

EFFECTS OF HYPERGLYCEMIA ON RED BLOOD CELL STORAGE LESION IN TRANSFUSION
MEDICINE

By

Yimeng Wang

A DISSERTATION

Submitted to
Michigan State University
in partial fulfillment of the requirements
for the degree of

Chemistry – Doctor of Philosophy

2013

ABSTRACT

EFFECTS OF HYPERGLYCEMIA ON RED BLOOD CELL STORAGE LESION IN TRANSFUSION MEDICINE

By

Yimeng Wang

Red blood cell (RBC) transfusions are an important component of critical healthcare. RBCs can be donated, processed, and stored in a blood bank for future transfusion. A review of RBC storage development, as well as RBC storage lesion, is presented here. Whole blood is collected into an anticoagulant-nutrient solution such as citrate phosphate dextrose (CPD). The RBCs separated from the plasma and platelets, are then added into an additive solution, such as AS-1, which supports the nutrient needs of the RBCs in storage. The glucose concentrations in CPD and AS-1 are 129 mM and 111 mM, respectively. Thus, the glucose level in this system (estimated > 40 mM) is much higher than the healthy glucose level *in vivo* (4-6 mM). This dissertation hypothesizes that the hyperglycemic conditions in the current storage system result in some changes in RBCs and thereby have adverse effects on vascular function.

In addition to the primary function of oxygen delivery, RBCs can function as a regulator of vascular tone. It is known that adenosine triphosphate (ATP) is released from intact RBCs in response to several stimuli and further stimulates nitric oxide (NO) production in the endothelium lining the blood vessels. This NO functions to relax the smooth muscle cells surrounding circulatory vessels, thereby increasing blood flow and oxygen delivery to the tissues. In order to investigate the effects of hyperglycemia, RBCs were processed

and stored in hyperglycemic and normoglycemic conditions. The vascular function and other properties of these cells were then studied.

In an *in vitro* microflow system, the RBCs stored in hyperglycemic conditions resulted in significantly less RBC-derived ATP for 4 weeks than the RBCs in normoglycemic conditions. During the same storage duration, microfluidic technologies enabled measurements of endothelium-derived NO that was stimulated by the ATP release from the stored RBCs. In comparison to normoglycemic solutions, the NO release decreased by more than 25% in the presence of the RBCs stored in the hyperglycemic conditions. Control experiments using inhibitors of ATP release from the RBCs, or ATP binding to the endothelium, strongly suggest that the decreased NO release by the endothelium is directly related to the ability of the stored RBCs to release ATP.

Furthermore, the mechanisms behind the effect of hyperglycemia on the ability of RBCs to release ATP were investigated and discussed. It was found that an osmotic imbalance was formed in RBCs in hyperglycemic conditions, which thereby reversibly impaired the ATP release from RBCs. In addition, longer hyperglycemic storage resulted in sorbitol accumulation within RBCs and cell membrane damage in terms of lipid peroxidation, which irreversibly impaired ability of the RBCs to release ATP. Therefore, the transfusion of those stored RBCs would result in inappropriate vasodilation, less blood flow, and insufficient oxygen delivery, which are often associated with post-transfusion complications. If the RBCs could be stored and maintained in normoglycemic conditions, it may be possible to reduce these complications to some extent and hopefully improve RBC transfusion efficacy.

Copyright by
YIMENG WANG
2013

ACKNOWLEDGEMENTS

First I would like to thank my advisor, Dr. Dana Spence, for his constant encouragement and guidance during my four and a half years at Michigan State University. His unique advising style allowed me to think and work independently. However, when I felt frustrated about the results, he'd like to discuss problems with me, provide suggestions in designing new experiments and encourage me to try more. Also, he gave a good example to show me how to write scientific papers and present attractive talks. In addition, I appreciate the helpful suggestions from my committee members, Dr. Bruening, Dr. Huang and Dr. Hrinchenko.

I sincerely thank the group members in Spence group, past and present. When I just joined in the group, the senior group members, Wathsala Medawala, Adam Giebink, Stephen Halpin, Kari Anderson, Suzanne Letourneau and Paul Vogel, provided their help generously. Without them I wouldn't get used to the graduate school life here soon. Really thanks to their critics and encouragements to my literature seminar, my second year oral examinations and other studies. They also introduced interesting American customs to me. I will miss the baking nights and crack barrel breakfasts. I would also like to thank the current group members: Jayda Erkal, Bethany Gross, Yueli Liu, Sarah Lockwood, Chengpeng Chen, Kristen Entwistle, and Ruipeng Mu. I enjoyed working with them very much. Additionally, due to the nature of the work in this dissertation, it was required blood samples from human. I would like to thank the group members'

donations and preparations. Special thanks to Suzanne, who read through this thesis and worked with me in the animal transfusion project.

I would like to thank my friends for making the graduate school life more enjoyable.

Finally, I really thank my parents for their love all of these years.

TABLE OF CONTENTS

LIST OF FIGURES	x
LIST OF TABLES	xix
Chapter 1 – Introduction	1
1.1 Brief Introduction of Red Blood Cell Transfusion.....	1
1.2 Red Blood Cell Storage History.....	1
1.3 Storage Lesion of RBCs	10
1.4 Vascular Effect of RBCs in Storage	15
1.5 Hyperglycemic Condition in Current Storage.....	19
REFERENCES	22
Chapter 2 – Flow-Induced Adenosine Triphosphate Release from Red Blood Cells Stored in Hyperglycemic and Normoglycemic Storage Solutions	30
2.1 Red Blood Cell-Derived ATP	30
2.2 Experimental	35
2.2.1 Experimental Storage Solutions Preparation	35
2.2.2 Blood Collection and Storage	36
2.2.3 Chemiluminescence Detection of ATP Release from RBCs in Flow-Based System	39
2.2.4 Lactate Accumulation in Stored RBCs	42
2.2.5 Determination of Glucose Level in Storage.....	45
2.2.6 Determination of Intracellular ATP in Stored RBCs	47
2.3 Results	48
2.3.1 Preliminary Study – 16 Days Storage.....	48
2.3.2 Glucose Feeding Treatment and 36 Days Storage	52
2.4 Discussion	59
REFERENCES	65
Chapter – 3 Endothelium-Derived Nitric Oxide Stimulated from RBC-Derived ATP	71
3.1 Nitric Oxide Stimulation in Vasodilation	71
3.2 NO Detection Based on Microfluidic Device	75

3.3 Experimental	78
3.3.1 Preparation of Microfluidic Devices	78
3.3.2 Culture of Endothelial Cells onto Microfluidic Device.....	82
3.3.3 Determination of Endothelium-Derived NO with Stimulation of ATP from Stored RBCs	83
3.3.4 The Effect of Glucose on NO Detection using Fluorescent Probe DAF-FM.....	87
3.3.5 Determination of RBC Hemolysis during Storage.....	89
3.4 Results	91
3.4.1 Endothelium-Derived NO Stimulated by ATP Release from 36-Day Stored RBCs	91
3.4.2 Results Verification by Two Control Experiments	92
3.4.3 The Effect of Glucose on NO Detection using Fluorescent Probe DAF-FM.....	94
3.4.4 Percent Hemolysis of RBCs Stored for 36 Days	97
3.5 Discussion	100
REFERENCES	105
Chapter 4 – Hyperglycemia and Reduced ATP Release from RBCs	112
4.1 Introduction.....	112
4.2 Experimental	123
4.2.1 Intracellular and Extracellular Glucose Measurement of RBCs	123
4.2.2 Osmotic Fragility Test of RBCs	124
4.2.3 Sorbitol Accumulation Measurement	126
4.2.4 Lipid Peroxidation Measurement	128
4.2.5 Protein Glycation Determination	130
4.2.6 Images, Mean Corpuscular Volume and Basal ATP Release of RBCs Suspended in Glucose Gradients.....	133
4.3 Results	137
4.3.1 Intracellular and Extracellular Glucose Level in Stored RBCs.....	137
4.3.2 Osmotic Fragility of Stored RBCs	137
4.3.3 Sorbitol Accumulation in Stored RBCs.....	139
4.3.4 Lipid Peroxidation in Stored RBCs	139
4.3.5 Protein Glycation in Stored RBCs	142

4.3.6 Images, Mean Corpuscular Volume, and Basal ATP Release of RBCs Suspended in Glucose Gradients.....	142
4.4 Discussion	148
REFERENCES	158
Chapter 5 – Conclusions and Future Directions	165
5.1 Overall Conclusions	165
5.2 Animal Model Determination of Posttransfusion Survival of RBCs Stored in Different Storage Solutions	171
5.2.1 Introduction	171
5.2.2 Optimization of Biotinylation of RBCs in Storage	175
5.2.3 Preliminary Posttransfusion Survival Study of Stored RBCs using a Rabbit Model.....	178
5.3 Glucose Slow Release Device/Membrane Development.....	182
REFERENCES	185

LIST OF FIGURES

Figure 1.1 – Collection of Blood in Additive Preservation Systems. A) The primary container contains 63 mL of CPD solution; one of the two satellite bags contains 100 mL of AS-1. B) ~ 450 mL of whole blood are collected into CPD in primary bag. C) The whole blood is centrifuged and RBCs (~ 220 mL) is transferred into 100 mL of AS-1 in the satellite bag, which can be separated and stored at 4°C for up to 42 days. For interpretation of the references to color in this and all other figures, the reader is referred to the electronic version of this dissertation.....9

Figure 1.2 – RBC Metabolism. The Embden-Meyerhof pathway (glycolysis) generates about 90% of ATP for energy. The pentose phosphate pathway provides the remaining 10% of ATP and generates NADPH that is used to reduce glutathione, which protects RBCs against oxidative stress. The generation of NADH maintains hemoglobin in a reduced state through the methemoglobin reductase pathway. The Luebering-Rapoport shunt regulates 2,3-DPG, which is a critical determinant of oxygen affinity of hemoglobin.....11

Figure 1.3 – Cross Section of a Blood Vessel and Proposed RBC-Mediated Vasodilation Mechanism. The blood components, such as RBCs, flow in the inner most core through the vessel. The endothelium lines the inner layer of the vessel interacting with blood. Outside of endothelial cells, there are thick layers of smooth muscle cells that are responsible for the expansion and contraction of the vessel. Vasodilation can be mediated by direct RBC-derived NO or endothelium-derived NO stimulated by RBC-derived ATP. For interpretation of the references to color in this and all other figures, the reader is referred to the electronic version of this dissertation.....17

Figure 2.1 – Proposed Signal Transduction Pathway for Regulated ATP Release from RBCs in Response to Mechanical Deformation. Conformational changes of GPCR results in activation of the heterotrimeric G protein, leading to activation of AC and production of cAMP; further with the activation of cAMP-dependent PKA, the CFTR protein becomes phosphorylated and thereby regulates ATP release through the plasma membrane via ion channels. For interpretation of the references to color in this and all other figures, the reader is referred to the electronic version of this dissertation.....32

Figure 2.2 – The Miniaturized RBC Collection and Storage in Lab. a) Injection of 1 mL of CPD or CPD-N into non-additive 10 mL glass Vacutainer tube; b) Draw about 7 mL of whole blood from donor into each Vacutainer tube; c) Sit at room temperature for at least 30 minutes and up to 2 hours, then centrifuge at 2000 g for 10 minutes; d) Plasma and buffy coat were discarded, as well as top 2-mm layer of packed RBCs to avoid remaining white cells; e) AS or AS-N were added into packed red blood cells at the ratio

of 1 to 2; f) 2 mL of mixed RBC concentrates were added into each PVC bag which was heat sealed and stored at 4°C; g) For normoglycemic one, blood bags were cut open and aliquot of glucose saline was added to feed RBCs every five days; bags were resealed and continued storing. All blood collection and storage processes were performed under sterile conditions. For interpretation of the references to color in this and all other figures, the reader is referred to the electronic version of this dissertation.....38

Figure 2.3 – Determination of Flow-Induced ATP Release from Stored RBCs using Microflow System. In dual syringe pump, one contained 7% RBCs, and the other contained luciferase/luciferin (L/L) solution. Both of them were pumped through microbore tubing at a rate of 6.7 $\mu\text{L}/\text{minute}$. RBCs flowed through the microbore tubing with an internal diameter of 50 μm resulting in ATP release into the solution, which met the L/L solution at a mixing T-junction. The combined stream was pumped through an additional segment of 75 μm internal diameter tubing, with a portion of the polyimide coating removed, over a PMT in a light excluding box. This allowed for the chemiluminescence (light) resulting from the reaction of ATP with L/L to be detected. For interpretation of the references to color in this and all other figures, the reader is referred to the electronic version of this dissertation.....41

Figure 2.4 – The Reaction Mechanism of Lactic Acid Assay. The lactate in the samples or standards is oxidized to pyruvate by LDH while NAD^+ reduced to NADH, which has an emission of fluorescence at 460 nm after excitation of 340 nm. The fluorescence intensity is proportional to the amount of NADH present as well as the lactate originally present. Thus, the lactate concentration in the samples can be quantified by using a calibration curve generated at the same time. An overall calibration curve (n = 6) is shown below, the limit of detection based on this curve is 11.4 μM43

Figure 2.5 – The Reaction Mechanism of Glucose Assay. The glucose in the samples or standards is first converted to G6P by HK, and subsequently oxidized to 6-phosphogluconate by G6PDH while NADP^+ reduced to NADPH, which has an emission of fluorescence at 460 nm after excitation of 340 nm. The fluorescence intensity is proportional to the amount of NADPH present as well as the glucose originally present. Thus the glucose concentration in the samples can be quantified by using a calibration curve generated at the same time. An overall calibration curve (n = 6) is shown below, the limit of detection based on this curve is 1.0 μM46

Figure 2.6 – ATP Release from the RBCs in Both Storage Conditions for 16-Day Preliminary Storage. The cells stored in normoglycemic condition (CPD-N/AS-1N, gray bars) show significantly higher ATP release than those in hyperglycemic condition (CPD/AS-1, black bars) for the first 8 days (*p < 0.005), the release gradually decreased as a function of storage duration. Furthermore, the ATP release from CPD-N/AS-1N cells on day 8 was statistically higher (p < 0.05) than the day 1 release from cells processed in CPD/AS-1. Data represent mean \pm s.e.m. (n = 4 for all).....50

Figure 2.7 – Lactate Accumulation in Hyperglycemic and Normoglycemic Conditions for the 16-Day Preliminary Storage. Lactate levels determined in the supernatant in both CPD/AS-1 (black bars) and CPD-N/AS-1N (grey bars) were at similar till day 8, whereas lactate stopped accumulating in the supernatant of RBCs stored in CPD-N/AS-1N around day 8. Data represent mean \pm s.e.m. (n = 4 for all).....51

Figure 2.8 – Extracellular Glucose Levels in Normoglycemic Storage Condition with Glucose Feeding Treatment for the 36-Day Storage. The black bars showed the glucose level was maintained at \sim 5 mM in the CPD-N/AS-1N storage with adding glucose saline every 5 days. Data represent mean \pm s.e.m. (n = 4 for all).....54

Figure 2.9 – Lactate Accumulation in Hyperglycemic and Normoglycemic Storage Conditions for the 36-Day Storage. Lactate accumulated in the supernatant in both CPD/AS-1 (black bars) and CPD-N/AS-1N with glucose feeding treatment (grey bars) increased equivalently till day 22. However, the CPD-N/AS-1N cells produced lactate slowly in the remaining storage period. Data represent mean \pm s.e.m. (n = 4 for all).....56

Figure 2.10 – ATP Release from the RBCs in Both Storage Conditions during 36 Days. The cells stored in normoglycemic condition with glucose feeding treatment (CPD-N/AS-1N, gray bars) consistently release significantly higher ATP than those in hyperglycemic condition (CPD/AS-1, black bars) through the 29-day storage duration (*p < 0.05), the release gradually decreased as a function of storage duration. In fact, the release from CPD-N/AS-1N cells on day 36 was statistically equivalent (p = 0.694) to the day 1 release from cells processed in CPD/AS-1. Data represent mean \pm s.e.m. (n = 4 for all).....57

Figure 2.11 – The Intracellular ATP Level in Stored RBCs in Hyperglycemic and Normoglycemic with and without Glucose Feeding Condition. The ATP concentration are highest for cells stored in CPD/AS-1 (black bars) and lowest for CPD-N/AS-1N without feeding (dark grey bars). The intracellular ATP concentrations for the CPD-N/AS-1N with feeding (light grey bars) is slightly lower than the CPD/AS-1, suggesting that the differences in ATP release from these cells is not necessarily due to the level of ATP reserved in the cell, since the amount of ATP release is just submicromolar level which is much smaller than the intracellular ATP level. Data represent mean \pm s.e.m. (n = 4 for all).....58

Figure 3.1 – ATP from RBCs Stimulates Endothelium-Derived NO Functions in Vascular Tone. RBC-derived ATP diffuses to endothelial cells and binds to P2Y receptors, resulting in an increase of intracellular free calcium, which activates the eNOS. The eNOS converts L-arginine into L-citrulline, as well as NO. NO diffuses to the smooth muscle cells, and binds to their sGC receptors, activating the conversion of GTP to cGMP. The increase of cGMP causes the relaxation of the muscle and facilitates dilation. For interpretation of the references to color in this and all other figures, the reader is referred to the electronic version of this dissertation.....73

Figure 3.2 – Fabrication of a Master for Microfluidic Device using Lithographic Method. Briefly, the clean silicon wafer is spin coated with SU-8 photoresist. After pre-baking, a transparent mask with the desired features is placed over the photoresist before exposing to UV light. The photoresist exposed to light cross links, forming a rigid structure of the feature. After a post-bake, the remaining unpolymerized photoresist is washed away in developer. Thus, a reusable master with raised features is created and can be used as a mold for PDMS. For interpretation of the references to color in this and all other figures, the reader is referred to the electronic version of this dissertation.....77

Figure 3.3 – Mechanism of NO Detection using DAF-FM. Shown in the upper panel are the structures of DAF-FM and its derivate, DAF-FM DA. DAF-FM DA permeates well into living cells and is rapidly transformed into water-soluble DAF-FM by cytosolic esterases. The lower panel shows the reaction between NO and DAF-FM, which requires oxygen, to form DAF-FM-NO. DAF-FM-NO fluorescence can be detected with a peak excitation wavelength of 485 nm and a peak emission of 515 nm.....79

Figure 3.4 – Fabrication of PDMS Slabs through Soft Lithography. The polymer and curing agent were mixed in 20:1 and 5:1 ratios in separate cups and degassed by vacuum. The 20:1 and 5:1 mixtures were poured over the masters and baked at 75°C for 13 minutes, after each layer. The PDMS was then removed from the master, after cooling. Both slabs were further modified to create the inlets of channels, the probe wells, and the waste wells.....81

Figure 3.5 – Experimental Setup for the Detection of Endothelium-Derived NO Stimulated by Flow-Induced ATP from Stored RBC Samples. The device, fabricated from PDMS and described in more detail elsewhere, enables RBCs processed in CPD/AS-1 or CPD-N/AS-1N to flow beneath a layer of endothelial cells. When the cells release ATP due to flow-induced deformation, the ATP in the suspension can diffuse through a porous membrane, stimulating NO production from the endothelium via purinergic receptor signaling. The fluorescent probe DAF-FM facilitates the measurement of NO released by the endothelium. The fluorescence signal can be measured directly in a plate reader with an excitation wavelength at 488 nm and emission wavelength of 515 nm. For interpretation of the references to color in this and all other figures, the reader is referred to the electronic version of this dissertation.....85

Figure 3.6 – Structures of GLI and PPADS. Glibenclamide, the CFTR inhibitor, was used to prevent ATP released from RBCs in the control experiments. PPADS, the purinergic receptor (P2Y) inhibitor, was used to inhibit the NO released from endothelium in the second control experiment.....88

Figure 3.7 – The NO Release from the Endothelium Stimulated from Flow-Induced ATP from Stored RBCs in Different Storage Solutions. The percent increase in NO release from the endothelial cells (> 25% for the first 3 weeks of storage) is significantly higher

when exposed to RBCs processed in CPD-N/AS-1N (*p < 0.02). Data represented as mean ± s.e.m., n = 4.....93

Figure 3.8 – The NO Release from the Endothelium in the Presence of RBCs Pretreated with GLI, an Inhibitor of RBC-Derived ATP Release. There is no significant increase in NO release (p = 0.742), regardless of the storage solution, when the stored RBCs are exposed to GLI, suggesting that this endothelium-derived NO is due to flow-induced ATP release from RBCs, not RBC lysis. Data represented as mean ± s.e.m., n = 4.....95

Figure 3.9 – The NO Release from the Endothelium Pretreated with PPADS, an Inhibitor of the ATP Binding Site, in the Presence of Stored RBCs. There is no significant increase in NO release (p = 0.623), regardless of the storage solution, when the endothelial cells in the presence of PPADS, suggesting that the increased NO signal is due to endothelial cell stimulation by ATP. Data represent mean ± s.e.m., n = 4.....96

Figure 3.10 – The Effect of Glucose across the Endothelium Cultured on the Microfluidic Device on the Detection of NO using DAF-FM. The upper panel a) demonstrates the glucose diffused above the endothelium when pumping 7% stored RBCs in CPD/AS-1 or CPD-N/AS-1N for 30 minutes at 37°C. The sample with CPD/AS-1 (dark grey bar) was 19.3 ± 0.6 mM and the one with CPD-N/AS-1N (grey bar) was 6.4 ± 0.1 mM in glucose concentration. Data represented as mean ± s.e.m., n = 6 wells. The lower panel b) shows the fluorescent intensity of 5 µM DAF-FM reacted with 0, 10, 100 µM of DEANO (NO donor) in glucose gradient ranging from 0 - 100 mM. Data represented as mean ± s.e.m., n = 3 wells. Data from these results indicates that glucose diffused above endothelium should have a negligible effect on the NO detection using 5 µM DAF-FM.....98

Figure 3.11 – The Percent Lysis of RBCs Stored in CPD/AS-1 (black circles), CPD-N/AS-1N with Periodic Glucose Feeding (white circles), and CPD-N/AS-1N without Periodic Glucose Feeding (black triangles). It is obvious from the data that AS-1N storage without glucose maintenance is detrimental to the RBCs. However, for those cells stored in AS-1N with glucose feeding, the extent of lysis is statistically equal to those cells stored in AS-1 (p = 0.366). Data represented as mean ± s.e.m., n = 4.....99

Figure 4.1 – Diagram of a Cross Section of the RBC Membrane. The RBC membrane is a composite of a lipid bilayer occupied by transmembrane proteins, supported by a spectrin-based cytoskeleton. Lipids are composed of cholesterol and phospholipids. The 4 major phospholipids are distributed asymmetrically within the two layers of membrane. Integral proteins, including glycophorin and the anion transport protein (Band 3) are embedded in the membrane via hydrophobic interactions with lipids. Peripheral proteins, including spectrin, ankyrin, actin, Band 4.1 and 4.2, are located on the inner cytoplasmic side of the lipid bilayer, forming the RBC cytoskeleton, anchored via integral proteins. For interpretation of the references to color in this and all other figures, the reader is referred to the electronic version of this dissertation.....115

Figure 4.2 – Simplified Reaction Pathway Involved in Protein Glycation and the Formation of AGEs. Reducing sugar, such as glucose, can chemically react with primary amine groups in proteins, initially forming the reversible Schiff base within minutes. During hours to weeks, it forms the more stable ketoamine product through an Amadori rearrangement and further converts to the reactive Amadori product. When large amounts of these products are accumulated, they tend to form a series of more reactive protein-bound moieties, AGEs.....118

Figure 4.3 – The Mechanism and Effect of the Hyperglycemia-Induced Polyol Pathway. Increased activity of aldose reductase, induced by hyperglycemia, converts glucose to sorbitol while oxidizing NADPH to NADP⁺. Next, sorbitol can be oxidized by sorbitol dehydrogenase to fructose while converting NAD⁺ to NADH. Increased performance of this pathway in RBCs leads to adverse effects, such as osmotic stress, oxidative stress, and even protein glycation. For interpretation of the references to color in this and all other figures, the reader is referred to the electronic version of this dissertation.....119

Figure 4.4 – Simplified Mechanism of Free Radical-Mediated Peroxidation of PFA. In the initiation step, ROS, such as hydroxyl radicals ($\cdot\text{OH}$), combine with a hydrogen atom of PFA to form a lipid radical and water. The unstable lipid radical reacts readily with oxygen to create lipid peroxy radical. This radical is also an unstable species that can either react with another PFA, producing more radicals and lipid peroxide (propagation), or react with itself to produce cyclic peroxide, which can further rearrange to create MDAs.....121

Figure 4.5 – The Mechanism behind the Sorbitol Assay and the Calibration Curve. The sorbitol assay is based on the oxidation of sorbitol to fructose catalysed by SDH in the presence of NAD⁺, resulting in the formation of NADH, which has an emission of fluorescence at 460 nm after excitation of 340 nm. The fluorescence intensity is proportional to the amount of NADH present as well as the sorbitol originally present. Thus, the sorbitol concentration in the samples can be quantified by using a calibration curve generated at the same time. An overall calibration curve (n = 3) is shown above; the limit of detection based on this curve is 10.0 μM127

Figure 4.6 – The Mechanism behind the TBARS Assay and the Calibration Curve. The MDA extracts from RBCs, representing the oxidative level and lipid peroxidation, can be determined using TBARS assay. The MDA-TBA adducts formed by the reaction of MDA and TBA at a high temperature (90-100°C) and acidic conditions are measured fluorometrically at an excitation wavelength of 530 nm and an emission wavelength of 550 nm. The net fluorescence intensity found by subtracting that of a blank as a background, is proportional to the amount of MDA-TBA adduct present as well as the MDA originally present. Thus, the MDA concentration in the samples can be quantified by using a calibration curve generated at the same time. An overall calibration curve (n = 6) is shown above; the limit of detection based on this curve is 10 nM.....131

Figure 4.7 – The Mechanism of Protein Glycation Assay and the Calibration Curve. The proteins, including Hb, in RBCs can be covalently modified by glucose linked as a stable ketoamine product. Through a mild hydrolysis of the ketoamine, glucose can be released from proteins as 5-HMF, which reacts with TBA to form a yellow HMF-TBA chromogen. This chromogen can be measured colorimetrically at 435 nm. The net absorbance at 435 nm, found by subtracting that at 500 nm as a background, is proportional to the amount of HMF-TBA chromogen present as well as the 5-HMF originally present. Thus, the 5-HMF concentration in the samples can be quantified by using a calibration curve generated at the same time. An overall calibration curve (n = 9) is shown above; the limit of detection based on this curve is 1.8 nM.....134

Figure 4.8 – Extracellular and Intracellular Glucose Levels in Stored RBCs for 36 Days. To monitor the glucose level of the RBCs stored in hyperglycemic (CPD/AS-1) and the normoglycemic (CPD-N/AS-1N) conditions, the intracellular and extracellular glucose levels were measured weekly. The extracellular glucose level in CPD/AS-1 storage (black dot) was at 66.2 ± 1.2 mM at day 1, decreasing to 53.9 ± 2.1 mM at day 36, while the intracellular level (black triangle) was at 51.8 ± 1.2 mM at day 1, decreasing to 44.1 ± 2.0 mM at day 36. With glucose feeding, both the extracellular (white dot) and intracellular (white triangle) glucose levels in CPD-N/AS-1N were stable around 5 mM with some fluctuations for 36 days. Data represented as mean \pm s.e.m. (n = 4).....138

Figure 4.9 – Osmotic Fragility of Stored RBCs. Osmotic fragility was determined by subtracting the absorbance of stored RBCs in 0.9% NaCl (blank) from that of all in 0.45%, then dividing by the absorbance of stored RBCs in DDW, representing 100% hemolysis of RBCs. The CPD-N/AS-1N RBCs (grey bars) showed a significantly lower percent hemolysis in 0.45% NaCl for the first 3 weeks, compared to the CPD/AS-1 RBCs (black bars), which had an approximate 50% hemolysis in 0.45% NaCl at day 1. However, the hemolysis percentage in both storages increased as a function of time, which indicated an increase in osmotic fragility of the RBCs. Data represented as mean \pm s.e.m. (n = 3).....140

Figure 4.10 – Sorbitol Accumulation in Stored RBCs. Sorbitol is produced through the hyperglycemia-induced polyol pathway and cannot cross the cell membrane and thereby accumulates in RBCs. Sorbitol accumulation was determined weekly during 36 days storage. At day 1, the sorbitol in CPD/AS-1 RBCs (black bars) was 52.8 ± 8.6 nmol/g Hb, while it was lower but not significantly so in CPD-N/AS-1N RBCs (grey bars), 43.1 ± 8.2 nmol/g Hb. However, the sorbitol increased dramatically in CPD/AS-1 RBCs during the first week to 147.5 ± 7.2 nmol/g Hb at day 8, whereas the one in normoglycemic storage at day 8 was statistically equivalent to day 1. For the remaining storage period, the sorbitol in both RBCs remained at the respective level. Data represented as mean \pm s.e.m. (n = 3).....141

Figure 4.11 – Lipid Peroxidation in Stored RBCs. MDA is a naturally occurring product of lipid peroxidation, which can be determined by a TBARS assay. In this assay, the MDA-

TBA adduct formed by the reaction of MDA and TBA is measured fluorometrically at 530 nm (excitation: 550 nm), and quantified with external standards. The MDA in CPD/AS-1 RBCs (black bars) and in CPD-N/AS-1N RBCs (grey bars) were 3.2 ± 0.2 nmol/g Hb and 3.1 ± 0.2 nmol/g Hb at day 1, respectively. However, the MDA in hyperglycemic conditions tended to increase as a function of time, while the amount in normoglycemic conditions seemed to remain at similar levels. At day 22, the MDA in CPD/AS-1 RBCs, 4.5 ± 0.2 nmol/g Hb, was significantly higher ($*p < 0.05$) than the level in CPD-N/AS-1N. Until day 36, the MDA in CPD/AS-1 RBCs increased to 5.6 ± 0.4 nmol/g Hb. Data represented as mean \pm s.e.m. (n = 4).....143

Figure 4.12 – Protein Glycation in Stored RBCs. The hydrolysis of protein glycation releases glucose from proteins as 5-HMF, which can be determined using TBA to form a yellow chromophore. The peripheral proteins (black bars), hemoglobin (light grey bars) and integral proteins (dark grey bars) of CPD/AS-1 RBCs and CPD-N/AS-1N RBCs were not significantly different from each other at various time points, (day 1, 15 and 36). Data represented as mean \pm s.e.m. (n = 4).....144

Figure 4.13 – Normalized Basal ATP Release of RBCs in Glucose Gradient. 7% RBCs were suspended in AS with different glucose concentrations indicated in horizontal axis (light grey bars). The dark grey bars represent RBCs washed with AS-1N. The samples were centrifuged, and the supernatants were used for measuring basal ATP release. The chemiluminescence intensities from each sample were normalized to the one from the “5.5” mM glucose sample. The basal ATP release from RBCs in “5.5” mM glucose sample was not significantly different from the ATP in “0” mM glucose sample, but it was significantly higher ($*p < 0.01$) than the ATP in “16.5”, “55” and “111” mM glucose sample. However, after washing with 5.5 mM AS, the ATP release of the RBC previously in “111” mM glucose sample increased and was significantly higher ($**p < 0.005$) than the one prior to washing. Data represented as mean \pm s.e.m. (n = 4).....147

Figure 4.14 – Mean Corpuscular Volume of RBCs in Glucose Gradient. The MCV of RBCs represents the average RBC volume, which is calculated by dividing the hematocrit by the total number of RBCs and multiplying by 10. The MCV of RBCs tended to decrease when they were exposed to high glucose; however, there was only significant decrease ($*p < 0.01$) in “111” mM glucose AS, compared to the sample in “5.5” mM glucose AS. Data represented as mean \pm s.e.m. (n = 4).....149

Figure 4.15 – Images of RBCs in Normoglycemic and Hyperglycemic Conditions. The images of RBCs suspended in 5.5 mM and 111 mM glucose AS are shown in a) and b), respectively. In a), RBCs had biconcave disk shapes, while RBCs shrank as shown in b). However, it is shown in d) that RBCs previously in hyperglycemic conditions returned to their normal shape after washing with 5.5 mM glucose AS. c) represents the RBCs previously in normoglycemic conditions after washing with 5.5 mM glucose AS.....150

Figure 4.16 – Long Term Study of ATP Release Reversibility of Stored RBCs. The basal ATP release in the supernatant from the 7% stored RBCs was determined weekly during 36 days of storage. The CPD/AS-1 RBCs were washed in hyperglycemic (black bars) and normoglycemic (grey bars) AS to remove the extracellular ATP from cell lysis in storage. The normoglycemic values are normalized to the hyperglycemic values. At day 1, after washing with AS-1N, the basal ATP from the CPD/AS-1 RBCs significantly (*p < 0.01) increased with comparison to the sample washed with AS-1. However, this increased basal ATP was no longer significant during the remaining storage. Data represented as mean ± s.e.m. (n = 4).....151

Figure 5.1 – The Mechanism of Biotinylation. NHS-biotin is the most popular type of biotinylation reagent. It reacts efficiently with primary amino groups of proteins to form stable amide bonds. The targets for labeling include the side chain of lysine residues and the N-terminus of each polypeptide.....173

Figure 5.2 – The Detection of Biotin-Labeled RBCs using Flow Cytometry. Panel a) represents the procedure of the biotinylation of RBCs using NHS-biotin and further labeling with streptavidin-conjugated fluorescein FITC for flow cytometry. Panel b) shows the results of biotinylation of RBCs using flow cytometer: pure biotin-labeled RBCs and different ratios of total RBCs and biotin-labeled RBCs mixtures (2:1, 5:1, 10:1, 20:1 and 30:1).The percentage of biotin-labeled RBCs is the ratio of the number of cells with fluorescent intensity > 10^3 to the total number of cells. For interpretation of the references to color in this and all other figures, the reader is referred to the electronic version of this dissertation.....177

Figure 5.3 – An Example of Posttransfusion Survival Data of Stored RBCs. Panel a) shows approximately 100% of stored RBCs were biotinylated before transfusion using the optimized method described previously. Panel b) represents that 8.1% of total RBCs circulating in that rabbit were the biotinylated stored RBCs at 10-minute time point. Panel c) shows the best fit curve plotted as percentage of stored RBCs survival versus time. The MPL of stored RBCs can be calculated based on the equation. For interpretation of the references to color in this and all other figures, the reader is referred to the electronic version of this dissertation.....180

LIST OF TABLES

Table 1.1 – Comparisons of CPD, CPDA-1, CPDA-2 and CPDA-3.....6

Table 1.2 – Content of Current Anticoagulant Solutions and Additive Solutions.....21

Table 2.1 – Contents of CPD/AS-1 and CPD-N/AS-1N System.....37

Table 2.2 – The Extracellular Glucose Level in CPD-N/AS-1N Storage without Glucose Feeding Treatment.....53

Table 3.1 – Different DEANO Concentrations in Glucose Gradient Preparation.....90

Table 4.1 – Glucose Level inside and outside of 7% RBCs in AS with Different Glucose Gradient.....146

Table 5.1 – Percentage of Posttransfusion Survival of Stored RBCs at Various Time Points.....181

Chapter 1 – Introduction

1.1 Brief Introduction of Red Blood Cell Transfusion

Mature human red blood cells (RBCs) lack nuclei and most organelles, and have a protein content that is 97% hemoglobin (Hb). The principal function of RBCs is the delivery of oxygen to the body tissue. They circulate in the vascular space and derive nutrients from and excrete waste into the plasma.¹ As a result of not containing mitochondria, RBCs largely rely on the breakdown of glucose to produce energy carrier adenosine triphosphate (ATP) by anaerobic glycolysis instead of using the oxygen they transport. RBCs can be donated, processed, and stored in a blood bank for blood transfusion. Blood transfusion is indeed vital to human health and applied in numerous clinical situations. The 2011 National Blood Collection and Utilization Survey (NBCUS) estimates that a total of 15,721,000 whole blood and red blood cell (RBC) units were collected and 13,785,000 units were transfused.² Typically, RBC concentrates are administered to sustain the oxygenation of tissues, and correct hemostasis imbalance or disorders under conditions such as severe haemorrhage (bleeding internally or externally), anaemia (a decrease in number of RBCs in the blood) or hypovolemia (blood volume contraction).³

1.2 Red Blood Cell Storage History

Historically, the first blood transfusions did not use stored blood, but instead directly transfused from donor to recipient by connecting their blood vessels, and thereby their circulations, before clotting intervened. In order to separate the donor and recipient in time and space, blood needed to be stored and transported.⁴ The first RBC storage solution, a mixture of citrate and glucose, was developed by Rous and Turner in 1915⁵ and was also used in the world's first blood bank by Robertson *et al.* during World War I in 1918.⁶ Through this remarkable work, two developments of vast importance to blood transfusion were made: the introduction of citrate as an anticoagulant, and the use of glucose as a RBC preservative.⁷ Specifically, 500 mL of blood were drawn into a mixture of 850 mL of 5.4% (300 mM) glucose and 350 mL of 3.8% (129 mM) trisodium citrate and stored in a "Winchester" bottle (a strong and heavy bottle with a capacity of 2.2 liters, made of amber glass). Though this solution allowed the storage of blood for up to 4 weeks, the blood could not be used immediately due to its large volume of solutions and high citrate content. The RBCs had to settle for 5 days to 800 - 900 mL and the high citrate containing supernatant was discarded.

Caramelization would occur when the mixture of sodium citrate and dextrose (D-glucose) was autoclaved for sterilization whereas citrate alone could be heated. Thus, the first blood bank standard was the collection of whole blood into autoclaved bottles of 3.8% sodium citrate solution and 5-day blood storage on ice. There is enough glucose in whole blood from healthy donors to support RBC storage for about 5 days. Later, it was

found that the original solution could be autoclaved if citric acid was added, dropping the pH below 5.8, and allowed the storage of whole blood for 21 days. This new solution was named acid citrate dextrose (ACD).⁸

The subsequent history of stored blood moved on to the quality control of the proportion of viable RBCs present at the time of transfusion. The RBCs are assumed to be viable in terms of intact and survival. This included a limit to the amount of free hemoglobin (Hb) in storage and the mean 24-hour *in vivo* survival at the time of transfusion. The amount of free Hb indicates the percentage of RBCs lysed during storage. 24-hour *in vivo* post-transfusion survival refers to the fraction of stored RBCs that stay in the circulation and will have a normal 100-day life span.

In the 1950s, plastic blood-storage bags were developed due to their distinct advantages: light weight and sturdier than glass bottles to transport, as well as providing a sterilized closed-collection system designed to avoid bacterial contamination.⁹⁻¹⁰ In addition, the polymeric materials used for plastic bags, require plasticizers to increase flexibility and stability. Of all available polymers, polyvinylchloride (PVC) has been chosen in conjunction with the two most common plasticizers, di-2-ethylhexylphthalate (DEHP) and tri-2-ethylhexyl trimellitate (TEHTM).⁹ Studies have shown that plasticizers improve gas exchange across the bag barrier, and the leakage of the plasticizer from bags into storage solution helps to stabilize the RBC membrane during storage.⁴

Meanwhile in the late 1950s, researchers were still dedicated to improving the quality of stored blood by modifying the storage solution. A new solution, citrate phosphate dextrose (CPD), was developed by adding sodium phosphate to ACD.¹¹ The purpose of adding inorganic phosphate is to reduce the gradient of phosphate between the inside and the outside of the stored RBCs. This prevents the loss of intracellular phosphate and supports the synthesis of ATP. Studies have shown that RBCs stored in CPD continue glycolytic activity for up to 28 days, whereas RBCs in ACD cease this process at day 15, due to a lack of required ATP.¹² The mean fraction of RBCs survived in 24 hours was raised from 75% in ACD to 79% in CPD (N = 4137).¹³ Also, Nakao *et al.* discovered a relationship between ATP levels and *in vivo* viability of RBCs in 1962.¹⁴ Adenine and inosine were added to the blood stored in ACD to increase ATP regeneration, which therefore was able to maintain the cell shape and increase the post-transfusion viability. Based on the results, citrate phosphate dextrose adenine (CPDA-1) solution was developed in 1968. This differs from CPD in that it has 1.25 times the glucose concentration and contains adenine, extending the storage to 5 weeks.¹⁵

The hematocrit of stored whole blood either in ACD, CPD or CPDA-1 was 70% or higher. Packing to higher hematocrit causes greater reduction in total nutrient reserves in plasma. When blood is drawn into an anticoagulant solution, the glucose and adenine quickly distribute to a quasiequilibrium between the plasma and RBCs.¹⁶ When the

plasma is removed, a share of the nutrients is lost. Thus, researchers started to modify the CPDA-1 solution by increasing glucose and adenine concentrations (see table 1.1).¹⁷

One solution, CPDA-2, contained higher adenine and 1.75 times the CPD glucose concentration; the other solution, CPDA-3, contained the same amount of adenine as CPDA-2, but 2 times the CPD glucose. These new solutions were evaluated for storage. Significantly enhanced ATP maintenance was provided by CPDA-2 and CPDA-3 in comparison to CPD and CPDA-1 beyond 4-week storage. Interestingly, higher ATP values were seen in CPDA-2 as compared with CPDA-3, though the glucose concentration in CPDA-3 was higher. However, adding more glucose would also result in unnecessary amounts of glucose present in the plasma and platelet components.

In the 1970s, RBC preparations replaced whole blood. However, after removing the plasma, high hematocrit (> 75%) suspension of packed RBCs is viscous and leads to slow administration. Therefore, additive solutions were developed to provide dilution and nutrients for packed RBCs in the 1980s.¹⁸ Blood was first drawn into an anticoagulant solution, such as CPD, followed by centrifugation to separate the RBCs (hematocrit ~ 90%) from plasma. Next, packed RBCs were added and mixed into an additive solution with some carryover of citrate, phosphate and dextrose from the first anticoagulant solution. It's worth noting that since the glucose distributes to a quasiequilibrium between plasma and RBCs as mentioned above, only 45% of the glucose is lost during the separation of the RBCs.¹⁷

Table 1.1 – Comparisons of CPD, CPDA-1, CPDA-2 and CPDA-3

	Dextrose	Adenine
CPD	129 mM	0 mM
CPDA-1	1.25x CPD	2 mM
CPDA-2	1.75x CPD	4 mM
CPDA-3	2x CPD	4 mM

The first additive solution (AS) was developed by Hogman *et al.* in 1978.¹⁹ It originated from diluting viscous packed RBCs with normal saline before transfusion. When the RBCs are stored for prolonged periods of time in saline, hemolysis due to storage has been shown to increase slightly. Thus, a solution containing sodium chloride (110 – 150 mM), adenine (1.25 mM) and glucose (45 – 80 mM), known as SAG, was evaluated for RBC storage. It turned out that RBCs could be stored for 35 days in SAG with 70% of the initial level of ATP maintenance and 82% of 24-hour RBC posttransfusion survival. When the volume of SAG added was half or less than the volume of packed RBCs (hematocrit ~ 55%), the leakage of intracellular potassium into storage was reduced, and thereby RBC water homeostasis was better maintained in comparison to CPDA-1 stored whole blood. The investigators also tried adding citrate and phosphate to the SAG solution, although there were no significant improvements or differences in RBC figures of merit. A major problem with this work was greater storage hemolysis than whole blood in CPD or packed RBCs.

Further studies showed that the high hemolysis was not related to the intracellular metabolic state of RBCs, but to the adverse effect of leukocytes remaining after separation from the plasma.¹⁹ Since human leukocytes are known to contain proteolytic enzymes,²⁰⁻²¹ it seems that leakage of leukocyte proteases to the surrounding environment can cause proteolysis in the membranes of RBCs (the activity of these proteases would be inhibited in plasma). Therefore, the removal of the buffy coat or

leukofiltration can prevent this damage, improve RBC recovery, and reduce storage hemolysis. Hogman *et al.* also showed that the addition of mannitol (10 – 30 mM) to the SAG solution was an effective way of reducing osmotic swelling and keeping the spontaneous lysis within normal limits (1%) during longer storage (6 weeks).²² This modified additive solution, SAGM, was named after the ingredients: sodium chloride (150 mM), adenine (1.25 mM), glucose (50 mM), and mannitol (28.8 mM). SAGM is the standard additive solution currently used in Europe.

In the USA, 3 modified versions based on the SAG solution that have been licensed by the Food and Drug Administration (FDA): AS-1 (Adsol Baxter; sodium chloride 154 mM, adenine 2 mM, dextrose 111 mM, mannitol 41 mM, pH 5.5), AS-3 (Nutricel Pall Medical; sodium chloride 70 mM, anhydrous monobasic sodium phosphate, 23 mM, citric acid 2 mM, sodium citrate 23 mM, dextrose 55 mM, pH 5.8), and AS-5 (Optisol Terumo; sodium chloride 150 mM, adenine 2.2mM, dextrose 45 mM, mannitol 45.5 mM, pH 5.5).²³ However, no new RBC additive solutions have been licensed for use in over 20 years.

Currently, as shown in figure 1.1, a typical RBC collection procedure (also intended for platelet production) involves 450 mL of whole blood drawn into a primary bag that contains 63 mL of the anticoagulant, CPD. After centrifugation, RBCs (~ 220 mL, containing ~ 40 mL of CPD-plasma) are sedimented and separated from the buffy coat (contains platelets and leukocytes) and plasma. With a semiautomated extractor,

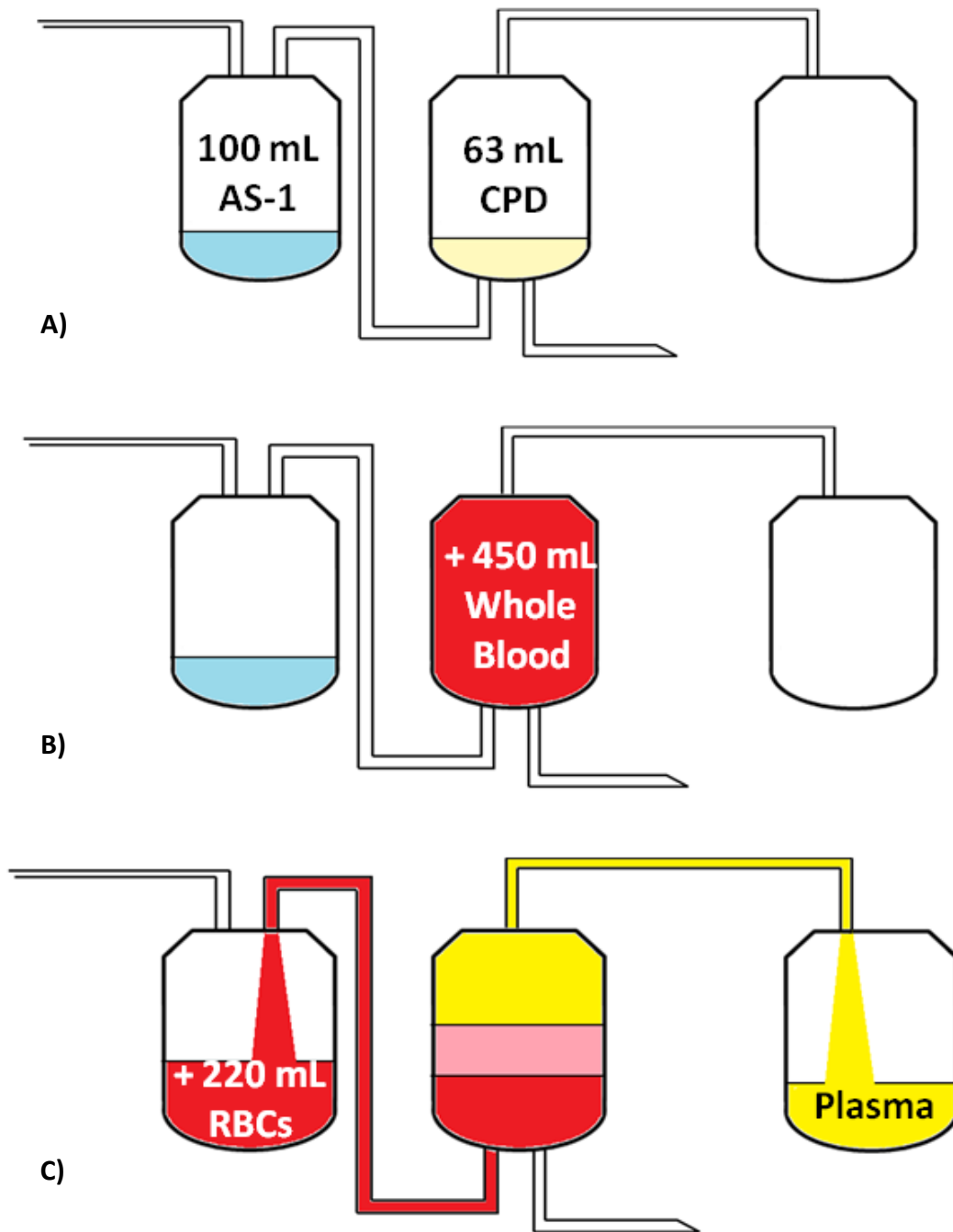


Figure 1.1 – Collection of Blood in Additive Preservation Systems. A) The primary container contains 63 mL of CPD solution; one of the two satellite bags contains 100 mL of AS-1. B) ~ 450 mL of whole blood are collected into CPD in primary bag. C) The whole blood is centrifuged and RBCs (~ 220 mL) is transferred into 100 mL of AS-1 in the satellite bag, which can be separated and stored at 4°C for up to 42 days. For interpretation of the references to color in this and all other figures, the reader is referred to the electronic version of this dissertation.

plasma is then exported out of the top port, and the RBCs are exported out of the bottom port into a satellite bag containing 100 mL of AS-1.²⁴ This procedure results in a final, stored RBC solution at ~ 55% - 60% hematocrit. RBCs can be further modified by passing through a leukoreduction filter prior to storage. RBC storage varies from bag to bag in term of RBC numbers and final volume, although the same procedure and amounts of solutions are used during processing.

1.3 Storage Lesion of RBCs

There are three areas of RBC biology that are crucial for normal RBC survival and function: 1) RBC metabolism; 2) hemoglobin structure and function; 3) normal chemical composition and structure of the RBC membrane. Due to the dramatic environmental change from *in vivo* to a closed system of solutions in the bag, RBCs undergo a series of metabolic and physical changes that are collectively known as storage lesions.

In storage, the solutions provide glucose, phosphate, and adenine to maintain ATP and 2,3-diphosphoglycerate (2,3-DPG) levels. The RBC generates about 90% of the ATP needed through the breakdown of glucose to lactate (anaerobic glycolytic pathway, shown in figure 1.2). Subsequently, lactic acid accumulates through glycolysis in the bag, and the RBC pH drops from 7.0 to 6.5 during storage.²⁵⁻²⁶ The decreasing pH slows down glycolysis by inhibiting hexokinase (HK) and phosphofructoskinase (PFK), so that less ATP is made during storage.²⁷ Although a quarter of intracellular ATP content is lost during storage, it is still considered as well maintained for RBC storage. The remaining

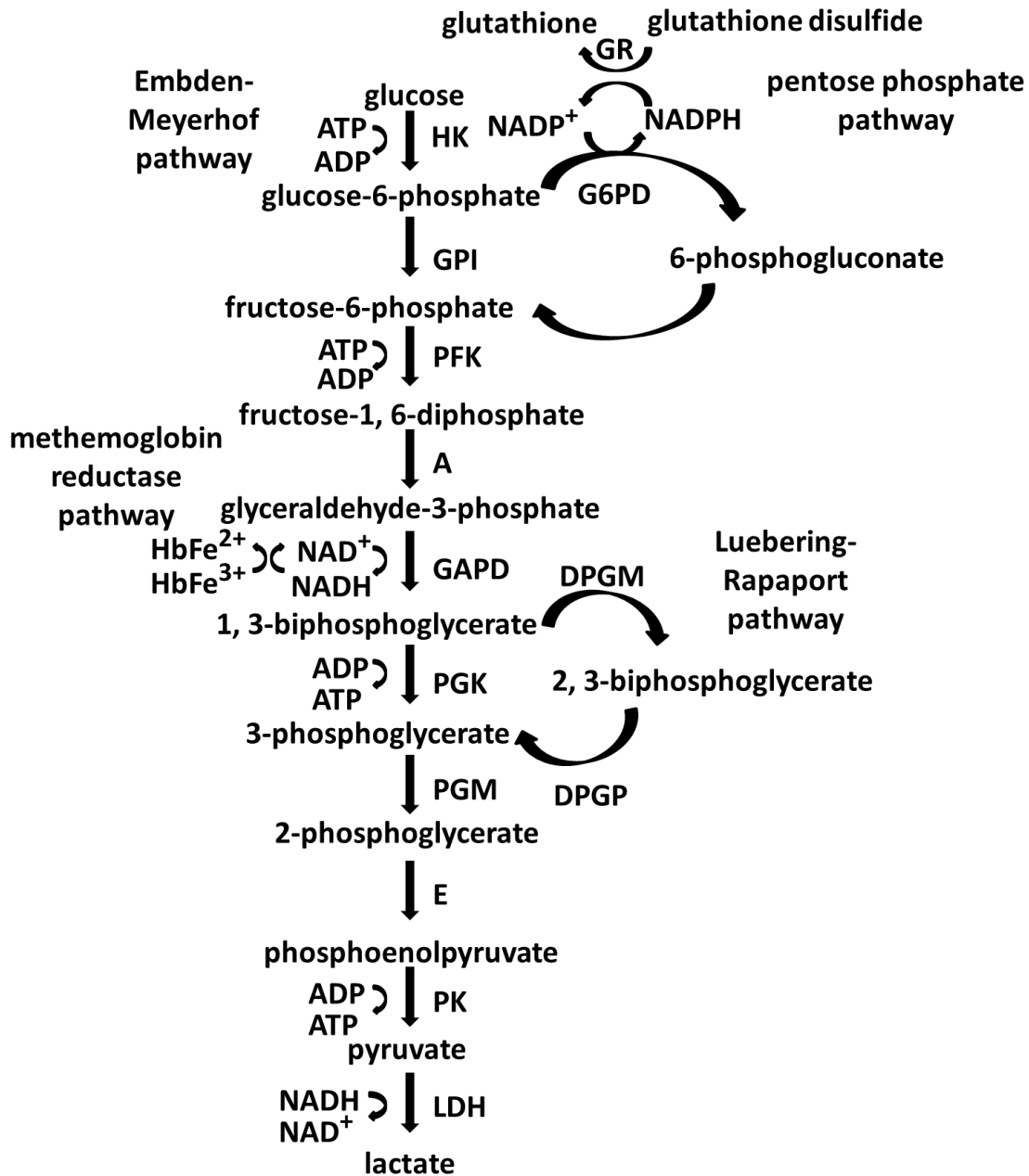


Figure 1.2 – RBC Metabolism. The Embden-Meyerhof pathway (glycolysis) generates about 90% of ATP for energy. The pentose phosphate pathway provides the remaining 10% of ATP and generates NADPH that is used to reduce glutathione, which protects RBCs against oxidative stress. The generation of NADH maintains hemoglobin in a reduced state through the methemoglobin reductase pathway. The Luebering-Rapoport shunt regulates 2,3-DPG, which is a critical determinant of oxygen affinity of hemoglobin.

10% of the ATP was generated by the pentose phosphate pathway. Besides, it contains other important pathways, although the mature RBC is often thought to be a simple cell with no organelles and biochemical significance beyond oxygen delivery. The Luebering-Rapoport shunt accumulates organic phosphate and 2,3-DPG. 2,3-DPG selectively binds to deoxyhemoglobin and stabilizes it,²⁵ so the oxygen is more likely to be released to adjacent tissue. However, diphosphoglyceromutase phosphatase (DPGP) is activated when the pH falls below 7.2, leading to the degradation of 90% of the 2,3-DPG after 42 days in storage. Thus, when initially transfused, Hb in stored RBCs binds surrounding oxygen tightly and is not able to release it to tissues. About 50-70% of the 2,3-DPG is able to be recovered *in vivo* within 24 h after transfusion.²⁸

RBCs are typically 75% saturated with oxygen when they are drawn into a storage solution.²⁹ There is a constant binding and dissociation between hemoglobin and oxygen. Occasionally, the oxygen takes an electron, leading to the formation of superoxide radical and increased methemoglobin, which is not able to bind oxygen. These consequences can be corrected immediately by superoxide dismutase and methemoglobin reductase *in vivo*. For example, the methemoglobin reductase pathway reduces methemoglobin (Fe^{3+}) back hemoglobin (Fe^{2+}) to be able to bind oxygen. However, these enzymes are not available in storage solutions. Methemoglobin is so unstable that free iron tends to come out into the solution. Also, because glycolysis in stored RBCs is 20-fold slower at 3°C than at 37°C,²⁶ the glutathione (GSH) and

nicotinamide adenine dinucleotide (NADH) concentrations fall.³⁰ This shortage of antioxidants and the existence of a superoxide radical, water, and free irons increase the chance of their transformation into a hydroxyl radical, which readily damages lipids and proteins. Unsaturated lipids can be oxidized whereas proteins can be decorated, or have alteration on their backbones and amino acid side-chains. The most common decoration occurring on proteins is the oxidative binding of glucose to hemoglobin to form glycated hemoglobin. One type of glycated hemoglobin, HbA1c, is an indicator of the hyperglycemia in blood over prolonged periods of time. While glycated Hb is common to an extent, RBCs form advanced glycation end products (AGEs), a heterogeneous group of chemically active compounds formed non-enzymatically through the reaction of reducing sugars, such as glucose, with the amino groups of free amino acids, peptides, and proteins.³¹⁻³² AGEs are cytotoxic compounds that may contribute to complications after RBC transfusion.³³ One study showed that the AGEs formed on the surface of stored RBCs can induce reactive oxygen species in human pulmonary microvascular endothelial cells through its receptor and thereby damage the endothelial cells.³²

The RBC has a 6-8 μm diameter biconcave disk shape with a volume of ~ 90 fL and undergoes morphological and physiological changes in membrane during storage.³⁴ The RBC membrane contains approximately 52% protein, 40% lipid and 8% carbohydrate.³⁵

It is required to maintain a certain level of ATP to preserve cell membrane integrity and cell functions.²⁵ The membrane is a semipermeable lipid bilayer supported by a protein cytoskeleton which maintains a critical role in two important RBC characteristics: deformability and permeability. The membranes of RBCs are larger than is necessary to contain their volume. The extra membrane makes RBCs flexible and deformable when they have to squeeze through small capillaries. However, RBCs tend to change from subtly bumpy discs to grossly bumpy spheres called spherocytosis during storage.³⁶ Thus, they have a smaller surface area through which oxygen and carbon dioxide can be exchanged and a higher osmotic fragility, which means when placed in water, they are more likely to burst, or lyse. This change, as well as decreasing ATP and 2,3-DPG levels, are generally reversible when the cells are in a warm, neutral pH, and nutrient-rich environment, such as under rejuvenation³⁷ or transfusion back to the human. Rejuvenation is a treatment in which a unit (bag) of stored RBCs are processed with 50 mL of the FDA-approved solution Rejuvesol (enCyte Systems, Braintree, Mass.) containing the substrates inosine, adenine, phosphate and pyruvate, and incubated in a 37°C water bath for 60 minutes. This treatment is currently approved for CPD/AS-1 RBCs within the 42-day storage period, but is not approved for same-day transfusion after rejuvenation. Thus, CPD/AS-1 RBCs are centrifuged to separate the rejuvenating solution, immediately prepared with a 40% glycerol solution and stored at -80°C for up to 3 years, and deglycerolized and washed before transfusion. This complicated freeze-thaw-wash

cycle has been used for long-term storage of RBCs from donors with rare or unusual phenotypes.³⁸

However, some changes that occur on RBC membranes during storage are irreversible. Phosphatidylserine (PS) exposure on the outer membrane surface is one of these changes.³⁹ PS is normally asymmetrically distributed on the inner membrane leaflet of RBC. When PS appears on the outer membrane, it promotes thrombin production and serves as a common recognition signal for clearance of stored RBC by macrophage from blood stream after transfusion.⁴⁰⁻⁴¹ In addition, RBCs tend to lose their membrane by shedding microparticles and therefore become more rigid and less flexible after 2 weeks of storage. The lipid microparticles, measuring 80 to 200 nm, are the lost membrane from the tips of the echinocytic spines and also contain high levels of exposed PS.⁴²

1.4 Vascular Effect of RBCs in Storage

Despite the long and slow development and improvement, RBC storage lesions still exist and may cause adverse events when transfused. Specifically, clinical studies have shown that increased morbidity and mortality is associated with the age of stored RBCs (often described as > 14-21 days) transfused.⁴³⁻⁴⁴ A study showed that cardiovascular patients who received older blood (median duration of storage = 20 days) had higher rates of in-hospital mortality (2.8% vs. 1.7%, P = 0.004, n = 6002 patients) as well as prolonged

intubation, renal failure and sepsis compared with those who received newer blood (median duration of storage = 11 days).⁴⁵

Recently, Roback *et al.* proposed a hypothesis about insufficient nitric oxide bioavailability (INOBA) to explain the increased morbidity and mortality observed in some patients after RBC transfusion.⁴⁶ It is proposed that nitric oxide (NO) levels in the vascular beds are markedly reduced, resulting in inappropriate vasoconstriction, decreased local blood flow, and insufficient oxygen delivery to end organs. It was discovered in the late 1980s that NO participates in vasodilation⁴⁷ by inducing rises in cyclic guanine monophosphate (cGMP) inside the smooth muscle⁴⁸ which, as a regulator of ion channel conductance, results in smooth muscle relaxation.⁴⁹

The concept of INOBA associated with the transfusion of stored RBCs is of particular interest to our group and others due to a wealth of literature describing the RBC as a determinant of blood flow.⁵⁰⁻⁵² RBCs can control local blood flow through the regulation of local NO concentration (figure 1.3). First, the RBC itself is able to release NO when oxygen tension is low.⁵³ NO is originally secreted from endothelial cells⁵⁴ and occasionally binds to the sulfur atoms on cysteine β -93 of Hb (SNO).⁵⁵ This SNO bond is so unstable that NO may be released during Hb deoxygenation. One study showed that the SNO-Hb in stored RBCs decreased rapidly to 1/5 of the fresh SNO-Hb levels 3 hours

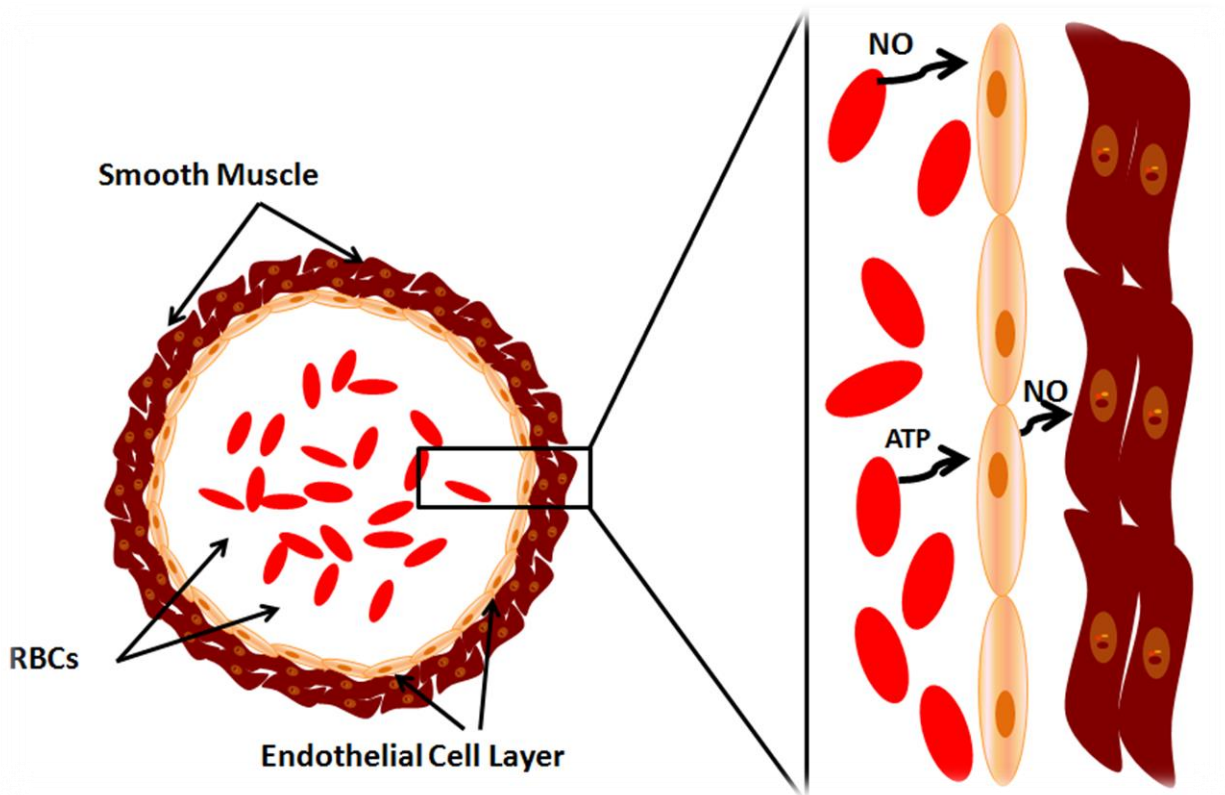


Figure 1.3 – Cross Section of a Blood Vessel and Proposed RBC-Mediated Vasodilation Mechanism. The blood components, such as RBCs, flow in the inner most core through the vessel. The endothelium lines the inner layer of the vessel interacting with blood. Outside of endothelial cells, there are thick layers of smooth muscle cells that are responsible for the expansion and contraction of the vessel. Vasodilation can be mediated by direct RBC-derived NO or endothelium-derived NO stimulated by RBC-derived ATP. For interpretation of the references to color in this and all other figures, the reader is referred to the electronic version of this dissertation.

after collection. Vasodilation by these cells was also significantly reduced.⁵⁶ However, this model has been debated due to another study using a mouse model expressing human Hb in which the β -cys93 residue was replaced, therefore inhibiting SNO-Hb synthesis, did not affect isolated RBC-dependent hypoxic vasodilation.⁵⁷

In another proposed mechanism related to INOBA, Gladwin *et al.* proposed that deoxygenated Hb can act as a nitrite reductase, reducing plasma nitrite to NO and producing SNO-Hb as well.⁵⁸ Several studies have provided evidence to support this mechanism: arteriovenous gradients in nitrite⁵⁹ and increased blood flow resulting from the addition of nitrite *in vivo*⁶⁰ were observed. However, there is a debate about the RBC-derived NO mechanism: NO, a short-lived free radical molecule, may not be able to diffuse from Hb to plasma, through an endothelial layer, and to the underlying smooth muscle.⁶¹

A third mechanism is proposed describing the RBC-mediated vasodilation through the release of ATP, which binds to purinergic receptors on the endothelium, activating endothelial nitric oxide synthase (eNOS) to produce NO, which is then able to diffuse to the smooth muscle.⁶²⁻⁶³ The RBC is capable of releasing ATP in response to flow-induced deformation,⁶⁴⁻⁶⁵ hypoxia,⁶⁶⁻⁶⁷ pharmaceutical stimuli like hydroxyurea,⁶⁸ and such small peptides as C-peptide.⁶⁹ This physiologically meaningful level of ATP released

from RBCs is known to be an active process, as opposed to cell lysis.⁷⁰⁻⁷¹ Endothelium-derived NO does not have to pass through a single layer of endothelial cells, which is more efficient and practical for NO to diffuse to muscle cells. Interestingly, some researchers have shown that the addition of nitrite can also induce the release of ATP from RBCs,⁷²⁻⁷³ which debates the evidence shown in the second mechanism.

Hb can also scavenge endothelium-derived NO by binding to β -93 cysteines.⁵⁴ In normal circulation, RBCs are mostly centered in the middle of the blood vessel, thereby forming a RBC-free zone close to the endothelium layer due to Fåhræus effect.⁷⁴ In addition, NO uptake by intact RBCs is \sim 333 times slower than by RBC microparticles, whereas uptake by RBC microparticles is \sim 3 times slower than cell-free Hb.⁷⁵ However, when microparticles and free Hb are present in a stored RBC suspension, scavenging of this NO becomes physiologically critical and may lead to adverse vascular effects.

1.5 Hyperglycemic Condition in Current Storage

Many RBC storage lesions, such as reduced deformability,⁵⁶ oxidative stress,⁷⁶ and advanced glycation endproducts (AGEs),³² also occur in the RBCs obtained from people with diabetes, even without storage.⁷⁷⁻⁷⁹ It would be premature to assume that the RBC storage lesions and diabetic complications have the same origin; however, an

examination of the processing solutions used to prepare RBCs for storage reveals a very interesting environment into which collection and storage occur.

As mentioned before, the mature RBC relies on the breakdown of glucose to maintain viability. Thus, glucose is indispensable in the storage solution. In order to provide enough “food” for RBCs in 6 week storage, researchers usually calculate the amount by considering the concept as how many grams or how many moles of glucose will be needed, as 3-4 millimoles of glucose are consumed per bag of RBCs during 5-6 weeks of storage.²⁶ However, when this concept translated to concentration, high millimolar concentrations of glucose exist in each solution, as shown in table 1.2.¹ CPD was originally designed as a whole blood storage solution for 3 weeks, and therefore it contains 8 millimoles of glucose in 63 mL for a 450 mL whole blood collection. For RBC storage, RBCs are separated from other components and some glucose is lost during this procedure. However, 100 mL of additive solution, such as AS-1 that contains glucose at a concentration of ~ 111 mM, was then added into 220 mL of packed RBCs. Thus, the estimated final glucose concentration is > 40 mM. To give this value some perspective, keep in mind that a normoglycemic, healthy individual has a bloodstream glucose level between 4 and 6 mM.⁸⁰ In short, the glucose concentrations in the collection and storage solutions are nearly an order of magnitude higher than a healthy individual and may adversely affect the stored RBC.

Table 1.2 – Content of Current Anticoagulant Solutions and Additive Solutions

Constituents (mM)	CPD	AS-1	AS-5	CP2D	AS-3
Sodium citrate	101.9	-	-	101.9	23
Monobasic sodium phosphate	16.1	-	-	16.1	23
Citric acid	15.6	-	-	15.6	2
Dextrose	129	111	45	258	55
Sodium chloride	-	154	150	-	70
Adenine	-	2	2.2	-	2
Mannitol	-	41	-	-	45.5
Anti-coagulant	-	CPD	CPD	-	CP2D

REFERENCES

REFERENCES

1. Hillyer, C. D., *Blood Banking and Transfusion Medicine: Basic Principles & Practice*. 2nd ed.; Philadelphia, PA : Churchill Livingstone/Elsevier: 2007.
2. Whitaker, B. I. *2011 National Blood Collection and Utilization Survey*; American Association of Blood Banks, 2011.
3. Rubin, O.; Crettaz, D.; Tissot, J. D.; Lion, N., Pre-Analytical and Methodological Challenges in Red Blood Cell Microparticle Proteomics. *Talanta* 2010, *82* (1), 1-8.
4. Hess, J. R., An Update on Solutions for Red Cell Storage. *Vox Sanguinis* 2006, *91* (1), 13-19.
5. Rous, P.; Turner, J. R., The Preservation of Living Red Blood Cells in Vitro : I. Methods of Preservation. *The Journal of Experimental Medicine* 1916, *23* (2), 219-237.
6. Robertson, O. H., Transfusion with Preserved Red Blood Cells. *British Medical Journal* 1918, *1* (2999), 691-695.
7. Mollison, P. L., The Introduction of Citrate as an Anticoagulant for Transfusion and of Glucose as a Red Cell Preservative. *British Journal of Haematology* 2000, *108* (1), 13-18.
8. Loutit, J. F.; Mollison, P. L., Disodium-Citrate-Glucose Mixture as a Blood Preservative. *British Medical Journal* 1943, *2* (4327), 744-745.
9. Carmen, R., The Selection of Plastic Materials for Blood Bags. *Transfusion Medicine Reviews* 1993, *7* (1), 1-10.
10. Hill, H. R.; Oliver, C. K.; Lippert, L. E.; Greenwalt, T. J.; Hess, J. R., The Effects of Polyvinyl Chloride and Polyolefin Blood Bags on Red Blood Cells Stored in a New Additive Solution. *Vox Sanguinis* 2001, *81* (3), 161-166.
11. Gibson, J. G., 2nd; Rees, S. B.; Mc, M. T.; Scheitlin, W. A., A Citrate-Phosphatedextrose Solution for the Preservation of Human Blood. *American Journal of Clinical Pathology* 1957, *28* (6), 569-578.
12. Gibson, J. G., 2nd; Gregory, C. B.; Button, L. N., Citrate-Phosphate-Dextrose Solution for Preservation of Human Blood: A Further Report. *Transfusion* 1961, *1*, 280-287.
13. Orlina, A. R.; Josephson, A. M., Comparative Viability of Blood Stored in Acid and Cpd. *Transfusion* 1969, *9* (2), 62-69.

14. Nakao, K.; Nagano, K.; Kamiyama, T.; Wada, T.; Nakao, M., A Direct Relationship between Adenosine Triphosphate-Level and in Vivo Viability of Erythrocytes. *Nature* 1962, *194* (4831), 877-&.
15. Zuck, T. F.; Bensinger, T. A.; Peck, C. C.; Chillar, R. K.; Beutler, E.; Button, L. N.; McCurdy, P. R.; Josephson, A. M.; Greenwalt, T. J., The in Vivo Survival of Red Blood Cells Stored in Modified Cpd with Adenine: Report of a Multi-Institutional Cooperative Effort. *Transfusion* 1977, *17* (4), 374-382.
16. Moore, G. L.; Ledford, M. E.; Brooks, D. E., Distribution and Utilization of Adenine in Red Blood-Cells During 42 Days of 4c Storage. *Transfusion* 1978, *18* (5), 538-545.
17. Moore, G. L.; Ledford, M. E.; Peck, C. C., The in Vitro Evaluation of Modifications in Cpd-Adenine Anticoagulated-Preserved Blood at Various Hematocrits. *Transfusion* 1980, *20* (4), 419-426.
18. Moore, G. L., Additive Solutions for Better Blood Preservation. *Critical Reviews in Clinical Laboratory Sciences* 1987, *25* (3), 211-229.
19. Hogman, C. F.; Hedlund, K.; Akerblom, O.; Venge, P., Red Blood Cell Preservation in Protein-Poor Media. I. Leukocyte Enzymes as a Cause of Hemolysis. *Transfusion* 1978, *18* (2), 233-241.
20. Odeberg, H.; Olsson, I.; Venge, P., Cationic Proteins of Human Granulocytes. Iv. Esterase Activity. *Laboratory Investigation; a Journal of Technical Methods and Pathology* 1975, *32* (1), 86-90.
21. Ohlsson, K.; Olsson, I., The Neutral Proteases of Human Granulocytes. Isolation and Partial Characterization of Two Granulocyte Collagenases. *European Journal of Biochemistry / FEBS* 1973, *36* (2), 473-481.
22. Hogman, C. F.; Hedlund, K.; Sahlestrom, Y., Red Cell Preservation in Protein-Poor Media. Iii. Protection against in Vitro Hemolysis. *Vox Sanguinis* 1981, *41* (5-6), 274-281.
23. Sparrow, R. L., Time to Revisit Red Blood Cell Additive Solutions and Storage Conditions: A Role for "Omics" Analyses. *Blood Transfusion = Trasfusione del sangue* 2012, *10 Suppl 2*, s7-11.
24. Hogman, C. F.; Eriksson, L.; Hedlund, K.; Wallvik, J., The Bottom and Top System: A New Technique for Blood Component Preparation and Storage. *Vox Sanguinis* 1988, *55* (4), 211-217.
25. Hogman, C. F., Preparation and Preservation of Red Cells. *Vox Sanguinis* 1998, *74 Suppl 2*, 177-187.
26. Hess, J. R., Red Cell Changes During Storage. *Transfusion and Apheresis Science* 2010, *43* (1), 51-59.

27. Hess, J. R., Red Cell Storage. *Journal of Proteomics* 2010, 73 (3), 368-373.
28. Beutler, E.; Wood, L., The in Vivo Regeneration of Red Cell 2,3 Diphosphoglyceric Acid (Dpg) after Transfusion of Stored Blood. *The Journal of Laboratory and Clinical Medicine* 1969, 74 (2), 300-304.
29. Meshalkin, E. N.; Vlasov Iu, A.; Shishkina, T. N.; Okuneva, G. N.; Pinegin, S. L., [Blood Oxygen Saturation in Various Regions of the Circulatory System in Healthy Persons]. *Kardiologiya* 1982, 22 (11), 45-49.
30. Dumaswala, U. J.; Wilson, M. J.; Wu, Y. L.; Wykle, J.; Zhuo, L.; Douglass, L. M.; Daleke, D. L., Glutathione Loading Prevents Free Radical Injury in Red Blood Cells after Storage. *Free Radical Research* 2000, 33 (5), 517-529.
31. Anderson, M. M.; Heinecke, J. W., Production of N(Epsilon)-(Carboxymethyl)Lysine Is Impaired in Mice Deficient in NADPH Oxidase: A Role for Phagocyte-Derived Oxidants in the Formation of Advanced Glycation End Products During Inflammation. *Diabetes* 2003, 52 (8), 2137-2143.
32. Mangalmurti, N. S.; Chatterjee, S.; Cheng, G.; Andersen, E.; Mohammed, A.; Siegel, D. L.; Schmidt, A. M.; Albelda, S. M.; Lee, J. S., Advanced Glycation End Products on Stored Red Blood Cells Increase Endothelial Reactive Oxygen Species Generation through Interaction with Receptor for Advanced Glycation End Products. *Transfusion* 2010, 50 (11), 2353-2361.
33. Lysenko, L.; Mierzchala, M.; Gamian, A.; Durek, G.; Kubler, A.; Kozlowski, R.; Sliwinski, M., The Effect of Packed Red Blood Cell Storage on Arachidonic Acid and Advanced Glycation End-Product Formation. *Archivum Immunologiae et Therapiae Experimentalis* 2006, 54 (5), 357-362.
34. Shohet, S. B.; Haley, J. E., Red Cell Membrane Shape and Stability: Relation to Cell Lipid Renewal Pathways and Cell ATP. *Nouvelle Revue Francaise d'Hematologie* 1972, 12 (6), 761-770.
35. Mohandas, N.; Evans, E., Mechanical Properties of the Red Cell Membrane in Relation to Molecular Structure and Genetic Defects. *Annual Review of Biophysics and Biomolecular Structure* 1994, 23, 787-818.
36. Hogman, C. F.; de Verdier, C. H.; Ericson, A.; Hedlund, K.; Sandhagen, B., Studies on the Mechanism of Human Red Cell Loss of Viability During Storage at +4 Degrees C in Vitro. I. Cell Shape and Total Adenylate Concentration as Determinant Factors for Posttransfusion Survival. *Vox Sanguinis* 1985, 48 (5), 257-268.
37. Lockwood, W. B.; Hudgens, R. W.; Szymanski, I. O.; Teno, R. A.; Gray, A. D., Effects of Rejuvenation and Frozen Storage on 42-Day-Old as-3 Rbcs. *Transfusion* 2003, 43 (11), 1527-1532.

38. Valeri, C. R.; Ragno, G., Cryopreservation of Human Blood Products. *Transfusion and Apheresis Science : Official Journal of the World Apheresis Association : Official Journal of the European Society for Haemapheresis* 2006, *34* (3), 271-287.
39. Lu, C.; Shi, J.; Yu, H.; Hou, J.; Zhou, J., Procoagulant Activity of Long-Term Stored Red Blood Cells Due to Phosphatidylserine Exposure. *Transfusion Medicine* 2011, *21* (3), 150-157.
40. Boas, F. E.; Forman, L.; Beutler, E., Phosphatidylserine Exposure and Red Cell Viability in Red Cell Aging and in Hemolytic Anemia. *Proceedings of the National Academy of Sciences of the United States of America* 1998, *95* (6), 3077-3081.
41. Zwaal, R. F.; Comfurius, P.; Bevers, E. M., Lipid-Protein Interactions in Blood Coagulation. *Biochimica et Biophysica Acta* 1998, *1376* (3), 433-453.
42. Laczko, J.; Szabolcs, M.; Jona, I., Vesicle Release from Erythrocytes During Storage and Failure of Rejuvenation to Restore Cell Morphology. *Haematologia* 1985, *18* (4), 233-248.
43. Tinmouth, A.; Chin-Yee, I., The Clinical Consequences of the Red Cell Storage Lesion. *Transfusion Medicine Reviews* 2001, *15* (2), 91-107.
44. Ho, J.; Sibbald, W. J.; Chin-Yee, I. H., Effects of Storage on Efficacy of Red Cell Transfusion: When Is It Not Safe? *Critical Care Medicine* 2003, *31* (12 Suppl), S687-697.
45. Koch, C. G.; Li, L.; Sessler, D. I.; Figueroa, P.; Hoeltge, G. A.; Mihaljevic, T.; Blackstone, E. H., Duration of Red-Cell Storage and Complications after Cardiac Surgery. *The New England Journal of Medicine* 2008, *358* (12), 1229-1239.
46. Roback, J. D.; Neuman, R. B.; Quyyumi, A.; Sutliff, R., Insufficient Nitric Oxide Bioavailability: A Hypothesis to Explain Adverse Effects of Red Blood Cell Transfusion. *Transfusion* 2011, *51* (4), 859-866.
47. Ignarro, L. J.; Buga, G. M.; Wood, K. S.; Byrns, R. E.; Chaudhuri, G., Endothelium-Derived Relaxing Factor Produced and Released from Artery and Vein Is Nitric Oxide. *Proceedings of the National Academy of Sciences of the United States of America* 1987, *84* (24), 9265-9269.
48. Ignarro, L. J.; Byrns, R. E.; Buga, G. M.; Wood, K. S., Endothelium-Derived Relaxing Factor from Pulmonary Artery and Vein Possesses Pharmacologic and Chemical Properties Identical to Those of Nitric Oxide Radical. *Circulation Research* 1987, *61* (6), 866-879.
49. Carvajal, J. A.; Germain, A. M.; Huidobro-Toro, J. P.; Weiner, C. P., Molecular Mechanism of Cgmp-Mediated Smooth Muscle Relaxation. *Journal of Cellular Physiology* 2000, *184* (3), 409-420.

50. Allen, B. W.; Piantadosi, C. A., How Do Red Blood Cells Cause Hypoxic Vasodilation? The Sno-Hemoglobin Paradigm. *The American Journal of Physiology - Heart and Circulatory Physiology* 2006, *291* (4), H1507-H1512.
51. Ellsworth, M. L., Red Blood Cell-Derived Atp as a Regulator of Skeletal Muscle Perfusion. *Medicine and Science in Sports and Exercise* 2004, *36* (1), 35-41.
52. Sprague, R. S.; Ellsworth, M. L.; Stephenson, A. H.; Lonigro, A. J., Atp: The Red Blood Cell Link to No and Local Control of the Pulmonary Circulation. *The American Journal of Physiology - Heart and Circulatory Physiology* 1996, *271* (6), H2717-H2722.
53. Bhatia, S. N.; Balis, U. J.; Yarmush, M. L.; Toner, M., Effect of Cell-Cell Interactions in Preservation of Cellular Phenotype: Cocultivation of Hepatocytes and Nonparenchymal Cells. *Faseb J* 1999, *13* (14), 1883-1900.
54. Bohlen, H. G.; Zhou, X.; Unthank, J. L.; Miller, S. J.; Bills, R., Transfer of Nitric Oxide by Blood from Upstream to Downstream Resistance Vessels Causes Microvascular Dilation. *The American Journal of Physiology - Heart and Circulatory Physiology* 2009, *297* (4), H1337-1346.
55. Stamler, J. S.; Simon, D. I.; Osborne, J. A.; Mullins, M. E.; Jaraki, O.; Michel, T.; Singel, D. J.; Loscalzo, J., S-Nitrosylation of Proteins with Nitric Oxide: Synthesis and Characterization of Biologically Active Compounds. *Proceedings of the National Academy of Sciences of the United States of America* 1992, *89* (1), 444-448.
56. Bennett-Guerrero, E.; Veldman, T. H.; Doctor, A.; Telen, M. J.; Ortel, T. L.; Reid, T. S.; Mulherin, M. A.; Zhu, H.; Buck, R. D.; Califf, R. M.; McMahan, T. J., Evolution of Adverse Changes in Stored Rbcs. *Proceedings of the National Academy of Sciences of the United States of America* 2007, *104* (43), 17063-17068.
57. Isbell, T. S.; Sun, C. W.; Wu, L. C.; Teng, X.; Vitturi, D. A.; Branch, B. G.; Kevil, C. G.; Peng, N.; Wyss, J. M.; Ambalavanan, N.; Schwiebert, L.; Ren, J.; Pawlik, K. M.; Renfrow, M. B.; Patel, R. P.; Townes, T. M., Sno-Hemoglobin Is Not Essential for Red Blood Cell-Dependent Hypoxic Vasodilation. *Nature Medicine* 2008, *14* (7), 773-777.
58. Lundberg, J. O.; Weitzberg, E.; Gladwin, M. T., The Nitrate-Nitrite-Nitric Oxide Pathway in Physiology and Therapeutics. *Nature reviews. Drug Discovery* 2008, *7* (2), 156-167.
59. Lauer, T.; Preik, M.; Rassaf, T.; Strauer, B. E.; Deussen, A.; Feelisch, M.; Kelm, M., Plasma Nitrite Rather Than Nitrate Reflects Regional Endothelial Nitric Oxide Synthase Activity but Lacks Intrinsic Vasodilator Action. *Proceedings of the National Academy of Sciences of the United States of America* 2001, *98* (22), 12814-12819.
60. Cosby, K.; Partovi, K. S.; Crawford, J. H.; Patel, R. P.; Reiter, C. D.; Martyr, S.; Yang, B. K.; Waclawiw, M. A.; Zalos, G.; Xu, X.; Huang, K. T.; Shields, H.; Kim-Shapiro, D. B.;

Schechter, A. N.; Cannon, R. O., 3rd; Gladwin, M. T., Nitrite Reduction to Nitric Oxide by Deoxyhemoglobin Vasodilates the Human Circulation. *Nature Medicine* 2003, 9 (12), 1498-1505.

61. Hakim, T. S.; Sugimori, K.; Camporesi, E. M.; Anderson, G., Half-Life of Nitric Oxide in Aqueous Solutions with and without Haemoglobin. *Physiological Measurement* 1996, 17 (4), 267-277.

62. Huh, D.; Hamilton, G. A.; Ingber, D. E., From 3d Cell Culture to Organs-on-Chips. *Trends in Cell Biology* 2011, 21 (12), 745-754.

63. Ellsworth, M. L.; Ellis, C. G.; Goldman, D.; Stephenson, A. H.; Dietrich, H. H.; Sprague, R. S., Erythrocytes: Oxygen Sensors and Modulators of Vascular Tone. *Physiology (Bethesda)* 2009, 24, 107-116.

64. Price, A. K.; Fischer, D. J.; Martin, R. S.; Spence, D. M., Deformation-Induced Release of Atp from Erythrocytes in a Poly(Dimethylsiloxane)-Based Microchip with Channels That Mimic Resistance Vessels. *Analytical Chemistry* 2004, 76 (16), 4849-4855.

65. Edwards, J.; Sprung, R.; Sprague, R.; Spence, D., Chemiluminescence Detection of Atp Release from Red Blood Cells Upon Passage through Microbore Tubing. *The Analyst* 2001, 126 (8), 1257-1260.

66. Ellsworth, M. L., The Red Blood Cell as an Oxygen Sensor: What Is the Evidence? *Acta Physiologica Scandinavica* 2000, 168 (4), 551-559.

67. Bergfeld, G. R.; Forrester, T., Release of Atp from Human Erythrocytes in Response to a Brief Period of Hypoxia and Hypercapnia. *Cardiovascular Research* 1992, 26 (1), 40-47.

68. Raththagala, M.; Karunaratne, W.; Kryziniak, M.; McCracken, J.; Spence, D. M., Hydroxyurea Stimulates the Release of Atp from Rabbit Erythrocytes through an Increase in Calcium and Nitric Oxide Production. *European Journal of Pharmacology* 2010, 645 (1-3), 32-38.

69. Meyer, J. A.; Froelich, J. M.; Reid, G. E.; Karunaratne, W. K. A.; Spence, D. M., Metal-Activated C-Peptide Facilitates Glucose Clearance and the Release of a Nitric Oxide Stimulus Via the Glut1 Transporter. *Diabetologia* 2008, 51 (1), 175-182.

70. Sprague, R. S.; Ellsworth, M. L.; Stephenson, A. H.; Kleinhenz, M. E.; Lonigro, A. J., Deformation-Induced Atp Release from Red Blood Cells Requires Cftr Activity. *The American Journal of Physiology - Heart and Circulatory Physiology* 1998, 275 (5), H1726-H1732.

71. Sprague, R. S.; Ellsworth, M. L.; Stephenson, A. H.; Lonigro, A. J., Participation of Camp in a Signal-Transduction Pathway Relating Erythrocyte Deformation to Atp Release. *American journal of physiology. Cell Physiology* 2001, *281* (4), C1158-1164.
72. Garcia, J. I.; Seabra, A. B.; Kennedy, R.; English, A. M., Nitrite and Nitroglycerin Induce Rapid Release of the Vasodilator Atp from Erythrocytes: Relevance to the Chemical Physiology of Local Vasodilation. *Journal of Inorganic Biochemistry* 2010, *104* (3), 289-296.
73. Cao, Z.; Bell, J. B.; Mohanty, J. G.; Nagababu, E.; Rifkind, J. M., Nitrite Enhances Rbc Hypoxic Atp Synthesis and the Release of Atp into the Vasculature: A New Mechanism for Nitrite-Induced Vasodilation. *The American Journal of Physiology - Heart and Circulatory Physiology* 2009, *297* (4), H1494-1503.
74. Fahraeus, R., The Suspension Stability of the Blood. *Physiological Reviews* 1929, *9* (2), 241-274.
75. Azarov, I.; Liu, C.; Reynolds, H.; Tsekouras, Z.; Lee, J. S.; Gladwin, M. T.; Kim-Shapiro, D. B., Mechanisms of Slower Nitric Oxide Uptake by Red Blood Cells and Other Hemoglobin-Containing Vesicles. *The Journal of Biological Chemistry* 2011, *286* (38), 33567-33579.
76. Lee, J. S.; Gladwin, M. T., Bad Blood: The Risks of Red Cell Storage. *Nature Medicine* 2010, *16* (4), 381-382.
77. Wautier, J. L.; Wautier, M. P.; Schmidt, A. M.; Anderson, G. M.; Hori, O.; Zoukourian, C.; Capron, L.; Chappey, O.; Yan, S. D.; Brett, J.; et al., Advanced Glycation End Products (Ages) on the Surface of Diabetic Erythrocytes Bind to the Vessel Wall Via a Specific Receptor Inducing Oxidant Stress in the Vasculature: A Link between Surface-Associated Ages and Diabetic Complications. *Proceedings of the National Academy of Sciences of the United States of America* 1994, *91* (16), 7742-7746.
78. Rattan, V.; Shen, Y.; Sultana, C.; Kumar, D.; Kalra, V. K., Diabetic Rbc-Induced Oxidant Stress Leads to Transendothelial Migration of Monocyte-Like HL-60 Cells. *The American Journal of Physiology* 1997, *273* (2 Pt 1), E369-375.
79. Brown, C. D.; Ghali, H. S.; Zhao, Z.; Thomas, L. L.; Friedman, E. A., Association of Reduced Red Blood Cell Deformability and Diabetic Nephropathy. *Kidney International* 2005, *67* (1), 295-300.
80. Engelgau, M. M.; Narayan, K. M.; Herman, W. H., Screening for Type 2 Diabetes. *Diabetes Care* 2000, *23* (10), 1563-1580.

Chapter 2 – Flow-Induced Adenosine Triphosphate Release from Red Blood Cells Stored in Hyperglycemic and Normoglycemic Storage Solutions

2.1 Red Blood Cell-Derived ATP

Human blood is composed of blood cells suspended in plasma. The blood plasma is mostly water containing components such as protein, glucose, inorganic salts, and carbon dioxide.¹ The blood cells are mainly erythrocytes (also called red blood cells, RBCs), leukocytes (also called white blood cells), and platelets. The primary function of the human RBC is to deliver oxygen to the tissues and to carry carbon dioxide from the plasma back to the lungs. The function of oxygen transport, as well as the preservation of the constituents of the RBC in an active form and the maintenance of ionic gradients across the cell membrane, all require the expenditure of metabolic energy.² Mature human RBCs lack nuclei and mitochondria, and therefore, they have to rely on anaerobic glycolysis to produce adenosine triphosphate (ATP) and maintain their viability. The breakdown of each glucose molecule to two lactate molecules provides a net gain of two ATP molecules, which is less efficient than glycolysis under aerobic condition.³

In addition to oxygen transport, RBCs have also been shown to release micromolar levels of ATP, a known stimulus of endothelium-derived nitric oxide (NO), in response to low levels of oxygen (hypoxia).⁴ This NO can function to relax the smooth muscle cells surrounding circulatory vessels, thereby increasing blood flow and oxygen delivery to hypoxic tissue. Furthermore, there are other modes of inducing ATP release from intact

RBCs, including lowering pH,⁵ changes to osmotic pressure,⁶ pharmaceutical stimuli, such as hydroxyurea,⁷ and small peptides, such as C-peptide.⁸

Mechanical deformation of RBCs has been also reported to stimulate the release of ATP.⁹⁻¹¹ Blood starts its flow from the heart through the arteries, arterioles and ultimately capillaries, where RBCs exchange oxygen for carbon dioxide. Arterioles and capillaries, having inside diameters of 25-100 and 5-25 μm , respectively, allow the rapid diffusion of oxygen and nutrients to tissues. These blood vessels are classified as resistance vessels, where RBCs undergo shear stress when they traverse through. Due to the resistance to flow, blood hematocrit (Hct) can be reduced from 40-45% to less than 10% in resistance vessels.¹² The flow-induced ATP release from RBCs can stimulate endothelium-derived NO and therefore dilate the vessel to improve blood flow to the area.

The mechanism for this ATP release from RBCs was proposed by Sprague *et al.* (figure 2.1). This signal transduction pathway involves the mechanical deformation of the RBC which induces a series of conformational changes in the G-protein coupled receptor (GPCR) that binds to and activates heterotrimeric G proteins.¹³⁻¹⁴ G-proteins then activate adenylate cyclase (AC) to produce cyclic adenosine monophosphate (cAMP) through the activation of cAMP-dependent protein kinase A (PKA). The cystic fibrosis transmembrane conductance regulator protein (CFTR) then becomes phosphorylated

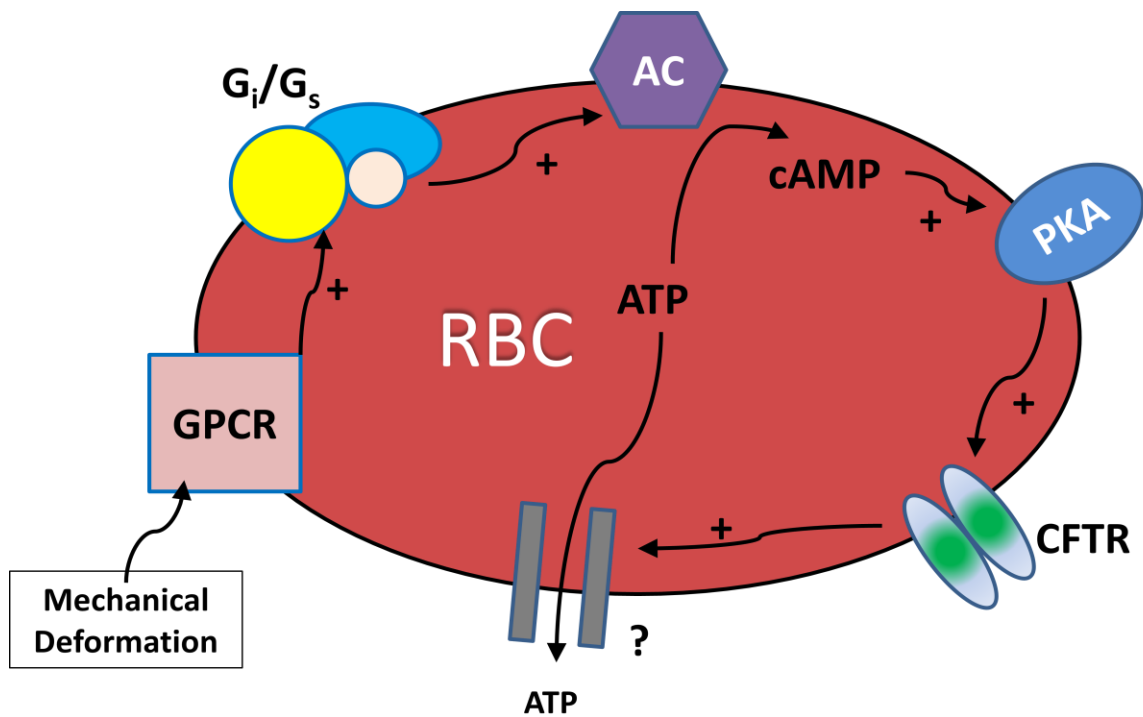


Figure 2.1 – Proposed Signal Transduction Pathway for Regulated ATP Release from RBCs in Response to Mechanical Deformation. Conformational changes of GPCR results in activation of the heterotrimeric G protein, leading to activation of AC and production of cAMP; further with the activation of cAMP-dependent PKA, the CFTR protein becomes phosphorylated and thereby regulates ATP release through the plasma membrane via ion channels. For interpretation of the references to color in this and all other figures, the reader is referred to the electronic version of this dissertation.

and regulates the passage of ATP through the plasma membrane.¹⁵⁻¹⁶ However, it has not been proven that CFTR is the ion channel that ATP passes through; rather it facilitates the passage of ATP through another secondary ion channel. Other hypotheses of channel-mediated ATP release, including the pannexin 1 hemichannel,¹⁷ connexin 43 hemichannels,¹⁸ a volume-regulated channel,¹⁹ and the purinergic receptor P2X7.²⁰

Reduced ATP release from RBCs purified from whole blood of people with primary pulmonary hypertension²¹ and cystic fibrosis¹⁶ has been reported. Furthermore, our group and others have reported that the ATP release from the RBCs of people with type 2 diabetes is also significantly lower in comparison to healthy, non-diabetic controls.²²⁻

²³ Interestingly, RBC-derived ATP has also been shown to be altered during storage.

McMahon *et al.* reported that RBCs stored for longer than one week were incapable of releasing ATP in response to hypoxia and also concluded that methods to enhance ATP release from the RBCs during storage would be beneficial to patients receiving a transfusion.²⁴

Deformability, one of the important characteristics of the RBC, refers to the change of shape of the cell under applied stress, without lysis. The major determinants of deformability include cell geometry, cell shape, and internal viscosity. Decreased RBC deformability is recognized as one of the storage lesions, which refers to the biochemical and physical changes of RBCs during storage. Loss of this characteristic

prevents the RBC membrane from deforming, thereby impairing the ability of the RBC (6-8 μm in diameter) to traverse capillaries of similar or even smaller diameter (5-10 μm).²⁵

Elevated glucose levels have been shown to decrease RBC deformability. Traykov *et al.* reported that high glucose can increase RBC rigidity almost immediately upon incubation.²⁶ It was also shown that acute exposure of RBCs from healthy volunteers to physiologically high glucose level (20 mM) in phosphate buffered saline (PBS) for only 5 minutes at 37°C would result in a significant decrease in membrane deformability.²⁷

Furthermore, Riquelme *et al.* reported that high glucose concentrations (55-555 mM) caused significant reductions in the viscoelastic properties of the membrane and also increased RBC membrane fragility.²⁸ Resmi *et al.* demonstrated a correlation between glucose (5-45 mM), protein oxidation, and cellular deformability with increasing incubation time (24-48 hours).²⁹

These reports involving reduced RBC deformability are potentially important when one considers the normoglycemic conditions of the bloodstream in healthy donor and the glucose levels in the solutions used during the processing of whole blood for RBC storage. The bloodstream glucose concentration of a healthy individual is typically between 4 and 6 mM.³⁰ As discussed in chapter 1, the concentration of glucose in the current solutions used to collect (citrate-phosphate-dextrose, CPD) and store (additive

solution-1, AS-1) RBCs, respectively, are both well above 100 mM. Thus, a microflow system was employed to determine the ATP release ability of RBCs stored in hyperglycemic and normoglycemic conditions in response to mechanical deformation. In addition, lactic acid accumulation, extracellular glucose levels, and intracellular ATP levels of the RBCs were also determined in both storage conditions.

2.2 Experimental

2.2.1 Experimental Storage Solutions Preparation

All reagents were purchased from Sigma-Aldrich (St. Louis, MO) unless otherwise indicated. Distilled deionized water (DDW) with 18.2 M Ω resistance was used for all experiments. CPD and AS-1 solutions were prepared according to standard compositions found in the literature.³¹ Specifically, 100 mL of CPD were prepared containing 89.4 mM sodium citrate, 15.6 mM citric acid, 128.8 mM dextrose, and 16.1 mM monobasic sodium phosphate. For AS-1, 200 mL were typically prepared containing 154.0 mM sodium chloride, 41.2 mM mannitol, 1.8 mM adenine, and 111.1 mM dextrose. All reagents were prepared from solid forms and used as received without further purification. Normoglycemic versions of CPD and AS-1 (CPD-N and AS-1N, respectively) were prepared in a manner identical to CPD and AS-1, but with the glucose level at 5.5 mM (See table 2.1). AS-1 and AS-1N were adjusted pH to 5.8 using hydrochloric acid (HCl) to avoid caramelization during autoclaved sterilization. All solutions used in collection and storage were sterilized at 10 bar and 121°C prior to use.

2.2.2 Blood Collection and Storage

All blood was collected by venipuncture under IRB-approved protocol. The collection process (figure 2.2) consisted of preparing 6 non-siliconized and untreated (i.e., no heparin or other anticoagulant) 10 mL glass Vacutainer tubes (BD, Franklin Lakes NJ); 1 mL of CPD was injected into 3 of the tubes using a syringe, while the other 3 contained 1 mL of CPD-N. Next, approximately 7 mL of whole blood were collected into each tube, resulting in a total volume of 8 mL. The blood remained in the collection solutions for at least 30 minutes, allowing the anticoagulant to completely work, but not more than 2 hours at room temperature ($\sim 20^{\circ}\text{C}$), prior to processing. Whole blood processing consisted of centrifugation at 2000 *g* for 10 minutes followed by removal of the plasma and buffy coat layers by aspiration. Importantly, an additional 2-mm layer off the top of the packed RBCs was also removed to minimize leukocyte presence during subsequent storage in the AS-1 or AS-1N solutions. The purified RBCs from the 3 tubes containing CPD were then combined into a single 15 mL tube, followed by the addition of AS-1 such that the ratio of packed RBC to AS-1 was 2:1. The same protocol was followed for RBCs collected in CPD-N and stored in AS-1N. Finally, 2 mL of the RBCs (stored in the AS-1 or AS-1N) were added to PVC bags and stored at 4°C. Prior to use, the polyvinyl chloride (PVC) bags were sterilized under UV light overnight. The PVC bags were prepared in-house using rolled PVC (ULINE, pleasant prairie WI) and a heat sealer. All blood collection and storage processes were performed under sterile conditions.

Table 2.1 – Contents of CPD/AS-1 and CPD-N/AS-1N System

Constituents (mM)	CPD	AS-1	CPD-N	AS-1N
Sodium Citrate	101.9	-	101.9	101.9
Monobasic Sodium Phosphate	16.1	-	16.1	16.1
Citric Acid	15.6	-	15.6	15.6
Dextrose	129	111	5.5	5.5
Sodium Chloride	-	154	150	154
Adnine	-	2	2.2	2
Mannitol	-	41	-	41
pH	5.6	5.8	5.6	5.8

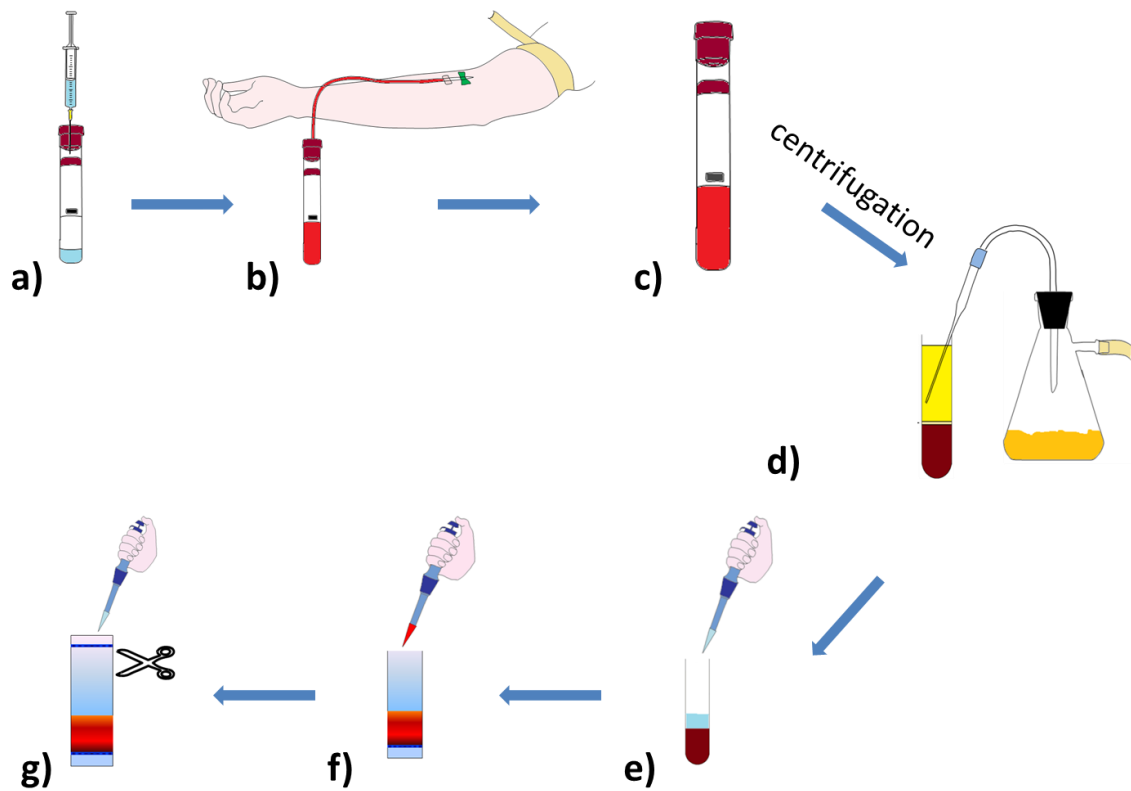


Figure 2.2 – The Miniaturized RBC Collection and Storage in Lab. a) Injection of 1 mL of CPD or CPD-N into non-additive 10 mL glass Vacutainer tube; b) Draw about 7 mL of whole blood from donor into each Vacutainer tube; c) Sit at room temperature for at least 30 minutes and up to 2 hours, then centrifuge at 2000 *g* for 10 minutes; d) Plasma and buffy coat were discarded, as well as top 2-mm layer of packed RBCs to avoid remaining white cells; e) AS or AS-N were added into packed red blood cells at the ratio of 1 to 2; f) 2 mL of mixed RBC concentrates were added into each PVC bag which was heat sealed and stored at 4°C; g) For normoglycemic one, blood bags were cut open and aliquot of glucose saline was added to feed RBCs every five days; bags were resealed and continued storing. All blood collection and storage processes were performed under sterile conditions. For interpretation of the references to color in this and all other figures, the reader is referred to the electronic version of this dissertation.

The RBCs stored in the normoglycemic AS-1N solution required periodic glucose feeding to provide enough nutrients for extended storage. These cells were “fed” by opening the PVC storage bag and adding a 20 μ L droplet of 400 mM glucose in saline to the RBCs, and then re-sealing the bag. The glucose saline was prepared by dissolving 0.72 g of dextrose in 10 mL of saline (a solution of 0.90% (weight/volume) of sodium chloride (NaCl)), in order to prevent cell lysis. This helped to maintain the glucose concentrations in the stored cells around 5 mM, while maintaining a constant volume into which the cells were stored.

2.2.3 Chemiluminescence Detection of ATP Release from RBCs in Flow-Based System

A 1000 μ M stock solution of ATP was prepared by dissolving 55 mg of ATP in 10 mL of DDW. ATP standards (0 – 1000 nM) were prepared by diluting aliquots of the stock ATP solution in AS-1 or AS-1N. To prepare the luciferin/luciferase (L/L) mixture required for the chemiluminescence determination of ATP, 2 mg of potassium luciferin (Gold Biotechnology, St. Louis, MO) were dissolved in 5 mL of DDW and then added to a vial containing firefly tail extract, which was used as the source of luciferase.

At various time points, one bag of each sample was removed from storage without interrupting the other samples. The Hct of samples were determined manually by collecting RBCs into microcapillary tubes, spinning in a microhematocrit centrifuge (CritSpin M960-22, StatSpin), and visually quantifying the percentage of packed red cells

using a microcapillary reader. For flow-induced ATP measurements involving RBCs, all RBC samples were diluted to 7% Hct in either AS-1 or AS-1N.

The measurement of flow-induced ATP release has been described previously.¹⁰ As shown in figure 2.3, to measure the ATP release, a 500 μ L syringe (Hamilton, Fisher Scientific) was filled with the L/L mixture described above. A second syringe was filled with either ATP standards (during calibration) or a 7% RBC solution (for measuring ATP release from the cells). Both solutions were pumped through 30 cm sections of microbore tubing with an internal diameter of 50 μ m (Polymicro Technologies, Phoenix, AZ) at a rate of 6.7 μ L/minute using a dual syringe pump (Harvard Apparatus, Boston, MA). The streams containing the L/L mixture and ATP standard, or 7% RBCs, combined at a mixing T-junction. The combined stream flowed through a segment (\sim 5 cm) of microbore tubing (i.d., 75 μ m) that had its polyimide coating removed, allowing for the detection of resultant chemiluminescent emission from the reaction using a photomultiplier tube (PMT, Hamamatsu Corporation, Hamamatsu, Japan) placed in a light excluding box. The ATP release from RBCs was measured soon (\sim 1-2 hours) after placement in the storage solutions (AS-1 or AS-1N) and weekly, through day 36 of storage. In order to account for any ATP already present in the sample prior to flow, an aliquot of the cells were centrifuged and supernatant analyzed for ATP. This value was subtracted from that obtained during the flow experiments to obtain a true value of the ATP that was released from the cells, as opposed to any ATP that was already present in the extracellular matrix.

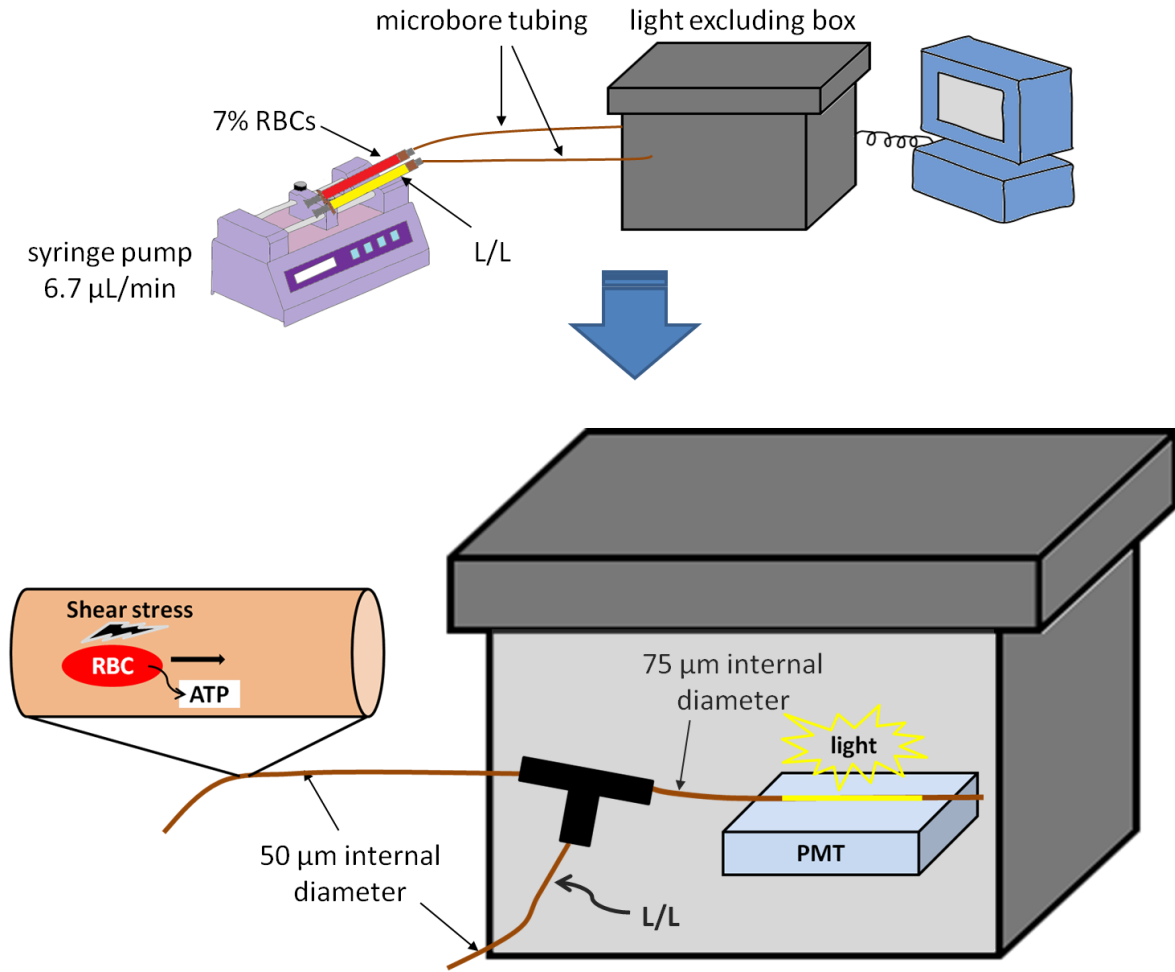


Figure 2.3 – Determination of Flow-Induced ATP Release from Stored RBCs using Microflow System. In dual syringe pump, one contained 7% RBCs, and the other contained luciferase/luciferin (L/L) solution. Both of them were pumped through microbore tubing at a rate of 6.7 µL/minute. RBCs flowed through the microbore tubing with an internal diameter of 50 µm resulting in ATP release into the solution, which met the L/L solution at a mixing T-junction. The combined stream was pumped through an additional segment of 75 µm internal diameter tubing, with a portion of the polyimide coating removed, over a PMT in a light excluding box. This allowed for the chemiluminescence (light) resulting from the reaction of ATP with L/L to be detected. For interpretation of the references to color in this and all other figures, the reader is referred to the electronic version of this dissertation.

2.2.4 Lactate Accumulation in Stored RBCs

Lactate that accumulated in the storage medium was measured to verify that RBCs are able to metabolize glucose normally under both conditions. This enzymatic reaction utilizes the oxidation of lactate to pyruvate while reducing nicotinamide adenine dinucleotide (NAD^+) to NADH. The protocol was modified from a previously described assay.³² The reaction mechanism and standard curve are shown in figure 2.4.

A 20 mM lactate stock solution was prepared by dissolving 18 mg L-lactic acid in 10 mL of DDW. Lactic acid, a weak acid with a pKa of 3.86, dissociates to lactate under the experimental circumstance. Standards of lactate ranging from 0-100 μM were prepared from the stock solution through a series of appropriate dilutions. The stock solution of NAD^+ was made by dissolving 50 mg of the solid with 1 mL of DDW, resulting in a final concentration of 50.2 mM. The L-lactic dehydrogenase (LDH) enzyme used in the assay was supplied already prepared in an ammonium sulfate suspension at ~ 8.62 units/ μL .

For the preliminary 16-day storage study, lactate accumulation was determined. In the experimental design, stored RBC samples were diluted to 7% Hct by the respective additive solutions. After centrifugation, the supernatants were prepared in a 96-well plate as part of a standard addition method. Briefly, 5 μL of the supernatant were added into 4 wells also containing 45 μL of DDW. To those 4 wells, lactate (50 μM) was added

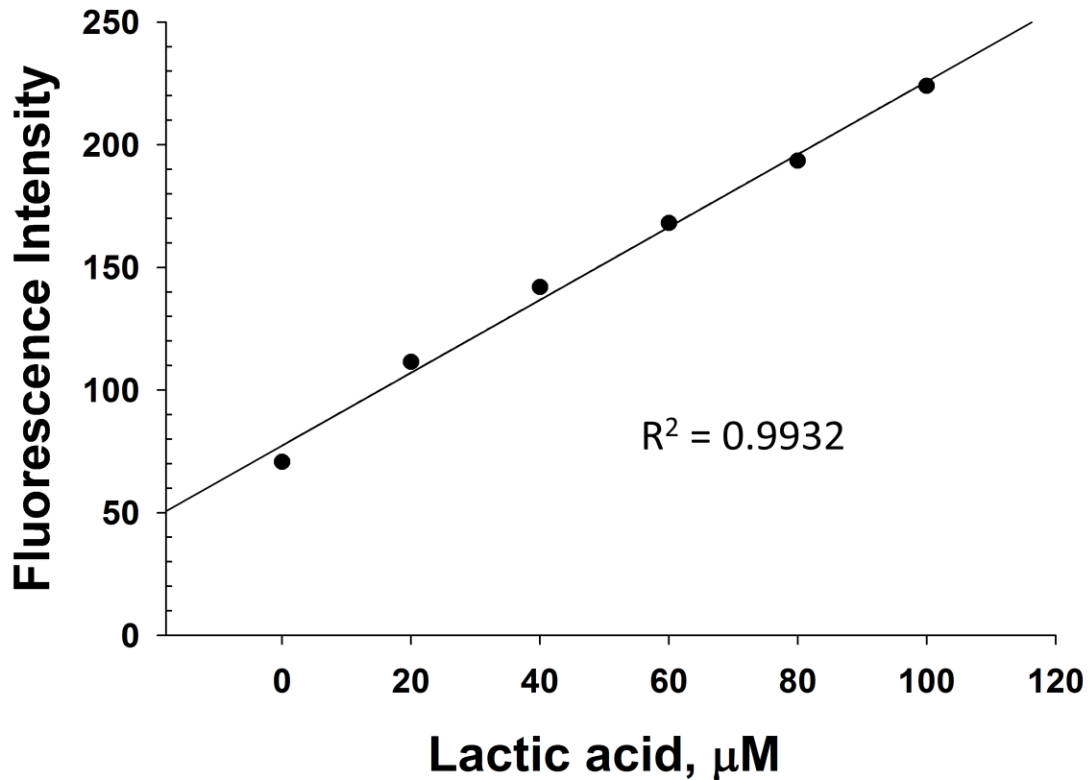
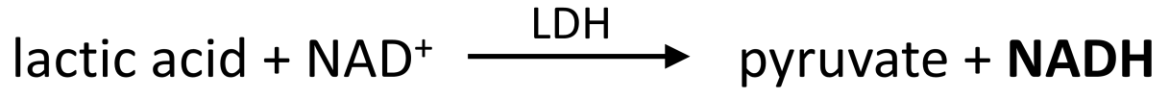


Figure 2.4 – The Reaction Mechanism of Lactic Acid Assay. The lactate in the samples or standards is oxidized to pyruvate by LDH while NAD^+ reduced to NADH, which has an emission of fluorescence at 460 nm after excitation of 340 nm. The fluorescence intensity is proportional to the amount of NADH present as well as the lactate originally present. Thus, the lactate concentration in the samples can be quantified by using a calibration curve generated at the same time. An overall calibration curve ($n = 6$) is shown below, the limit of detection based on this curve is 11.4 μM .

in volumes of 0, 10, 25, and 50 μL . DDW was then added to each well to bring the final volume to 100 μL .

For the 36-day storage study, the samples were processed in a different manner. Supernatant samples were prepared directly by centrifuging the stored RBC samples (55-60% Hct) at 2000 g for 10 minutes and then further centrifuging again at 15,000 g for 15 minutes. Next, 5 μL of supernatant were diluted to 100 μL with DDW. These dilutions resulted in lactate concentrations within the range of a calibration curve that was prepared with external lactic acid standards ranging from 0 to 100 μM . In this way, the direct lactate production in storage could be evaluated with simplicity, and the experimental procedures were simplified as well.

To perform the assay, 100 μL of an enzyme solution containing LDH (5.0 U/mL) and NAD^+ (5 mM) in trizma buffer (0.1 M, pH 8.9) were added to 100 μL of standards or samples described above. The buffer was prepared by dissolving 1.21 g Trisma base in 100 mL of DDW and adjusting the pH to 8.9 by adding 2 M sodium hydroxide (NaOH) drop wise. The mixture was then allowed to react for 15 minutes at 37°C prior to the measurement of fluorescence intensity at 460 nm (excitation at 340 nm). The fluorescence was read in a commercial plate reader (Spectramax M4, Molecular Devices), and has an intensity that is proportional to the amount of NADH and lactate present. The concentration of lactate can be determined using the calibration curve generated at the same time.

2.2.5 Determination of Glucose Level in Storage

To verify the maintenance of normoglycemic conditions in CPD-N/AS-1N storage, glucose levels of the storage medium were determined. The extracellular glucose is first converted into glucose-6-phosphate (G6P) by hexokinase (HK). G6P is subsequently converted into 6-phospho-gluconate by glucose-6-phosphate dehydrogenase (G6PDH) while converting nicotinamide adenine dinucleotide phosphate (NADP^+) to its reduced form (NADPH). The protocol was modified from a previously described assay.³² The reaction mechanism and standard curve are shown in figure 2.5.

For quantification using the glucose assay, a 20 mM glucose stock solution was prepared by dissolving 36 mg of D-glucose into 10 mL of DDW. Standards (0 - 100 μM) were prepared from the stock solution with a series of appropriate dilutions. NADP^+ was prepared at a final working concentration of 12.5 mM by dissolving 100 mg in 10.76 mL of DDW and aliquotted into 500 μL and storing in freezer (-20°C) until use. A 20 mM ATP stock solution was prepared by dissolving 11 mg in 1000 μL of DDW. The magnesium chloride (MgCl_2) stock solution was prepared at 100 mM by dissolving 203 mg in 10 mL of DDW. The enzyme, G6PDH was supplied in an ammonium sulfate suspension at ~ 2.5 units/ μL . The other enzyme, HK, was prepared as a stock solution with a concentration of 57 units/mL by dissolving 10 mg of the lyophilized enzyme in 10 mL of DDW.

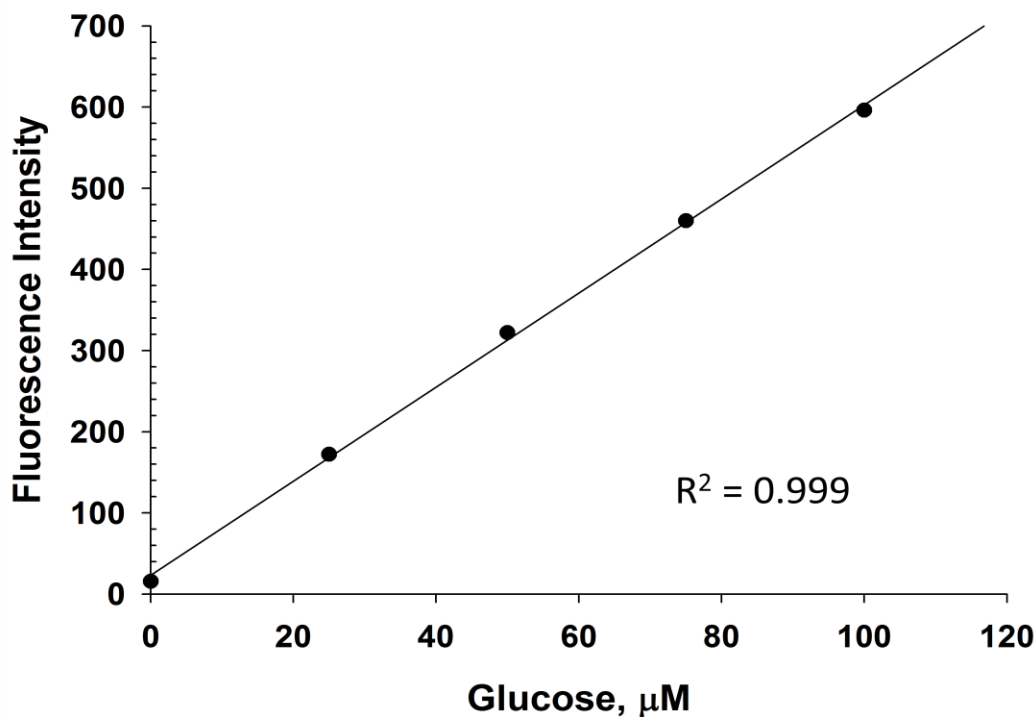
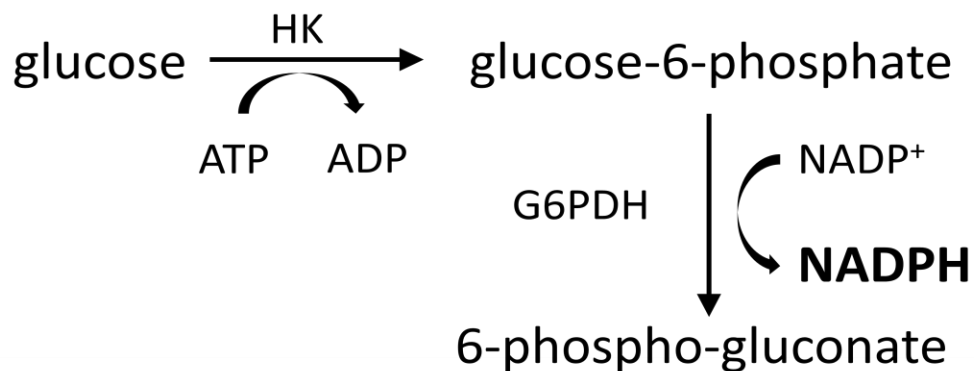


Figure 2.5 – The Reaction Mechanism of Glucose Assay. The glucose in the samples or standards is first converted to G6P by HK, and subsequently oxidized to 6-phospho-gluconate by G6PDH while NADP^+ reduced to NADPH, which has an emission of fluorescence at 460 nm after excitation of 340 nm. The fluorescence intensity is proportional to the amount of NADPH present as well as the glucose originally present. Thus the glucose concentration in the samples can be quantified by using a calibration curve generated at the same time. An overall calibration curve ($n = 6$) is shown below, the limit of detection based on this curve is 1.0 μM .

Due to the high Hct of stored RBCs, the supernatant had to be separated by a two-step centrifugation process. Supernatant samples were prepared by first centrifuging the stored RBCs at 2000 *g* for 10 minutes and then centrifuging again at 15,000 *g* for 15 minutes. Next, supernatant from AS-1N one was diluted to 1/100 with DDW, while supernatant from AS-1 was diluted 1/1000. These dilutions resulted in glucose concentrations within the range of a calibration curve that was prepared with external glucose standards ranging from 0 to 100 μM .

To perform the assay, 100 μL of an enzyme solution containing G6PD (0.9 U/mL), ATP (2 mM), MgCl_2 (2 mM), NADP^+ (1.25 mM), and HK (1.7 U/mL) in a 0.3 M triethanolamine (TEA) buffer at a pH of 7.6 were added to the 100 μL samples described in the previous paragraph. The TEA buffer was prepared by dissolving 4.48 g TEA in 100 mL of DDW and adjusting the pH to 7.6 using HCl. This mixture was then allowed to react for 15 minutes prior to the measurement of fluorescence intensity at 460 nm (excitation at 340 nm). The fluorescence intensity is proportional to the amount of NADPH present, as well as the glucose present. The concentration of glucose can be determined using the generated calibration curve.

2.2.6 Determination of Intracellular ATP in Stored RBCs

In order to compare the levels of intracellular ATP of RBCs stored in both versions of the solutions at various time points, samples were removed from storage bags, centrifuged and washed 4X with tris buffered saline (TBS) to remove any extracellular ATP. TBS was

prepared by dissolving 6.05 g Tris and 8.76 g NaCl in 1L of DDW and adjusting the pH to 7.5 with 1 M HCl. The intracellular ATP was determined at 7% Hct to allow for comparison with ATP release. Based on the Hct of the packed RBCs, a small aliquot of these RBCs (typically between 2-3 μL) was removed and diluted with the appropriate volume of TBS to create 50 μL of a RBC solution with a Hct of 7%. Due to the millimolar level of ATP in the RBC, a series of dilutions of samples were performed to obtain a measurable chemiluminescence signal. These dilutions also minimized the matrix effects of the cell lysate present (red color from hemoglobin). The RBCs in this 50 μL solution were lysed and diluted by the addition of 1000 μL of DDW. After 50 μL of this lysed solution were further diluted with 950 μL of TBS, 100 μL aliquots of the diluted sample were mixed with 100 μL of a L/L mixture, and the resultant chemiluminescence intensity was measured by the PMT in a plate reader. The quantitative amounts of ATP in the RBC samples were determined based on a calibration curve generated with authentic ATP standards (0-0.5 μM), also prepared in the TBS.

2.3 Results

2.3.1 Preliminary Study – 16 Days Storage

As described previously, RBCs were collected and stored using the miniaturized storage system. To start, a short interval of days was chosen to determine the ability of RBCs to release ATP when stored in hyperglycemic and normoglycemic system. Day 1 indicates the very first day of collection and storage. Thus, 2 bags of stored RBCs were removed

every 3-4 days: one contained RBCs collected and stored in CPD and AS-1, respectively, while the other contained RBCs collected and stored in CPD with 5.5 mM glucose (CPD-N) and AS-1 with 5.5 mM glucose (AS-1N). The cells in these samples were first evaluated for their ability to release ATP while flowing through a microbore tubing system described in the experimental section.

The results in figure 2.6 show that the RBCs collected and stored in the CPD-N and AS-1N, released a significantly higher ($p < 0.005$) amount of ATP though the first 8 days of storage ($0.312 \pm 0.008 \mu\text{M}$ on day 1 to $0.178 \pm 0.019 \mu\text{M}$ on day 8) than those collected and stored in the CPD and AS-1 ($0.126 \pm 0.002 \mu\text{M}$ on day 1 to $0.070 \pm 0.011 \mu\text{M}$ on day 8). Furthermore, the ATP release from the CPD-N/AS-1N cells on day 8 was statistically higher ($p < 0.05$) than the day 1 release from cells processed in CPD/AS-1. However, this favorable trend was not able to be maintained longer than 1 week, and the ATP release from the RBCs processed in CPD-N/AS-1N also decreased rapidly.

Based on the calculation of the rate of RBC metabolism at 4°C , the amount of glucose in the CPD-N/AS-1 system was determined to not to be enough for RBCs stored longer than 1 week. Results from additional experiments measuring lactate levels in the supernatant of the storage solutions, performed on the same day as the ATP release studies, verified this calculation. The results in figure 2.7 show that the concentration of extracellular lactate in the supernatant was $145 \pm 13 \mu\text{M}$ and $143 \pm 9 \mu\text{M}$ on day 1 for RBCs stored in CPD/AS-1 and CPD-N/AS-1N, respectively. Lactate accumulated rapidly in both storage solutions until day 8 (444 ± 12 and $446 \pm 6 \mu\text{M}$, respectively). However, the

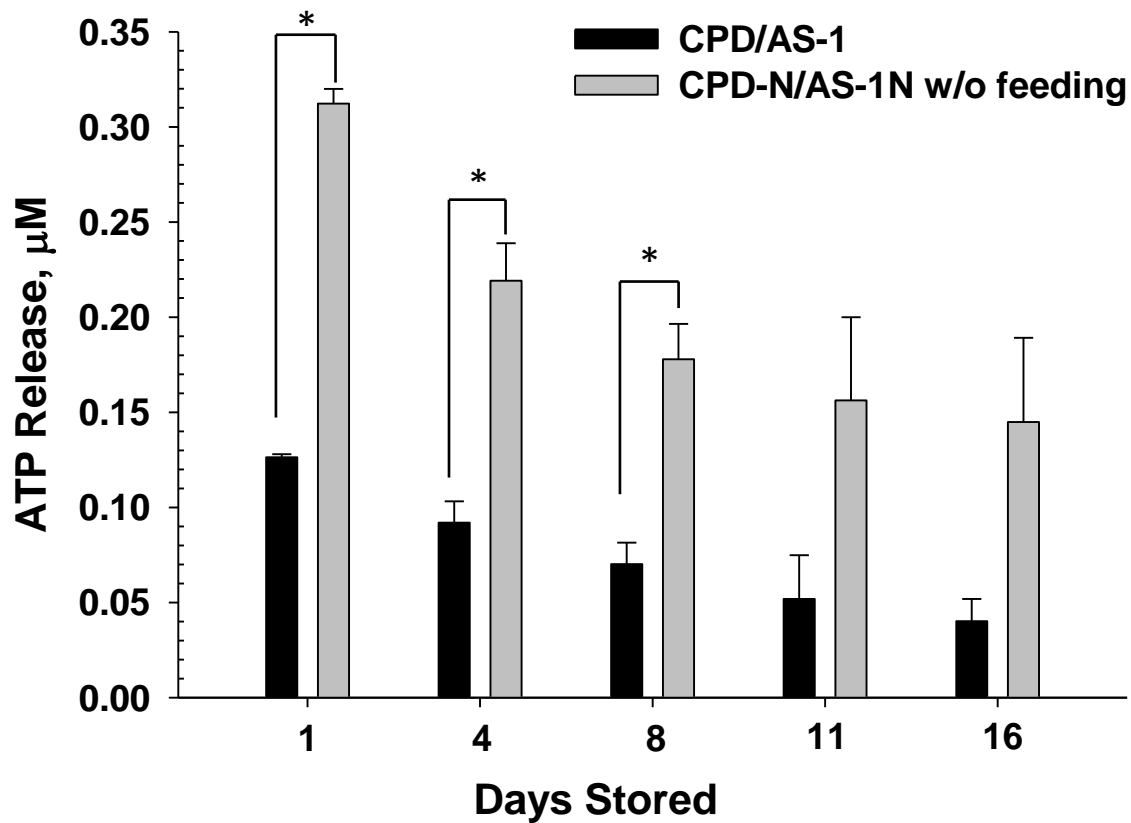


Figure 2.6 – ATP Release from the RBCs in Both Storage Conditions for 16-Day Preliminary Storage. The cells stored in normoglycemic condition (CPD-N/AS-1N, gray bars) show significantly higher ATP release than those in hyperglycemic condition (CPD/AS-1, black bars) for the first 8 days (* $p < 0.005$), the release gradually decreased as a function of storage duration. Furthermore, the ATP release from CPD-N/AS-1N cells on day 8 was statistically higher ($p < 0.05$) than the day 1 release from cells processed in CPD/AS-1. Data represent mean \pm s.e.m. ($n = 4$ for all).

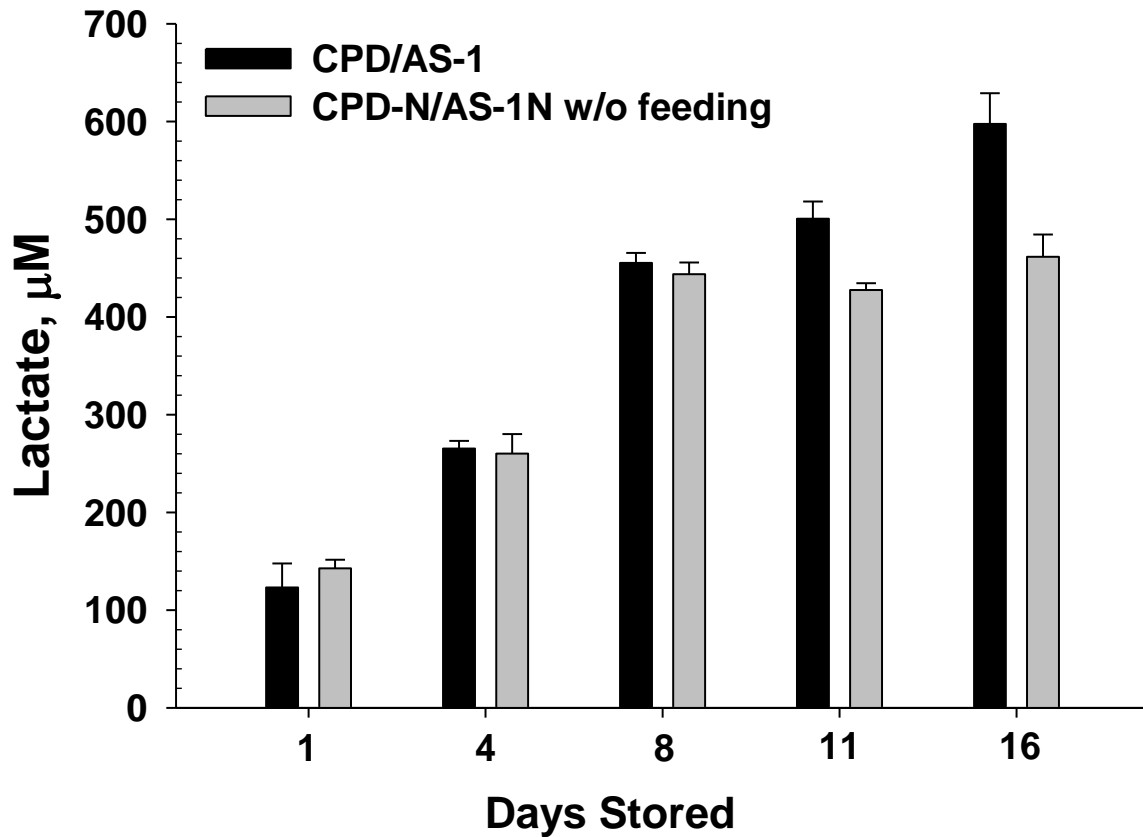


Figure 2.7 – Lactate Accumulation in Hyperglycemic and Normoglycemic Conditions for the 16-Day Preliminary Storage. Lactate levels determined in the supernatant in both CPD/AS-1 (black bars) and CPD-N/AS-1N (grey bars) were at similar till day 8, whereas lactate stopped accumulating in the supernatant of RBCs stored in CPD-N/AS-1N around day 8. Data represent mean \pm s.e.m. (n = 4 for all).

lactate levels in the supernatant of RBCs stored in CPD-N/AS-1N stopped increasing after day 8.

The decrease in lactate accumulation was also verified by a quantitative determination of glucose concentration in the AS-1N supernatant, which was found to be exhausted by day 8 as well (shown in table 2.2). Collectively, these results suggest that while a normoglycemic collection and storage protocol may be beneficial for increased of ATP release from stored RBCs, it is not necessarily conducive for storage periods beyond 1 week.

2.3.2 Glucose Feeding Treatment and 36 Days Storage

Based on the glucose concentration and lactic acid accumulation in the supernatant of the storage solutions, a consuming rate of glucose in the CPD-N/AS-1N system was evaluated as 0.8 millimoles per liter per day. Thus, in order to maintain glucose levels at ~ 5 mM, a periodic glucose feeding treatment was performed in CPD-N/AS-1N storage as described in the experimental section. Briefly, 2 μ L of 400 mM of glucose in saline were added per milliliters of stored RBCs per day for every 5 days. Due to the pH drops of lactate accumulations, the rate of glucose consumption decreases during the later storage.³³ Thus, reduced amount of glucose saline was added into storage after 2 weeks.

The results shown in figure 2.8 suggest that the extracellular glucose level of RBCs in CPD-N/AS-1N with feeding was stable, with a slight increase, at 5.1 ± 0.8 mM through 36 days of storage.

Table 2.2 – The Extracellular Glucose Level in CPD-N/AS-1N Storage without Glucose Feeding Treatment

Days stored	Extracellular glucose / mM
1	6.3
2	4.1
3	2.9
4	2.4
5	1.4
6	0.4
7	0.0
8	-0.1
9	-0.1
10	-0.1

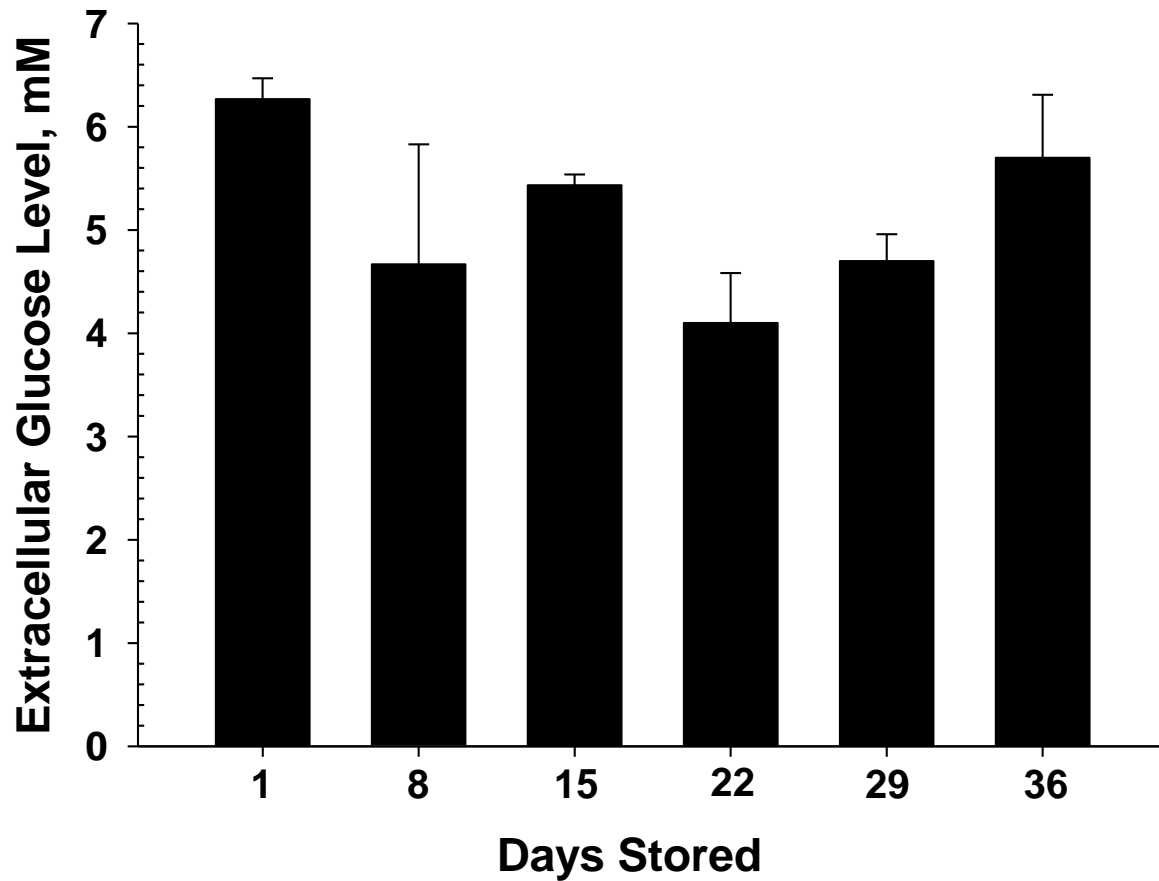


Figure 2.8 – Extracellular Glucose Levels in Normoglycemic Storage Condition with Glucose Feeding Treatment for the 36-Day Storage. The black bars showed the glucose level was maintained at ~ 5 mM in the CPD-N/AS-1N storage with adding glucose saline every 5 days. Data represent mean \pm s.e.m. (n = 4 for all).

With the periodic glucose feeding, RBCs were able to be stored in the CPD-N/AS-1N system for 36 days. Lactate accumulation was determined again to verify the metabolism activity of stored RBCs. As shown in figure 2.9, the periodic feeding of RBCs stored in the CPD-N/AS-1N solutions enabled glycolytic processes as shown by the continued lactate accumulation throughout the storage period. Lactic acid accumulation of RBCs increased equivalently for both RBCs stored in CPD/AS-1 and CPD-N/AS-1N until day 22. However, the former kept increasing to 24.5 mM on day 36, while the latter increased slowly to 15.2 mM on day 36.

As shown in figure 2.10, the ATP release from RBCs processed in CPD-N/AS-1N with feeding was significantly higher ($0.285 \pm 0.028 \mu\text{M}$) than those processed in CPD/AS-1 ($0.079 \pm 0.021 \mu\text{M}$) through 29 days ($p < 0.05$), and were also maintained at certain level statistically. In addition, RBCs collected and stored in CPD-N/AS-1N released ATP at a level on day 36 ($0.178 \pm 0.046 \mu\text{M}$) of storage that was statistically equivalent ($p = 0.694$) to the amount of ATP released from RBCs collected and stored in the CPD/AS-1 on day 1 ($0.152 \pm 0.042 \mu\text{M}$).

To further verify the activity of the metabolism of RBCs stored in hyperglycemic and normoglycemic conditions, intracellular ATP was determined as well. Intracellular levels of ATP in the RBC are typically in the single-digit millimolar range, and the amount released is sub-micromolar.⁴ Thus, it can be determined if the difference in the amount of ATP released is the result of the difference in ATP reserved in the cells. The data in figure 2.11 show that intracellular concentrations of ATP for all three storage protocols

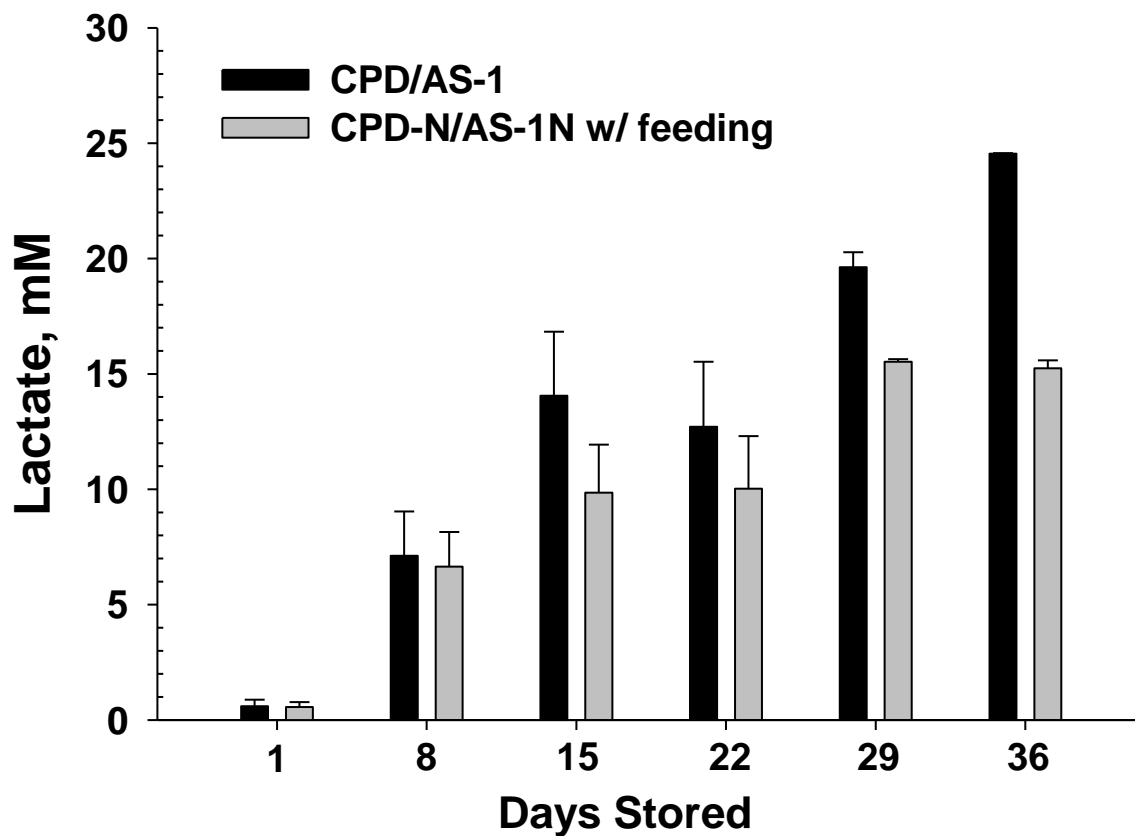


Figure 2.9 – Lactate Accumulation in Hyperglycemic and Normoglycemic Storage Conditions for the 36-Day Storage. Lactate accumulated in the supernatant in both CPD/AS-1 (black bars) and CPD-N/AS-1N with glucose feeding treatment (grey bars) increased equivalently till day 22. However, the CPD-N/AS-1N cells produced lactate slowly in the remaining storage period. Data represent mean \pm s.e.m. (n = 4 for all).

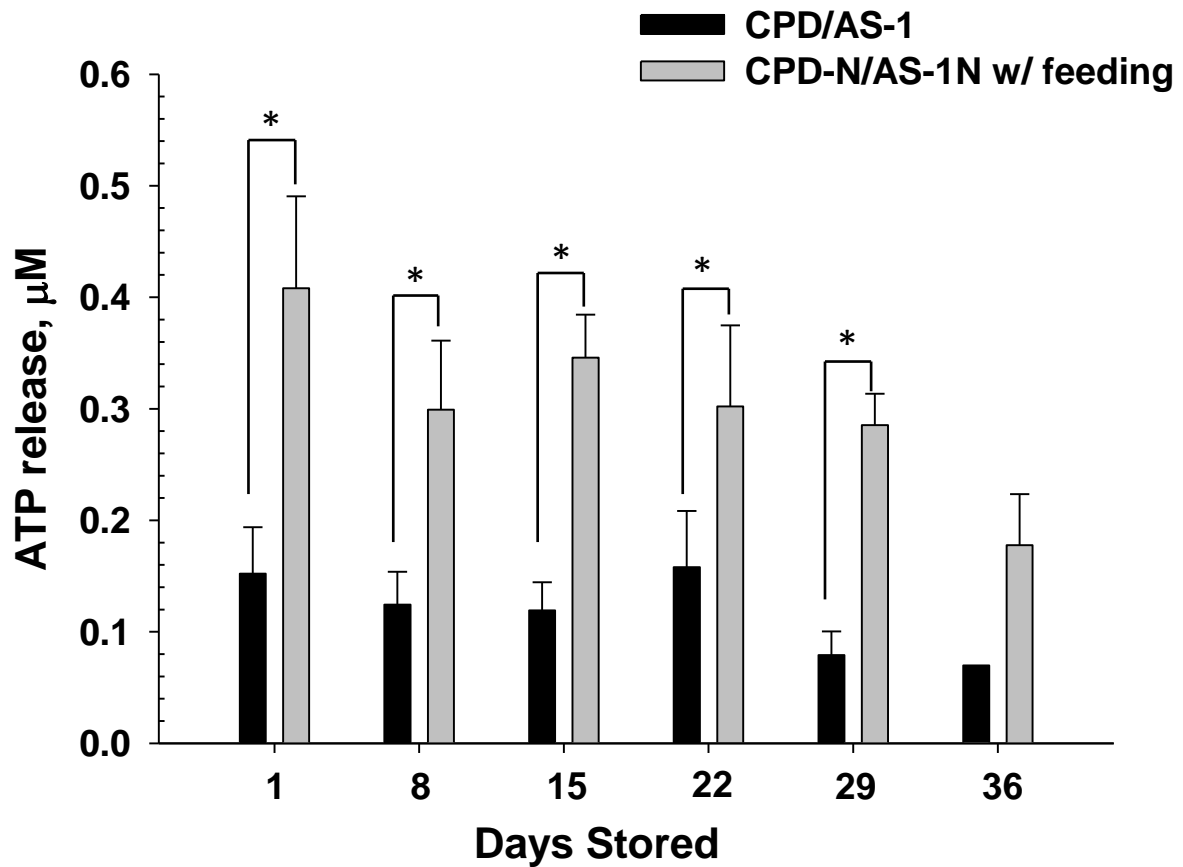


Figure 2.10 – ATP Release from the RBCs in Both Storage Conditions during 36 Days. The cells stored in normoglycemic condition with glucose feeding treatment (CPD-N/AS-1N, gray bars) consistently release significantly higher ATP than those in hyperglycemic condition (CPD/AS-1, black bars) through the 29-day storage duration (* $p < 0.05$), the release gradually decreased as a function of storage duration. In fact, the release from CPD-N/AS-1N cells on day 36 was statistically equivalent ($p = 0.694$) to the day 1 release from cells processed in CPD/AS-1. Data represent mean \pm s.e.m. ($n = 4$ for all).

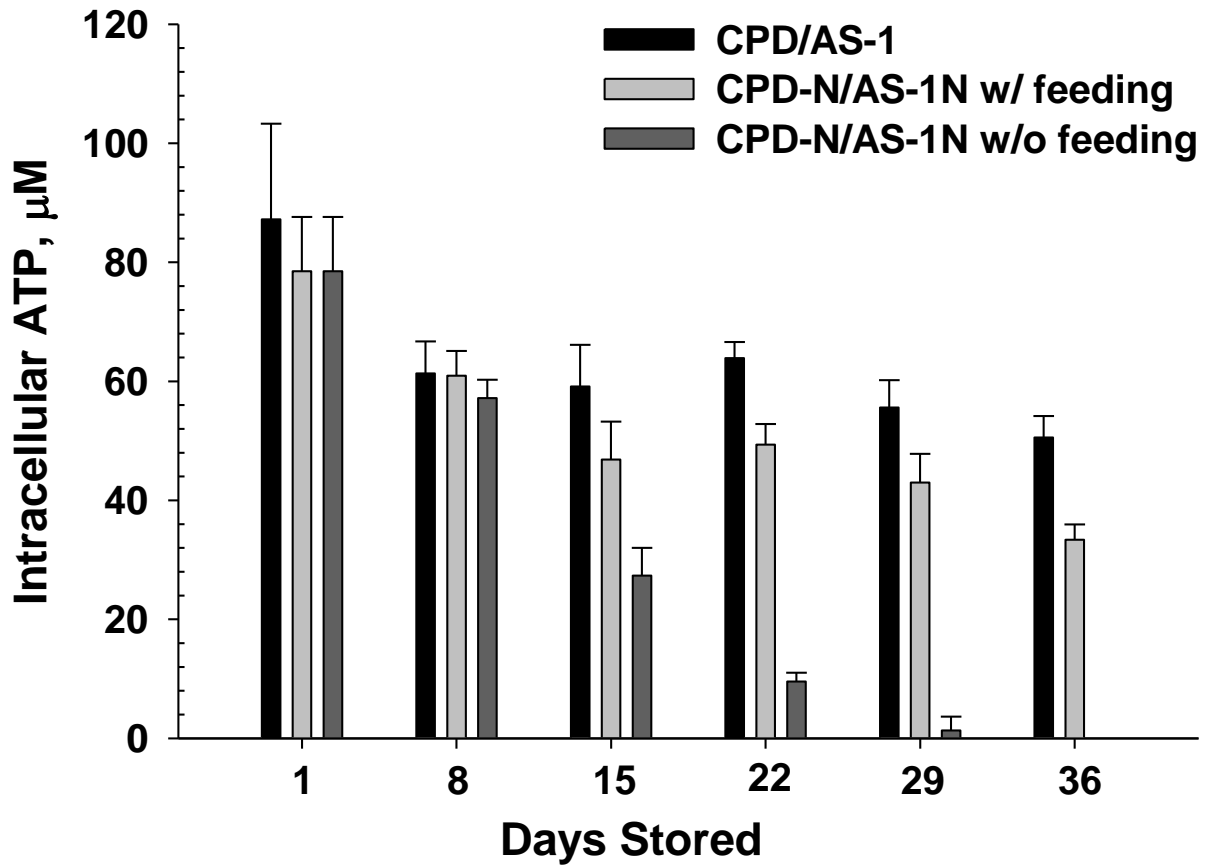


Figure 2.11 – The Intracellular ATP Level in Stored RBCs in Hyperglycemic and Normoglycemic with and without Glucose Feeding Condition. The ATP concentration are highest for cells stored in CPD/AS-1 (black bars) and lowest for CPD-N/AS-1N without feeding (dark grey bars). The intracellular ATP concentrations for the CPD-N/AS-1N with feeding (light grey bars) is slightly lower than the CPD/AS-1, suggesting that the differences in ATP release from these cells is not necessarily due to the level of ATP reserved in the cell, since the amount of ATP release is just submicromolar level which is much smaller than the intracellular ATP level. Data represent mean \pm s.e.m. ($n = 4$ for all).

are nearly identical for the first week of storage. However, the RBCs stored in CPD-N/AS-1N, whose glucose levels were not maintained by periodic feeding, had intracellular ATP concentrations approaching zero by week 4 of storage. The cells processed in CPD/AS-1 or CPD-N/AS-1N with glucose addition had intracellular ATP concentrations that were maintained above 0.5 mM/RBC over the course of 5 weeks of storage. As shown, the RBCs processed in the higher glucose-containing collection and storage solutions maintained slightly higher levels of ATP than those stored in the CPD-N/AS-1N, though this did not translate to higher ATP release.

2.4 Discussion

In the United States, the National Blood Collection and Utilization Survey (NBCUS) reported 15.7 million units were donated in its most recent survey, a value exceeding the number of units of RBCs transfused during that period by over 1 million.³⁴ However, even though there was not a numerical shortage of stored units of RBCs, according to the NBCUS, post-transfusion complications are still an area of concern in transfusion medicine. It is increasingly being recognized that these complications are mediated, at least in part, by storage dependent changes to the RBC itself.³⁵ Various reports have suggested that, in some instances, people are less likely to survive after receiving a transfusion, in comparison to those who did not receive any units of stored blood components.³⁶⁻³⁹ The positive association between the age of transfused RBCs with an increased incidence of transfusion related pathologies indicates that the RBC storage

lesion is the key factor in microcirculatory dysfunction and inflammatory tissue injury.⁴⁰

However, the manner in which the RBC storage lesions induces these complications remains unclear.⁴¹

To fulfill its primary function, oxygen transport, the transfused RBC must be intact, have sufficient survival rates *in vivo*, and circulate.⁴² These three properties translate to a required reduction in RBC lysis, the ability of the transfused RBCs to avoid removal due to cell apoptotic or cell senescence mechanisms, and the ability of the transfused RBCs to traverse blood vessels. Through the history of storage solution development, researchers have been dedicated to improving the quality of stored RBCs by reducing the hemolysis rate and improving the post-transfusion survival percentage. However, less effort is made on how good the stored RBCs are at circulating and functioning after transfusion.

The RBC has been shown to participate in the regulation of blood flow directly and actively through the RBC-derived ATP-stimulated NO production from endothelial cells through the mechanism described previously. In current clinical RBC storage, intracellular ATP levels are relatively well maintained,⁴³ whereas less is known related to the ability of stored RBCs to release ATP. McMahon *et al.* recently demonstrated that the hypoxia-induced or even the normoxic (basal) ATP release from stored RBC declined as a function of the storage time and defined this impaired ATP release as a novel RBC

storage lesion.⁴⁴ Transfusion of stored RBCs back to a nude mouse model was also shown in this work. Storage-induced impaired ATP release resulted in a rapid endothelial adhesion of RBCs *in vitro* and RBC sequestration in the lungs of transfused mice *in vivo*, which implies its contribution to adverse pathophysiology, such as acute coronary syndromes, especially when considering the recipients are the critically ill patient. Thus, it suggests that maintaining RBC responsiveness to stimuli that release ATP may be as important as intracellular ATP maintenance.⁴⁵ In our study presented here, efforts were made to improve the ability of stored RBC to release ATP under shear stress by providing a normoglycemic storage condition.

At beginning of this study, a miniaturized storage system was set up as the experimental section described. The procedures of collection and storage we used mimicked the gold standard in clinical settings, but on a smaller scale (collection of ~ 15 mL of whole blood, 1-2 mL of stored RBCs in each bag). The leukoreduction was not applied because the filtration procedure requires a large volume of blood sample with a hold-up volume of at least 8 mL. However, as described previously, the top 2-mm of packed RBCs were discarded with the plasma and buffy coat to avoid any remaining white cells. The miniaturized storage system allowed an individual storage bag to be removed at various time points without disturbing or contaminating other bags. Also, due to microliter amount of sample needed in each experiment, less blood was wasted in the miniaturized storage system.

The data in figure 2.6 provides evidence that the ability of the RBC to release ATP in response to mechanical deformation is compromised when processed using the standard CPD/AS-1 collection and storage solutions. When a separate aliquot of these RBCs was analyzed in normoglycemic versions of these solutions (CPD-N/AS-1N), the ATP release was significantly increased. In fact, our results show that the ATP release on day 16 in the CPD-N/AS-1N system was statistically equal ($p = 0.735$) to that of the CPD/AS-1 system on day 1. Such results are important considering that complications associated with transfusions generally increase when using RBCs that have been stored for more than 2 weeks.

Unfortunately, storing the RBCs in a normoglycemic solution (AS-1N) resulted in the complete exhaustion of glucose in the storage bag, as indicated by both lactate accumulation measurements (figure 2.7) and direct determination of glucose (table 2.2). Therefore, a rudimentary feeding protocol was developed that allowed for normoglycemic levels of glucose to be maintained in the miniaturized storage bags without affecting the overall sample volume. When this protocol was implemented, the ATP release remained steady throughout storage; in fact, the data in figure 2.10 show that the level of ATP release on day 36 is still statistically equivalent ($p = 0.694$) to the release on day 1 using standard CPD/AS-1 collection and storage solutions.

In order to compare the amount of intracellular ATP with the level of ATP released from stored RBCs, the former was determined for a 7% Hct of stored RBC sample and the data in figure 2.11 show that the intracellular ATP was at 2-digits micromolar level.

From these data, it is clear that the amount of ATP released ($\sim 0.2 \mu\text{M}$) is much smaller than the amount of ATP ($\sim 80 \mu\text{M}$) reserved in the cells. Thus, even though the intracellular levels of ATP were actually slightly higher in those RBCs stored in the higher glucose-containing AS-1 solutions, this ATP was not able to be released. This is not completely surprising as Sprague *et al.* have shown that people with primary pulmonary hypertension (PPH) release less ATP in response to stimulation, even though their RBCs contained levels of intracellular ATP statistically equal to those of non-PPH controls.⁴⁶

Furthermore, the high amount of glucose in the CPD/AS-1 storage solutions did not accelerate the metabolism of stored RBCs; on the contrary, it may be the cause of the impaired ATP release. Evaluated glucose levels may result in decreased membrane deformability, or even protein oxidation of stored RBCs, and thereby impair the ATP release in response to mechanical deformation. This mechanism will be discussed further in chapter 4.

However, this glucose feeding treatment is not perfect. As the data show in figure 2.8, the extracellular glucose level in normoglycemic storage was stable around 5 mM with fluctuations. Based on the data in table 2.2, glucose levels would decrease to ~ 1.4 mM by day 5 when the first glucose was added. Although RBCs in this condition were still viable and able to release ATP, the metabolism slowed due to the lack of sufficient glucose, which results in less lactate accumulation and intracellular ATP, as shown in figures 2.9 and 2.11, compared to the cells stored in CPD/AS-1. Specifically, the intracellular ATP maintenance in CPD-N/AS-1N was better (77% of the amount on day 1)

than the one in CPD/AS-1 (70% of the amount on day 1) during first week of storage. However, the fluctuations of glucose level in storage may decrease this advantage through the remaining storage period. Therefore, a continuous glucose feeding device/method is required and will be discussed in the future directions.

REFERENCES

REFERENCES

1. Krebs, H. A., Chemical Composition of Blood Plasma and Serum. *Annual Review of Biochemistry* 1950, *19*, 409-430.
2. Gov, N.; Safran, S. A., Red Blood Cell Shape and Fluctuations: Cytoskeleton Confinement and ATP Activity. *Journal of Biological Physics* 2005, *31* (3-4), 453-464.
3. Rose, I. A.; Warms, J. V., Control of Glycolysis in the Human Red Blood Cell. *The Journal of Biological Chemistry* 1966, *241* (21), 4848-4854.
4. Bergfeld, G. R.; Forrester, T., Release of ATP from Human Erythrocytes in Response to a Brief Period of Hypoxia and Hypercapnia. *Cardiovascular Research* 1992, *26* (1), 40-47.
5. Ellsworth, M. L.; Forrester, T.; Ellis, C. G.; Dietrich, H. H., The Erythrocyte as a Regulator of Vascular Tone. *The American Journal of Physiology* 1995, *269* (6 Pt 2), H2155-2161.
6. Light, D. B.; Capes, T. L.; Gronau, R. T.; Adler, M. R., Extracellular ATP Stimulates Volume Decrease in Necturus Red Blood Cells. *The American Journal of Physiology* 1999, *277* (3 Pt 1), C480-491.
7. Raththagala, M.; Karunaratne, W.; Kryziniak, M.; McCracken, J.; Spence, D. M., Hydroxyurea Stimulates the Release of ATP from Rabbit Erythrocytes through an Increase in Calcium and Nitric Oxide Production. *European Journal of Pharmacology* 2010, *645* (1-3), 32-38.
8. Meyer, J. A.; Froelich, J. M.; Reid, G. E.; Karunaratne, W. K. A.; Spence, D. M., Metal-Activated C-Peptide Facilitates Glucose Clearance and the Release of a Nitric Oxide Stimulus Via the Glut1 Transporter. *Diabetologia* 2008, *51* (1), 175-182.
9. Adak, S.; Chowdhury, S.; Bhattacharyya, M., Dynamic and Electrokinetic Behavior of Erythrocyte Membrane in Diabetes Mellitus and Diabetic Cardiovascular Disease. *Biochimica et Biophysica Acta* 2008, *1780* (2), 108-115.
10. Edwards, J.; Sprung, R.; Sprague, R.; Spence, D., Chemiluminescence Detection of ATP Release from Red Blood Cells Upon Passage through Microbore Tubing. *The Analyst* 2001, *126* (8), 1257-1260.
11. Price, A. K.; Fischer, D. J.; Martin, R. S.; Spence, D. M., Deformation-Induced Release of ATP from Erythrocytes in a Poly(Dimethylsiloxane)-Based Microchip with Channels That Mimic Resistance Vessels. *Analytical Chemistry* 2004, *76* (16), 4849-4855.

12. Pries, A. R.; Secomb, T. W., Microvascular Blood Viscosity in Vivo and the Endothelial Surface Layer. *The American Journal of Physiology - Heart and Circulatory Physiology* 2005, 289 (6), H2657-2664.
13. Olearczyk, J. J.; Stephenson, A. H.; Lonigro, A. J.; Sprague, R. S., Heterotrimeric G Protein Gi Is Involved in a Signal Transduction Pathway for ATP Release from Erythrocytes. *The American Journal of Physiology - Heart and Circulatory Physiology* 2004, 286 (3), H940-945.
14. Olearczyk, J. J.; Stephenson, A. H.; Lonigro, A. J.; Sprague, R. S., Receptor-Mediated Activation of the Heterotrimeric G-Protein Gs Results in ATP Release from Erythrocytes. *Medical Science Monitor : International Medical Journal of Experimental and Clinical Research* 2001, 7 (4), 669-674.
15. Sprague, R. S.; Ellsworth, M. L.; Stephenson, A. H.; Lonigro, A. J., Participation of Camp in a Signal-Transduction Pathway Relating Erythrocyte Deformation to ATP Release. *The American Journal of Physiology - Cell Physiology* 2001, 281 (4), C1158-1164.
16. Sprague, R. S.; Ellsworth, M. L.; Stephenson, A. H.; Kleinhenz, M. E.; Lonigro, A. J., Deformation-Induced ATP Release from Red Blood Cells Requires Cftr Activity. *The American Journal of Physiology - Heart and Circulatory Physiology* 1998, 275 (5), H1726-H1732.
17. Locovei, S.; Bao, L.; Dahl, G., Pannexin 1 in Erythrocytes: Function without a Gap. *Proceedings of the National Academy of Sciences of the United States of America* 2006, 103 (20), 7655-7659.
18. Cotrina, M. L.; Lin, J. H.; Alves-Rodrigues, A.; Liu, S.; Li, J.; Azmi-Ghadimi, H.; Kang, J.; Naus, C. C.; Nedergaard, M., Connexins Regulate Calcium Signaling by Controlling ATP Release. *Proceedings of the National Academy of Sciences of the United States of America* 1998, 95 (26), 15735-15740.
19. Hisadome, K.; Koyama, T.; Kimura, C.; Droogmans, G.; Ito, Y.; Oike, M., Volume-Regulated Anion Channels Serve as an Auto/Paracrine Nucleotide Release Pathway in Aortic Endothelial Cells. *The Journal of General Physiology* 2002, 119 (6), 511-520.
20. Parpura, V.; Scemes, E.; Spray, D. C., Mechanisms of Glutamate Release from Astrocytes: Gap Junction "Hemichannels", Purinergic Receptors and Exocytotic Release. *Neurochemistry International* 2004, 45 (2-3), 259-264.
21. Sprague, R. S.; Stephenson, A. H.; Ellsworth, M. L.; Keller, C.; Lonigro, A. J., Impaired Release of ATP from Red Blood Cells of Humans with Primary Pulmonary Hypertension. *Experimental Biology and Medicine (Maywood)* 2001, 226 (5), 434-439.
22. Carroll, J. S.; Ku, C. J.; Karunaratne, W.; Spence, D. M., Red Blood Cell Stimulation of Platelet Nitric Oxide Production Indicated by Quantitative Monitoring of

the Communication between Cells in the Bloodstream. *Analytical Chemistry* 2007, 79 (14), 5133-5138.

23. Sprague, R.; Stephenson, A.; Bowles, E.; Stumpf, M.; Ricketts, G.; Lonigro, A., Expression of the Heterotrimeric G Protein Gi and ATP Release Are Impaired in Erythrocytes of Humans with Diabetes Mellitus. *Advances in Experimental Medicine and Biology* 2006, 588, 207-216.

24. Zhu, H.; Zennadi, R.; Xu, B. X.; Eu, J. P.; Torok, J. A.; Telen, M. J.; McMahon, T. J., Impaired Adenosine-5'-Triphosphate Release from Red Blood Cells Promotes Their Adhesion to Endothelial Cells: A Mechanism of Hypoxemia after Transfusion. *Critical Care Medicine* 2011, 39 (11), 2478-2486.

25. Baskurt, O. K.; Meiselman, H. J., Blood Rheology and Hemodynamics. *Seminars in Thrombosis and Hemostasis* 2003, 29 (5), 435-450.

26. Traykov, T. T.; Jain, R. K., Effect of Glucose and Galactose on Red Blood Cell Membrane Deformability. *International Journal of Microcirculation, Clinical and Experimental / Sponsored by the European Society for Microcirculation* 1987, 6 (1), 35-44.

27. Livshits, L.; Srulevich, A.; Raz, I.; Cahn, A.; Barshtein, G.; Yedgar, S.; Eldor, R., Effect of Short-Term Hyperglycemia on Protein Kinase C Alpha Activation in Human Erythrocytes. *The Review of Diabetic Studies : RDS* 2012, 9 (2-3), 94-103.

28. Riquelme, B.; Foresto, P.; D'Arrigo, M.; Valverde, J.; Rasia, R., A Dynamic and Stationary Rheological Study of Erythrocytes Incubated in a Glucose Medium. *Journal of Biochemical and Biophysical Methods* 2005, 62 (2), 131-141.

29. Resmi, H.; Akhunlar, H.; Temiz Artmann, A.; Guner, G., In Vitro Effects of High Glucose Concentrations on Membrane Protein Oxidation, G-Actin and Deformability of Human Erythrocytes. *Cell Biochemistry and Function* 2005, 23 (3), 163-168.

30. Engelgau, M. M.; Narayan, K. M.; Herman, W. H., Screening for Type 2 Diabetes. *Diabetes Care* 2000, 23 (10), 1563-1580.

31. Hillyer, C. D., *Blood Banking and Transfusion Medicine: Basic Principles & Practice*. 2 nd ed.; Philadelphia, PA : Churchill Livingstone/Elsevier: 2007.

32. Liddell, J. R.; Zwingmann, C.; Schmidt, M. M.; Thiessen, A.; Leibfritz, D.; Robinson, S. R.; Dringen, R., Sustained Hydrogen Peroxide Stress Decreases Lactate Production by Cultured Astrocytes. *Journal of Neuroscience Research* 2009, 87 (12), 2696-2708.

33. Hess, J. R., Red Cell Changes During Storage. *Transfusion and Apheresis Science : Official Journal of the World Apheresis Association : Official Journal of the European Society for Haemapheresis* 2010, 43 (1), 51-59.

34. Whitaker, B. I. *2011 National Blood Collection and Utilization Survey*; American Association of Blood Banks, 2011.
35. Vandromme, M. J.; McGwin, G., Jr.; Weinberg, J. A., Blood Transfusion in the Critically Ill: Does Storage Age Matter? *Scandinavian Journal of Trauma, Resuscitation and Emergency Medicine* 2009, *17*, 35.
36. Koch, C. G.; Li, L.; Sessler, D. I.; Figueroa, P.; Hoeltge, G. A.; Mihaljevic, T.; Blackstone, E. H., Duration of Red-Cell Storage and Complications after Cardiac Surgery. *The New England Journal of Medicine* 2008, *358* (12), 1229-1239.
37. Hebert, P. C.; Wells, G.; Blajchman, M. A.; Marshall, J.; Martin, C.; Pagliarello, G.; Tweeddale, M.; Schweitzer, I.; Yetisir, E., A Multicenter, Randomized, Controlled Clinical Trial of Transfusion Requirements in Critical Care. Transfusion Requirements in Critical Care Investigators, Canadian Critical Care Trials Group. *The New England Journal of Medicine* 1999, *340* (6), 409-417.
38. Gong, M. N.; Thompson, B. T.; Williams, P.; Pothier, L.; Boyce, P. D.; Christiani, D. C., Clinical Predictors of and Mortality in Acute Respiratory Distress Syndrome: Potential Role of Red Cell Transfusion. *Critical Care Medicine* 2005, *33* (6), 1191-1198.
39. Kneyber, M. C.; Hersi, M. I.; Twisk, J. W.; Markhorst, D. G.; Plotz, F. B., Red Blood Cell Transfusion in Critically Ill Children Is Independently Associated with Increased Mortality. *Intensive Care Medicine* 2007, *33* (8), 1414-1422.
40. Weinberg, J. A.; Barnum, S. R.; Patel, R. P., Red Blood Cell Age and Potentiation of Transfusion-Related Pathology in Trauma Patients. *Transfusion* 2011, *51* (4), 867-873.
41. Glynn, S. A., The Red Blood Cell Storage Lesion: A Method to the Madness. *Transfusion* 2010, *50* (6), 1164-1169.
42. Hess, J. R., Red Cell Storage: When Is Better Not Good Enough? *Blood Transfusion = Trasfusione Del Sangue* 2009, *7* (3), 172-173.
43. Hess, J. R.; Rugg, N.; Knapp, A. D.; Gormas, J. F.; Hill, H. R.; Oliver, C. K.; Lippert, L. E.; Greenwalt, T. J., The Role of Electrolytes and Ph in Rbc Ass. *Transfusion* 2001, *41* (8), 1045-1051.
44. Zhu, H.; Zennadi, R.; Xu, B. X.; Eu, J. P.; Torok, J. A.; Telen, M. J.; McMahon, T. J., Impaired Adenosine-5'-Triphosphate Release from Red Blood Cells Promotes Their Adhesion to Endothelial Cells: A Mechanism of Hypoxemia after Transfusion. *Critical Care Medicine* 2011, *39* (11), 2478-2486.
45. Patel, R. P., Losing Control over Adenosine 5'-Triphosphate Release: Implications for the Red Blood Cell Storage Lesion. *Critical Care Medicine* 2011, *39* (11), 2573-2574.

46. Sprague, R. S.; Stephenson, A. H.; Ellsworth, M. L.; Keller, C.; Lonigro, A. J., Impaired Release of ATP from Red Blood Cells of Humans with Primary Pulmonary Hypertension. *Experimental Biology and Medicine (Maywood)* 2001, 226 (5), 434-439.

Chapter – 3 Endothelium-Derived Nitric Oxide Stimulated from RBC-Derived ATP

3.1 Nitric Oxide Stimulation in Vasodilation

The endothelium is the thin layer of cells lining the inside of a blood vessel, directly in contact with both circulating blood, and the smooth muscle layer surrounding the vessel. The vascular endothelial cells line the entire circulatory system, including the end-most capillaries. They function in vasoconstriction and vasodilation through the release of different factors that determine the activity of the underlying smooth muscle, and hence, control blood pressure.¹ One of these relaxing factors, nitric oxide (NO), was first reported in 1987.²

Many stimuli of NO exist, and the hypothesis proposed by Sprague *et al.* that adenosine triphosphate (ATP) from red blood cells (RBCs) stimulates endothelium-derived NO functions in vascular tone is now well established.³ RBCs release ATP in response to a number of stimuli, including hypoxia (low oxygen levels),⁴ mechanical deformation,⁵⁻⁷ changes in osmotic pressure⁸ and pharmaceutical agents.⁹⁻¹⁰ When ATP is released from RBCs, it can bind to the purinergic receptor, P2Y, on the endothelial cells.¹¹⁻¹² This binding increases calcium transport into the cell, thereby activating endothelial nitric oxide synthase (eNOS), the interaction of Ca²⁺-calmodulin (CaM) with the eNOS at the Ca²⁺-CaM-binding domain.¹³⁻¹⁴ The stimulation of eNOS results in the conversion of L-

arginine to L-citrulline, requiring the reduced form of nicotinamide adenine dinucleotide phosphate (NADPH), oxygen and calcium as cofactors, releasing NO as a by-product.¹⁵

The NO is then able to diffuse from the endothelium to the smooth muscle cells, where it binds to its receptor, soluble guanylyl cyclase (sGC), activating the synthesis of cyclic guanosine monophosphate (cGMP).¹⁶ The increase of cGMP, which is a regulator of ion channel conductance, results in smooth muscle relaxation and dilation.¹⁷ This mechanism is shown in figure 3.1.

RBCs also release NO in response to hypoxia¹⁸ and mechanical stress.¹⁹⁻²⁰ However, to participate in vasodilation, the RBC-derived NO, a short-lived free radical molecule,²¹ must diffuse a longer distance through the oxidizing environment of blood and plasma, and through an endothelial layer, to regulate smooth muscle relaxation. Preliminary studies in our group show that RBC-derived NO would not be able to participate in smooth muscle relaxation.²² Thus, the focus of this work is ATP-stimulated NO.

The RBC works as a regulator of vascular tone. RBCs release ATP in response to low oxygen levels and mechanical deformation. Proper vasodilation should increase blood flow and allow RBCs to deliver oxygen to tissues in need of reoxygenation. Thus, NO physiology has important implications for transfusion medicine.²³ Roback *et al.*

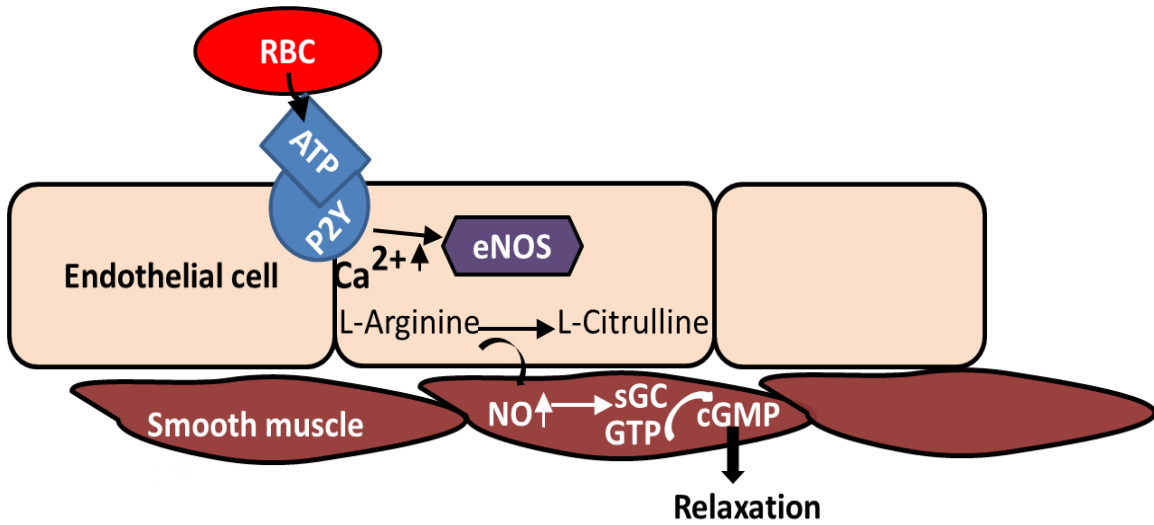


Figure 3.1 – ATP from RBCs Stimulates Endothelium-Derived NO Functions in Vascular Tone. RBC-derived ATP diffuses to endothelial cells and binds to P2Y receptors, resulting in an increase of intracellular free calcium, which activates the eNOS. The eNOS converts L-arginine into L-citrulline, as well as NO. NO diffuses to the smooth muscle cells, and binds to their sGC receptors, activating the conversion of GTP to cGMP. The increase of cGMP causes the relaxation of the muscle and facilitates dilation. For interpretation of the references to color in this and all other figures, the reader is referred to the electronic version of this dissertation.

proposed a hypothesis about insufficient NO bioavailability (INOBA) to explain the increased morbidity and mortality observed in some patients after RBC transfusion.²⁴ It is known that NO levels in the vascular beds are often markedly reduced, after transfusion. However, the origin of the INOBA is not completely understood, and when stored RBCs are transfused, it is not clear if the INOBA is due to a reduction in RBC-derived NO, or RBC-stimulated endothelial NO. Based on the results in chapter 2, showing decreased amount of ATP were released from RBCs stored in standard CPD/AS-1 solutions, compared to the RBCs in normoglycemic solutions, further studies of RBC-stimulated endothelial NO were performed to investigate a possible cause of INOBA.

Importantly, local NO levels can be modulated by the hemoglobin (Hb) in RBCs. Hb can scavenge the endothelium-derived NO by binding to β -93 cysteines.²⁵ In normal or healthy circulation, this scavenging does not have a serious effect on NO bioavailability, for multiple reasons. First, RBCs are mostly centered in the middle of the blood vessel, forming a RBC-free zone close to the endothelium layer, called Fåhræus effect.²⁶ Additionally, the scavenging can be inhibited by the encapsulation of Hb in intact RBCs.²⁷⁻²⁸ However, considering the hemolysis occurring during RBC storage, Hb-containing microparticles and free Hb may be present *in vivo* after blood transfusion. The NO uptake by RBC microparticles is ~ 333 times faster than by intact RBCs, and uptake by free Hb is ~ 1000 times faster than by intact RBCs.²⁹ Thus, the ability of RBCs to remain intact is critical to maintaining the levels of bioavailable NO.

In this chapter, using a microfluidic device, the effect of ATP release from RBCs stored in hyperglycemic (CPD/AS-1) and normoglycemic (CPD-N/AS-1N) conditions on endothelium-derived NO production at various storage time points was investigated. The percentage of hemolysis of RBCs stored in both conditions was also determined using Drabkin's method,³⁰ the standard technique used to determine the concentration of Hb.

3.2 NO Detection Based on Microfluidic Device

Microfluidics is a multidisciplinary science of the practical applications that involves small volumes of fluids flowing through channels with micrometer, or tens of micrometers, dimensions. Microfluidic-based systems have significant advantages in the investigation of cell-cell communication.³¹⁻³³ The investigation of intercellular communication using microfluidic devices enables replication of the chemical, mechanical, and physical cellular microenvironment *in vitro*. The ability to culture and flow different cell types at physiologically relevant time and length scales, allows studying the basic mechanisms, and avoids the challenges of isolating the functional unit *in vivo*.³⁴⁻³⁵

The most popular material used for the fabrication of microfluidic devices in cell-based studies is poly(dimethylsiloxane), or PDMS. PDMS is a silicon-based elastomeric material with a number of advantageous properties.³⁶ First, it is non-toxic and gas permeable,

which is critical to cell culture. Secondly, PDMS has optical transparency and low autofluorescence, which allow for imaging applications. In addition, soft lithography enables it to be easily molded, reliably replicated, and readily integrated with different materials, such as PDMS, glass, polystyrene, or even different devices, such as built-in valves and pumps.³⁷ Soft lithography for microfluidics was first reported by Whitesides *et al.* in 1998,³⁸ and expanded rapidly in the field of microfabrication for biochemistry and biology.³⁹ In a typical fabrication of a microfluidic device using PDMS, a master with raised features is created by coating photoresist onto a silicon wafer, covered by a transparent mask with the desired feature design, and exposing it to ultraviolet (UV) light.⁴⁰ The photoresist polymerizes under UV light, becoming insoluble to the photoresist developer, thus the remaining areas can be washed away.⁴¹ These procedures are shown in figure 3.2, where a master is created to mold PDMS, forming the recessed channels.

An *in vitro* model employed in intercellular communication between RBCs and bovine pulmonary artery endothelial cells (bPAECs), using a PDMS-based microfluidic device, was reported by our group in 2007.⁴² A modified microfluidic device for NO detection with the advantages of high throughput and rapid measurement in plate reader as also been reported.⁴³ Increased RBC-derived ATP, under a chemical stimulus or hypoxia, can interact with the endothelial cells cultured in these devices and result in elevated NO

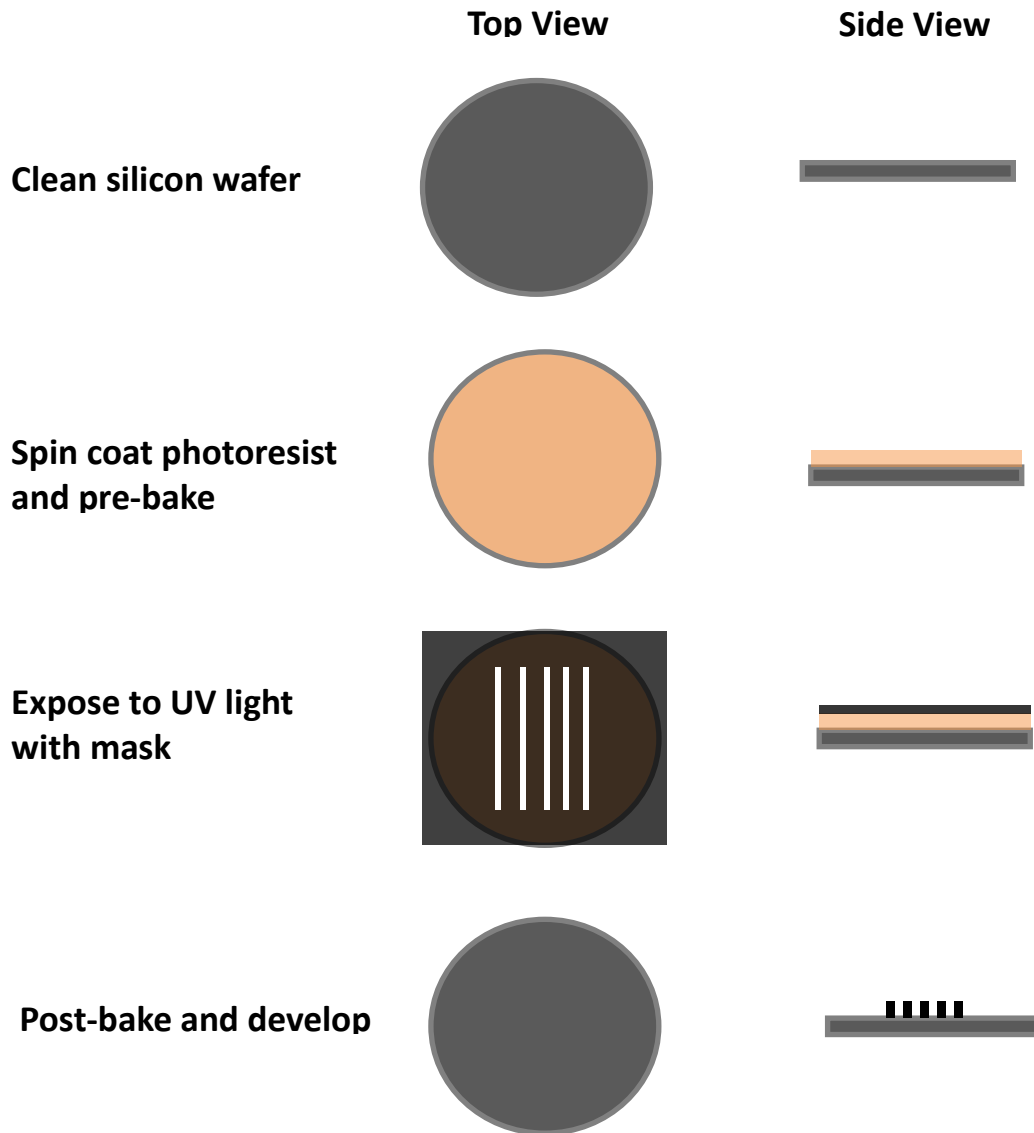


Figure 3.2 – Fabrication of a Master for Microfluidic Device using Lithographic Method. Briefly, the clean silicon wafer is spin coated with SU-8 photoresist. After pre-baking, a transparent mask with the desired features is placed over the photoresist before exposing to UV light. The photoresist exposed to light cross links, forming a rigid structure of the feature. After a post-bake, the remaining unpolymerized photoresist is washed away in developer. Thus, a reusable master with raised features is created and can be used as a mold for PDMS. For interpretation of the references to color in this and all other figures, the reader is referred to the electronic version of this dissertation.

production. Considering NO is a short-lived, free radical molecule,⁴⁴ these microfluidic devices enable the determination of NO production directly in wells, where endothelial cells are cultured. A fluorescent probe, 4-amino-5-methylamino-2',7'-difluorofluorescein (DAF-FM), reacts with NO to form a fluorescent product.⁴⁵ Its derivate, DAF-FM diacetate (DA) is able to cross the cell membrane and is transformed by esterases to DAF-FM, losing its cell permeability in meanwhile. The structures of DAF-FM and DAF-FM DA and the reaction mechanism are shown in figure 3.3.

3.3 Experimental

3.3.1 Preparation of Microfluidic Devices

Endothelium-derived NO production was determined using a microfluidic device fabricated by the soft photolithographic method.⁴⁶ First, a silicon master was prepared by spin-coating it with SU8-50 photoresist (MicroChem Corporation, Newton, MA), which had been loaded into a 50 mL syringe over night to enable gases to escape. The silicon wafer was spun with 4 mL of photoresist at 500 rpm for 15 seconds, then 1000 rpm for 30 seconds, followed by a 15-minute pre-bake at 95°C. A transparency mask with feature designs was placed over the prepared wafer and exposed to ultraviolet (UV) light at 340 nm for 30 seconds. During this process, the cross-linking of the photoresist was induced where the UV light could pass through the mask. After a 5-minute post-bake at 95°C, the wafer was developed in propylene glycol monomethyl ether acetate to

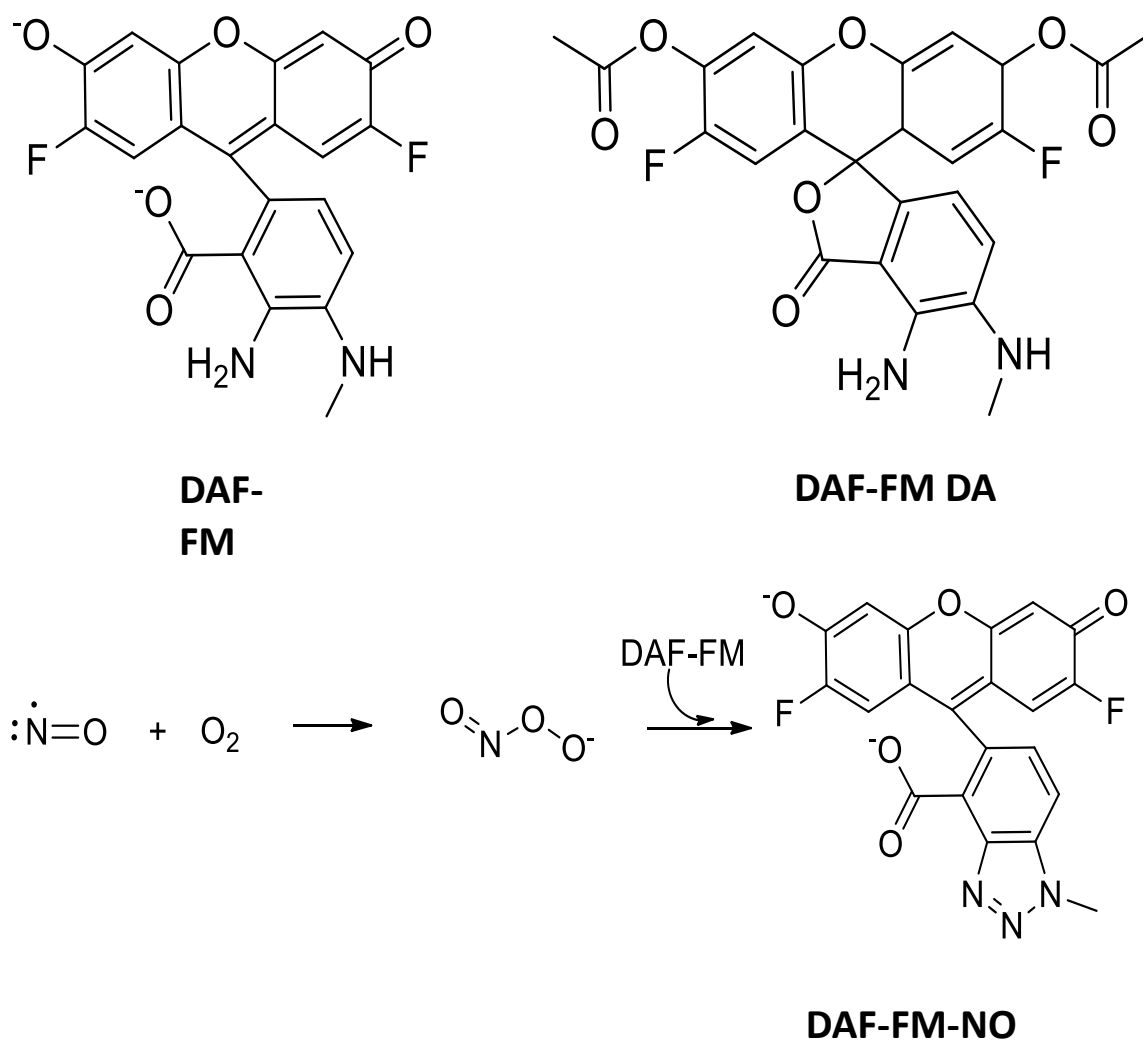
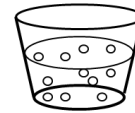


Figure 3.3 – Mechanism of NO Detection using DAF-FM. Shown in the upper panel are the structures of DAF-FM and its derivate, DAF-FM DA. DAF-FM DA permeates well into living cells and is rapidly transformed into water-soluble DAF-FM by cytosolic esterases. The lower panel shows the reaction between NO and DAF-FM, which requires oxygen, to form DAF-FM-NO. DAF-FM-NO fluorescence can be detected with a peak excitation wavelength of 485 nm and a peak emission of 515 nm.

remove the photoresist that was not cross-linked, creating desired features with a height of 100 μm .

The microfluidic device was comprised of two individual PDMS slabs, with slight modifications from previous work.⁴³ The fabrication of this device, shown as figure 3.4, was performed with two layers of PDMS of different properties. The first layer was made by mixing Sylgard 184 elastomer and curing agent (Ellsworth Adhesives, Germantown, WI) in a 20:1 ratio, which was used on surfaces to increase sealing. The second layer having a 5:1 mixture of elastomer and curing agent was coated on to the 20:1 layer, after the first layer had been cured by heating at 75°C for 13 minutes, to add rigidity to the device. After another 13-minute bake at 75°C, the slabs were cooled to room temperature and removed from the wafer. The bottom slab of PDMS contained 200 μm wide by 100 μm tall, L-shape channels. Inlets to these channels were punched using 20 gauge stainless steel tubing (New England Small Tube Company) at the same position on the short arm of the “L”. A second slab of PDMS, with no lithographically features, except for 1/8 inch holes that were created using a paper-hole punch, was used as the top layer of the microfluidic device. 1/8 inch holes were employed instead of 7/32 inch holes (originally designed) in order to reduce background signal while still containing sufficient volume. These two slabs were aligned and sealed with a track-etched polycarbonate membrane (pore diameter of 0.4 μm , Steriltech Inc., Kent, WA) over the area of all wells except those used for waste. Finally, this device was irreversibly cured together by baking at 75°C for 20 minutes. In the finished device, the

Pour and mix polymer and curing agent

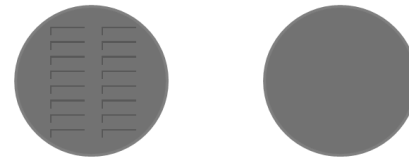


De-gas by vacuum



Bottom Slab Top Slab

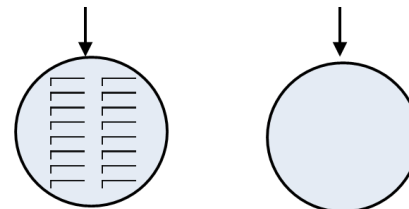
Pour 20:1 mixture over master
Bake 13 min at 75°C



Pour 5:1 mixture over master
Bake 13 min at 75°C



Remove PDMS from master



Further modify PDMS for the device

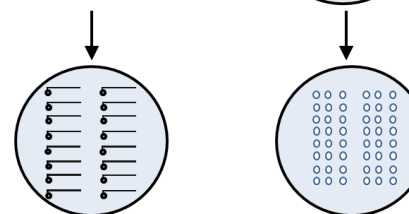


Figure 3.4 – Fabrication of PDMS Slabs through Soft Lithography. The polymer and curing agent were mixed in 20:1 and 5:1 ratios in separate cups and degassed by vacuum. The 20:1 and 5:1 mixtures were poured over the masters and baked at 75°C for 13 minutes, after each layer. The PDMS was then removed from the master, after cooling. Both slabs were further modified to create the inlets of channels, the probe wells, and the waste wells.

membrane represents the bottom of a “well” where portions of the PDMS were removed by the paper-hole punch. Importantly, cells can be cultured on the polycarbonate membrane surface. This device, specifically the probe-well area, was designed to fit the size of a standard 96-well plate.

3.3.2 Culture of Endothelial Cells onto Microfluidic Device

In order to investigate the effect of RBC-derived ATP on endothelial cells, a confluent layer of bPAECs (Lonza, Walkersville, MD) was cultured in each probe well of the microfluidic device. The cells were originally cultured in T-25 culture flasks (TPP brand – MIDSCI, St. Louis, MO) at 37°C and 5% CO₂ with Dulbecco’s modified eagle medium (DMEM, from MIDSCI) containing 5.5 mM glucose, 10% (v/v) fetal bovine serum (Lonza), and penicillin/streptomycin (MIDSCI) until they were ~ 80% confluent in the flasks. To detach the cells from the flask, they were rinsed with 4-(2-hydroxyethyl)-1-piperazineethanesulfonic acid (HEPES) solution, followed by a short incubation (~ 2 minutes) with a trypsin solution. After removing the trypsin solution by aspiration, DMEM was added to wash the cells off the flask surface by pipetting and scraping. The DMEM suspension containing the cells was transferred into a 15-mL tube and centrifuged at 1500 rpm for 5 minutes. A pellet of cells remained at the bottom of the tube after the supernatant was discarded, and the cells were resuspended in 600 µL of the DMEM media.

Meanwhile, the microfluidic device described above was prepared for cell culture by covering the polycarbonate membrane in each well with 10 μL of a 50 $\mu\text{g}/\text{mL}$ fibronectin solution, air-blow drying, and exposing to UV light to sterilize. Next, 10 μL of the prepared cell suspension were added into each well and allowed to incubate at 37°C. The 1-hour incubation allowed the cells settle down on the bottom of the wells. Then, the media solution was removed carefully, followed by the addition of 10 μL of the fresh media. The device was prepared \sim 12 hours before experimentation, with media change hourly, followed by incubation.

3.3.3 Determination of Endothelium-Derived NO with Stimulation of ATP from Stored RBCs

All reagents were purchased from Sigma-Aldrich (St. Louis, MO) unless indicated otherwise. Distilled deionized water (DDW) with 18.2 $\text{M}\Omega$ resistance was used for all experiments.

After a 12-hour incubation, the cells had become immobilized and confluent on the membrane in the microfluidic device. The endothelial cells in each well were rinsed with Hank's balanced salt solution (HBSS) to remove the culture media. The fluorescent probe, DAF-FM (Molecular Probes, Carlsbad, CA), was prepared by dissolving 1 mg into water free DMSO to make a 5 mM stock solution and stored in the dark at -20°C. A 5 μM DAF-FM working solution was prepared by diluting the stock solution with HBSS. Next, 10 μL of this working solution were added into each probe well. DAF-FM is an

extracellular probe for fluorescence detection of NO with the structure shown in figure 3.3. This probe is not cell-permeable but is more sensitive to NO and is photo-stable.

The RBC samples were prepared with the RBCs stored in hyperglycemic and normoglycemic conditions as described in chapter 2. Briefly, these RBCs were removed from storage at various time points and diluted to a 7% hematocrit (Hct) suspension with the additive solutions they were stored in. The experimental setup is shown in figure 3.5. The 7% RBC suspension was pumped through a 30-cm section of microbore tubing with an internal diameter of 50 μm (Polymicro Technologies, Phoenix, AZ) at 1 $\mu\text{L}/\text{minute}$ and 37°C. The microbore tubing was prepared to be attached to the 20 gauge stainless tube by removing 1 cm of the polyimide coating, and then securing with JB Weld. The 20 gauge tube was connected into the inlet of the L-shape channel, allowing the RBC suspension to flow underneath the probe well where ATP would diffuse to the endothelial cell layer through the pores of the membrane. The RBCs are too large to diffuse through these pores and continue to flow to a waste well on the device. The pumping was performed for a 30-minute period to allow sufficient time for NO production. NO production was stimulated via purinergic receptor signaling on the endothelial cells by RBC-derived ATP. This NO interacts with the probe contained in the well and an increase in fluorescence intensity was measured by a plate reader using an excitation wavelength of 488 nm and emission wavelength of 515 nm.

Two control experiments, inhibition studies of ATP release from the RBCs and endothelial NO production, were performed to ensure the NO production detected was

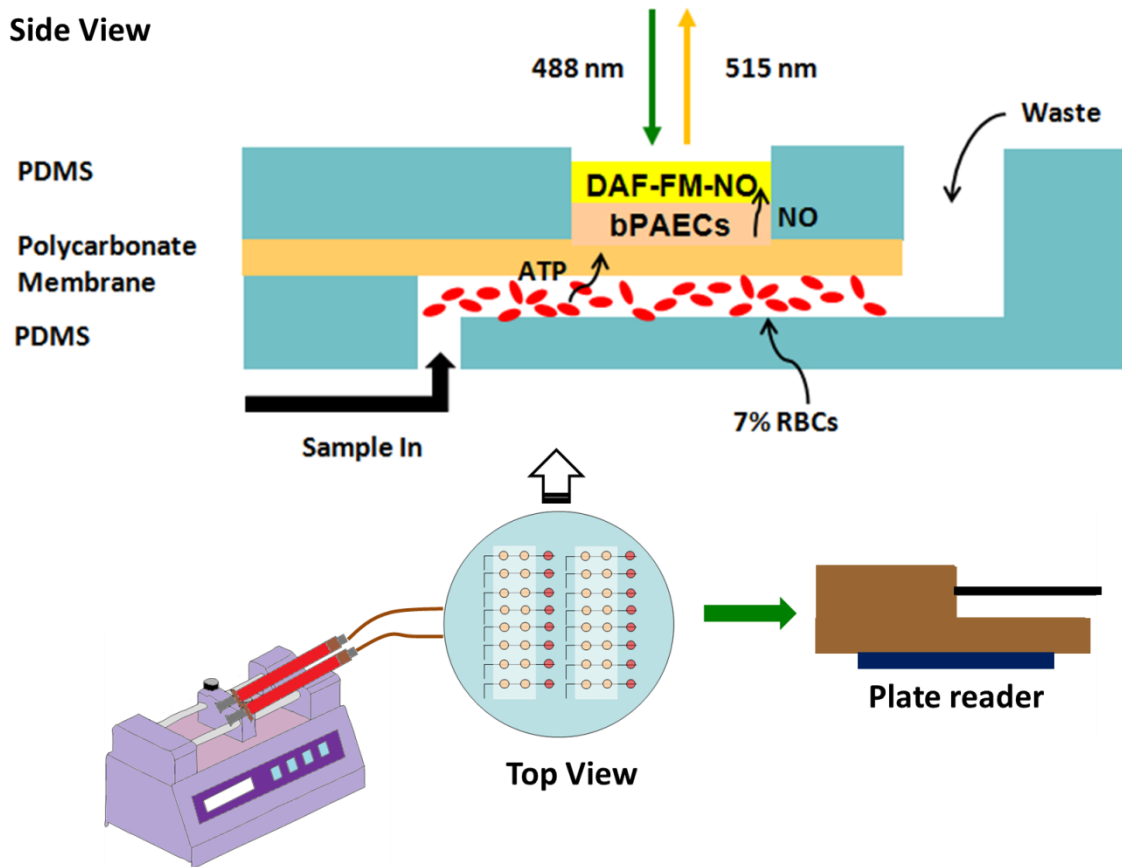


Figure 3.5 – Experimental Setup for the Detection of Endothelium-Derived NO Stimulated by Flow-Induced ATP from Stored RBC Samples. The device, fabricated from PDMS and described in more detail elsewhere, enables RBCs processed in CPD/AS-1 or CPD-N/AS-1N to flow beneath a layer of endothelial cells. When the cells release ATP due to flow-induced deformation, the ATP in the suspension can diffuse through a porous membrane, stimulating NO production from the endothelium via purinergic receptor signaling. The fluorescent probe DAF-FM facilitates the measurement of NO released by the endothelium. The fluorescence signal can be measured directly in a plate reader with an excitation wavelength at 488 nm and emission wavelength of 515 nm. For interpretation of the references to color in this and all other figures, the reader is referred to the electronic version of this dissertation.

endothelium derived and stimulated by the RBC ATP release. The first control experiment was performed by inhibiting the activity of the cystic fibrosis transmembrane conductance regulator (CFTR) protein. CFTR is either the ion channel that ATP passes through the RBC membrane, or it facilitates the passage of ATP through another ion channel.⁴⁷⁻⁴⁸ Thus, the inhibition of CFTR by glibenclamide (GLI) results in less, or no, ATP release from RBCs in response to stimulation.⁴⁷

The GLI was prepared by dissolving 0.0247 g into 10 mL of 0.05 M sodium hydroxide (NaOH) solution to generate a 5 mM solution. A hot water bath (~ 50°C) incubation was used to accelerate the dissolving process. Next, 20 µL of this GLI solution were added into 1 mL of a 7% RBC suspension to create a final concentration of 100 µM. RBC samples were incubated for 30 minutes at room temperature. These samples, as well as the samples without GLI treatment, were pumped simultaneously through the microfluidic device as described above.

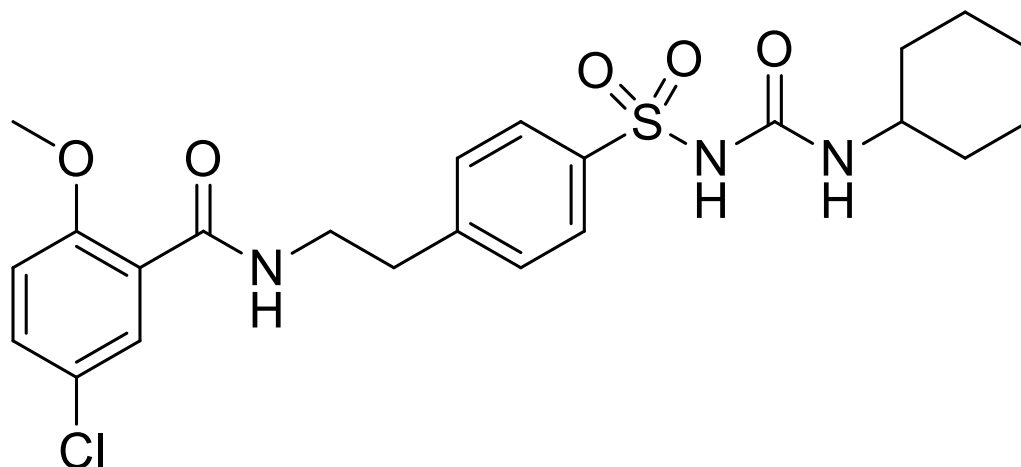
The second control experiment was performed by inhibiting the purinergic receptor, P2Y, on the endothelial cells. The P2Y receptor is the receptor that binds ATP and stimulates NO production via activation of eNOS. The PPADS, a non-selective P2 purinergic antagonist, was used to block the receptor.⁴⁹ A PPADS working solution was prepared by diluting 50 µL of 100 mM PPADS stock solution (in DMSO) with 450 µL of HBSS to create a final solution of 10 mM just prior to use. Cell culture media was removed from the wells in the microfluidic device, followed by rinsing of the wells with HBSS. Next, 10

μL of the PPADS working solution was added to the wells. After a 30-minute incubation at 37°C , the wells were rinsed with HBSS several times (usually 3-4 times) to remove excess PPADS solution, which has a dark orange color, before the addition of the DAF-FM probe. Meanwhile, the 7% RBC samples were pumped underneath both the PPADS-treated and non-treated endothelial cells for subsequent stimulation by RBC-derived ATP. The structures of GLI and pyridoxalphosphate-6-azophenyl-2',4'-disulfonic acid (PPADS) are shown in figure 3.6.

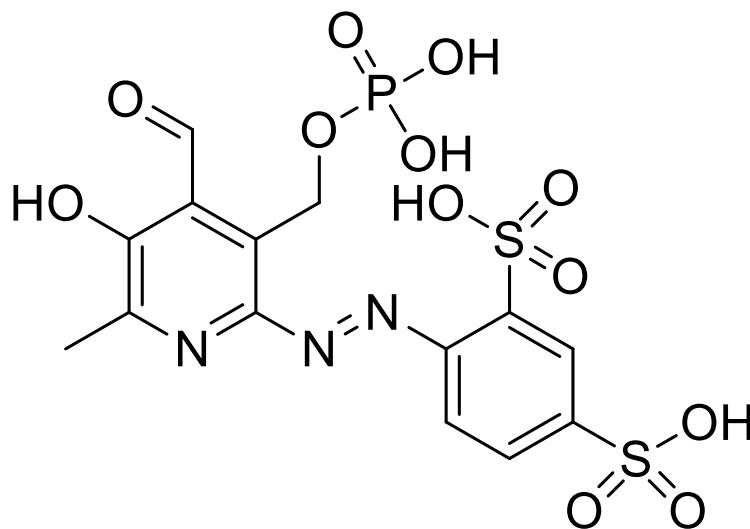
3.3.4 The Effect of Glucose on NO Detection using Fluorescent Probe DAF-FM

Unpublished studies in our group suggest that intracellular NO detection using DAF-FM DA is influenced by the surrounding glucose concentration. DAF-FM DA is a fluorescent probe for NO, as it can cross the cell membrane and transform to DAF-FM, which is cell-impermeable. In order to evaluate the effect of glucose on the detection of endothelium-derived NO, studies were performed to determine glucose diffusion across the endothelial cell coated membrane, and levels of NO detection in the glucose gradient solution.

Briefly, the microfluidic device with the endothelium was prepared as described above. 7% hematocrit RBC samples were prepared in AS-1 (with 111.1 mM glucose) and AS-1N (with 5.5 mM glucose), respectively. RBC samples were pumped at 37°C under the wells containing 10 μL of HBSS (glucose free). After 30 minutes, the glucose concentration in the HBSS was determined using the method described in chapter 2.



Glibenclamide



PPADS

Figure 3.6 – Structures of GLI and PPADS. Glibenclamide, the CFTR inhibitor, was used to prevent ATP released from RBCs in the control experiments. PPADS, the purinergic receptor (P2Y) inhibitor, was used to inhibit the NO released from endothelium in the second control experiment.

Next, various levels of NO in the glucose gradient solution were determined. NO standards were prepared using diethylamine NONOate (DEANO). DEANO is an NO donor that releases NO spontaneously under physiological conditions, with a half-life of approximately 3 minutes. A vial containing 10 mg of DEANO was dissolved in 1 mL of 0.01 M NaOH; 10.3 μ L of this solution were diluted by the addition of 489.7 μ L of HBSS to generate a 1000 μ M stock solution. A 500 mM glucose stock solution was prepared and used to generate three sets of the same glucose gradient (0, 10, 20, 40, 60, 100, and 200 mM) in HBSS, with different DEANO concentrations (0, 20, and 200 μ M), as shown in table 3.1. Then, 50 μ L of each gradient was pipetted into a 96-well plate, along with 50 μ L of DAF-FM in different concentrations. The mixtures were incubated at 37°C for 30 minutes. Finally, the fluorescence intensity was measured in the plate reader using an excitation wavelength of 488 nm and emission wavelength of 515 nm.

3.3.5 Determination of RBC Hemolysis during Storage

Percent hemolysis was determined as the ratio of free Hb released into the surrounding media to the total Hb contained in the sample. Determination of Hb is based on a quantitative colorimetric method using Drabkin's solution. Drabkin's solution was prepared using a commercially available kit. Briefly, a vial of the Drabkin's reagent, which contains sodium bicarbonate, potassium ferricyanide, and potassium cyanide, was reconstituted in 1000 mL of DDW and 0.5 mL of 30% Brij 35 solution. This solution is hypotonic and able to lyse RBCs. The solution was then stored in an amber bottle and is stable for at least 6 months. Drabkin's solution oxidizes Hb and its derivatives to

Table 3.1 – Different DEANO Concentrations in Glucose Gradient Preparation

200 μ L total		DEANO, 0 μ M		DEANO, 20 μ M		DEANO, 200 μ M	
Glucose/mM	Glucose stock/ μ L	DEANO stock/ μ L	HBSS/ μ L	DEANO stock/ μ L	HBSS/ μ L	DEANO stock/ μ L	HBSS/ μ L
0	0	0	200	4	196	40	160
10	4	0	196	4	192	40	156
20	8	0	192	4	188	40	152
40	16	0	184	4	180	40	144
60	24	0	176	4	172	40	136
100	40	0	160	4	156	40	120
200	80	0	120	4	116	40	80

methemoglobin and further converts them to cyanmethemoglobin (HbCN), a colored compound having a maximum absorption at 540 nm.

Supernatant samples were prepared by 2-step centrifugation due to the high Hct of stored RBCs. Supernatant samples were prepared by first centrifuging the stored RBCs at 2000 *g* for 10 minutes and then centrifuging again at 15,000 *g* for 15 minutes. The resulting supernatant was then diluted 1/10 in Drabkin's solution. Similarly, the total Hb samples were prepared by diluting RBC samples 1/1000 in Drabkin's solution so that the final HbCN concentration fell within the range of the calibration curve (0-0.8 g/L HbCN). A 7.2 g/L HbCN stock standard was prepared by dissolving 72 mg of human Hb lyophilized powder into 10 mL of Drabkin's solution. Standards (0-0.8 g/L) were prepared from the stock solution with a series of appropriate dilutions. After mixing, samples and standards were incubated at room temperature, in the dark, for at least 30 minutes. Absorbance was read at 550 nm in the plate reader. The Hb concentration was then calculated from the calibration curve that was simultaneously generated. The sample Hct was determined as described previously. Hemolysis was then calculated according to the formula:⁵⁰

$$\% \text{ Hemolysis} = (\text{Supernatant Hb (g/l)} \times [100 - \text{Hct (\%)}]) / (\text{Total Hb (g/l)})$$

3.4 Results

3.4.1 Endothelium-Derived NO Stimulated by ATP Release from 36-Day Stored RBCs

The potential importance of increased ATP release from RBCs processed in CPD-N/AS-1N, shown in figure 2.10, is related to its well-established role as a stimulus of NO production in various cell types. A microfluidic device enabled RBC-derived ATP to diffuse to an endothelial layer and stimulate NO production. Devices similar to this one have been previously employed by our group to investigate the cellular communication mediated by ATP release from RBCs.⁴³ However, this is the first time that such a device has been used to investigate properties of stored RBCs.

The NO released from the endothelial cells was measured using the fluorogenic probe, DAF-FM. The amount of NO produced from endothelial cells stimulated by ATP released from flowing RBCs processed in CPD-N/AS-1N was normalized to the NO stimulated by ATP released from RBCs in CPD/AS-1 on each analysis day. In figure 3.7, the results are shown as the percent increase in NO release. The NO production by endothelial cells in the presence of RBCs processed with CPD-N/AS-1N was significantly increased ($p < 0.02$) by at least 25% throughout the first 22 days of storage, in comparison to RBCs processed in CPD/AS-1.

3.4.2 Results Verification by Two Control Experiments

Two negative control experiments were performed to ensure that this NO release was stimulated by flowing RBC-derived ATP. First, RBCs in CPD/AS-1 and CPD-N/AS-1N were incubated with GLI, an inhibitor of ATP release from RBCs.⁴⁷ The data in figure 3.8 show that the inhibition of RBCs stored in AS-1N with GLI decreased the NO release to a level

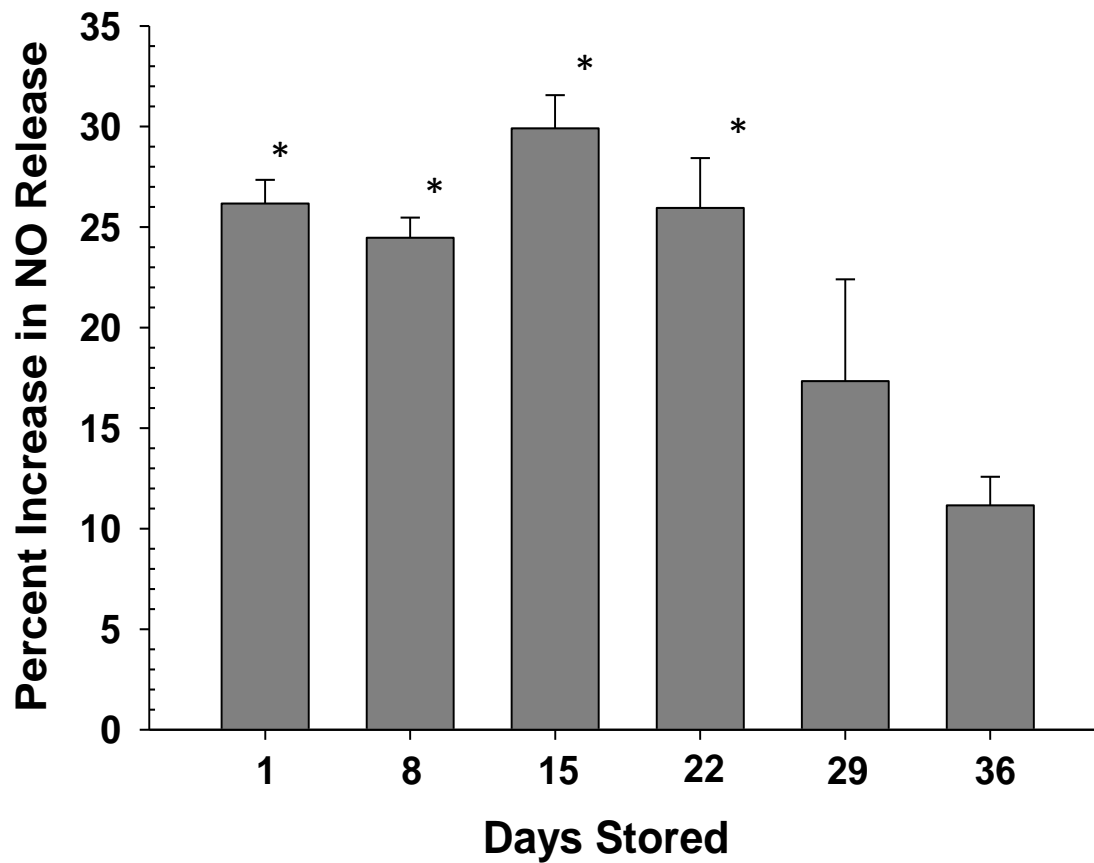


Figure 3.7 – The NO Release from the Endothelium Stimulated from Flow-Induced ATP from Stored RBCs in Different Storage Solutions. The percent increase in NO release from the endothelial cells (> 25% for the first 3 weeks of storage) is significantly higher when exposed to RBCs processed in CPD-N/AS-1N (* $p < 0.02$). Data represented as mean \pm s.e.m., n = 4.

that is statistically equal ($p = 0.742$) to cells stored in AS-1 with GLI. This strongly suggests that the increase in endothelium-derived NO is not due to stimulation by ATP resulting from RBC lysis. If ATP due to lysis was the stimulus for the enhanced NO production, GLI inhibition would have no effect on the results.

In addition to inhibition at the RBC level, a second control was performed at the endothelial level. Specifically, endothelial cells cultured on the microfluidic device were incubated with PPADS, which is a recognized inhibitor of the P2Y purinergic receptor for ATP.⁴⁹ As shown in figure 3.9, NO production in the presence of CPD-N/AS-1N processed RBCs, which had been significantly higher than when exposed to RBCs processed in CPD/AS-1, was unable to be stimulated to such increases when the endothelium was inhibited with PPADS. This provides further evidence that the increase in NO production from the endothelial cells is a direct result of ATP stimulation.

The combined data in figures 3.8 and 3.9 suggest that endothelium-derived levels of NO are strongly related to the ability of the RBC to release ATP, which, in turn, is affected by glucose levels in the collection and storage solutions.

3.4.3 The Effect of Glucose on NO Detection using Fluorescent Probe DAF-FM

Previous studies by our group have shown that glucose concentration has an effect on NO detection using the fluorescent probe DAF-FM DA, which a derivate of DAF-FM, used in the studies shown above. Thus, experiments were designed to evaluate this.

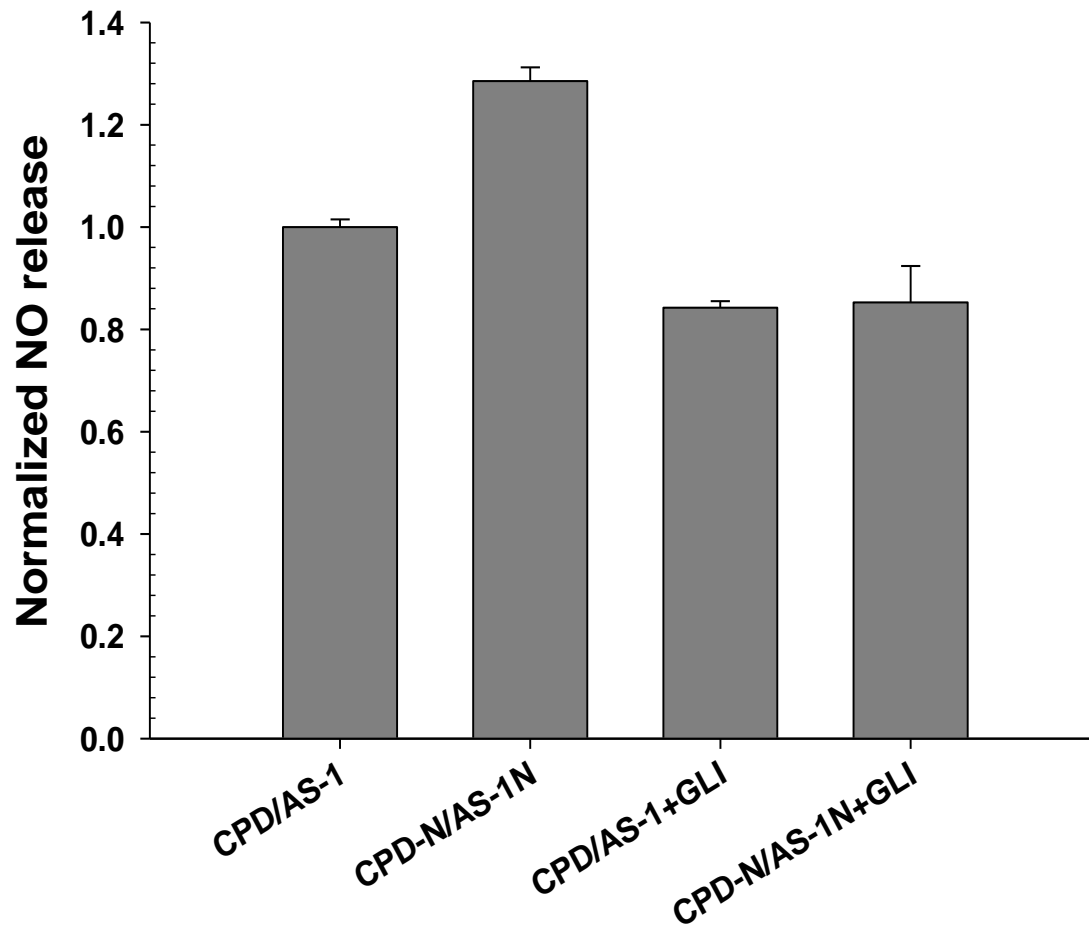


Figure 3.8 – The NO Release from the Endothelium in the Presence of RBCs Pretreated with GLI, an Inhibitor of RBC-Derived ATP Release. There is no significant increase in NO release ($p = 0.742$), regardless of the storage solution, when the stored RBCs are exposed to GLI, suggesting that this endothelium-derived NO is due to flow-induced ATP release from RBCs, not RBC lysis. Data represented as mean \pm s.e.m., $n = 4$.

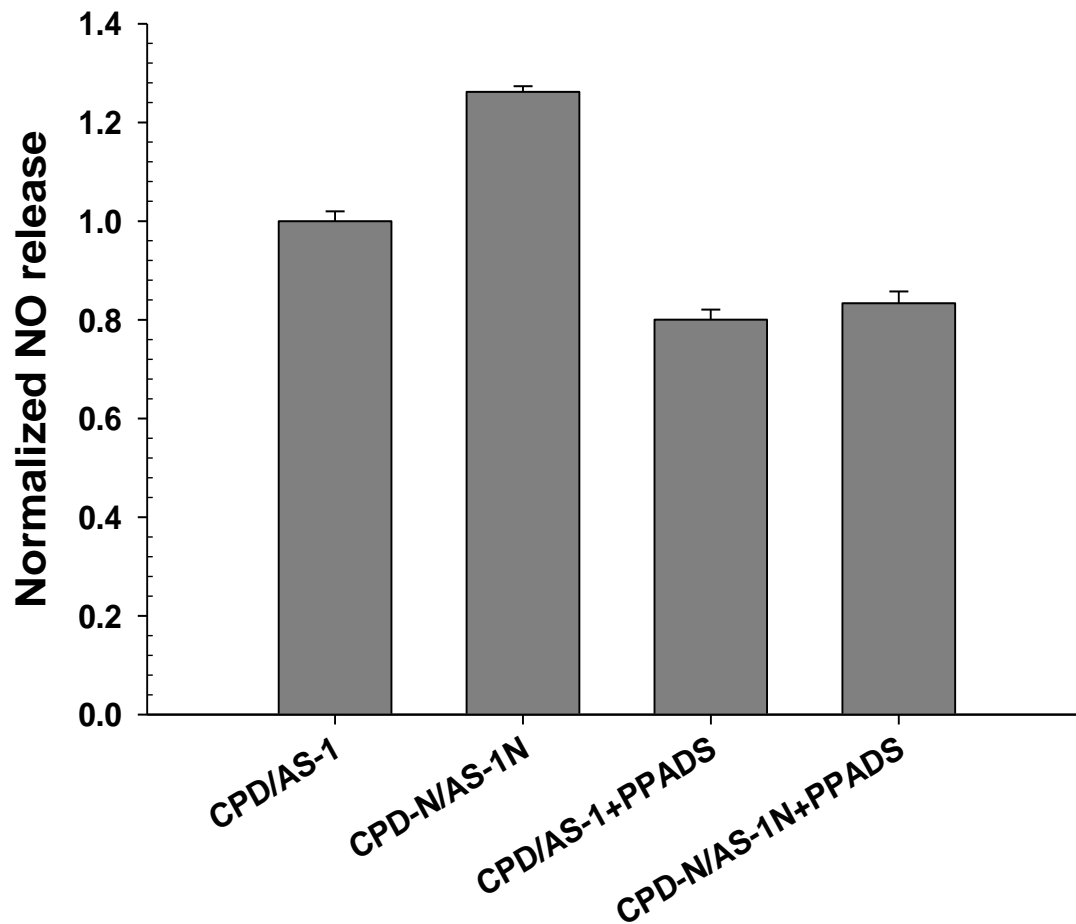


Figure 3.9 – The NO Release from the Endothelium Pretreated with PPADS, an Inhibitor of the ATP Binding Site, in the Presence of Stored RBCs. There is no significant increase in NO release ($p = 0.623$), regardless of the storage solution, when the endothelial cells in the presence of PPADS, suggesting that the increased NO signal is due to endothelial cell stimulation by ATP. Data represent mean \pm s.e.m., $n = 4$.

First, the amount of glucose that can diffuse across the endothelium layer cultured on the membrane of the previously described microfluidic device was determined. As shown in figure 3.10a, after pumping for 30 minutes at 37°C, the glucose levels in the HBSS obtained from the wells were 19.3 ± 0.6 mM and 6.4 ± 0.1 mM for 7% RBCs in AS-1 and AS-1N, respectively. Next, DEANO, the NO donor, was used to investigate the detection of different NO concentrations in the glucose gradient. The fluorescent signal tended to increase when the glucose concentration was higher than 50 mM; and this increase become larger when more DAF-FM was added (data not shown). However, as shown in figure 3.10b, when the final concentration of DAF-FM was 5 μ M, the concentration used in sections 3.4.1 and 3.4.2, the fluorescent intensity detected was statistically equivalent in 0, 10, and 100 μ M of DEANO with the glucose gradient from 0 to 100 mM. The combined data in figure 3.10, suggests that the glucose level in the probe well should not affect the NO detection using 5 μ M DAF-FM.

3.4.4 Percent Hemolysis of RBCs Stored for 36 Days

In the US, the Food and Drug Administration (FDA) requires that hemolysis of stored RBCs does not exceed 1%, while in Europe the recommendation is lower at 0.8%.⁵¹ Due to the importance of ATP in the maintenance of cell membrane integrity, the hemolysis of the RBCs processed in the CPD/AS-1 was compared to that of cells stored in CPD-N/AS-1N versions with and without periodic feeding with glucose. Figure 3.11 shows that the percent hemolysis remained statistically the same in the 3 conditions for the initial 3 weeks of storage. It remained statistically equivalent to 1% throughout 5 weeks

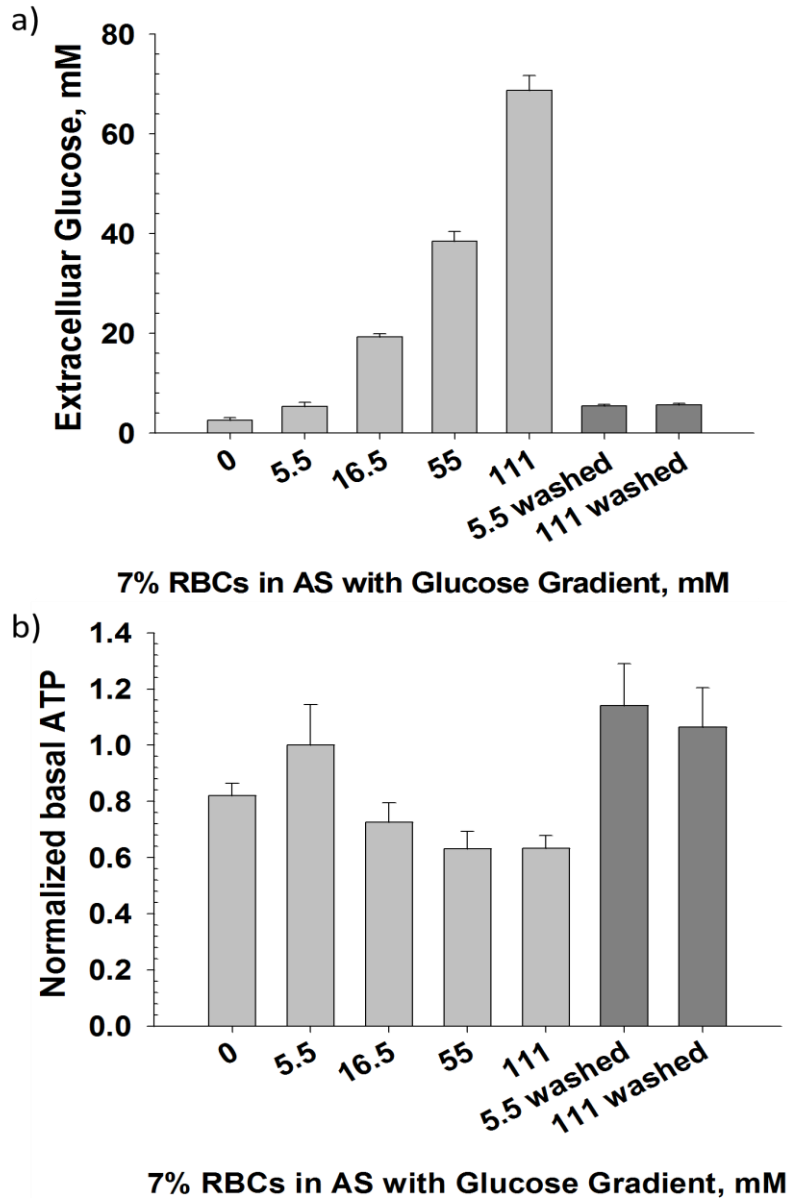


Figure 3.10 – The Effect of Glucose across the Endothelium Cultured on the Microfluidic Device on the Detection of NO using DAF-FM. The upper panel a) demonstrates the glucose diffused above the endothelium when pumping 7% stored RBCs in CPD/AS-1 or CPD-N/AS-1N for 30 minutes at 37°C. The sample with CPD/AS-1 (dark grey bar) was 19.3 ± 0.6 mM and the one with CPD-N/AS-1N (grey bar) was 6.4 ± 0.1 mM in glucose concentration. Data represented as mean \pm s.e.m., $n = 6$ wells. The lower panel b) shows the fluorescent intensity of 5 μ M DAF-FM reacted with 0, 10, 100 μ M of DEANO (NO donor) in glucose gradient ranging from 0 - 100 mM. Data represented as mean \pm s.e.m., $n = 3$ wells. Data from these results indicates that glucose diffused above endothelium should have a negligible effect on the NO detection using 5 μ M DAF-FM.

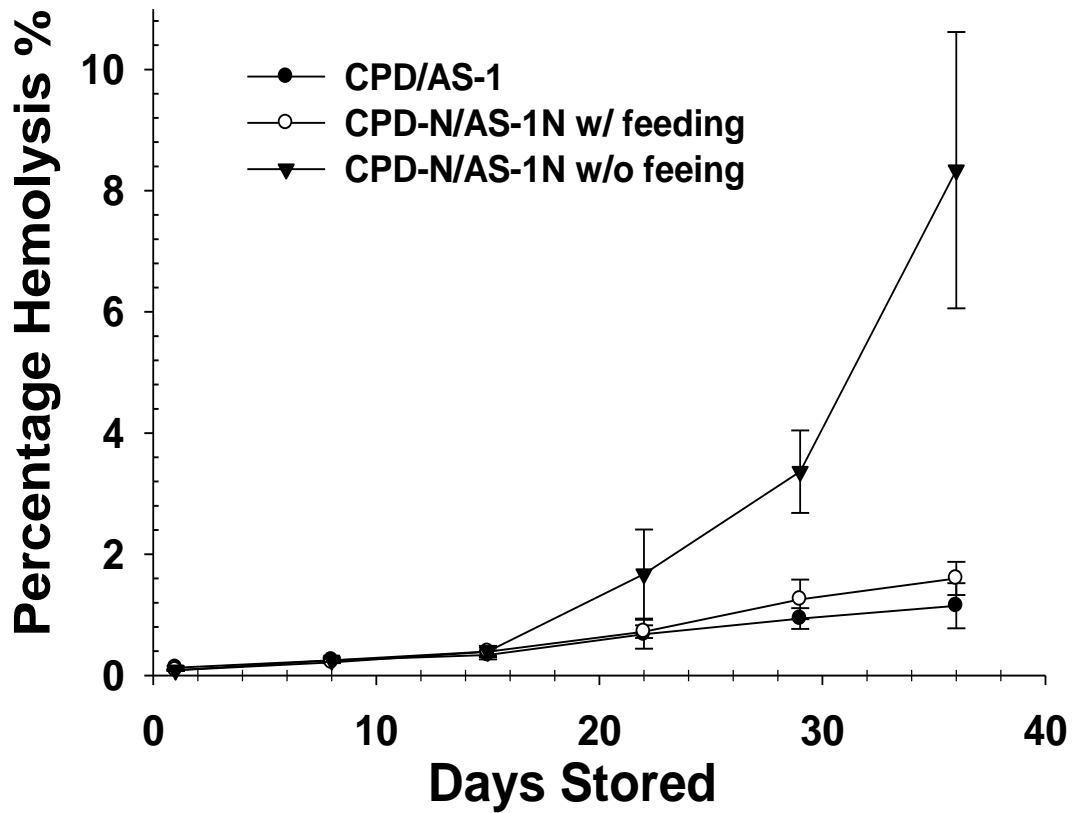


Figure 3.11 – The Percent Lysis of RBCs Stored in CPD/AS-1 (black circles), CPD-N/AS-1N with Periodic Glucose Feeding (white circles), and CPD-N/AS-1N without Periodic Glucose Feeding (black triangles). It is obvious from the data that AS-1N storage without glucose maintenance is detrimental to the RBCs. However, for those cells stored in AS-1N with glucose feeding, the extent of lysis is statistically equal to those cells stored in AS-1 ($p = 0.366$). Data represented as mean \pm s.e.m., $n = 4$.

of storage for both CPD/AS-1 and CPD-N/AS-1N with glucose maintenance. Importantly, the hemolysis values for these solutions were statistically equivalent ($p = 0.366$), suggesting that the normoglycemic storage solutions with feeding do not increase the rate of lysis in comparison to the currently accepted CPD/AS-1 processing protocol. In the absence of glucose (non-feeding protocol), the CPD-N/AS-1N solutions were not sufficient for maintaining acceptable hemolysis rates.

3.5 Discussion

The endothelium releases mediators to regulate the contraction and relaxation of underlying smooth muscle and thereby to actively adjust the blood vessel caliber to match blood flow to local tissue oxygen needs in the microcirculation.⁵²⁻⁵³ NO is one of the mediators that can relax the smooth muscle and can be both synthesized and released by RBCs and the endothelium. Roback *et al.* recently proposed the hypothesis of INOBA: that the reduced NO levels below a critical threshold in vascular beds would lead to increased vasoconstriction that results in less blood flow and insufficient oxygen delivery to end organs in patients who receive RBC transfusions.⁵⁴ In the hypothesis, it was also proposed that the factors leading to posttransfusion complications include impaired NO production, increased NO scavenging by stored RBCs, and reduced NO synthesis by the dysfunctional endothelial cells of critically ill patients. However, as mentioned in chapter 2, RBC-derived ATP stimulated NO release from the endothelium is the focus here in the investigation of the benefits of RBCs stored in normoglycemic

storage solution. The ATP release from RBCs processed in normoglycemic solutions (CPD-N/AS-1N), shown in figure 2.10, was increased in comparison to those processed with current protocols (CPD/AS-1). However, these data alone do not provide requisite evidence that INOBA in transfusion medicine is simply the result of decreased ATP release from RBCs due to high glucose levels in the solutions used to process whole blood. Therefore, a microfluidic device was employed to determine the origin of NO measured above an endothelium that was exposed to the RBCs processed in the different collection and storage solutions.

Once reliable cell culture on the microfluidic device and the manipulation of flow-induced RBC ATP were achieved, the cell-cell communication between the RBC and the endothelium was able to be investigated. The extracellular probe, DAF-FM, instead of the intracellular probe, DAF-FM DA, was used to determine how much NO was released from the endothelium for possible diffusion to the smooth muscle. The results from the microfluidic device experiments, shown in figures 3.7 - 3.9, suggest that the NO measured above the endothelium is a result of eNOS stimulation from RBC-derived ATP binding to the endothelium. The data in figure 3.7 indicate that the increased ATP release from RBCs stored in CPD-N/AS-1N stimulated more NO release from the endothelium, which has the potential for better vasodilation *in vivo*. The notion of ATP stimulating NO was enhanced by the use of GLI (an inhibitor of ATP release from RBC) and PPADS (a purinergic receptor inhibitor that blocks the ATP binding site). NO levels were not statistically increased when these antagonists were employed. Both of these

antagonists would affect endothelium-derived NO, but not necessarily RBC-derived NO. Furthermore, previous work by our group showed that RBC-derived NO is unable to diffuse across the endothelium layer cultured in this device. In these prior studies, half of the wells in the device were cultured with a confluent layer of endothelial cells, while the other half was not. Standards from the NO donor, DEANO, were pumped into the device, showing that the concentration of NO that crossed the polycarbonate membrane in the presence of endothelial cells was significantly lower than crossing the polycarbonate membrane alone. Thus, the data presented here provide evidence that the NO being measured in figure 3.7 is not RBC-derived, but rather, RBC-stimulated by ATP.

The glucose level in the experimental conditions minimally affected NO determinations using low concentration of DAF-FM (figure 3.10). However, another concern was the effect of the diffused glucose on the endothelial cells in the probe wells. Studies have shown that an elevated glucose level influences not only the functions of RBCs, but also endothelial cells. Madar *et al.* have shown that bovine aortic endothelial cells (bAECs) pretreated with 22 mM glucose for at least 2 weeks had decreased eNOS protein expression when compared to cells treated with 5 mM glucose.⁵⁵ Brownlee *et al.* demonstrated that eNOS activity of bAECs cultured in 30 mM glucose medium was inhibited through mitochondrial overproduction of superoxide.⁵⁶ On the contrary, Luscher *et al.* have shown that human aortic endothelial cells (hAECs) exposed to 22.2 mM glucose for 5 days had increased expression of eNOS mRNA and higher NO

production.⁵⁷ Thus, another control experiment of inhibiting eNOS function may need to be performed to eliminate this concern. eNOS inhibitors are mostly analogues of L-arginine and are therefore competitive inhibitors for eNOS, such as L-NG-nitroarginine methyl ester (L-NAME).⁵⁸ However, pumping the 7% RBCs in AS-1 would lead to a diffusion of ~20 mM glucose across the membrane to the probe well, which is a sufficiently high enough glucose level to result in dysfunctional endothelial cells based on the literature, though the 30-minute experiment period may be not long enough to manipulate the NO production.

The modified collection and storage solutions seem to have a beneficial effect on ATP release and subsequent NO production, which could be advantageous *in vivo*. However, another key component to successful blood transfusion is that the RBCs remain intact. In fact, regardless of how much NO is being stimulated or produced by the RBC, if RBC lysis is present, the bioavailability of NO will more than likely drop due to NO scavenging by free Hb. While no measurements involving cell survival were performed in this study, the percentage of RBCs that underwent hemolysis did not significantly increase when stored in the normoglycemic versions of the collection and storage solutions when followed by maintenance of glucose levels. When these cells were not maintained with physiological levels of glucose by periodic feeding, the lysis did increase, as to be expected as glucose and ATP are both key components in maintaining proper cellular membrane structure and functionality. It is noteworthy that the hemolysis rates for the RBCs stored during this study would most likely improve, i.e., a reduction in the

hemolysis rate would be seen if the collected whole blood had been leukocyte reduced by buffy coat removal and filtration. It has been shown that mean hemolysis rates are significantly lowered when stored products are leukoreduced by filtration.⁵⁹ This method was avoided here due to the small volume of samples that were collected from donors. However, future studies involving standard collection volumes would most certainly benefit from leukoreduction by filtration methods.

The data shown here and in chapter 2 demonstrate that RBCs stored in the standard CPD/AS-1 solutions have impaired ability to release ATP in response to mechanical deformation compared to the RBCs stored in the normoglycemic condition. This decreased RBC-derived ATP would further adversely affect the healthy endothelium to release NO. In addition, the RBCs stored in normoglycemic condition, maintaining by periodic glucose feeding had a not significantly different hemolysis rate during 36 day storage from the RBCs stored in CPD/AS-1. This indicates that the influence of free Hb scavenging on NO bioavailability is equivalent for the normoglycemic and hyperglycemic storage. Although the RBC-derived NO was not determined here, the previous work in our group implied that this NO may not diffuse through the endothelium to smooth muscle. Thus, the origin of INOBA may be the reduced endothelium-derived NO weakly stimulated by the impaired ATP release from the RBCs stored in hyperglycemic solutions, which would result in reduced dilation, less blood flow and insufficient oxygen delivery, further leading to possible posttransfusion complications.

REFERENCES

REFERENCES

1. Vanhoutte, P. M., The Endothelium--Modulator of Vascular Smooth-Muscle Tone. *The New England Journal of Medicine* 1988, 319 (8), 512-513.
2. Palmer, R. M. J.; Ferrige, A. G.; Moncada, S., Nitric-Oxide Release Accounts for the Biological-Activity of Endothelium-Derived Relaxing Factor. *Nature* 1987, 327 (6122), 524-526.
3. Sprague, R. S.; Ellsworth, M. L.; Stephenson, A. H.; Lonigro, A. J., ATP: The Red Blood Cell Link to NO and Local Control of the Pulmonary Circulation. *The American Journal of Physiology - Heart and Circulatory Physiology* 1996, 271 (6), H2717-H2722.
4. Bergfeld, G. R.; Forrester, T., Release of ATP from Human Erythrocytes in Response to a Brief Period of Hypoxia and Hypercapnia. *Cardiovascular Research* 1992, 26 (1), 40-47.
5. Adak, S.; Chowdhury, S.; Bhattacharyya, M., Dynamic and Electrokinetic Behavior of Erythrocyte Membrane in Diabetes Mellitus and Diabetic Cardiovascular Disease. *Biochimica et Biophysica Acta* 2008, 1780 (2), 108-115.
6. Edwards, J.; Sprung, R.; Sprague, R.; Spence, D., Chemiluminescence Detection of ATP Release from Red Blood Cells Upon Passage through Microbore Tubing. *The Analyst* 2001, 126 (8), 1257-1260.
7. Price, A. K.; Fischer, D. J.; Martin, R. S.; Spence, D. M., Deformation-Induced Release of ATP from Erythrocytes in a Poly(Dimethylsiloxane)-Based Microchip with Channels That Mimic Resistance Vessels. *Analytical Chemistry* 2004, 76 (16), 4849-4855.
8. Light, D. B.; Capes, T. L.; Gronau, R. T.; Adler, M. R., Extracellular ATP Stimulates Volume Decrease in Necturus Red Blood Cells. *The American Journal of Physiology* 1999, 277 (3 Pt 1), C480-491.
9. Meyer, J. A.; Froelich, J. M.; Reid, G. E.; Karunarathne, W. K. A.; Spence, D. M., Metal-Activated C-Peptide Facilitates Glucose Clearance and the Release of a Nitric Oxide Stimulus Via the Glut1 Transporter. *Diabetologia* 2008, 51 (1), 175-182.
10. Raththagala, M.; Karunarathne, W.; Kryziniak, M.; McCracken, J.; Spence, D. M., Hydroxyurea Stimulates the Release of ATP from Rabbit Erythrocytes through an Increase in Calcium and Nitric Oxide Production. *European Journal of Pharmacology* 2010, 645 (1-3), 32-38.
11. Busse, R.; Ogilvie, A.; Pohl, U., Vasomotor Activity of Diadenosine Triphosphate and Diadenosine Tetraphosphate in Isolated Arteries. *American Journal of Physiology* 1988, 254 (5), H828-H832.

12. Communi, D.; Raspe, E.; Piroton, S.; Boeynaems, J. M., Coexpression of P-2y and P-2u Receptors on Aortic Endothelial-Cells - Comparison of Cell Localization and Signaling Pathways. *Circulation Research* 1995, 76 (2), 191-198.
13. Arnal, J. F.; Dinh-Xuan, A. T.; Pueyo, M.; Darblade, B.; Rami, J., Endothelium-Derived Nitric Oxide and Vascular Physiology and Pathology. *Cellular and Molecular Life Sciences : CMLS* 1999, 55 (8-9), 1078-1087.
14. Marrero, M. B.; Venema, V. J.; Ju, H.; He, H.; Liang, H.; Caldwell, R. B.; Venema, R. C., Endothelial Nitric Oxide Synthase Interactions with G-Protein-Coupled Receptors. *The Biochemical Journal* 1999, 343 Pt 2, 335-340.
15. Bogle, R. G.; Coade, S. B.; Moncada, S.; Pearson, J. D.; Mann, G. E., Bradykinin and ATP Stimulate L-Arginine Uptake and Nitric-Oxide Release in Vascular Endothelial-Cells. *Biochemical and Biophysical Research Communications* 1991, 180 (2), 926-932.
16. Ignarro, L. J.; Byrns, R. E.; Wood, K. S., Endothelium-Dependent Modulation of Cgmp Levels and Intrinsic Smooth Muscle Tone in Isolated Bovine Intrapulmonary Artery and Vein. *Circulation Research* 1987, 60 (1), 82-92.
17. Carvajal, J. A.; Germain, A. M.; Huidobro-Toro, J. P.; Weiner, C. P., Molecular Mechanism of Cgmp-Mediated Smooth Muscle Relaxation. *Journal of Cellular Physiology* 2000, 184 (3), 409-420.
18. Halpin, S. T.; Spence, D. M., Direct Plate-Reader Measurement of Nitric Oxide Released from Hypoxic Erythrocytes Flowing through a Microfluidic Device. *Analytical Chemistry* 2010, 82 (17), 7492-7497.
19. Ulker, P.; Sati, L.; Celik-Ozenci, C.; Meiselman, H. J.; Baskurt, O. K., Mechanical Stimulation of Nitric Oxide Synthesizing Mechanisms in Erythrocytes. *Biorheology* 2009, 46 (2), 121-132.
20. Baskurt, O. K.; Ulker, P.; Meiselman, H. J., Nitric Oxide, Erythrocytes and Exercise. *Clinical Hemorheology and Microcirculation* 2011, 49 (1-4), 175-181.
21. Hakim, T. S.; Sugimori, K.; Camporesi, E. M.; Anderson, G., Half-Life of Nitric Oxide in Aqueous Solutions with and without Haemoglobin. *Physiological Measurement* 1996, 17 (4), 267-277.
22. Halpin, S. T. Modeling the Vascular System with Microfluidic Technology. Ph D, Michigan State University, Chemistry, 2012.
23. Wallis, J. P., Nitric Oxide and Blood: A Review. *Transfusion Medicine* 2005, 15 (1), 1-11.

24. Roback, J. D.; Neuman, R. B.; Quyyumi, A.; Sutliff, R., Insufficient Nitric Oxide Bioavailability: A Hypothesis to Explain Adverse Effects of Red Blood Cell Transfusion. *Transfusion* 2011, 51 (4), 859-866.
25. Bohlen, H. G.; Zhou, X.; Unthank, J. L.; Miller, S. J.; Bills, R., Transfer of Nitric Oxide by Blood from Upstream to Downstream Resistance Vessels Causes Microvascular Dilation. *The American Journal of Physiology - Heart and Circulatory Physiology* 2009, 297 (4), H1337-1346.
26. Fahraeus, R., The Suspension Stability of the Blood. *Physiological Reviews* 1929, 9 (2), 241-274.
27. Chen, K.; Pittman, R. N.; Popel, A. S., Nitric Oxide in the Vasculature: Where Does It Come from and Where Does It Go? A Quantitative Perspective. *Antioxidants & Redox Signaling* 2008, 10 (7), 1185-1198.
28. Chen, K.; Piknova, B.; Pittman, R. N.; Schechter, A. N.; Popel, A. S., Nitric Oxide from Nitrite Reduction by Hemoglobin in the Plasma and Erythrocytes. *Nitric Oxide : Biology and Chemistry / Official Journal of the Nitric Oxide Society* 2008, 18 (1), 47-60.
29. Azarov, I.; Liu, C.; Reynolds, H.; Tsekouras, Z.; Lee, J. S.; Gladwin, M. T.; Kim-Shapiro, D. B., Mechanisms of Slower Nitric Oxide Uptake by Red Blood Cells and Other Hemoglobin-Containing Vesicles. *The Journal of Biological Chemistry* 2011, 286 (38), 33567-33579.
30. Balasubramaniam, P.; Malathi, A., Comparative Study of Hemoglobin Estimated by Drabkin's and Sahli's Methods. *Journal of Postgraduate Medicine* 1992, 38 (1), 8-9.
31. Kumar, N. M.; Gilula, N. B., The Gap Junction Communication Channel. *Cell* 1996, 84 (3), 381-388.
32. Pawson, T., Protein Modules and Signalling Networks. *Nature* 1995, 373 (6515), 573-580.
33. Guo, F.; French, J. B.; Li, P.; Zhao, H.; Chan, C. Y.; Fick, J. R.; Benkovic, S. J.; Huang, T. J., Probing Cell-Cell Communication with Microfluidic Devices. *Lab on a Chip* 2013, 13 (16), 3152-3162.
34. El-Ali, J.; Sorger, P. K.; Jensen, K. F., Cells on Chips. *Nature* 2006, 442 (7101), 403-411.
35. Huh, D.; Hamilton, G. A.; Ingber, D. E., From 3d Cell Culture to Organs-on-Chips. *Trends in Cell Biology* 2011, 21 (12), 745-754.
36. Young, E. W.; Beebe, D. J., Fundamentals of Microfluidic Cell Culture in Controlled Microenvironments. *Chemical Society Reviews* 2010, 39 (3), 1036-1048.

37. Unger, M. A.; Chou, H. P.; Thorsen, T.; Scherer, A.; Quake, S. R., Monolithic Microfabricated Valves and Pumps by Multilayer Soft Lithography. *Science* 2000, *288* (5463), 113-116.
38. Xia, Y. N.; Whitesides, G. M., Soft Lithography. *Annual Review of Materials Research* 1998, *28*, 153-184.
39. Whitesides, G. M.; Ostuni, E.; Takayama, S.; Jiang, X. Y.; Ingber, D. E., Soft Lithography in Biology and Biochemistry. *Annual Review of Biomedical Engineering* 2001, *3*, 335-373.
40. Duffy, D. C.; McDonald, J. C.; Schueller, O. J. A.; Whitesides, G. M., Rapid Prototyping of Microfluidic Systems in Poly(Dimethylsiloxane). *Analytical Chemistry* 1998, *70* (23), 4974-4984.
41. Zhang, J.; Tan, K. L.; Hong, G. D.; Yang, L. J.; Gong, H. Q., Polymerization Optimization of Su-8 Photoresist and Its Applications in Microfluidic Systems and MemS. *Journal of Micromechanics and Microengineering* 2001, *11* (1), 20-26.
42. Genes, L. I.; Tolan, N. V.; Hulvey, M. K.; Martin, R. S.; Spence, D. M., Addressing a Vascular Endothelium Array with Blood Components Using Underlying Microfluidic Channels. *Lab on a Chip* 2007, *7* (10), 1256-1259.
43. Halpin, S. T.; Spence, D. M., Direct Plate-Reader Measurement of Nitric Oxide Released from Hypoxic Erythrocytes Flowing through a Microfluidic Device. *Analytical Chemistry* 2010, *82* (17), 7492-7497.
44. Hakim, T. S.; Sugimori, K.; Camporesi, E. M.; Anderson, G., Half-Life of Nitric Oxide in Aqueous Solutions with and without Haemoglobin. *Physiological Measurement* 1996, *17* (4), 267-277.
45. Kojima, H.; Nakatsubo, N.; Kikuchi, K.; Urano, Y.; Higuchi, T.; Tanaka, J.; Kudo, Y.; Nagano, T., Direct Evidence of NO Production in Rat Hippocampus and Cortex Using a New Fluorescent Indicator: Daf-2 Da. *Neuroreport* 1998, *9* (15), 3345-3348.
46. McDonald, J. C.; Duffy, D. C.; Anderson, J. R.; Chiu, D. T.; Wu, H. K.; Schueller, O. J. A.; Whitesides, G. M., Fabrication of Microfluidic Systems in Poly(Dimethylsiloxane). *Electrophoresis* 2000, *21* (1), 27-40.
47. Sprague, R. S.; Ellsworth, M. L.; Stephenson, A. H.; Kleinhenz, M. E.; Lonigro, A. J., Deformation-Induced ATP Release from Red Blood Cells Requires Cfr Activity. *The American Journal of Physiology - Heart and Circulatory Physiology* 1998, *275* (5), H1726-H1732.
48. Sprague, R. S.; Ellsworth, M. L.; Stephenson, A. H.; Lonigro, A. J., Participation of Camp in a Signal-Transduction Pathway Relating Erythrocyte Deformation to ATP

Release. *The American Journal of Physiology - Cell Physiology* 2001, 281 (4), C1158-C1164.

49. Lambrecht, G.; Friebe, T.; Grimm, U.; Windscheif, U.; Bungardt, E.; Hildebrandt, C.; Baumert, H. G.; Spatz-Kumbel, G.; Mutschler, E., Ppads, a Novel Functionally Selective Antagonist of P2 Purinoceptor-Mediated Responses. *European Journal of Pharmacology* 1992, 217 (2-3), 217-219.

50. Han, V.; Serrano, K.; Devine, D. V., A Comparative Study of Common Techniques Used to Measure Haemolysis in Stored Red Cell Concentrates. *Vox Sanguinis* 2010, 98 (2), 116-123.

51. Sawant, R. B.; Jathar, S. K.; Rajadhyaksha, S. B.; Kadam, P. T., Red Cell Hemolysis During Processing and Storage. *Asian Journal of Transfusion Science* 2007, 1 (2), 47-51.

52. Villar, I. C.; Francis, S.; Webb, A.; Hobbs, A. J.; Ahluwalia, A., Novel Aspects of Endothelium-Dependent Regulation of Vascular Tone. *Kidney International* 2006, 70 (5), 840-853.

53. Singel, D. J.; Stamler, J. S., Chemical Physiology of Blood Flow Regulation by Red Blood Cells: The Role of Nitric Oxide and S-Nitrosohemoglobin. *Annual Review of Physiology* 2005, 67, 99-145.

54. Roback, J. D.; Neuman, R. B.; Quyyumi, A.; Sutliff, R., Insufficient Nitric Oxide Bioavailability: A Hypothesis to Explain Adverse Effects of Red Blood Cell Transfusion. *Transfusion* 2011, 51 (4), 859-866.

55. Noyman, I.; Marikovsky, M.; Sasson, S.; Stark, A. H.; Bernath, K.; Seger, R.; Madar, Z., Hyperglycemia Reduces Nitric Oxide Synthase and Glycogen Synthase Activity in Endothelial Cells. *Nitric Oxide : Biology and Chemistry / Official Journal of the Nitric Oxide Society* 2002, 7 (3), 187-193.

56. Du, X. L.; Edelstein, D.; Dimmeler, S.; Ju, Q.; Sui, C.; Brownlee, M., Hyperglycemia Inhibits Endothelial Nitric Oxide Synthase Activity by Posttranslational Modification at the Akt Site. *The Journal of Clinical Investigation* 2001, 108 (9), 1341-1348.

57. Cosentino, F.; Hishikawa, K.; Katusic, Z. S.; Luscher, T. F., High Glucose Increases Nitric Oxide Synthase Expression and Superoxide Anion Generation in Human Aortic Endothelial Cells. *Circulation* 1997, 96 (1), 25-28.

58. Rees, D. D.; Palmer, R. M.; Schulz, R.; Hodson, H. F.; Moncada, S., Characterization of Three Inhibitors of Endothelial Nitric Oxide Synthase in Vitro and in Vivo. *British Journal of Pharmacology* 1990, 101 (3), 746-752.

59. Heaton, W. A.; Holme, S.; Smith, K.; Brecher, M. E.; Pineda, A.; AuBuchon, J. P.; Nelson, E., Effects of 3-5 Log₁₀ Pre-Storage Leucocyte Depletion on Red Cell Storage and Metabolism. *British Journal of Haematology* 1994, 87 (2), 363-368.

Chapter 4 – Hyperglycemia and Reduced ATP Release from RBCs

4.1 Introduction

The term hyperglycemia usually describes a condition in which an excessive amount of glucose, generally higher than 11 mM, exists in the blood plasma. Hyperglycemia is a hallmark sign of diabetes, which is a medical condition with uncontrolled, elevated blood glucose levels and is associated with a large variety of diabetic complications. Specifically, red blood cells (RBCs) obtained from people with diabetes are usually less deformable,¹ have elevated oxidative stress,² and form advanced glycation endproducts (AGEs).³ Interestingly, these impaired properties also occur in RBCs stored in modern aqueous storage solutions used in transfusion medicine. Collectively these properties are referred to as the RBC storage lesions.⁴⁻⁶

Changes in the RBC are not completely surprising considering the glucose level in modern storage solutions. As described in chapter 1, ~ 450 mL of whole blood is drawn into 63 mL of the anticoagulant, citrate phosphate dextrose (CPD) solution, which has a glucose level of 129 mM prior to the collection of whole blood. After centrifugation, the RBC suspension (~ 220 mL, containing ~ 40 mL of CPD-plasma) is separated and added to 100 mL of an additive solution (AS-1) that contains glucose at a concentration of 111 mM.⁷ Therefore, a unit of stored RBCs in this system should have a hematocrit (Hct) of 55-60% with the estimated final glucose concentration greater than 40 mM.

Due to similarities of diabetic and stored RBCs, normoglycemic versions of the collection and storage solutions (CPD-N/AS-1N) were prepared and used to store the purified RBCs. This system was compared with the CPD/AS-1 systems, to investigate various properties of the RBCs during storage. As discussed previously, collection and storage in CPD-N/AS-1N followed by periodic feeding of the stored cells to maintain normoglycemic levels, results in statistically higher adenosine triphosphate (ATP) release values 4 weeks into storage (when compared to the values for cells processed in typical CPD/AS-1 solutions). This RBC-derived ATP has a significant impact on endothelium-derived nitric oxide (NO).⁸⁻¹⁰ However, the mechanism behind this phenomenon is unclear.

RBCs have millimolar concentrations of intracellular ATP and are able to release portions of that ATP under a variety of external stimuli, such as hypoxia (low oxygen),¹¹ mechanical stress,¹²⁻¹³ low pH¹⁴ and changes in osmotic pressure.¹⁵ A signal transduction pathway of the deformation-induced ATP release has been proposed by Sprague *et al.*¹⁶⁻¹⁸ Mechanical deformation of the cell membrane activates the G-protein coupled receptor (GPCR), resulting in adenylyl cyclase that converts ATP to cyclic adenosine monophosphate (cAMP), which directly leads to the phosphorylation of cystic fibrosis transmembrane conductance regulator (CFTR) protein by protein kinase A, stimulating ATP release through a yet unknown separate ATP releasing channel.¹⁷⁻²¹

The mechanism of ATP release responding to low oxygen has been also proposed to

occur through this pathway.²² Specifically, hemoglobin (Hb), with a significant amount binding to the RBC membrane,²³ undergoes a conformational change as it releases oxygen,²⁴ resulting in similar mechanical activation of G-protein in the RBC. Furthermore, physiological low pH increases the tendency of Hb to release oxygen by altering its structure, which may also lead to a similar mechanism of increasing ATP release. Sprague *et al.* have also demonstrated that decreased deformability of RBC membranes reduces the release of ATP in response to low oxygen, by treating RBCs with diamide, a compound that decreases RBC deformability, but does not directly inhibit the signaling pathways of ATP release.²² In addition, Adler *et al.* have shown that increased osmotic fragility of RBCs decreases cell volume recovery in response to hypotonic stock and reduces endogenous extracellular ATP.¹⁵ Therefore, some physical and biochemical changes, which alter the deformability and osmotic fragility of RBC membrane, may occur during storage in hyperglycemic conditions and thereby impair the ability of the RBC to release ATP.

The RBC membrane is a composite of a lipid bilayer occupied by transmembrane proteins, supported by a spectrin-based cytoskeleton (figure 4.1).²⁵ Lipids are composed of cholesterol and phospholipids. The 4 major phospholipids, including those on the outer surface of RBC membrane, such as phosphatidyl ethanolamine (PE) and sphingomyelin (SM), and the ones on the inner surface, such as phosphatidyl serine (PS)

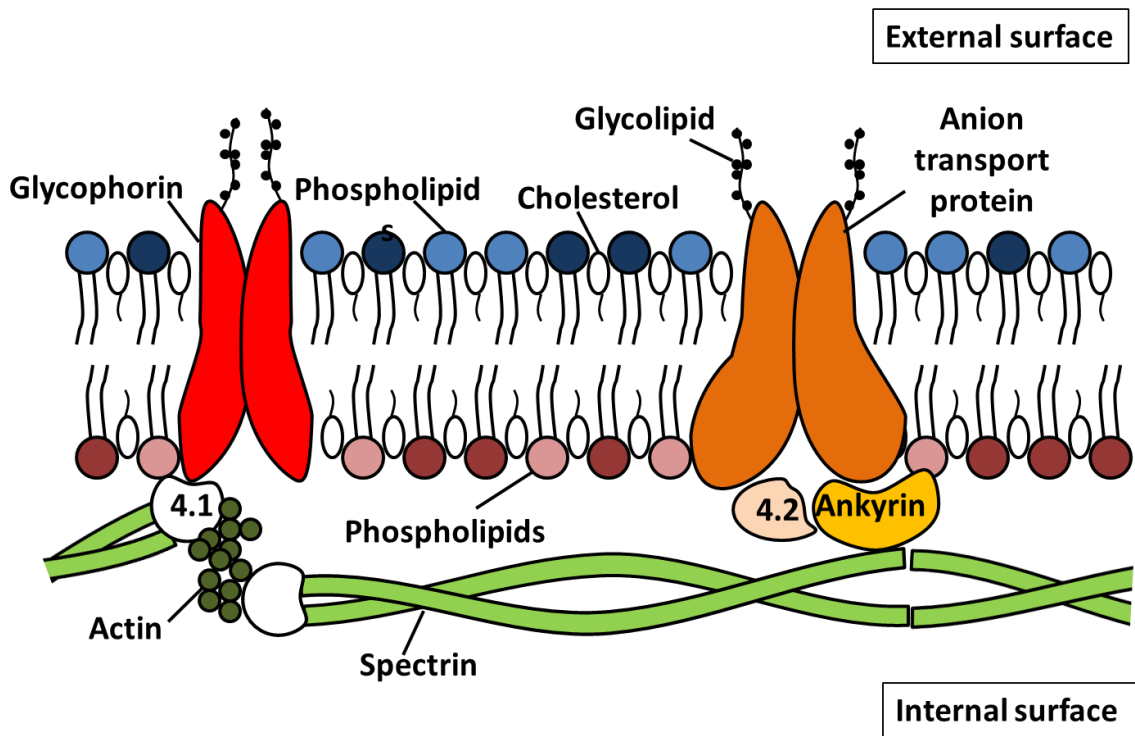


Figure 4.1 – Diagram of a Cross Section of the RBC Membrane. The RBC membrane is a composite of a lipid bilayer occupied by transmembrane proteins, supported by a spectrin-based cytoskeleton. Lipids are composed of cholesterol and phospholipids. The 4 major phospholipids are distributed asymmetrically within the two layers of membrane. Integral proteins, including glycophorin and the anion transport protein (Band 3) are embedded in the membrane via hydrophobic interactions with lipids. Peripheral proteins, including spectrin, ankyrin, actin, Band 4.1 and 4.2, are located on the inner cytoplasmic side of the lipid bilayer, forming the RBC cytoskeleton, anchored via integral proteins. For interpretation of the references to color in this and all other figures, the reader is referred to the electronic version of this dissertation.

and phosphatidyl ethanolamine (PE), are distributed within the two layers of membrane. Proteins are also not organized equally in the membrane. Proteins that are embedded in the membrane via hydrophobic interactions with lipids, such as glycophorin and band 3 (the anion transport protein), are termed integral proteins (IP). A second class of membrane proteins, the peripheral proteins (PP), which are located on the inner cytoplasmic side of the lipid bilayer, are anchored via integral proteins. The PPs, including spectrin, ankyrin, actin, band 4.1 and 4.2, form the RBC cytoskeleton, responsible for membrane elasticity and stability.

Studies in proteomics have shown that oxidation, as well as the breakdown of structural proteins, already occurs in the first weeks of storage.²⁶⁻²⁸ Specifically, signs of oxidation are observed in band 3 and the cytoskeletal proteins 4.1, 4.2, and spectrin during the first several days, followed by breakdown of actin and ankyrin, as well as crosslinking of spectrin.²⁶ Membrane protein oxidation, glycation, and breakdown of actin filaments have also been observed when RBCs were exposed to high glucose (>25 mM).²⁹ This protein damage may cause dysfunction in the RBC membrane in terms of deformability. Hyperglycemia-induced membrane damage seems to be related to glucose-based reactions, including glucose autoxidation, protein glycation, and formation of advanced glycation end-products (AGEs).³⁰⁻³² Glucose chemically reacts with primary amine groups in proteins, initially forming reversible Schiff base products within minutes, and then undergoing an Amadori rearrangement to form the Amadori product, a more

stable ketoamine compound, within hours to weeks, as shown in figure 4.2.³³ During Amadori reorganization, the highly reactive intermediate carbonyl groups, such as α -dicarbonyls, may react with amino, sulfhydryl, and guanidine functional groups in proteins, which results in denaturation, and cross-linking of the targeted proteins.³⁴ In addition, reactions between lysine and arginine functional groups on proteins and α -dicarbonyls, lead to the irreversible formation of stable AGE compounds, such as N^ε-(carboxymethyl)lysine (CML).³⁵

Hyperglycemia can also induce the polyol pathway in the RBC. Through this pathway, as shown in figure 4.3, glucose is reduced to sorbitol via aldose reductase (AR), which oxidizes the reducing form of nicotinamide adenine dinucleotide phosphate (NADPH) to NADP⁺. Sorbitol dehydrogenase (SDH) can then oxidize sorbitol to fructose while converting nicotinamide adenine dinucleotide (NAD⁺) to NADH. This can return to the glycolysis pathway by phosphorylating fructose to fructose-6-phosphate through hexokinase (HK). Glucose uptake at the normal ambient glucose level (5.5 mM) only accounts for about 2-3% of total glucose metabolism; however, this increases to 11% when the glucose concentration reaches 50 mM.³⁶ The normal function of the polyol pathway in human RBCs is unknown. However, when the activity of the polyol pathway in the RBC increases with rising glucose levels, this pathway contributes to oxidative stress by depleting the cofactor NADPH, which is required for the regeneration of

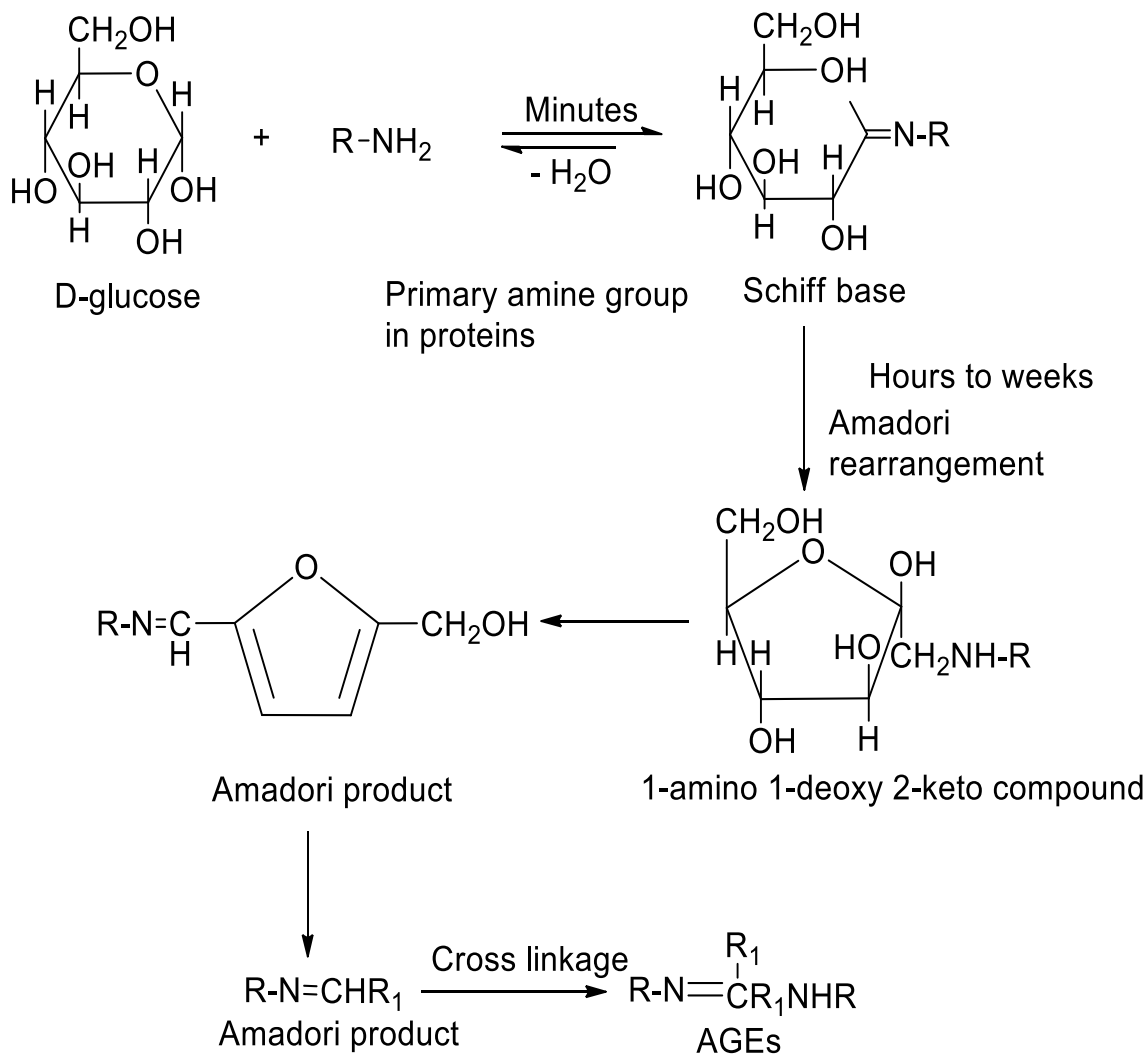


Figure 4.2 – Simplified Reaction Pathway Involved in Protein Glycation and the Formation of AGEs. Reducing sugar, such as glucose, can chemically react with primary amine groups in proteins, initially forming the reversible Schiff base within minutes. During hours to weeks, it forms the more stable ketoamine product through an Amadori rearrangement and further converts to the reactive Amadori product. When large amounts of these products are accumulated, they tend to form a series of more reactive protein-bound moieties, AGEs.

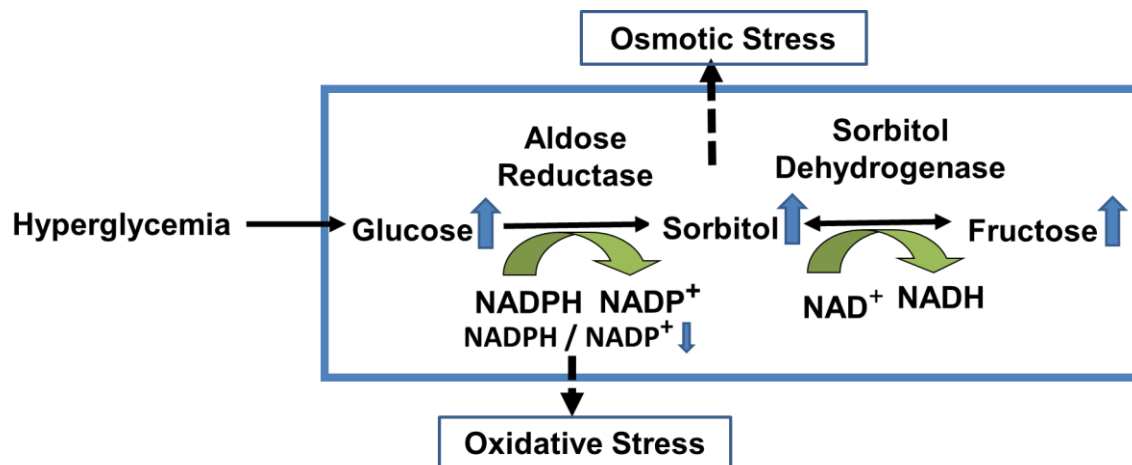


Figure 4.3 – The Mechanism and Effect of the Hyperglycemia-Induced Polyol Pathway. Increased activity of aldose reductase, induced by hyperglycemia, converts glucose to sorbitol while oxidizing NADPH to NADP⁺. Next, sorbitol can be oxidized by sorbitol dehydrogenase while converting NAD⁺ to NADH. Increased performance of this pathway in RBCs leads to adverse effects, such as osmotic stress, oxidative stress, and even protein glycation. For interpretation of the references to color in this and all other figures, the reader is referred to the electronic version of this dissertation.

glutathione (GSH), and the depletion of NAD⁺ in the second phase leads to more glucose entering into the polyol pathway. The oxidative stress rising from storage conditions may result in lipid peroxidation of the RBC membrane, which may further affect the deformability of RBCs. The membrane lipids, both polyunsaturated fatty acid (PFA) and cholesterol, can be oxidized through non-enzymatic mechanisms.³⁷ The free radical-mediated peroxidation (shown in figure 4.4) of PFA forms reactive carbonyl end-products in the cell, one of which is malondialdehyde (MDA), a commonly known marker of oxidative stress.³⁸

In addition, the high-glucose induced polyol pathway leads to osmotic stress. Sorbitol, the product from the polyol pathway, cannot pass the cell membrane and accumulates intracellularly, and thereby has an effect on the osmotic pressure and, consequently, the deformability of RBCs. Bareford *et al.* have been demonstrated that the incubation of RBCs obtained from healthy controls in a 50 mM glucose buffer at 37°C for 2 hours resulted in a pronounced accumulation of sorbitol and a significantly decreased ability ($p < 0.02$) of RBCs to filter through 3 μm diameter straight channel pores, as compared to RBCs incubated in 5 mM glucose buffer.³⁹ This work also showed that when sorbinil, an inhibitor preventing sorbitol accumulation, was added to the incubation buffer, there was no longer a decreased filterability of RBCs in hyperglycemic conditions.

The RBC membrane is semipermeable, which allows water and anions pass through freely. Thus, RBCs are sensitive to osmosis occurring across the membrane. The

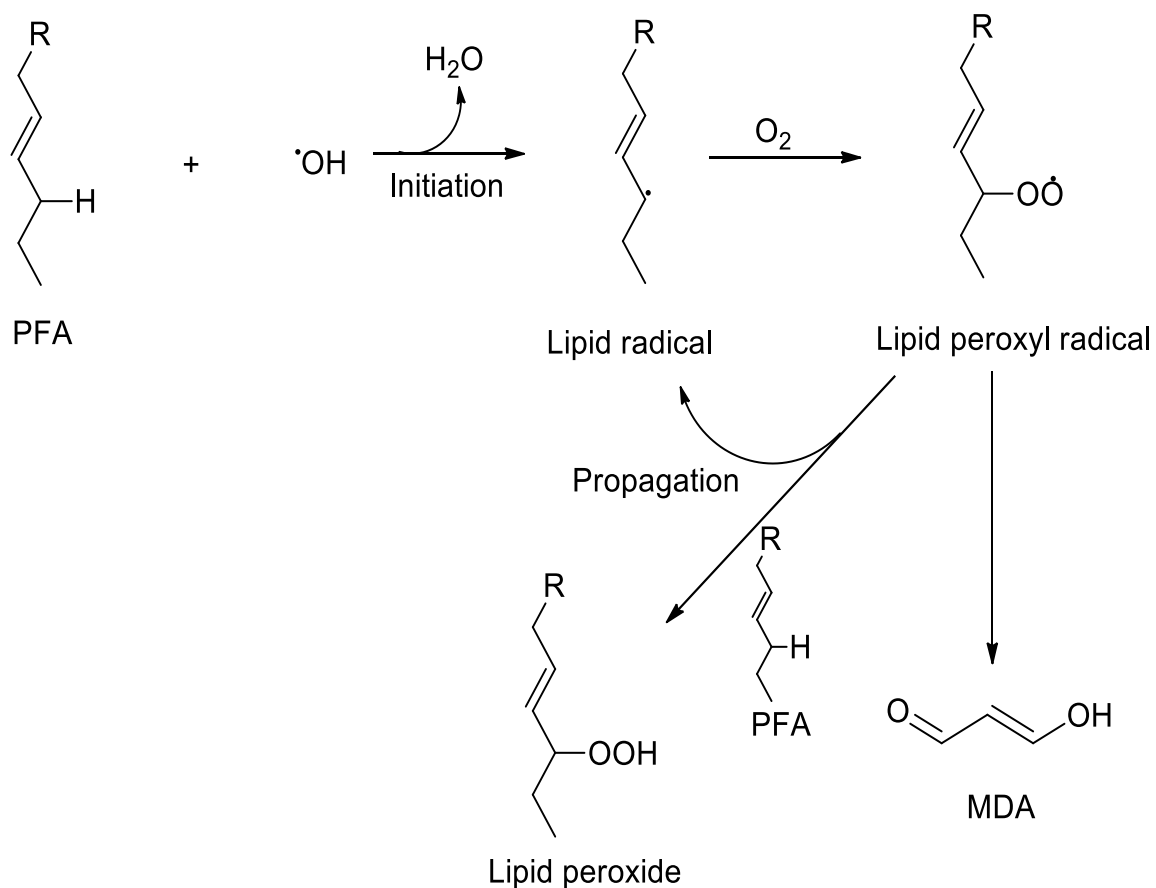


Figure 4.4 – Simplified Mechanism of Free Radical-Mediated Peroxidation of PFA. In the initiation step, ROS, such as hydroxyl radicals ($\cdot\text{OH}$), combine with a hydrogen atom of PFA to form a lipid radical and water. The unstable lipid radical reacts readily with oxygen to create lipid peroxy radical. This radical is also an unstable species that can either react with another PFA, producing more radicals and lipid peroxide (propagation), or react with itself to produce cyclic peroxide, which can further rearrange to create MDAs.

accumulation of 1 mole of solute per liter of tissue water is equivalent to 1 osmole per liter or 1 osmolar in osmotic pressure. For RBCs, an isotonic solution is 0.9% NaCl with 0.3 osmolarity. In a hypertonic solution (> 0.31 osmolar), the water inside the RBC exits the cell in an attempt to equalize the osmotic pressure, causing the cell to shrink and crenate (form a scalloped shape). In contrast, the RBC absorbs water when it is in a hypotonic solution (< 0.28 osmolar) to balance the osmotic pressure, resulting in swelling and potential bursting. Although glucose distributes to quasiequilibrium between the plasma and RBCs with a half life < 30 seconds,⁴⁰ high glucose concentration may still lead to osmotic pressure and further the dehydration and crenation of the RBC. It has been shown that increasing osmotic pressure makes the RBC become stiff and compromises its membrane elasticity.⁴¹

In addition to the properties of the membrane and osmotic effect, the deformability of RBCs is also influenced by cell shape and cytoplasmic viscosity.²⁵ The RBC has a normal biconcave shape with an average volume of 90 fL. With 40% excess surface area, the RBC maintains a ratio of surface area to volume (S/V), that allows these cells to deform. Cytoplasmic viscosity is mainly determined by the mean cellular hemoglobin concentration (MCHC). For a normal human RBC, the MCHC should be in the range of 27 (with a viscosity of 5 centipoises (cp)) to 37 g/dL (with a viscosity of 15 cp) with a mean value at 33 g/dL. The viscosity of Hb increases sharply when the concentration is above 37 g/dL, such as 45 cp at 40 g/dL, 170 cp at 45 g/dL and 650 cp at 50 g/dL.⁴²⁻⁴³ Both an

increase and a decrease in S/V, and an increase in MCHC may lead to a decrease in deformability.

As previously discussed, RBCs stored in CPD/AS-1 have been shown to have a decrease in RBC-derived ATP release, which may result from impaired deformability of RBCs due to hyperglycemia. In this chapter, several factors that influence the deformability of RBCs are determined and discussed. A comparison of RBCs stored in hyperglycemic conditions (CPD/AS-1) and normoglycemic conditions (CPD-N/AS-1N) allows for the investigation of the effect of hyperglycemia on the ability of RBC to release ATP.

4.2 Experimental

4.2.1 Intracellular and Extracellular Glucose Measurement of RBCs

All reagents were purchased from Sigma-Aldrich (St. Louis, MO) unless indicated otherwise. Distilled deionized water (DDW) with 18.2 M Ω resistance was used for all experiments.

In this study, glucose levels both inside and outside of the RBCs in storage were determined for 36 days. Glucose measurements were based on the fluorescence of NADH. Glucose is phosphorylated by ATP, in the presence of hexokinase, to glucose-6-phosphate (G6P), which is then oxidized to 6-phosphogluconate in the presence of NAD⁺ in a reaction catalyzed by glucose-6-phosphate dehydrogenase (G6PD). During

this oxidation, an equimolar amount of NAD^+ is reduced to the fluorescent NADH , the levels of which are proportional to glucose concentration.

For extracellular glucose measurements, samples were prepared using the 2-step centrifugation. Supernatant samples were prepared by centrifuging the RBCs at $2000g$ for 10 minutes, followed by further centrifuging at $15,000g$ for 15 minutes. The resulting supernatant from the AS-1N sample was diluted to 1:100 with distilled and deionized water (DDW), while supernatant from AS-1 sample was diluted 1:1000. These dilutions resulted in glucose concentrations within the range of a calibration curve that was prepared with external glucose standards ranging from 0 to $100 \mu\text{M}$.

For intracellular glucose measurements, packed RBCs from the first centrifugation were lysed 1:10 with DDW. The red color of the lysate has a matrix effect on the assay, thus mandating the use of the standard addition method. Specifically, $5 \mu\text{L}$ of the lysate (the lysate from AS-1N sample had to be diluted to 1:10 with DDW before this step) were diluted to $100 \mu\text{L}$ in a solution that contained glucose at concentrations ranging from 0 to $100 \mu\text{M}$ to establish a standard curve.

To perform the reaction described above, $100 \mu\text{L}$ of a solution containing G6PD (0.9 U/mL), ATP (2 mM), MgCl_2 (2 mM), NADP^+ (1.25 mM), and hexokinase (1.7 U/mL) in a triethanolamine buffer (0.23 M , $\text{pH } 7.6$) were added to the $100 \mu\text{L}$ samples described in the preceding paragraph. This mixture was then allowed to react for 15 minutes prior to the measurement of fluorescence intensity at 460 nm (excitation at 340 nm).

4.2.2 Osmotic Fragility Test of RBCs

Osmotic fragility of RBCs stored in hyperglycemic and normoglycemic conditions were determined weekly for 36 days. The osmotic fragility test measures the resistance to hemolysis of RBCs exposed to hypotonic solutions. In a hypotonic medium, the rupture of the RBC membrane occurs, releasing Hb from the cell. By measuring the Hb concentration, the percentage of hemolysis at different NaCl concentrations can be calculated. For normal RBCs, initial hemolysis begins at $0.45 \pm 0.05\%$ NaCl solution and is complete at $\sim 0.3 \pm 0.05\%$ NaCl solution. The standard osmotic fragility test is performed using median corpuscular fragility (MCF), which is the concentration of NaCl solution causing 50% lysis of RBCs.

Here, a simplified method was used to test the osmotic fragility of RBCs stored in CPD/AS-1 and CPD-N/AS-1N.⁴⁴ RBCs were removed from storage and warmed to room temperature. 25 μL of the RBC samples were gently transferred into 3 tubes containing 500 μL of 0.9% sodium chloride (NaCl), 0.45% NaCl, and DDW, respectively. Suspensions were gently mixed and incubated at room temperature for 30 minutes. Next, the suspensions were centrifuged at 1500 g for 5 minutes. The absorbance (Abs) of the supernatant, containing various concentrations of Hb derived from the lysed RBCs, was determined in a clear, 96-well plate using a plate reader set at 540 nm. The signal in 0.9% NaCl was assumed as the blank, which should induce no hemolysis of RBC, and was subtracted from the signal in 0.45% NaCl. The signal in DDW was assumed to be 100%

hemolysis. Thus, the percentage of hemolysis in 0.45% NaCl was calculated as the following equation:

$$\text{Percentage hemolysis for 0.45\% NaCl} = (\text{Abs}_{0.45\% \text{NaCl}} - \text{Abs}_{0.9\% \text{NaCl}}) / \text{Abs}_{\text{DDW}} \times 100$$

4.2.3 Sorbitol Accumulation Measurement

To investigate the effect of the high glucose level in CPD/AS-1 storage on the polyol pathway, sorbitol accumulation was determined in both storage systems. RBC sorbitol can be measured using an enzymatic method with fluorometric detection.⁴⁵⁻⁴⁶ This method is based on the oxidation of sorbitol to fructose, catalysed by SDH in the presence of NAD^+ , resulting in the formation of NADH. The reaction mechanism and standard curve are described in figure 4.5.

100 μL of stored RBC samples were lysed with 500 μL of DDW with vigorous vortexing. 5 μL of this lysate were diluted to determine the Hb concentration of the sample using Drabkin's method described in chapter 3. 100 μL of 0.3 M zinc sulfate (ZnSO_4) solution and 100 μL of 0.475 M sodium hydroxide solution (NaOH) were added into the remaining cell lysates to precipitate the protein. The supernatant was prepared by centrifuging these samples at 2000 g for 10 minutes. The 20 mM sorbitol stock solution was prepared by dissolving 0.036 g of D-sorbitol in 10 mL of DDW. The working standards, ranging from 0-80 μM , were prepared by a series of dilutions from the stock solution before each assay and were treated similarly to the samples described above.

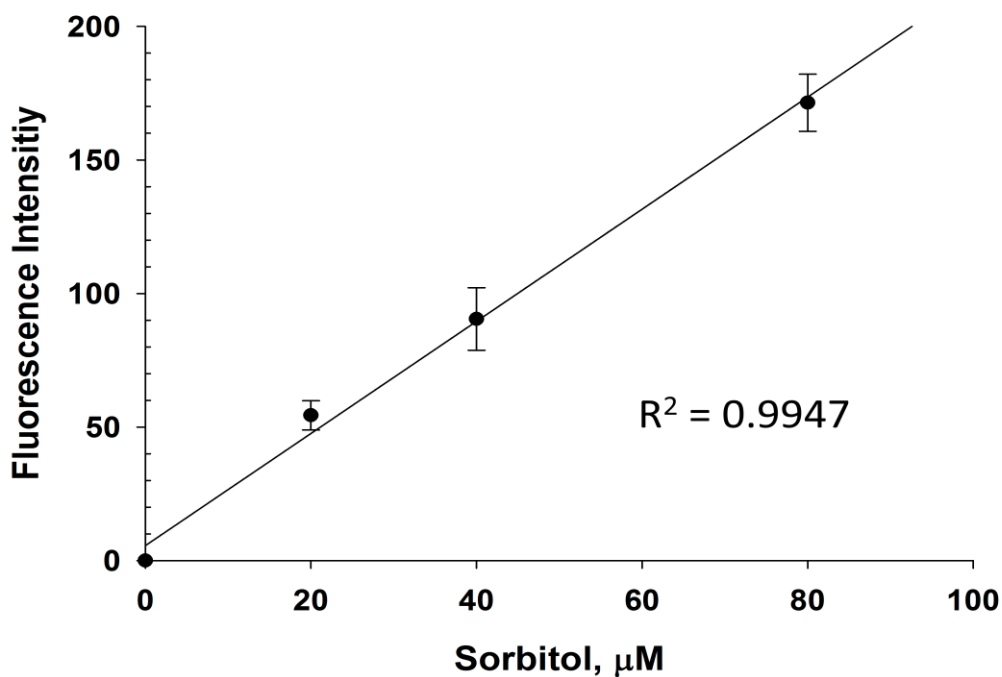
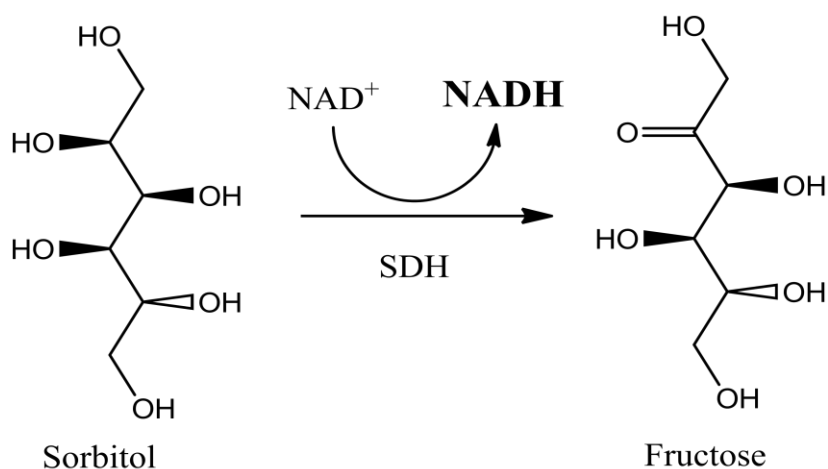


Figure 4.5 – The Mechanism behind the Sorbitol Assay and the Calibration Curve. The sorbitol assay is based on the oxidation of sorbitol to fructose catalysed by SDH in the presence of NAD⁺, resulting in the formation of NADH, which has an emission of fluorescence at 460 nm after excitation of 340 nm. The fluorescence intensity is proportional to the amount of NADH present as well as the sorbitol originally present. Thus, the sorbitol concentration in the samples can be quantified by using a calibration curve generated at the same time. An overall calibration curve (n = 3) is shown above; the limit of detection based on this curve is 10.0 µM.

Next, 100 μL of the supernatant resulting from the samples and standards were each added into a well of a 96-well plate. 50 μL of the enzyme mixture, containing SDH (2 kU/L), NAD^+ (3 mM), and disodium ethylenediaminetetraacetic acid (EDTA, 10 mM) in glycine-NaOH buffer (0.15 M, pH 9.0), were added into each well. For the blank assay (both the samples and standards), the enzyme mixture was prepared in the same manner, with the exception of the omission of SDH. After incubation at 37°C for 30 minutes, the fluorescence emitted from the formation of NADH was measured at room temperature at 460 nm (excitation at 340 nm). To generate a standard curve, the net fluorescence intensities, obtained by subtracting those of the blank from those of enzymatic reaction, were plotted as a function of the sorbitol concentration. The sorbitol levels in the samples were then calculated from this curve using the respective net fluorescence intensities. The final sorbitol concentrations were expressed as nmol/g Hb.

4.2.4 Lipid Peroxidation Measurement

The amount of lipid peroxidation in stored RBCs was determined by measuring MDAs. The mechanism has been proposed that reactive oxygen species (ROS), such as hydroxyl radicals ($\cdot\text{OH}$), react with PFAs, followed by a series of chain reactions to create MDAs.⁴⁷⁻⁴⁸ The thiobarbituric acid reactive substances (TBARS) assay is the most widely used assay to determine lipid peroxidation, based on the reaction between MDAs with thiobarbituric acid (TBA), resulting in the chromophore TBARS.⁴⁹⁻⁵¹

Stored RBCs were diluted in AS-1N to a final Hct of 6%. 10 μ L of this suspension were used to determine the Hb concentration in the samples using Drabkin's method. Next, 10 μ L of 0.5 M butylated hydrotoluene (BHT) in acetonitrile was added into 1000 μ L of the RBC suspension to generate a final concentration of 5 mM. BHT works as an antioxidant, and its addition prevents autooxidation of the sample during the assay.⁵²

Then, 28% (w/v) trichloroacetic acid (TCA) was added into the RBC suspensions at a ratio of 1:2. The samples were vortexed before being incubated on ice for 10 minutes to precipitate proteins. The supernatants were prepared by centrifuging at 22,000 *g* for 10 minutes and carefully collected to avoid contamination with cell debris. 400 μ L of the supernatant, containing MDA extracts, were added into 100 μ L of 1% TBA in 0.05 M NaOH or 0.05 M NaOH alone (sample blank) in a 2-mL tube. The tubes were capped and sealed with parafilm (to avoid evaporation), incubated in a boiling water bath for 15 minutes, and immediately cooled on ice for 10 minutes. 200 μ L of the samples were then transferred into a 96-well plate in a duplicate manner. The fluorescence of TBARS was measured using an excitation wavelength of 532 nm and an emission wavelength of 553 nm. The TBARS level in a sample was quantified using an MDA standard curve generated at the same time. A 1 M MDA standard stock was prepared by dissolving 166 μ L malonaldehyde bis(dimethyl acetal) in 834 μ L ethanol. This MDA stock was further diluted with AS-1N to produce standards ranging from 0-400 nM. The standards were treated in a similar manner to the samples. Thus, the final TBARS values in the RBC

samples are presented as nmol/g Hb. The reaction mechanism and the standard curve are shown in figure 4.6.

4.2.5 Protein Glycation Determination

The proteins in the RBC, including peripheral proteins, integral proteins and Hb, can be covalently modified by glucose linked as a stable ketoamine adduct. A chemical procedure, the TBA assay, was used to quantify the nonenzymatic glycation of proteins.⁵³ This assay uses mild acid hydrolysis to release glucose from protein as 5-hydroxymethylfurfural (5-HMF), which is then reacted with TBA to form a yellow chromophore. The original procedure was used to assay serum protein, so the sample preparation was modified for this study.

Stored RBCs were washed with saline (0.9% NaCl) 3 times to remove extracellular glucose. Hb samples were prepared by lysing 350 μ L of washed RBCs in 1000 μ L of DDW, followed by centrifugation at 22,000 *g* for 10 minutes to sediment the membrane protein. The Hb concentration in the supernatant was determined using Drabkin's method, and the supernatant was frozen at -20°C until assay. The remaining washed RBCs were lysed using 5 mM phosphate buffer (pH 8.0) containing 350 μ M EDTA, and incubated on ice for 10 minutes. Next, the RBC membrane ghosts were collected by centrifugation at 22,000 *g* for 10 minutes at 4°C, and the supernatant was removed. This process was repeated until the Hb-free RBC ghosts (white) were obtained for glycation assay. Next, peripheral membrane proteins were separated from the integral proteins

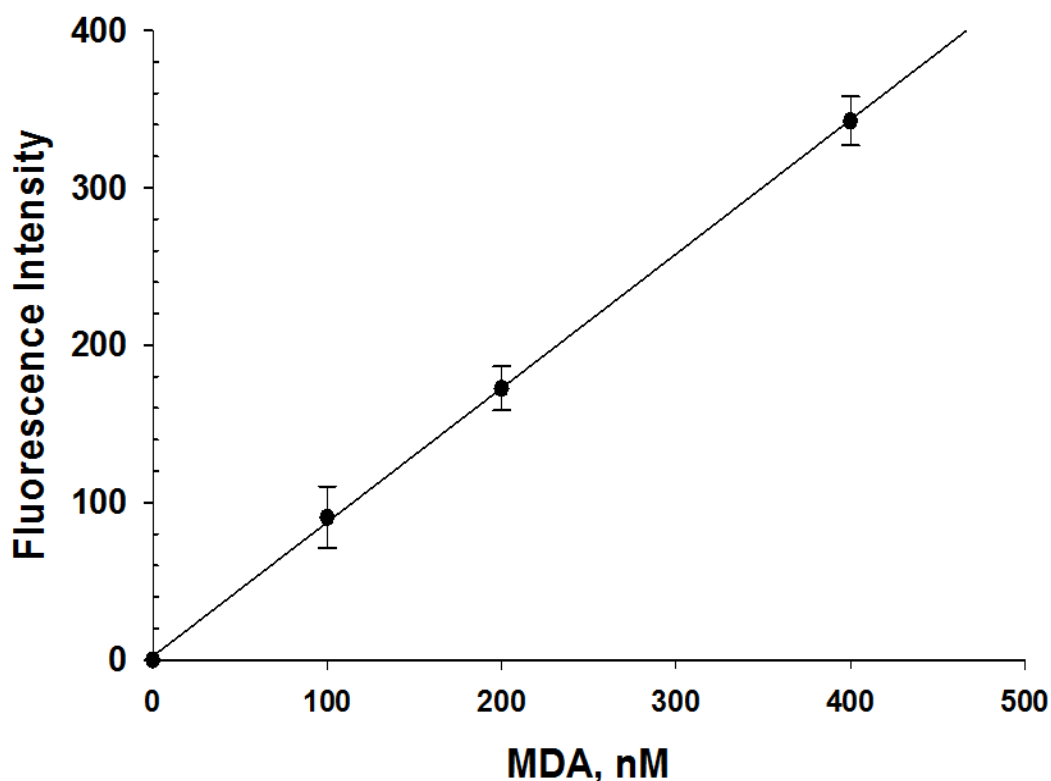
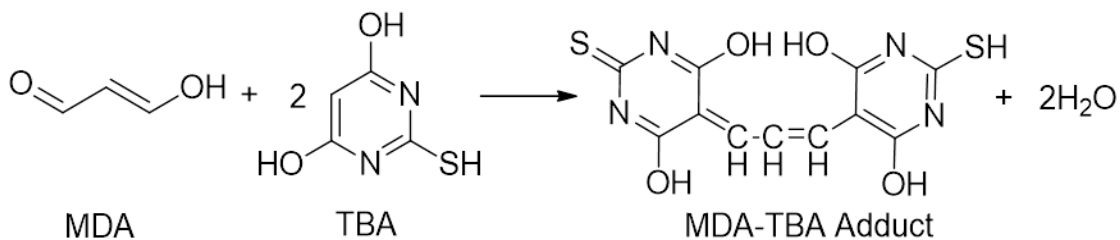


Figure 4.6 – The Mechanism behind the TBARS Assay and the Calibration Curve. The MDA extracts from RBCs, representing the oxidative level and lipid peroxidation, can be determined using TBARS assay. The MDA-TBA adducts formed by the reaction of MDA and TBA at a high temperature (90-100°C) and acidic conditions are measured fluorometrically at an excitation wavelength of 530 nm and an emission wavelength of 550 nm. The net fluorescence intensity found by subtracting that of a blank as a background, is proportional to the amount of MDA-TBA adduct present as well as the MDA originally present. Thus, the MDA concentration in the samples can be quantified by using a calibration curve generated at the same time. An overall calibration curve (n = 6) is shown above; the limit of detection based on this curve is 10 nM.

by adding 0.1 M NaOH (containing 200 μ M EDTA, pH 12.0) into the membrane ghost and incubating on ice for 15 minutes.⁵⁴ After centrifugation at 27,000 *g* for 10 minutes, the concentration of the peripheral protein in the supernatant and the integral protein in the pellet were determined using a BCA (bicinchoninic acid) protein assay kit (Thermo Scientific Pierce, Rockford, IL USA) and frozen at -20°C until assay.

For the TBA assay, the amount of protein was adjusted to 1 mg in each sample based on the concentrations. Then, 100% (w/v) TCA was added into each sample at the volume ratio of 1 to 10. The samples were incubated in the refrigerator overnight to precipitate all the proteins. The following day, the sample pellets were collected by centrifuging at 22,000 *g* for 10 minutes and discarding the supernatants. 100 μ L of DDW and 600 μ L of 0.33 M oxalic acid were added into the pellets. The tubes were capped and tightly sealed with Teflon tape and parafilm. The samples were autoclaved at 121°C for 2 hours to accelerate the hydrolysis.⁵⁵ After cooling on ice, 25 μ L of 100% TCA and 150 μ L TBA were added into the hydrolyzed samples, which were incubated at 37°C for 40 minutes. After a second cooling, 25 μ L of 4 M NaCl in 10% TCA were added to prevent the formation of emulsions during extraction using an organic solvent.⁵³ 600 μ L of isobutnaol were then added to the tubes, which were vortexed to extract the HMF-TBA chromophore from the aqueous phase. The tubes were then centrifuged at 1,500 *g* for 5 minutes. A 200 μ L aliquot of the upper isobutanol phase was added into each well of a clear-bottom 96-well plate, which allows measurement of the absorbance at 435 nm

and 500 nm. The HMF-TBA adduct has an Abs maximum at 435 nm. Due to the similarity of Abs at 500 nm and the background Abs in the sample assay without TBA (blank), the net Abs at 435 nm can be made by subtraction of the 500 nm Abs from that at 435 nm. The reaction mechanism and the standard curve are shown in figure 4.7.

In this method, fructose can serve as a standard: after conversion to 5-HMF during hydrolysis with weak acid. A set of standards was prepared by diluting 20 mM fructose stock to 0-75 nM with DDW. 100 μ L of the fructose standards were treated exactly the same as the samples, starting from the hydrolysis procedure. Thus, the amount of HMF detected from the samples could be quantified from the standard curve generated at various fructose concentrations against the net Abs measured at 435 nm. The final glycation was represented as nmol HMF/ mg protein or Hb.

4.2.6 Images, Mean Corpuscular Volume and Basal ATP Release of RBCs Suspended in Glucose Gradients

In this study, whole blood was collected in CPD or CPD-N as described in chapter 2. The RBCs processed in CPD-N were suspended in AS without glucose and with 5.5 mM glucose (AS-1N); the RBCs in CPD were suspended in AS with 16.5 mM, 55 mM and 111 mM glucose (AS-1) at a ratio of 2 to 1. Next, a series of studies were performed on the RBCs in glucose gradients.

The Hct, total Hb concentration, and intracellular and extracellular glucose of RBCs suspended in the glucose gradients were determined as previously described. Mean corpuscular volume (MCV) of the RBCs represents the average RBC volume. MCV is

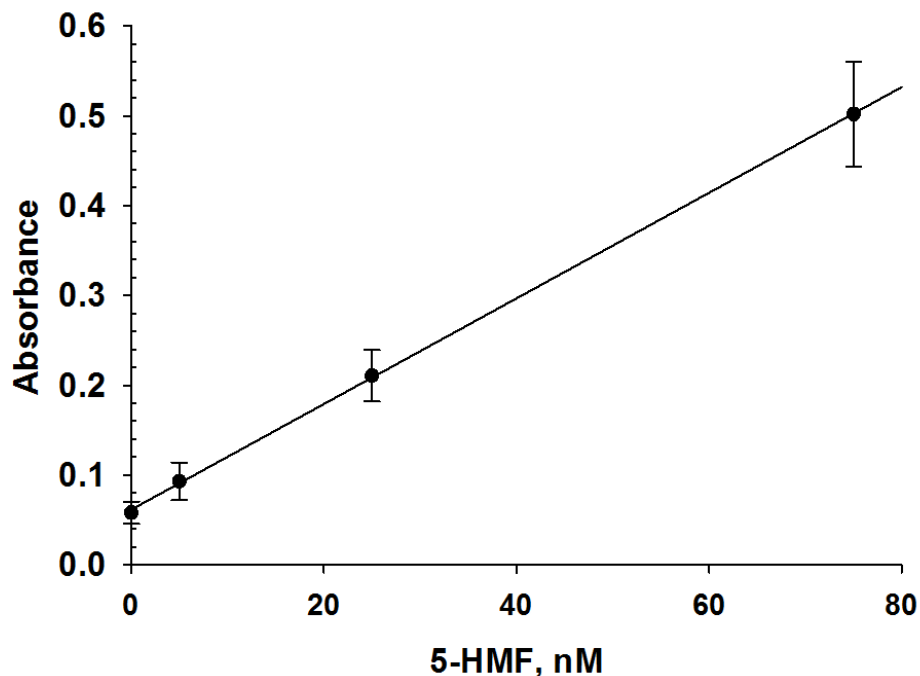
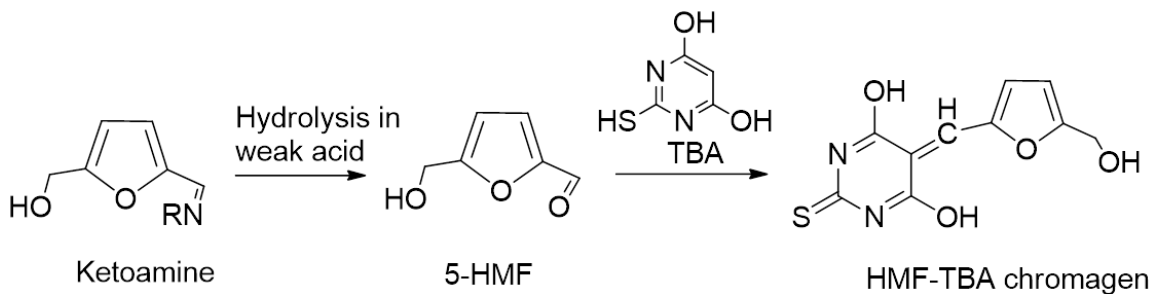


Figure 4.7 – The Mechanism of Protein Glycation Assay and the Calibration Curve. The proteins, including Hb, in RBCs can be covalently modified by glucose linked as a stable ketoamine product. Through a mild hydrolysis of the ketoamine, glucose can be released from proteins as 5-HMF, which reacts with TBA to form a yellow HMF-TBA chromagen. This chromagen can be measured colorimetrically at 435 nm. The net absorbance at 435 nm, found by subtracting that at 500 nm as a background, is proportional to the amount of HMF-TBA chromagen present as well as the 5-HMF originally present. Thus, the 5-HMF concentration in the samples can be quantified by using a calibration curve generated at the same time. An overall calibration curve ($n = 9$) is shown above; the limit of detection based on this curve is 1.8 nM.

calculated by dividing the total volume of packed RBCs (the Hct), by RBC count (millions/ μL), and multiplying by 10.⁵⁶ The number of RBCs was counted in a hemocytometer. Specifically, each RBC sample (\sim Hct 60%) was diluted 1/200 fold with the respective AS and inverted gently to generate a homogenous suspension. To prepare the hemocytometer (Bright-Line, Hausser Scientific, Horsham, PA), the mirror-like polished surface was carefully cleaned with a Kim-wipe and ethanol. The rectangular clean coverslip of the same brand was then placed over the counting surface prior to adding the cell suspension. The cell suspension (\sim 10 μL) was introduced into the V-shaped well using a pipette, till the area under the coverslip was filled by capillary action. The counting chamber was then placed under the microscope, and the counting grid was brought into focus. The gridded area of the hemocytometer consists of 25 squares, each 1 mm^2 in area, which are subdivided into smaller grids for counting different blood cell type. The central 1 mm^2 grid was divided into 9, 0.04 mm^2 squares and the RBCs in the four corner squares and the middle one were counted. If a cell overlaps a line, the cell is counted as “in” if it overlaps the top or right line, and “out” if it overlaps the bottom or left line. Since the depth of the chamber is 0.1 mm, each 1 mm^2 square contains 100 nL of RBC suspension. Thus, the original concentration of RBCs can be calculated as shown below:

$$\# \text{ of RBCs in original storage per mL} = \text{average \# of RBCs in the square} \times 25 \times 10^4 \times 200$$

The cell images in the glucose gradients were then taken under 40X magnification.

The basal level of ATP was determined in the supernatant of samples by chemiluminescence using the luciferase/luciferin (L/L) assay. A 7% RBC suspension was prepared in the respective AS for each sample. After 10 minutes of incubation at room temperature, the RBC suspensions were centrifuged at 500 *g* for 5 minutes. 100 μ L of the supernatant were transferred into a 96-well plate in triplicate. The chemiluminescence was then measured 6 seconds after adding 30 μ L of L/L using a plate reader.

In order to investigate if the effect of glucose on the RBCs was reversible, RBCs in AS-1 were washed in normoglycemic AS (AS-1N). Specifically, the AS-1 RBCs were resuspended in AS-1N at a ratio of 1 to 10 and centrifuged at 500 *g* for 5 minutes, discarding the supernatant. This process was repeated 5 times to remove excess intracellular and extracellular glucose existing in the AS-1 RBCs. The RBCs in AS-1N had the same washing procedure performed for comparison. These two washed samples were also used for glucose measurements, basal ATP release, corpuscular cell volume, and obtaining images discussed above.

For a long term ATP reversibility study, the CPD/AS-1 RBCs were analyzed for basal ATP release on a weekly basis. However, since the RBCs may lyse during storage, the CPD/AS-1 RBCs were washed as described above in AS-1 and AS-1N for comparison. A 7% RBC suspension was then prepared with the respective AS, and ATP in the supernatant was determined using the L/L assay.

4.3 Results

4.3.1 Intracellular and Extracellular Glucose Level in Stored RBCs.

Figure 4.8 shows the glucose level inside and outside the RBCs stored in hyperglycemic (CPD/AS-1) and normoglycemic (CPD-N/AS-1N) storage solutions, monitored weekly, during 36 days of storage. The extracellular glucose level in CPD/AS-1 storage was at 66.2 ± 1.2 mM at day 1, decreasing to 53.9 ± 2.1 mM at day 36, while the intracellular level was at 51.8 ± 1.2 mM at day 1, decreasing to 44.1 ± 2.0 mM at day 36. The extracellular glucose level was consistently higher than the intracellular level during the 36 days. Both of the glucose levels in CPD/AS-1 indicated that the glucose amount was in excess during storage. For CPD-N/AS-1N storage, both the extracellular and intracellular glucose levels were stable around 5 mM with glucose feeding treatment every 5 days. However, fluctuations existed in intracellular glucose levels more often than in the extracellular levels.

4.3.2 Osmotic Fragility of Stored RBCs

Osmotic fragility of stored RBCs was determined weekly during storage by using a simplified test, the percent hemolysis of RBCs in 0.45% NaCl. This could be determined by subtracting the absorbance of stored RBCs in 0.9% NaCl (non-induced hemolysis, blank) from that of those in 0.45% NaCl, then dividing by the absorbance of stored RBCs in DDW, which represents 100% hemolysis of the RBCs. For a normal RBC, initial hemolysis begins at $0.45 \pm 0.05\%$ NaCl solution and completes at $0.3 \pm 0.05\%$ NaCl

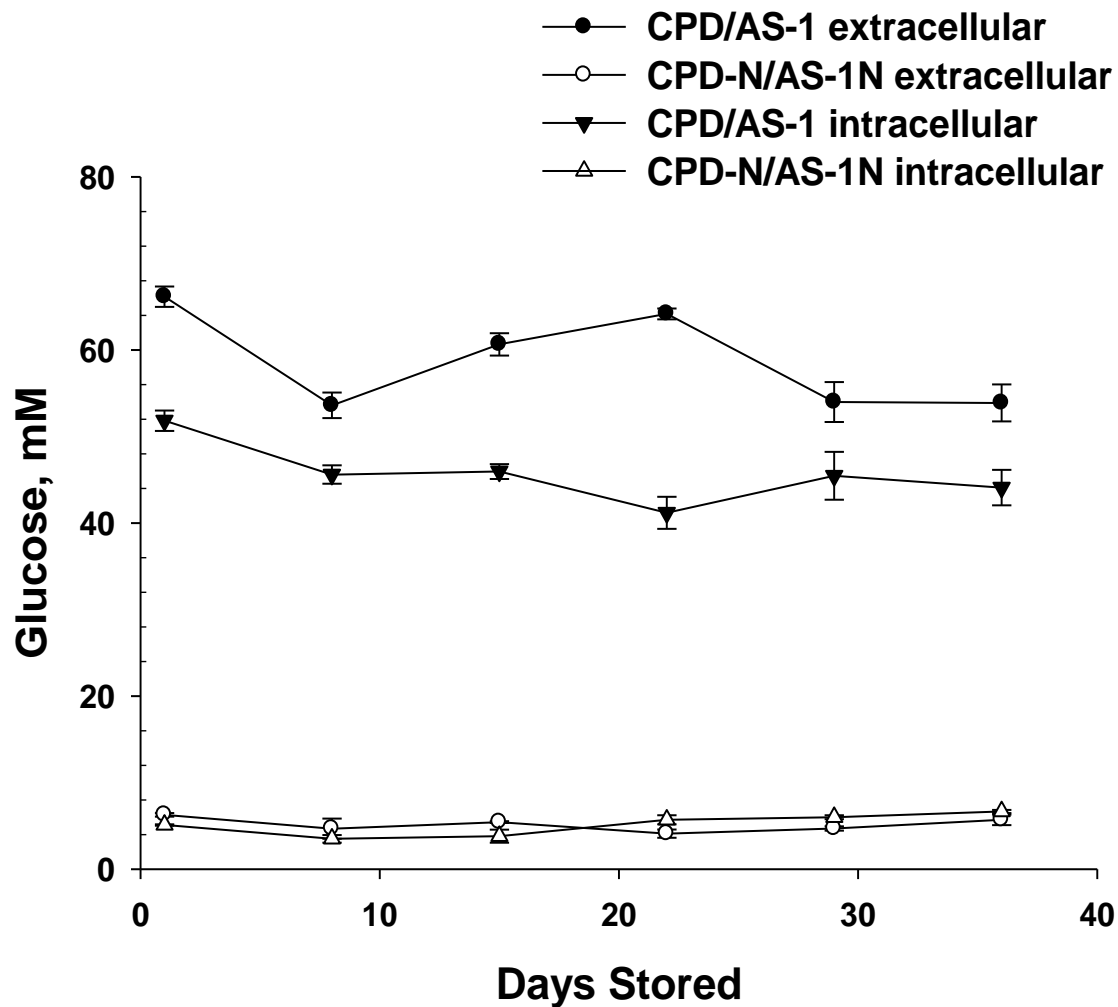


Figure 4.8 – Extracellular and Intracellular Glucose Levels in Stored RBCs for 36 Days. To monitor the glucose level of the RBCs stored in hyperglycemic (CPD/AS-1) and the normoglycemic (CPD-N/AS-1N) conditions, the intracellular and extracellular glucose levels were measured weekly. The extracellular glucose level in CPD/AS-1 storage (black dot) was at 66.2 ± 1.2 mM at day 1, decreasing to 53.9 ± 2.1 mM at day 36, while the intracellular level (black triangle) was at 51.8 ± 1.2 mM at day 1, decreasing to 44.1 ± 2.0 mM at day 36. With glucose feeding, both the extracellular (white dot) and intracellular (white triangle) glucose levels in CPD-N/AS-1N were stable around 5 mM with some fluctuations for 36 days. Data represented as mean \pm s.e.m. (n = 4).

solution. Thus, the more hemolysis occurs in 0.45% NaCl, the more fragile the RBCs. As shown in figure 4.9, the CPD-N/AS-1N RBCs showed a significantly lower percent hemolysis ($5.6 \pm 0.6\%$, $9.1 \pm 0.8\%$, $27.3 \pm 1.1\%$) in 0.45% NaCl for the first 3 weeks, compared to the CPD/AS-1 RBCs ($51.7 \pm 6.0\%$ hemolysis at day 1). However, the hemolysis percentage in both storage solutions increased as a function of time, which indicated an increased osmotic fragility of RBCs.

4.3.3 Sorbitol Accumulation in Stored RBCs

Sorbitol is produced through the hyperglycemia-induced polyol pathway, and because it cannot cross the cell membrane, it accumulates in the RBCs. Sorbitol accumulation represents the activity of the polyol pathway and may have adverse effect on RBCs. As shown in figure 4.10, the sorbitol accumulated in both hyperglycemic and normoglycemic conditions was determined weekly during 36 days of storage. At day 1, the concentration of sorbitol in the CPD/AS-1 RBCs was 52.8 ± 8.6 nmol/g Hb; it was lower, but not significantly so, in CPD-N/AS-1N RBCs, 43.1 ± 8.2 nmol/g Hb. However, the sorbitol increased dramatically in the CPD/AS-1 RBCs during the first week to 147.5 ± 7.2 nmol/g Hb at day 8, whereas those in normoglycemic storage at day 8 remained at 40.3 ± 7.0 nmol/g Hb, statistically equivalent to day 1. For the remainder of the storage period, the sorbitol levels in the CPD-N/AS-1N RBCs and the CPD/AS-1 RBCs were stable around 45 and 150 nmol/g Hb, respectively.

4.3.4 Lipid Peroxidation in Stored RBCs

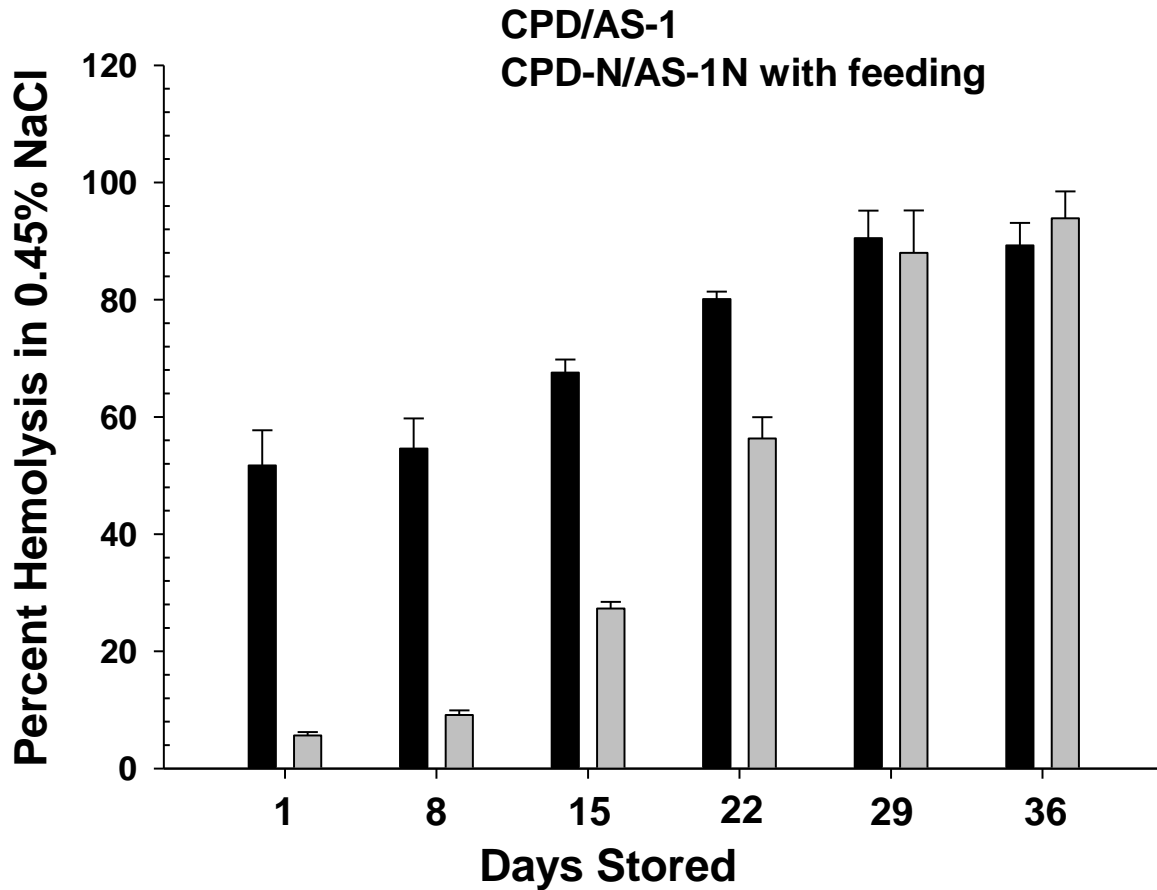


Figure 4.9 – Osmotic Fragility of Stored RBCs. Osmotic fragility was determined by subtracting the absorbance of stored RBCs in 0.9% NaCl (blank) from that of all in 0.45%, then dividing by the absorbance of stored RBCs in DDW, representing 100% hemolysis of RBCs. The CPD-N/AS-1N RBCs (grey bars) showed a significantly lower percent hemolysis in 0.45% NaCl for the first 3 weeks, compared to the CPD/AS-1 RBCs (black bars), which had an approximate 50% hemolysis in 0.45% NaCl at day 1. However, the hemolysis percentage in both storages increased as a function of time, which indicated an increase in osmotic fragility of the RBCs. Data represented as mean \pm s.e.m. (n = 3).

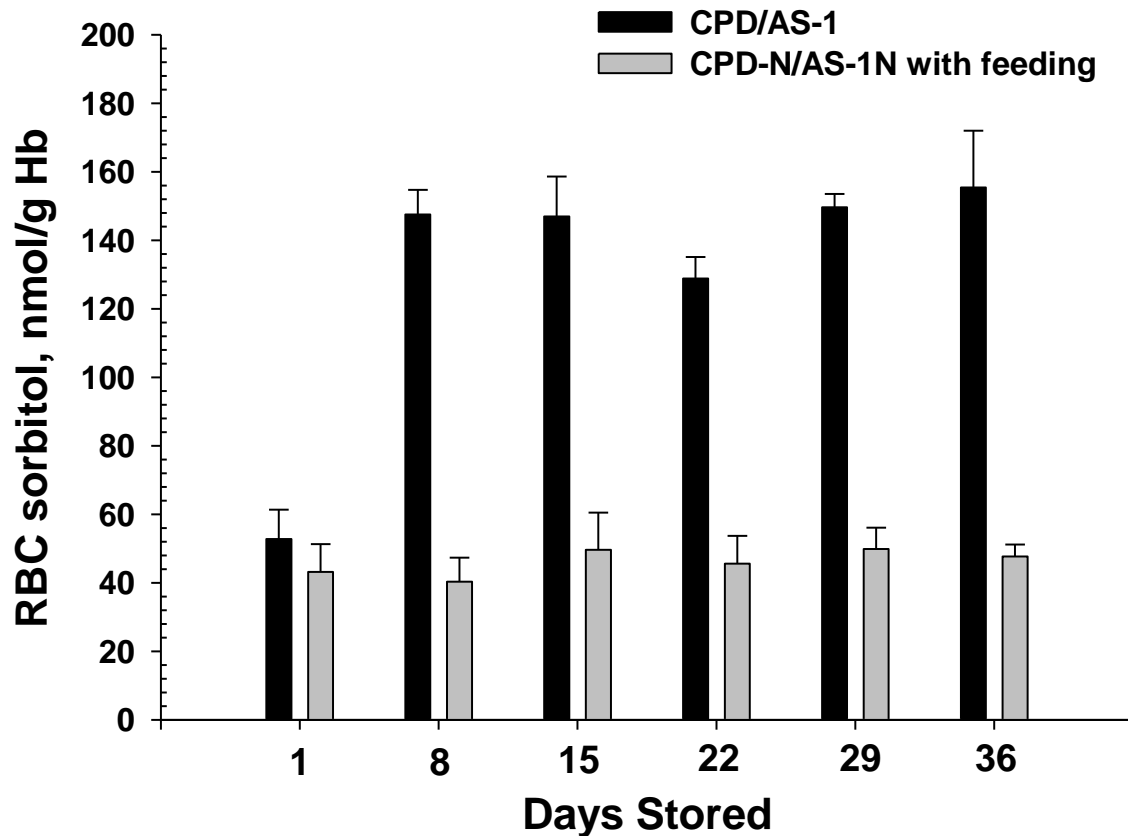


Figure 4.10 – Sorbitol Accumulation in Stored RBCs. Sorbitol is produced through the hyperglycemia-induced polyol pathway and cannot cross the cell membrane and thereby accumulates in RBCs. Sorbitol accumulation was determined weekly during 36 days storage. At day 1, the sorbitol in CPD/AS-1 RBCs (black bars) was 52.8 ± 8.6 nmol/g Hb, while it was lower but not significantly so in CPD-N/AS-1N RBCs (grey bars), 43.1 ± 8.2 nmol/g Hb. However, the sorbitol increased dramatically in CPD/AS-1 RBCs during the first week to 147.5 ± 7.2 nmol/g Hb at day 8, whereas the one in normoglycemic storage at day 8 was statistically equivalent to day 1. For the remaining storage period, the sorbitol in both RBCs remained at the respective level. Data represented as mean \pm s.e.m. (n = 3).

MDA is a naturally occurring product of lipid peroxidation and can be determined by the TBARS assay. In this assay, the MDA-TBA adduct formed by the reaction of MDA and TBA is measured fluorometrically at 550 nm (excitation: 530 nm) and quantified with external standards. In figure 4.11, the MDA levels in the CPD/AS-1 RBCs and in the CPD-N/AS-1N RBCs were 3.2 ± 0.2 nmol/g Hb and 3.1 ± 0.2 nmol/g Hb at day 1, respectively. However, the MDA in the hyperglycemic conditions tended to increase as a function of time, while the MDA in normoglycemic conditions remained at similar levels. At day 22, the MDA in the CPD/AS-1 RBCs, 4.5 ± 0.2 nmol/g Hb, was significantly higher ($p < 0.05$) than that in the CPD-N/AS-1N RBCs, 3.1 ± 0.5 nmol/g Hb. By day 36, the MDA in the CPD/AS-1 RBCs increased to 5.6 ± 0.4 nmol/g Hb, which was still significantly higher ($p < 0.005$) than the 3.2 ± 0.4 nmol/g Hb of the normoglycemic cells. The increased MDA level in hyperglycemic conditions is an indicator of increased oxidative stress in RBCs.

4.3.5 Protein Glycation in Stored RBCs

Reducing sugars react with the primary amino group of proteins and form a stable ketoamine adduct. The hydrolysis process of the glycated protein releases glucose from protein as 5-HMF, which can be determined using the TBA assay. The yellow chromophore formed in the assay can be then measured colorimetrically. As shown in figure 4.12, the peripheral proteins, hemoglobin and integral proteins of CPD/AS-1 RBCs and CPD-N/AS-1N RBCs were not significantly different from each other at days 1, 15, and 36. The hemoglobin had the highest level of glycation, above 25 nmol/g Hb, and the peripheral proteins had the lowest level, below 10 nmol/g Hb.

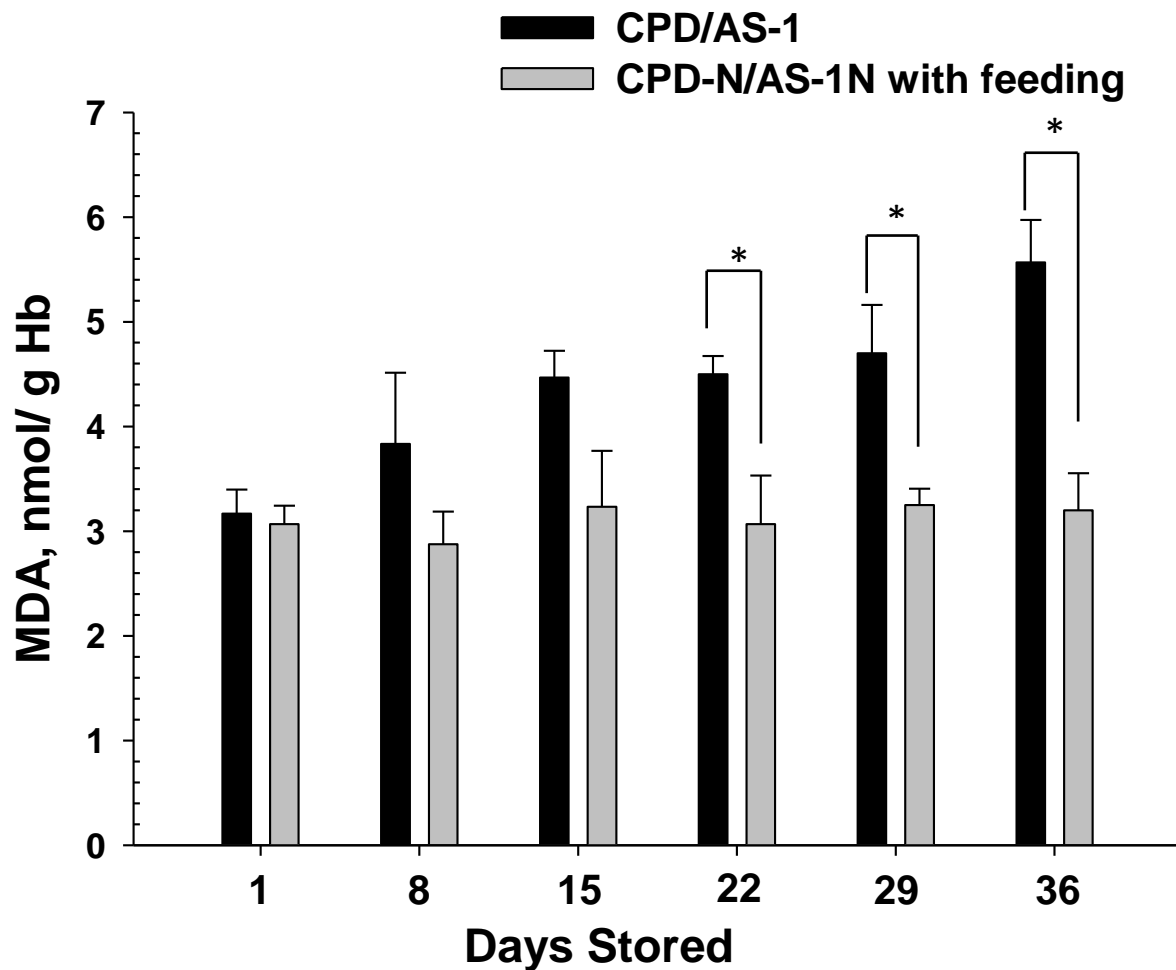


Figure 4.11 – Lipid Peroxidation in Stored RBCs. MDA is a naturally occurring product of lipid peroxidation, which can be determined by a TBARS assay. In this assay, the MDA-TBA adduct formed by the reaction of MDA and TBA is measured fluorometrically at 530 nm (excitation: 550 nm), and quantified with external standards. The MDA in CPD/AS-1 RBCs (black bars) and in CPD-N/AS-1N RBCs (grey bars) were 3.2 ± 0.2 nmol/g Hb and 3.1 ± 0.2 nmol/g Hb at day 1, respectively. However, the MDA in hyperglycemic conditions tended to increase as a function of time, while the amount in normoglycemic conditions seemed to remain at similar levels. At day 22, the MDA in CPD/AS-1 RBCs, 4.5 ± 0.2 nmol/g Hb, was significantly higher (* $p < 0.05$) than the level in CPD-N/AS-1N. Until day 36, the MDA in CPD/AS-1 RBCs increased to 5.6 ± 0.4 nmol/g Hb. Data represented as mean \pm s.e.m. ($n = 4$).

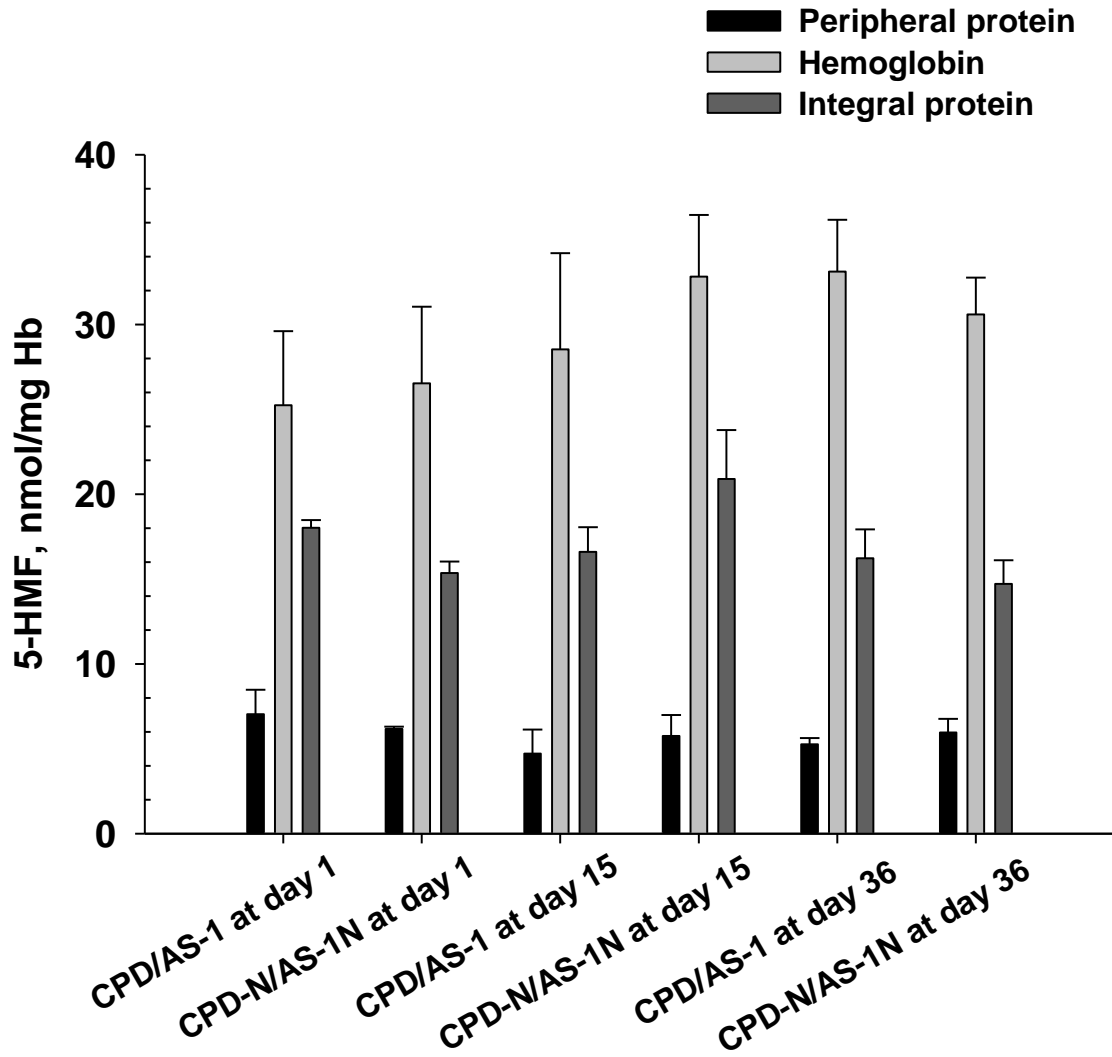


Figure 4.12 – Protein Glycation in Stored RBCs. The hydrolysis of protein glycation releases glucose from proteins as 5-HMF, which can be determined using TBA to form a yellow chromophore. The peripheral proteins (black bars), hemoglobin (light grey bars) and integral proteins (dark grey bars) of CPD/AS-1 RBCs and CPD-N/AS-1N RBCs were not significantly different from each other at various time points, (day 1, 15 and 36). Data represented as mean \pm s.e.m. (n = 4).

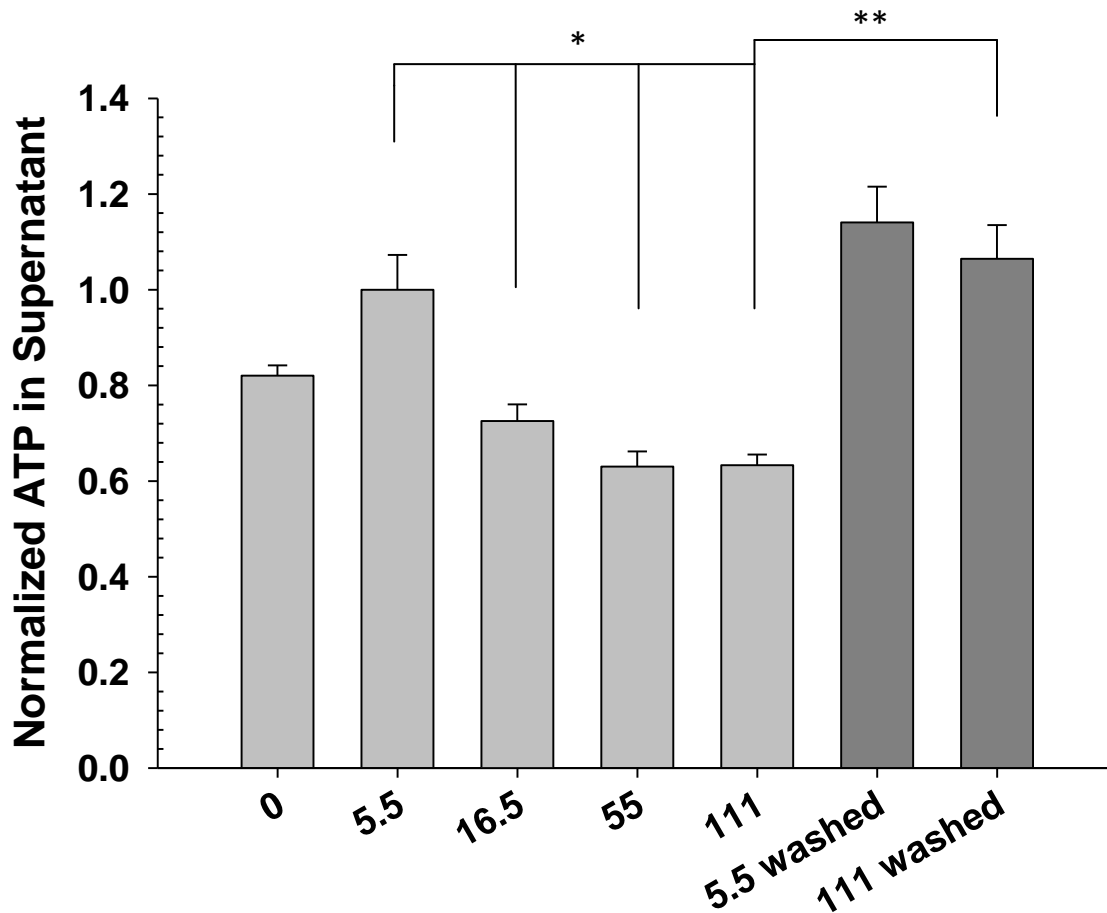
4.3.6 Images, Mean Corpuscular Volume, and Basal ATP Release of RBCs Suspended in Glucose Gradients

The RBCs processed in CPD-N (5.5 mM glucose) were suspended in AS without glucose and with 5.5 mM glucose (AS-1N); 2 aliquots of the RBCs in CPD (~ 129 mM glucose) were suspended in 1 aliquots of AS with 16.5 mM, 55 mM and 111 mM glucose (AS-1. "Washed" represents that the RBCs in 5.5 and 111 mM glucose AS were resuspended in AS-1N and washed 5 times by centrifugation and resuspension. In table 4.1, it is shown that the real glucose levels inside and outside of RBCs in AS with different glucose gradients. Since the RBCs were first collected in CPD-N or CPD, it would subsequently affect the intracellular and extracellular glucose level of RBCs in the AS. Also, the results showed that after washing 5 times, both the intracellular and extracellular glucose levels of the RBCs in the 111 mM glucose AS decreased to normoglycemic level.

Next, the basal ATP release was determined in the supernatant of 7% RBCs suspended in AS with glucose gradients as described above. The chemiluminescence generated from the reaction of L/L and ATP in the supernatant obtained from each sample was normalized to the value from the "5.5" mM glucose sample. As shown in figure 4.13, the basal ATP release from RBCs in "5.5" mM sample was not significantly different from that ATP release from RBCs in the "0" mM glucose sample. This may due to the real intracellular glucose level of RBCs in the "0" mM glucose sample (4.0 ± 0.4 mM), which was from the residual glucose existing in CPD-N and plasma. The basal ATP release from RBCs in the "5.5" mM sample was significantly higher ($p < 0.01$) than the ATP release from RBCs in the "16.5", "55" and "111" mM glucose sample. However, this impaired

Table 4.1 – Glucose Level inside and outside of 7% RBCs in AS with Different Glucose Gradient

Glucose level in AS, mM	Intracellular glucose, mM	Extracellular glucose, mM
0	4.0 ± 0.4	2.5 ± 0.3
5.5	6.4 ± 0.5	5.3 ± 0.4
16.5	18.0 ± 1.1	19.3 ± 0.3
55	34.9 ± 2.6	38.5 ± 1.0
111	61.8 ± 0.8	68.8 ± 1.5
Washed 5.5	5.7 ± 0.3	5.4 ± 0.2
Washed 111	5.8 ± 0.5	5.6 ± 0.2



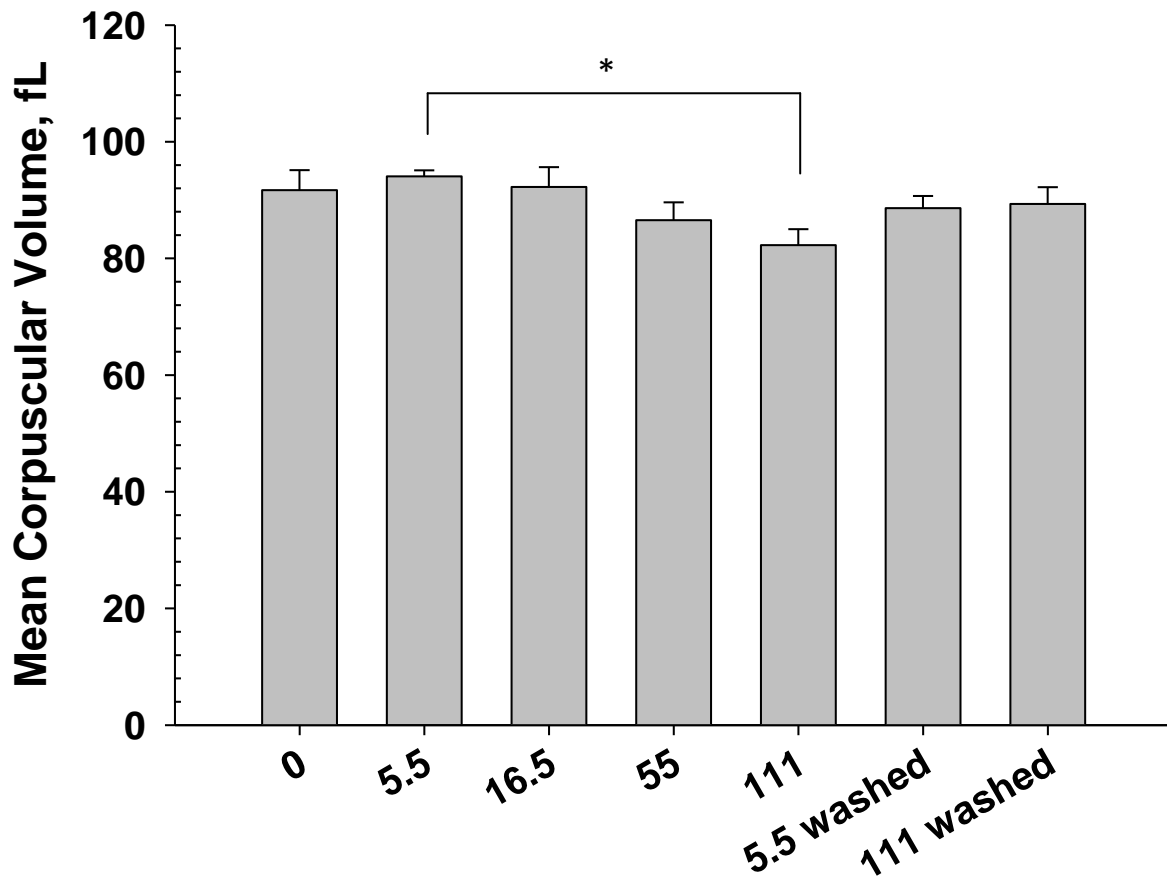
7% RBCs in AS with Different Glucose Gradient, mM

Figure 4.13 – Normalized Basal ATP Release of RBCs in Glucose Gradient. 7% RBCs were suspended in AS with different glucose concentrations indicated in horizontal axis (light grey bars). The dark grey bars represent RBCs washed with AS-1N. The samples were centrifuged, and the supernatants were used for measuring basal ATP release. The chemiluminescence intensities from each sample were normalized to the one from the “5.5” mM glucose sample. The basal ATP release from RBCs in “5.5” mM glucose sample was not significantly different from the ATP in “0” mM glucose sample, but it was significantly higher (* $p < 0.01$) than the ATP in “16.5”, “55” and “111” mM glucose sample. However, after washing with 5.5 mM AS, the ATP release of the RBC previously in “111” mM glucose sample increased and was significantly higher (** $p < 0.005$) than the one prior to washing. Data represented as mean \pm s.e.m. (n = 4).

basal ATP release due to hyperglycemia was reversible after removing excess glucose. The basal ATP release from the RBCs in washed “111” mM glucose sample was significantly higher ($p < 0.005$) than the basal ATP release from RBCs in “111” mM glucose sample, but not significantly higher than that in the “5.5” mM glucose sample.

The MCV of RBCs represents the average RBC volume and is calculated by dividing the hematocrit by the total number of RBCs in the sample and multiplying by 10. For normal RBCs, the MCV has a range of 80-96 fL.⁵⁶ In figure 4.14, it is shown that the MCV of RBCs tended to decrease when they were exposed to high amounts of glucose; however, it only showed a significant decrease to 82.3 ± 2.7 fL ($*p < 0.01$) in the “111” mM glucose AS compared to the cells in the “5.5” mM glucose AS, 94.1 ± 1.0 fL. Also, as shown in figure 4.15, RBCs had biconcave disk shapes when exposed to normoglycemic condition, whereas RBCs shrunk in hyperglycemic condition. After washing with 5.5 mM AS, the MCV of RBCs previously in 111 mM glucose AS increased to 89.3 ± 2.9 fL, but this was not a significant increase. However, the image in figure 4.15 shows that the shape of the RBCs returned to the disk shape without shrinkage.

For the long term study of ATP reversibility, the CPD/AS-1 RBCs were washed in hyperglycemic and normoglycemic AS to remove the extracellular ATP from cell lysis during storage. As shown in figure 4.16, the basal ATP release from the CPD/AS-1 RBCs significantly ($p < 0.01$) increased after washing with AS-1N, compared to the sample washed with AS-1 at day 1. However, this increased basal ATP was not significant during the remaining storage.



RBCs in AS with Different Glucose Gradient, mM

Figure 4.14 – Mean Corpuscular Volume of RBCs in Glucose Gradient. The MCV of RBCs represents the average RBC volume, which is calculated by dividing the hematocrit by the total number of RBCs and multiplying by 10. The MCV of RBCs tended to decrease when they were exposed to high glucose; however, there was only significant decrease (* $p < 0.01$) in “111” mM glucose AS, compared to the sample in “5.5” mM glucose AS. Data represented as mean \pm s.e.m. (n = 4).

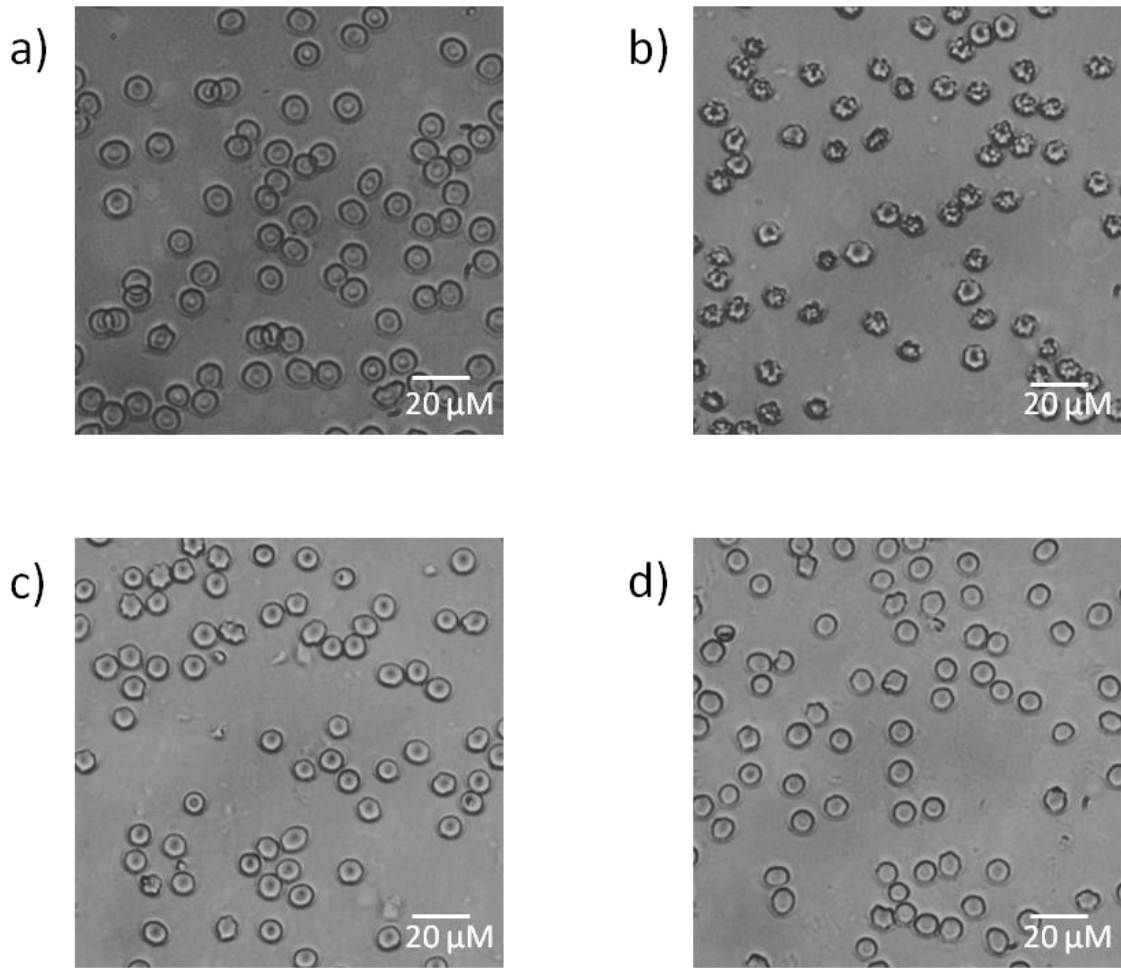


Figure 4.15 – Images of RBCs in Normoglycemic and Hyperglycemic Conditions. The images of RBCs suspended in 5.5 mM and 111 mM glucose AS are shown in a) and b), respectively. In a), RBCs had biconcave disk shapes, while RBCs shrank as shown in b). However, it is shown in d) that RBCs previously in hyperglycemic conditions returned to their normal shape after washing with 5.5 mM glucose AS. c) represents the RBCs previously in normoglycemic conditions after washing with 5.5 mM glucose AS.

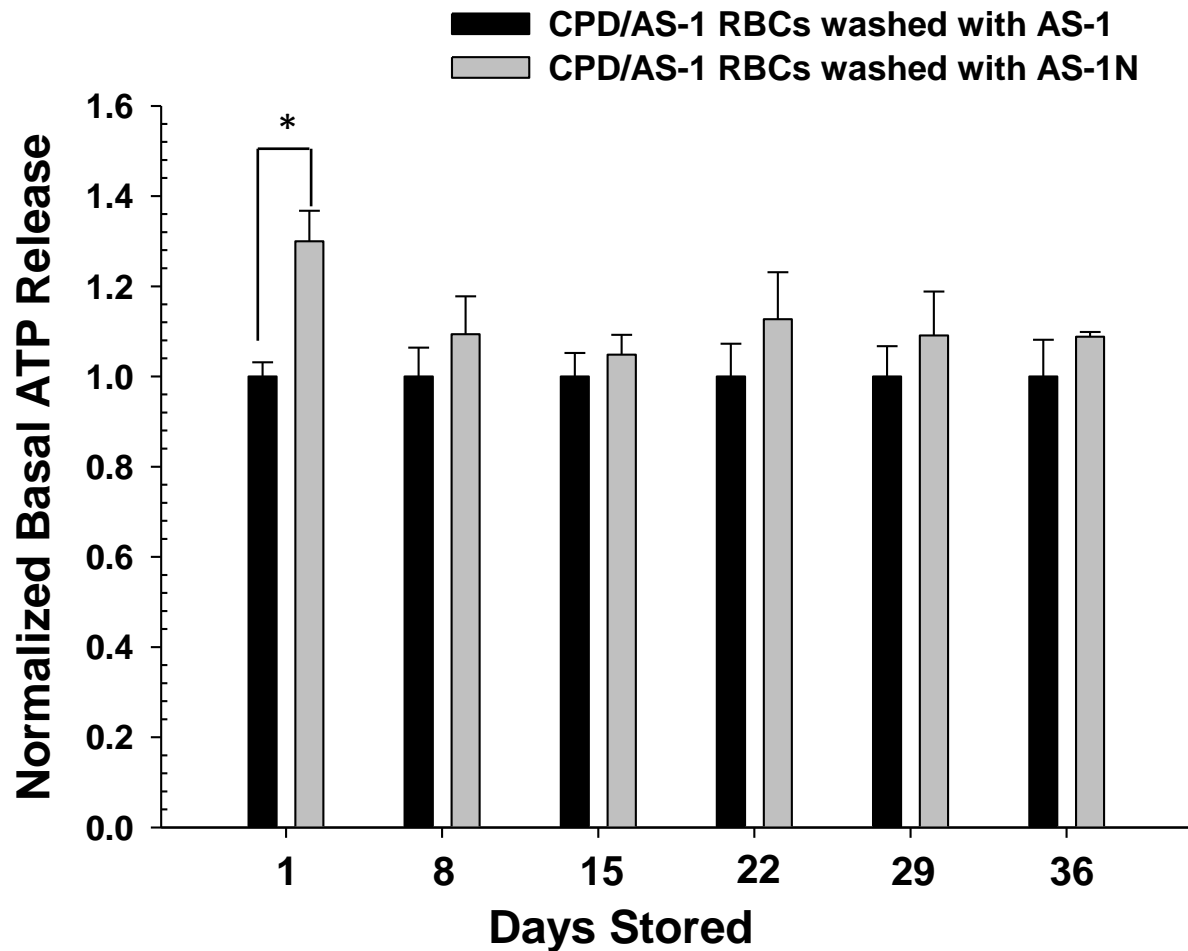


Figure 4.16 – Long Term Study of ATP Release Reversibility of Stored RBCs. The basal ATP release in the supernatant from the 7% stored RBCs was determined weekly during 36 days of storage. The CPD/AS-1 RBCs were washed in hyperglycemic (black bars) and normoglycemic (grey bars) AS to remove the extracellular ATP from cell lysis in storage. The normoglycemic values are normalized to the hyperglycemic values. At day 1, after washing with AS-1N, the basal ATP from the CPD/AS-1 RBCs significantly (* $p < 0.01$) increased with comparison to the sample washed with AS-1. However, this increased basal ATP was no longer significant during the remaining storage. Data represented as mean \pm s.e.m. (n = 4).

4.4 Discussion

When whole blood is drawn from a healthy donor who has a blood glucose level at ~ 5.5 mM into CPD with a glucose level at 129 mM, at a ratio of 1 to 7, the glucose quickly distributes to a quasiequilibrium between the plasma and RBCs.⁴⁰ Thus, after separating the RBCs from the plasma, the RBCs may contain ~ 20 mM glucose inside. When AS-1, with glucose level at 111 mM, is added into RBCs at a ratio of 1 to 2, the glucose level in the storage should be around 50 mM. As shown in figure 4.8, the intracellular and extracellular glucose levels in CPD/AS-1 storage were 51.8 ± 1.2 mM and 66.2 ± 1.2 mM at day 1. However, at day 36, the glucose levels were still as high as 44.1 ± 2.0 mM and 53.9 ± 2.1 mM, intracellular and extracellular, respectively. The results indicate that the amount of glucose in CPD/AS-1 is much higher than the needs of the metabolism of RBCs in storage, which may also lead to adverse effects.

Human blood plasma has an osmotic concentration of about 300. If RBCs are placed in distilled water, water molecules will rapidly cross the cell membrane by osmosis, and the cells will swell and rupture, releasing their cytoplasmic contents. By contrast, if RBCs are placed in a 300 mM solution of sucrose, which is a non-electrolyte and non permeable to the membrane, the cells do not lyse or change shape, since the osmotic concentration of the extracellular sucrose solution balances that of the intracellular fluid. However, since RBCs take up glucose by a facilitated diffusion carrier, glucose transporter 1 (GLUT1), with a half life < 30 seconds,^{40, 57} the total osmotic

concentration within the RBCs placed in a high glucose solution will quickly increase until glucose is distributed to quasiequilibrium. The data in figure 4.8 suggest that the intracellular glucose concentration was constantly lower than the extracellular one, which creates an osmotic imbalance, so the RBCs lose water into the media, and thereby undergo crenation due to the rapid osmotic efflux of water, as shown in figure 4.15b.

The increased intracellular osmotic concentration of RBCs in CPD/AS-1 may also explain the osmotic fragility shown in figure 4.9. The CPD/AS-1 RBCs had a $51.7 \pm 6.0\%$ hemolysis level in 0.45% NaCl at day 1, while normal RBCs should be on the verge of lysing at this concentration of NaCl. The sample in CPD-N/AS-1N had $5.6 \pm 0.6\%$ hemolysis. However, the difference in the osmotic fragility at day 1 was reversible. When the CPD/AS-1 RBCs, as well as CPD-N/AS-1N RBCs, were washed with saline 3 times, followed by the same procedure to determine osmotic fragility, the percent hemolysis of the two types of cells were equivalent to each other (data not shown). Given that the study of the RBCs suspended in a glucose gradient, as shown in table 4.1 and figures 4.13 and 4.14, less basal ATP is released from RBCs in high glucose AS, however, after washing with AS-1N, the RBCs without excess glucose were able to return to their original volume and release as much ATP as the RBCs in normal glucose AS. Therefore, this leads the hypothesis that RBCs collected in hyperglycemic CPD/AS-1 forms an osmotic imbalance, leading to cell dehydration and crenation, increasing

osmotic fragility, which may further impair the ability of ATP release at the beginning of storage.

In addition, the data of sorbitol accumulation in figure 4.10 shows the activity of the polyol pathway in CPD/AS-1 and CPD/AS-1N RBCs. Since the RBC membrane is not permeable to sorbitol, the intracellular sorbitol level simply reflects an equilibrium between its formation by aldose reductase and its depletion by sorbitol dehydrogenase.³⁶ The sorbitol level in the CPD-N/AS-1N RBCs was stable around 45 nmol/g Hb during storage, which is slightly higher than the clinical cut-off value between normal subjects and diabetic subjects (40 nmol/g Hb).⁴⁵ This small amount of sorbitol production may be due to a concentrated glucose portion for a short period created by the glucose feeding treatment. However, the rapid increase of sorbitol in CPD/AS-1 RBCs during the first week indicates the high activity of the polyol pathway occurred in CPD/AS-1 RBCs due to hyperglycemia. Following this, the sorbitol level was then stable around 130 nmol/g Hb for the remaining period. Since sorbitol is the intermediate of the polyol pathway, it may require further measurement of the fructose to determine the reason of this equilibrium. Thus, this increased activity of the polyol pathway implies a quick depletion of NADPH, which induces oxidative stress during storage.

One of the consequences of increased oxidative stress in RBCs is lipid peroxidation. The assessment of lipid peroxidation has relied largely on the analyses of secondary or end products derived from hydroperoxide transformation, metabolism, or decomposition,

such as MDA.⁵⁸ The measurement of MDA based on TBARS is a well-established method for screening and monitoring lipid peroxidation. There are several commercially available TBARS assay kits, however, they are not suitable for RBCs due to Hb interference and the presence of iron, which may catalyze sample oxidation.⁵⁹ Thus, the method used here is modified for RBCs by several aspects: the extraction MDAs from RBC using TCA to precipitate proteins, the addition of the antioxidant BHT to reduce sample autoxidation, and the usage of a sample blank to eliminate other interference, such as glucose. Jain *et al.* have shown that glucose-induced lipid peroxidation of the RBC could be blocked by dimethylfuran, the scavenger for singlet oxygen, which may indirectly suggest a possible generation of oxygen radicals and their contribution in lipid peroxidation in RBC treated with elevated glucose levels.⁶⁰ The data in figure 4.11 shows that the MDA levels increased as a function of storage time in CPD/AS-1 RBCs, which became significantly higher than the CPD-N/AS-1N RBCs at week 3 ($p < 0.05$). The MDA level in CPD-N/AS-1N RBCs was stable around 3 nmol/g Hb during storage, which is similar to the level in fresh RBCs reported in literature.^{49, 60} It has been shown that the exposure of RBCs to tertiary butyl hydroperoxide, an agent that induces the peroxidation of unsaturated fatty acids in membrane phospholipids, markedly increases membrane rigidity and decreases cellular deformability.⁶¹ Furthermore, it has been also shown that RBCs treated with 5 μ M MDA, which is more than an order of magnitude greater than the level that might be formed from endogenous phospholipids, had no

change in the resting morphology from the normal biconcave shape, but expressed decreased cellular deformability.⁶² Thus, the increased MDA observed in CPD/AS-1 RBCs with a longer storage period was induced by the oxidative stress resulting from hyperglycemia. This may further impair the membrane deformability of RBCs and be another cause of the reduced ability of stored RBC to release ATP.

In addition, increased production of ROS and alteration in membrane proteins might also result in less deformability of stored RBCs. As shown in figure 4.12, there was no significant difference of either peripheral proteins, hemoglobin, or integral proteins at day 1, week 2 and week 5, respectively. Although several efforts were done to improve the sensitivity, including the separation of membrane proteins and the extraction of chromophores using organic solvent, this measurement might be not specific enough for a glycation determination. The results also suggest that the glycation formed through the Amadori rearrangement, which takes hours to weeks, may occur slowly in the cold storage condition and therefore not be detectable, even though the reversible Schiff base formed between proteins and glucose may still affect the function of RBC membrane. However, it may be worth trying to measure a specific AGE, CML, using a competitive enzyme-linked immunosorbent assay (ELISA), which has been reported to form in RBCs during storage.⁴

There is an unexplained result from the data in figure 4.9: the osmotic fragility of the CPD-N/AS-1N RBCs increased dramatically after 2 weeks and become equivalent to the

CPD/AS-1 RBCs at day 29. This may be due to the periodic low glucose concentration in the RBCs between glucose feeding, leading to slower glycolysis and lower intracellular ATP reserves as shown in figures 2.9 and 2.11. This may have an adverse effect on the membrane properties in the later period of storage. In order to overcome this disadvantage of glucose feeding treatment, more discussion will be provided in chapter 5.

Overall, the osmotic fragility resulting from high glucose induced osmotic imbalance impaired the ability of the RBCs in CPD/AS-1 to release as much ATP as the cells in normoglycemic conditions at the beginning of storage. This is reversible after washing the RBCs with normoglycemic AS at day 1. However, as shown in figure 4.16, the RBCs stored in hyperglycemic conditions could not release increased amounts of ATP when they were washed with normoglycemic AS after 1 week of storage. This irreversibility may result from further cellular and membrane changes of RBCs in storage due to hyperglycemia, such as sorbitol accumulation and lipid peroxidation. The results shown here indicate that hyperglycemia may cause membrane damage of stored RBCs permanently and therefore irreversibly impair the ability of ATP release from RBCs in storage after a week. As mentioned in previous chapters, impaired RBC-derived ATP may lead to reduced endothelium-derived NO, and consequently inappropriate dilation and insufficient oxygen delivery. These adverse effects of RBCs stored in hyperglycemic condition on patients who need blood transfusion would result in possible posttransfusion complications.

REFERENCES

REFERENCES

1. Brown, C. D.; Ghali, H. S.; Zhao, Z.; Thomas, L. L.; Friedman, E. A., Association of Reduced Red Blood Cell Deformability and Diabetic Nephropathy. *Kidney International* 2005, *67* (1), 295-300.
2. Rattan, V.; Shen, Y.; Sultana, C.; Kumar, D.; Kalra, V. K., Diabetic Rbc-Induced Oxidant Stress Leads to Transendothelial Migration of Monocyte-Like HI-60 Cells. *American Journal of Physiology* 1997, *273* (2 Pt 1), E369-375.
3. Wautier, J. L.; Wautier, M. P.; Chappey, O.; Zoukourian, C.; Guillausseau, P. J.; Capron, L., Diabetic Erythrocytes Bearing Advanced Glycation End Products Induce Vascular Dysfunctions. *Clinical Hemorheology* 1996, *16* (5), 661-667.
4. Mangalmurti, N. S.; Chatterjee, S.; Cheng, G.; Andersen, E.; Mohammed, A.; Siegel, D. L.; Schmidt, A. M.; Albelda, S. M.; Lee, J. S., Advanced Glycation End Products on Stored Red Blood Cells Increase Endothelial Reactive Oxygen Species Generation through Interaction with Receptor for Advanced Glycation End Products. *Transfusion* 2010, *50* (11), 2353-2361.
5. Bennett-Guerrero, E.; Veldman, T. H.; Doctor, A.; Telen, M. J.; Ortel, T. L.; Reid, T. S.; Mulherin, M. A.; Zhu, H.; Buck, R. D.; Califf, R. M.; McMahon, T. J., Evolution of Adverse Changes in Stored Rbcs. *Proceedings of the National Academy of Sciences of the United States of America* 2007, *104* (43), 17063-17068.
6. Lee, J. S.; Gladwin, M. T., Bad Blood: The Risks of Red Cell Storage. *Nature Medicine* 2010, *16* (4), 381-382.
7. Hogman, C. F.; Eriksson, L.; Hedlund, K.; Wallvik, J., The Bottom and Top System: A New Technique for Blood Component Preparation and Storage. *Vox Sanguinis* 1988, *55* (4), 211-217.
8. Busse, R.; Ogilvie, A.; Pohl, U., Vasomotor Activity of Diadenosine Triphosphate and Diadenosine Tetraphosphate in Isolated Arteries. *The American Journal of Physiology* 1988, *254* (5 Pt 2), H828-832.
9. Arnal, J. F.; Dinh-Xuan, A. T.; Pueyo, M.; Darblade, B.; Rami, J., Endothelium-Derived Nitric Oxide and Vascular Physiology and Pathology. *Cellular and Molecular Life Sciences : CMLS* 1999, *55* (8-9), 1078-1087.
10. Bogle, R. G.; Coade, S. B.; Moncada, S.; Pearson, J. D.; Mann, G. E., Bradykinin and ATP Stimulate L-Arginine Uptake and Nitric Oxide Release in Vascular Endothelial Cells. *Biochemical and Biophysical Research Communications* 1991, *180* (2), 926-932.

11. Bergfeld, G. R.; Forrester, T., Release of ATP from Human Erythrocytes in Response to a Brief Period of Hypoxia and Hypercapnia. *Cardiovascular Research* 1992, 26 (1), 40-47.
12. Price, A. K.; Fischer, D. J.; Martin, R. S.; Spence, D. M., Deformation-Induced Release of ATP from Erythrocytes in a Poly(Dimethylsiloxane)-Based Microchip with Channels That Mimic Resistance Vessels. *Analytical Chemistry* 2004, 76 (16), 4849-4855.
13. Sprung, R.; Sprague, R.; Spence, D., Determination of ATP Release from Erythrocytes Using Microbore Tubing as a Model of Resistance Vessels in Vivo. *Analytical Chemistry* 2002, 74 (10), 2274-2278.
14. Ellsworth, M. L.; Forrester, T.; Ellis, C. G.; Dietrich, H. H., The Erythrocyte as a Regulator of Vascular Tone. *American Journal of Physiology* 1995, 269 (6 Pt 2), H2155-2161.
15. Light, D. B.; Capes, T. L.; Gronau, R. T.; Adler, M. R., Extracellular ATP Stimulates Volume Decrease in Necturus Red Blood Cells. *American Journal of Physiology* 1999, 277 (3 Pt 1), C480-491.
16. Sprague, R. S.; Ellsworth, M. L.; Stephenson, A. H.; Lonigro, A. J., Participation of Camp in a Signal-Transduction Pathway Relating Erythrocyte Deformation to ATP Release. *The American Journal of Physiology - Cell Physiology* 2001, 281 (4), C1158-1164.
17. Olearczyk, J. J.; Stephenson, A. H.; Lonigro, A. J.; Sprague, R. S., Heterotrimeric G Protein Gi Is Involved in a Signal Transduction Pathway for ATP Release from Erythrocytes. *The American Journal of Physiology - Heart and Circulatory Physiology* 2004, 286 (3), H940-945.
18. Olearczyk, J. J.; Stephenson, A. H.; Lonigro, A. J.; Sprague, R. S., Receptor-Mediated Activation of the Heterotrimeric G-Protein Gs Results in ATP Release from Erythrocytes. *Medical Science Monitor : International Medical Journal of Experimental and Clinical Research* 2001, 7 (4), 669-674.
19. Li, C.; Ramjeesingh, M.; Bear, C. E., Purified Cystic Fibrosis Transmembrane Conductance Regulator (Cftr) Does Not Function as an ATP Channel. *The Journal of Biological Chemistry* 1996, 271 (20), 11623-11626.
20. Braunstein, G. M.; Roman, R. M.; Clancy, J. P.; Kudlow, B. A.; Taylor, A. L.; Shylonsky, V. G.; Jovov, B.; Peter, K.; Jilling, T.; Ismailov, II; Benos, D. J.; Schwiebert, L. M.; Fitz, J. G.; Schwiebert, E. M., Cystic Fibrosis Transmembrane Conductance Regulator Facilitates ATP Release by Stimulating a Separate ATP Release Channel for Autocrine Control of Cell Volume Regulation. *The Journal of Biological Chemistry* 2001, 276 (9), 6621-6630.

21. Sprague, R. S.; Ellsworth, M. L.; Stephenson, A. H.; Kleinhenz, M. E.; Lonigro, A. J., Deformation-Induced ATP Release from Red Blood Cells Requires Cftr Activity. *American Journal of Physiology* 1998, 275 (5 Pt 2), H1726-1732.
22. Sprague, R. S.; Ellsworth, M. L., Erythrocyte-Derived ATP and Perfusion Distribution: Role of Intracellular and Intercellular Communication. *Microcirculation* 2012, 19 (5), 430-439.
23. Sridharan, M.; Sprague, R. S.; Adderley, S. P.; Bowles, E. A.; Ellsworth, M. L.; Stephenson, A. H., Diamide Decreases Deformability of Rabbit Erythrocytes and Attenuates Low Oxygen Tension-Induced ATP Release. *Experimental Biology and Medicine (Maywood)* 2010, 235 (9), 1142-1148.
24. Jagger, J. E.; Bateman, R. M.; Ellsworth, M. L.; Ellis, C. G., Role of Erythrocyte in Regulating Local O₂ Delivery Mediated by Hemoglobin Oxygenation. *The American Journal of Physiology - Heart and Circulatory Physiology* 2001, 280 (6), H2833-2839.
25. Mohandas, N.; Gallagher, P. G., Red Cell Membrane: Past, Present, and Future. *Blood* 2008, 112 (10), 3939-3948.
26. D'Amici, G. M.; Rinalducci, S.; Zolla, L., Proteomic Analysis of Rbc Membrane Protein Degradation During Blood Storage. *Journal of Proteome Research* 2007, 6 (8), 3242-3255.
27. Kriebardis, A. G.; Antonelou, M. H.; Stamoulis, K. E.; Economou-Petersen, E.; Margaritis, L. H.; Papassideri, I. S., Storage-Dependent Remodeling of the Red Blood Cell Membrane Is Associated with Increased Immunoglobulin G Binding, Lipid Raft Rearrangement, and Caspase Activation. *Transfusion* 2007, 47 (7), 1212-1220.
28. Bosman, G. J.; Lasonder, E.; Lutten, M.; Roerdinkholder-Stoelwinder, B.; Novotny, V. M.; Bos, H.; De Grip, W. J., The Proteome of Red Cell Membranes and Vesicles During Storage in Blood Bank Conditions. *Transfusion* 2008, 48 (5), 827-835.
29. Resmi, H.; Akhunlar, H.; Temiz Artmann, A.; Guner, G., In Vitro Effects of High Glucose Concentrations on Membrane Protein Oxidation, G-Actin and Deformability of Human Erythrocytes. *Cell Biochemistry and Function* 2005, 23 (3), 163-168.
30. Hunt, J. V.; Bottoms, M. A.; Mitchinson, M. J., Oxidative Alterations in the Experimental Glycation Model of Diabetes Mellitus Are Due to Protein-Glucose Adduct Oxidation. Some Fundamental Differences in Proposed Mechanisms of Glucose Oxidation and Oxidant Production. *The Biochemical Journal* 1993, 291 (Pt 2), 529-535.
31. Pokharna, H. K.; Pottenger, L. A., Glycation Induced Crosslinking of Link Proteins, in Vivo and in Vitro. *The Journal of Surgical Research* 2000, 94 (1), 35-42.

32. Dolhofer-Bliesener, R.; Lechner, B.; Gerbitz, K. D., Possible Significance of Advanced Glycation End Products in Serum in End-Stage Renal Disease and in Late Complications of Diabetes. *European Journal of Clinical Chemistry and Clinical Biochemistry : Journal of the Forum of European Clinical Chemistry Societies* 1996, 34 (4), 355-361.
33. Nawale, R. B.; Mourya, V. K.; Bhise, S. B., Non-Enzymatic Glycation of Proteins: A Cause for Complications in Diabetes. *Indian Journal of Biochemistry & Biophysics* 2006, 43 (6), 337-344.
34. Lo, T. W.; Westwood, M. E.; McLellan, A. C.; Selwood, T.; Thornalley, P. J., Binding and Modification of Proteins by Methylglyoxal under Physiological Conditions. A Kinetic and Mechanistic Study with N Alpha-Acetylarginine, N Alpha-Acetylcysteine, and N Alpha-Acetyllysine, and Bovine Serum Albumin. *The Journal of Biological Chemistry* 1994, 269 (51), 32299-32305.
35. Ahmed, M. U.; Thorpe, S. R.; Baynes, J. W., Identification of N Epsilon-Carboxymethyllysine as a Degradation Product of Fructoselysine in Glycated Protein. *The Journal of Biological Chemistry* 1986, 261 (11), 4889-4894.
36. Morrison, A. D.; Clements, R. S., Jr.; Travis, S. B.; Oski, F.; Winegrad, A. I., Glucose Utilization by the Polyol Pathway in Human Erythrocytes. *Biochemical and Biophysical Research Communications* 1970, 40 (1), 199-205.
37. Niki, E.; Yoshida, Y.; Saito, Y.; Noguchi, N., Lipid Peroxidation: Mechanisms, Inhibition, and Biological Effects. *Biochemical and Biophysical Research Communications* 2005, 338 (1), 668-676.
38. Marnett, L. J., Lipid Peroxidation-DNA Damage by Malondialdehyde. *Mutation Research* 1999, 424 (1-2), 83-95.
39. Bareford, D.; Jennings, P. E.; Stone, P. C.; Baar, S.; Barnett, A. H.; Stuart, J., Effects of Hyperglycaemia and Sorbitol Accumulation on Erythrocyte Deformability in Diabetes Mellitus. *Journal of Clinical Pathology* 1986, 39 (7), 722-727.
40. Moore, G. L.; Ledford, M. E.; Brooks, D. E., Distribution and Utilization of Adenine in Red Blood-Cells During 42 Days of 4c Storage. *Transfusion* 1978, 18 (5), 538-545.
41. Wu, J.; Li, Y.; Lu, D.; Liu, Z.; Cheng, Z.; He, L., Measurement of the Membrane Elasticity of Red Blood Cell with Osmotic Pressure by Optical Tweezers. *Cryo Letters* 2009, 30 (2), 89-95.
42. Mohandas, N.; Chasis, J. A., Red Blood Cell Deformability, Membrane Material Properties and Shape: Regulation by Transmembrane, Skeletal and Cytosolic Proteins and Lipids. *Seminars in Hematology* 1993, 30 (3), 171-192.

43. Cokelet, G. R.; Meiselman, H. J., Rheological Comparison of Hemoglobin Solutions and Erythrocyte Suspensions. *Science* 1968, *162* (3850), 275-277.
44. Meamarbashi, A.; Rajabi, A., Erythrocyte Osmotic Fragility Test Revealed Protective Effects of Supplementation with Saffron and Cinnamon on Red Blood Cell Membrane. *Asian Journal of Experimental Biological Sciences* 2013, *4*(2), 322-326.
45. Umeda, M.; Otsuka, Y.; Ii, T.; Matsuura, T.; Shibata, H.; Ota, H.; Sakurabayashi, I., Determination of D-Sorbitol in Human Erythrocytes by an Enzymatic Fluorometric Method with an Improved Deproteinization Procedure. *Annals of Clinical Biochemistry* 2001, *38* (Pt 6), 701-707.
46. Hayashi, R.; Hayakawa, N.; Makino, M.; Nagata, M.; Kakizawa, H.; Uchimura, K.; Hamada, M.; Aono, T.; Fujita, T.; Shinohara, R.; Nagasaka, A.; Itoh, M., Changes in Erythrocyte Sorbitol Concentrations Measured Using an Improved Assay System in Patients with Diabetic Complications and Treated with Aldose Reductase Inhibitor. *Diabetes care* 1998, *21* (4), 672-673.
47. Halliwell, B.; Chirico, S., Lipid Peroxidation: Its Mechanism, Measurement, and Significance. *The American Journal of Clinical Nutrition* 1993, *57* (5 Suppl), 715S-724S; discussion 724S-725S.
48. Clemens, M. R.; Waller, H. D., Lipid Peroxidation in Erythrocytes. *Chemistry and Physics of Lipids* 1987, *45* (2-4), 251-268.
49. Kaniyas, T.; Wong, K.; Acker, J. P., Determination of Lipid Peroxidation in Desiccated Red Blood Cells. *Cell Preservation Technology* 2007, *5* (3), 165-174.
50. Yagi, K., Simple Assay for the Level of Total Lipid Peroxides in Serum or Plasma. *Methods in Molecular Biology* 1998, *108*, 101-106.
51. Armstrong, D.; Browne, R., The Analysis of Free Radicals, Lipid Peroxides, Antioxidant Enzymes and Compounds Related to Oxidative Stress as Applied to the Clinical Chemistry Laboratory. *Advances in Experimental Medicine and Biology* 1994, *366*, 43-58.
52. Pikul, J.; Leszczynski, D. E.; Kummerow, F. A., Elimination of Sample Autoxidation by Butylated Hydroxytoluene Additions before Thiobarbituric Acid Assay for Malonaldehyde in Fat from Chicken Meat. *Journal of Agricultural and Food Chemistry* 1983, *31* (6), 1338-1342.
53. Murtiashaw, M. H.; Young, J. E.; Strickland, A. L.; Mcfarland, K. F.; Thorpe, S. R.; Baynes, J. W., Measurement of Nonenzymatically Glucosylated Serum-Protein by an Improved Thiobarbituric Acid Assay. *Clinica Chimica Acta* 1983, *130* (2), 177-187.

54. Yu, J.; Steck, T. L., Selective Solubilization, Isolation, and Characterization of a Predominant Polypeptide from Human Erythrocyte Membranes. *Journal of Cell Biology* 1973, 59 (2), A374-A374.
55. Parker, K. M.; England, J. D.; Dacosta, J.; Hess, R. L.; Goldstein, D. E., Improved Colorimetric Assay for Glycosylated Hemoglobin. *Clinical Chemistry* 1981, 27 (5), 669-672.
56. Brugnara, C.; Mohandas, N., Red Cell Indices in Classification and Treatment of Anemias: From M.M. Wintrob's Original 1934 Classification to the Third Millennium. *Current Opinion in Hematology* 2013, 20 (3), 222-230.
57. Lienhard, G. E.; Slot, J. W.; James, D. E.; Mueckler, M. M., How Cells Absorb Glucose. *Scientific American* 1992, 266 (1), 86-91.
58. Janero, D. R., Malondialdehyde and Thiobarbituric Acid-Reactivity as Diagnostic Indices of Lipid Peroxidation and Peroxidative Tissue Injury. *Free Radical Biology & Medicine* 1990, 9 (6), 515-540.
59. Pyles, L. A.; Stejskal, E. J.; Einzig, S., Spectrophotometric Measurement of Plasma 2-Thiobarbituric Acid-Reactive Substances in the Presence of Hemoglobin and Bilirubin Interference. *Proceedings of the Society for Experimental Biology and Medicine* 1993, 202 (4), 407-419.
60. Jain, S. K., Hyperglycemia Can Cause Membrane Lipid Peroxidation and Osmotic Fragility in Human Red Blood Cells. *The Journal of Biological Chemistry* 1989, 264 (35), 21340-21345.
61. Corry, W. D.; Meiselman, H. J.; Hochstein, P., T-Butyl Hydroperoxide-Induced Changes in the Physicochemical Properties of Human Erythrocytes. *Biochimica et Biophysica Acta* 1980, 597 (2), 224-234.
62. Pfafferott, C.; Meiselman, H. J.; Hochstein, P., The Effect of Malonyldialdehyde on Erythrocyte Deformability. *Blood* 1982, 59 (1), 12-15.

Chapter 5 – Conclusions and Future Directions

5.1 Overall Conclusions

Red blood cell (RBC) transfusion is a key element of modern medical care. In modern RBC storage systems, whole blood is collected into an anticoagulant-nutrient solution such as citrate phosphate dextrose (CPD). The RBCs are separated from the plasma and platelets and added into an additive solution, such as AS-1, which supports the nutrient needs of the RBCs in storage. This system allows for RBCs to be stored for 35-42 days at 4°C. Unfortunately, this storage is not perfect, as the RBCs undergo storage lesions, which include metabolic effects, shape change, membrane loss, oxidative injury to lipid and proteins, changes in oxygen affinity and delivery, shedding of active proteins, lipids, and microvesicles, and reduced RBC lifespan.¹

The RBC is a highly specialized cell without a nucleus and other organelles such as mitochondria; thus, it has to rely on the breakdown of glucose to adenosine triphosphate (ATP) for cellular metabolism. Both CPD and AS-1 contain glucose, but in a much higher concentration than the glucose level *in vivo* (4-6 mM). As shown in figure 4.8, the glucose level inside and outside of RBCs were 51.8 ± 2.4 mM and 66.2 ± 2.4 mM, respectively, just after collecting and storing in CPD/AS-1. They decreased to 44.1 ± 4.1 mM intracellular and 53.9 ± 4.3 mM extracellular at day 36. This indicates that the amount of glucose added into the storage solutions is much higher than the needs of the RBCs.

The results presented in this dissertation show the effects of hyperglycemia on various parameters of red blood cells (RBCs) in storage. Evidence is provided to explain the mechanism of these effects. In addition to the primary function of oxygen delivery, RBCs can function as a regulator of vascular tone. ATP is released from intact RBCs in response to several stimuli and further stimulates nitric oxide (NO) production in the endothelium lining the blood vessels.²⁻³ This NO can function to relax the smooth muscle cells surrounding circulatory vessels, thereby increasing blood flow and oxygen delivery to the tissues.

The major finding of this study is shown in figure 2.10: RBCs stored in a hyperglycemic condition (CPD/AS-1) release significantly less ATP under mechanical deformation, as compared to the RBCs stored in a normoglycemic environment. In addition, it has been demonstrated that impaired ATP release is a novel RBC storage lesion.⁴ As discussed in chapter 2, the normoglycemic storage of RBCs was achieved by storing RBCs in the normoglycemic version (5.5 mM glucose) of CPD/AS-1 (CPD-N/AS-1N), followed by a periodic glucose feeding regimen. With the maintenance of a healthy glucose level during storage, RBCs were not only able to metabolize normally (as the lactate accumulation data in figure 2.9 shows), but were also capable of releasing normal amounts of ATP for 4 weeks. Although the intracellular ATP level of the RBCs was significantly higher in hyperglycemic storage than in normoglycemic storage after 3 weeks, this ATP reservoir does not convert into released ATP.

To further investigate the vascular function of stored RBCs, a microfluidic device was employed to study the cell-cell communication between flowing RBCs and endothelial cells immobilized on the membrane of the device, as presented in chapter 3. The results in figure 3.7 suggest that the impaired ATP release from RBCs stored in a hyperglycemic condition would result in decreased NO release from healthy endothelial cells. Two control experiments were performed to confirm that the detected NO was from endothelium and was stimulated by RBC-derived ATP, as shown in figures 3.8 and 3.9. It has been proposed that NO levels in the vascular beds are markedly reduced, leading to the impaired vasodilation in patients who have received a transfusion.⁵ This hypothesis of insufficient NO bioavailability (INOBA) may explain the increased morbidity and mortality observed in some patients after RBC transfusion. In addition, the percent hemolysis of stored RBCs was not affected by the normoglycemic storage.

Several cellular properties were studied to investigate a possible reason for impaired ATP release from RBCs stored in a hyperglycemic condition. It has been shown that RBCs can release ATP through a signal transduction pathway involving the G-protein coupled receptor (GPCR), cyclic adenosine monophosphate (cAMP), and the cystic fibrosis transmembrane conductance regulation (CFTR) protein.⁶⁻⁸ Specifically, the initiation of this pathway is a series of conformational changes in the GPCR under mechanical deformation or changes in the deformability of the membrane due to other stimuli. Thus, the factors that influence the deformability of RBCs may also affect ATP release from RBCs.

The data in figure 4.9 indicates the osmotic fragility of stored RBCs in hyperglycemic conditions was much higher than that of RBCs in normoglycemic conditions even at day 1. This increased osmotic fragility resulted from the osmotic imbalance inside and outside of the RBCs, which was induced by the high amount of glucose in the solutions. This also led to the shrinkage and crenation of RBCs, as shown in figures 4.14 and 4.15. This osmotic effect on RBCs, due to hyperglycemia, may decrease their deformability and therefore impair the ability of the RBCs to release ATP initially.

The effect of hyperglycemia on RBCs is reversible at the beginning of storage. The reversibility experiments indicate that RBCs can return to normal shape and volume after the removal of the excess glucose at day 1. At the same time, the basal ATP release from these RBCs was equivalent to the basal ATP release from the RBCs in the normoglycemic condition, as shown in figure 4.13. However, the longer the RBCs are stored in a hyperglycemic condition, the more irreversible the changes become. From the long term reversibility study, shown in figure 4.16, it is shown that RBCs stored in a hyperglycemic condition for more than a week did not release appreciable levels of ATP, even after the removal of excess amount of glucose.

Within the first week of storage, sorbitol started to accumulate due to the polyol pathway activation induced by hyperglycemic conditions. The accumulation of sorbitol would further increase the osmotic effect. Another effect of the polyol pathway is the depletion of the cofactor NADP^+ , which is required for the regeneration of glutathione (GSH), the antioxidant against the cellular reactive oxygen species (ROS). Thus, the

oxidative stress induced by the polyol pathway further causes damage to important cellular components, such as the RBC membrane. As shown in figure 4.11, the level of the malondialdehyde (MDA), an indicator of lipid peroxidation, increased as a function of time in the RBCs stored in hyperglycemic conditions. This damage of phospholipids, the major component of the cell membrane, may alter the mechanical behavior of the membrane and therefore lead to an irreversible change in the ability of RBCs to release ATP. Another concern of hyperglycemic storage conditions is the effect on proteins, such as membrane proteins and hemoglobin, in terms of glycation and oxidation. However, based on the results in the study shown in figure 4.12, there was no significant increase of protein glycation either with longer storage time or when compared to the RBCs stored in normoglycemic condition. The formation of protein glycation may need a longer time to become detectable using the thiobarbituric (TBA) assay, due to the cold temperature of storage decreasing reaction rates. However, it is interesting to consider the high amount of glucose interacting with the proteins, especially the primary amine groups, forming a reversible Schiff base, which may also impact the function of proteins to some extent.

Although the normoglycemic storage cannot eliminate all of the storage lesions, it helps the RBCs by reducing the osmotic effect and oxidative stress, and therefore, RBCs appear to be in better health. However, the periodic glucose feeding treatment needs to improve to become a continuous method of providing “food” to RBCs. The 5-day

interval between each feeding may also cause some adverse effects during RBC storage, such as slow glucose metabolism.

Overall, hyperglycemic storage used currently results in the irreversibly impaired ATP release from RBCs, an important vascular regulator, due to the osmotic effect and oxidative stress. This decreased ATP release will subsequently reduce the endothelium-derived NO. When a patient loses 30-40% of total blood volume, approximately 1.5 to 2 L, it is necessary to perform a blood transfusion. Imagine that tons of stored RBCs, especially old stored RBCs (often described as > 14-21 days), were transfused into the patient; however, those transfused RBCs could not release ATP in response to the physiological stimuli, and therefore result in low bioavailability of NO in the patient. The adverse consequence of the transfusion would be inappropriate vasodilation, less blood flow, and insufficient oxygen delivery. Thus, although the transfused RBCs replace the lost component of whole blood, they do not function well. Not to mention that the high amount of residual glucose and oxidative species are brought into the patient with transfusion. Clinical studies have shown that increased morbidity and mortality occurred in the patients who received old blood.⁹⁻¹⁰ The adverse vascular effects of RBCs associated with hyperglycemic conditions are often associated with those post-transfusion complications. If the RBCs could be stored and maintained in normoglycemic conditions, it may be possible to reduce these complications to some extent and hopefully improve RBC transfusion efficacy.

5.2 Animal Model Determination of Posttransfusion Survival of RBCs Stored in Different Storage Solutions

5.2.1 Introduction

The previous chapters have introduced and discussed several benefits of RBCs stored in normoglycemic conditions. However, there is no *in vitro* method that can predict with great accuracy how a given sample of stored RBCs will survive in the circulation. RBC survival is a general term describing the persistence of RBCs in circulation. When stored RBCs are injected into the circulation, some cells are cleared within a few hours, but the rest survive normally. Thus, in order to investigate the viability of stored RBCs *in vivo*, direct measurement of posttransfusion survival has to be performed.

Labeling of RBCs with ^{51}Cr is a practical method for measuring RBC survival and has such advantages as ease of RBC labeling, excellent RBC uptake, low toxicity, and low and stable elution rate. It is commonly performed by using the radioisotope disodium chromate ^{51}Cr ($\text{Na}_2^{51}\text{CrO}_4$), since the hemoglobin (Hb) within the RBC has a very high affinity for chromium. RBC survival can be determined using either the single-label technique with back-extrapolation or the double-label technique with direct measurement of the RBC mass. Other cell radiolabels are used in the double-label technique, such as technetium ($^{99\text{m}}\text{Tc}$) and indium (^{111}In).¹¹

A non-radiolabeled method of measuring RBC survival has been developed based on biotinylation of RBCs.¹²⁻¹³ Biotinylation of intact RBCs is performed by covalent attachment to the amino groups by means of biotin N-hydrosuccinimide ester (NHS-biotin), as shown in figure 5.1. NHS-biotin has poor solubility in aqueous solutions, which has to first be dissolved in an organic solvent, such as DMF and DMSO, and then diluted into the aqueous reaction mixture. After reacting with RBCs, biotin can still bind to streptavidin and avidin with an extremely high affinity and high specificity, and is resistant to extremes of heat, pH, and proteolysis. Thus, the principle of this method is based on the determination of the number of biotin-labeled RBCs that persist in the circulation by using fluorescein-labeled streptavidin and flow cytometry. Since the biotinylated RBCs are examined and enumerated individually by flow cytometry, they are counted accurately to as low as 0.06% of the circulating RBCs.¹⁴ In addition, this alternative method avoids radiation exposure to the test subjects.

To determine RBC survival, biotinylated RBCs are transfused back into the subjects, and blood samples are obtained at 10 minutes after transfusion and at approximately 1, 2, 4, 6, 24, 48 hours, and 7, 14 days thereafter. The survival variable can be determined from post-transfusion recovery at 24 hours (PTR_{24}), which reflects the intravascular recovery of RBCs 24 hours after transfusion. In order to have an accurate determination of the PTR_{24} , the 10-minute sample is used to represent 100% survival, since the infused RBCs are mixed completely by 3 minutes after transfusion in a normal person.¹⁵ Thus the

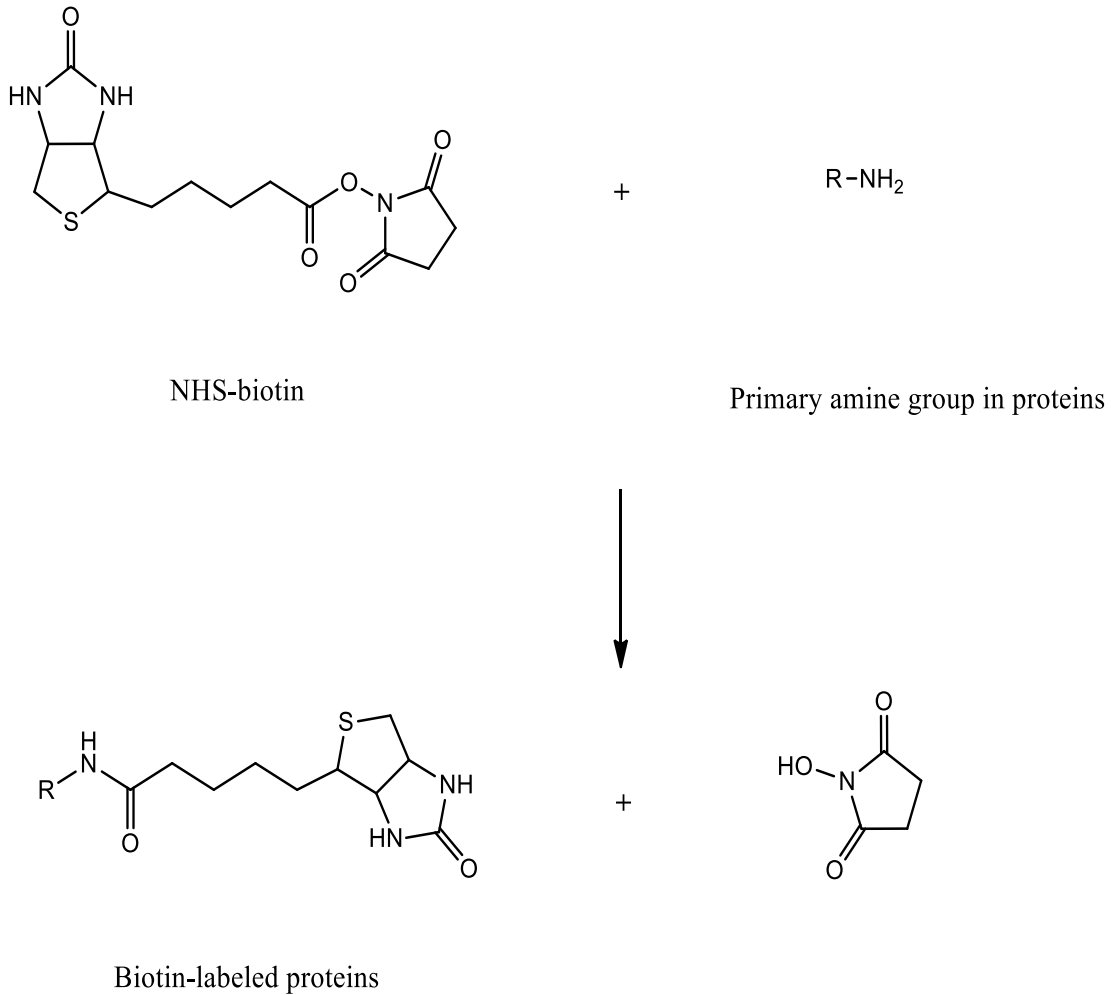


Figure 5.1 – The Mechanism of Biotinylation. NHS-biotin is the most popular type of biotinylation reagent. It reacts efficiently with primary amino groups of proteins to form stable amide bonds. The targets for labeling include the side chain of lysine residues and the N-terminus of each polypeptide.

PTR₂₄ can be calculated as the percentage of biotinylated RBCs circulating 24 hours after transfusion divided by the percentage of biotinylated RBCs circulating 10 minutes after transfusion. Another variable is called the mean potential RBC life span (MPL). The percentage of biotinylated RBCs measured at various time points are expressed as a percentage of the value for the 10-minute sample and plotted versus time. Since the population distribution for the age of RBCs is even in a healthy adult subject, this survival curve should demonstrate a linear decline if all RBCs are uniformly labeled. Thus, the value obtained by extrapolation of this linear disappearance curve to the time axis is referred to as the MPL. The MPL reflects the average life span of the stored RBCs that are transfused into the circulation until they are removed.¹⁶

Several animal models are employed in preclinical studies of blood transfusion and blood substitutes, including mouse, rabbit, dog, horse, and baboon.¹⁷⁻²¹ However, animal models may not be perfect for all studies. It has been reported that the storage of rat RBCs for 1 week in CPDA-1 produces a storage lesion similar in extent to human RBCs stored for 4 weeks.²² In addition, dog RBCs are known to contain amounts of ATP similar to those of rabbit, but do not release that ATP under physiological conditions, so they are not suitable for this study.²³ Here, a rabbit model was chosen because it is easy to access and previous work indicated that the results would be applicable to human blood.²⁴⁻²⁵ Autologous blood transfusion is the collection of blood from a

subject and retransfusion back to the same subject, which can reduce the risks of disease transmission and immune-mediated reactions, and thereby provide an accurate prediction of the survival of the transfused RBCs.²⁶

5.2.2 Optimization of Biotinylation of RBCs in Storage

The biotinylation of RBCs was first optimized with human RBCs. The first attempt of biotinylation of RBCs was based on the method developed by Chiarantini *et al.*²⁷ Briefly, RBCs from human donors were washed 3 times and adjusted to 10% hematocrit (Hct) with phosphate buffered saline (PBS, pH 7.4). A 0.1 M NHS-biotin solution (ApexBio, Houston TX) was prepared in dimethylformamide (DMF) and added into the 10% RBCs at a ratio of 3 μ L per ml of RBC suspension. After a 20-minute incubation at room temperature (RT) on the shaker, the RBCs were washed 3 times with PBS and adjusted to 10% Hct suspension again. Biotin-labeled RBCs were further labeled with fluorescent streptavidin-FITC (S-FITC). A 0.01 mg/ μ L of S-FITC (BioLegend, San Diego, CA) was prepared by diluting the stock 50-fold with PBS. Next, 20 μ L of S-FITC were added into 5 μ L of biotin-labeled RBC suspension. Following a 30-minute incubation in the dark at 4°C, the RBC suspension was carefully washed 3 times with PBS and resuspended into 2 mL with PBS. Samples were evaluated via flow cytometer (BD Accuri C6, San Joes CA); 10⁴ of cells were analyzed. The percentage of biotin-labeled RBCs was the ratio of the number of the cells with fluorescent intensity (FL) > 10³ to the total number of cells. The results in figure 5.2 show that human RBCs can be biotinylated completely using this

method. In addition, to determine whether a measurable percentage of RBCs could reliably be recovered, different ratios of total RBCs and biotin-labeled RBCs mixtures (2:1, 5:1, 10:1, 20:1 and 30:1) were prepared and further labeled with fluorescent S-FITC as described above. As shown in figure 5.2, all ratios can be successfully achieved without excess biotinylation.

In order to use the biotinylation method to determine the posttransfusion survival rate of stored RBCs, the method had to be modified and optimized. The stored RBCs (~ 60% Hct) cannot be diluted to 10% Hct and washed with PBS for biotinylation before transfusion. Thus, the amount of biotin added has to be the exact amount for the RBCs to avoid excess labeling after transfusion into the recipient. Owens *et al.* have shown that 0.04 pg of biotin/RBC is the optimal biotin concentration for the post-transfusion survival study in horses.²⁶ However, none of the RBCs could be biotinylated using a NHS-biotin solution with the concentration of 42 mM to achieve 0.04 pg of biotin/RBC directly in storage conditions without washing. Surprisingly, once those “non-biotinylated RBCs” were mixed with unbiotinylated RBCs at a ratio higher than 10:1, it would show the correct percentage of biotin-labeled RBCs. Inspired by this fact, the amount of biotin should be enough for biotinylation, but the high concentration of biotin could induce aggregation and therefore no biotin-labeled RBCs were shown. After several trials of reducing concentration and repeat labeling, the optimal concentration of NHS-biotin was determined to be 2 mM. In addition, biotinylation was also optimized based on the volume of stored RBCs, the incubation time, and temperature.

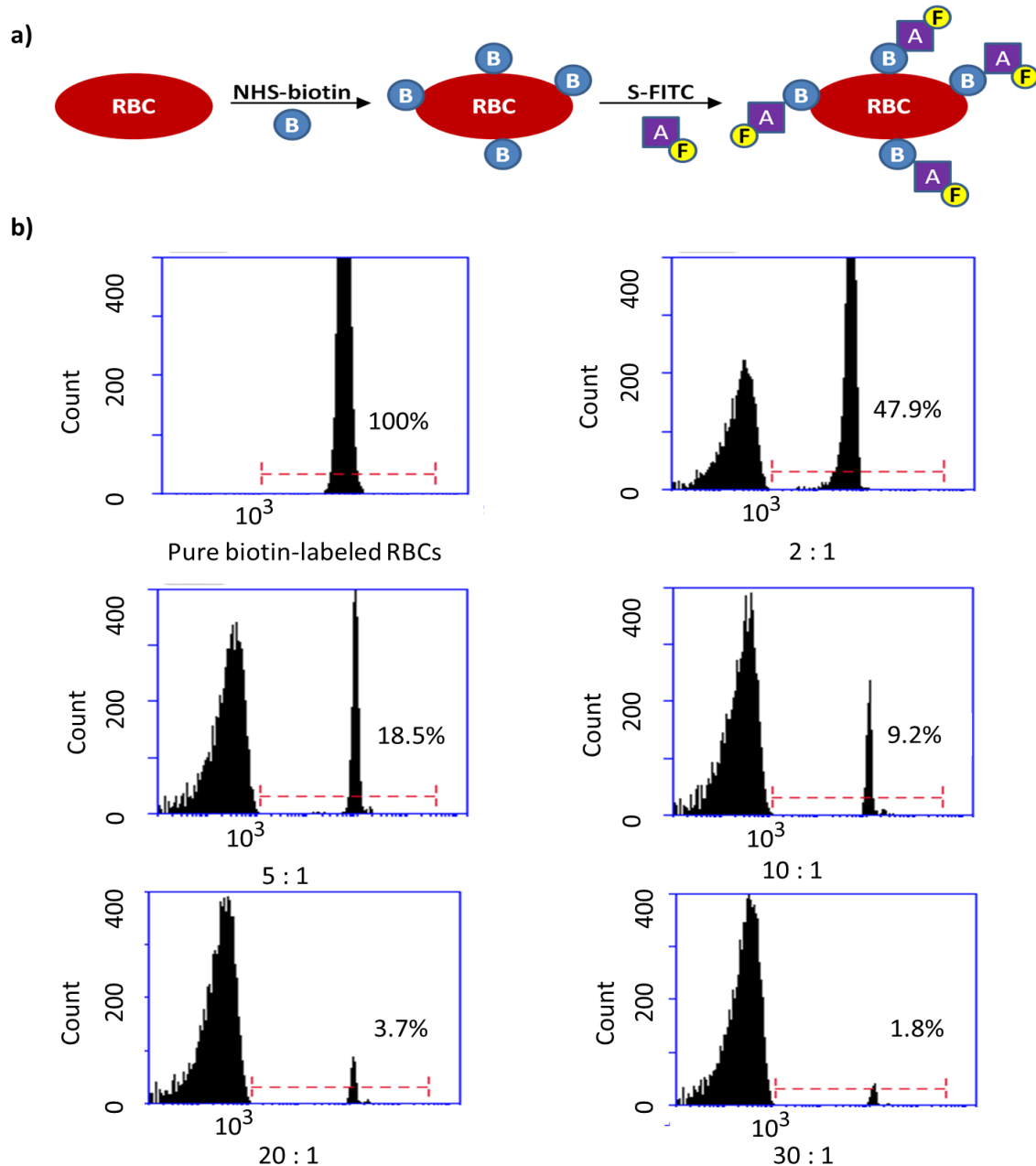


Figure 5.2 – The Detection of Biotin-Labeled RBCs using Flow Cytometry. Panel a) represents the procedure of the biotinylation of RBCs using NHS-biotin and further labeling with streptavidin-conjugated fluorescein FITC for flow cytometry. Panel b) shows the results of biotinylation of RBCs using flow cytometer: pure biotin-labeled RBCs and different ratios of total RBCs and biotin-labeled RBCs mixtures (2:1, 5:1, 10:1, 20:1 and 30:1). The percentage of biotin-labeled RBCs is the ratio of the number of cells with fluorescent intensity $> 10^3$ to the total number of cells. For interpretation of the references to color in this and all other figures, the reader is referred to the electronic version of this dissertation.

Therefore, the stored RBCs could be completely biotinylated by adding the correct volume (based on 0.04 pg of biotin/RBC) of the NHS-biotin with the concentration of 2 mM, directly in storage (either CPD/AS-1 or CPD-N/AS-1N) without dilution or washing. The volume of stored RBCs could be scaled up to 5 mL for both human and rabbit RBCs. The incubation was extended to 1 hour but still at RT, since biotinylation of RBCs did not occur at 4°C. The further labeling with S-FITC was the same as described above.

5.2.3 Preliminary Posttransfusion Survival Study of Stored RBCs using a Rabbit Model

This study was in collaboration with In Vivo Facility at Michigan State University to evaluate the post-transfusion survival of stored RBCs in CPD/AS-1 and CPD-N/AS-1N. Briefly, 4 male New Zealand White rabbits, weighing approximately 3-4 kg and in good health were assigned to the study. Rabbits were first anesthetized with isoflurane. Approximately 14 mL of whole blood from each of 4 rabbits were drawn and collected in either CPD or CPD-N. After a 30 minute incubation at RT, the whole blood was centrifuged, followed by discarding the plasma and the buffy coat. Next, the packed RBCs were added into AS-1 or AS-1N (resulting in 7-9 mL of stored RBCs) for storage. The following day, after 24 hours of storage, the stored RBCs were biotinylated and then autotransfused back into the respective donor rabbits. Before transfusion, 50 µL of biotin-labeled stored RBCs were saved to prove the complete biotinylation. Transfusion took approximately 10 minutes for each rabbit. 1 mL of blood was collected from each rabbit for analysis at 0, 1, 2, 4, 6, 24 and 48 hours post-transfusion, and at 7 and 14 days post-transfusion. The post-transfusion whole blood was washed with PBS once before

treating with S-FITC. The samples were prepared in a duplicate manner. The measurement of biotin-labeled RBCs using flow cytometry allowed for the comparison of RBC survival between the RBCs stored in hyperglycemic and normoglycemic conditions.

The results in figure 5.3 show an example of post-transfusion survival data of the RBCs stored in CPD/AS-1 from rabbit No. 1: approximately 100% of stored RBCs were biotinylated before transfusion, and 8.1% of biotinylated RBCs were determined at 10-minute time point, using the optimized method described above. The fluorescence intensity shifted to left compared to the results obtained in the optimization experiments. This might indicate higher amount of biotin per RBC should be used in the bulk labeling for further study. The MPL of stored RBCs were calculated based on the best fit curve plotted as percentage versus time (figure 5.3 c)). The stored RBCs have the MPL of 35.8 ± 4.9 days and 31.0 ± 3.4 days, in hyperglycemic and normoglycemic conditions, respectively. The results in table 5.1 show that the percentage of biotinylated RBCs increased irregularly compared to the value at 10-minute time point during the first two days after transfusion. The increased value might represent the non-favored biotinylation of the RBCs *in vivo* by the excess biotin in the storage. However, this was never observed *in vitro* in the optimization experiments. Although there was a fluctuation in the percentage of biotin, the value at 10-minute value was still used to representing 100% survival. Thus, the PTR₂₄ of the stored RBCs were $95 \pm 10\%$ and $98 \pm 2\%$, in hyperglycemic and normoglycemic conditions, respectively. Since these RBCs

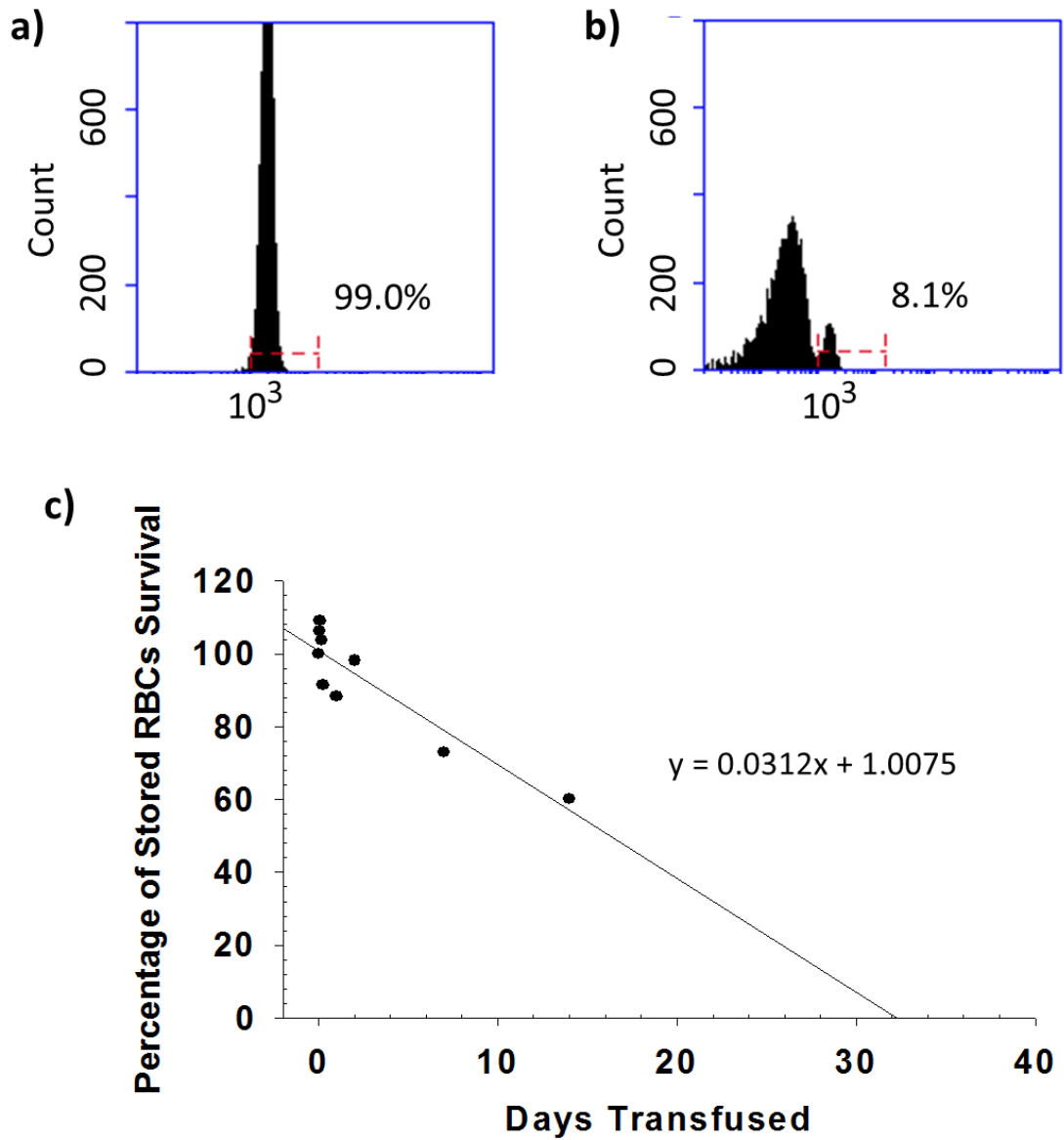


Figure 5.3 – An Example of Posttransfusion Survival Data of Stored RBCs. Panel a) shows approximately 100% of stored RBCs were biotinylated before transfusion using the optimized method described previously. Panel b) represents that 8.1% of total RBCs circulating in that rabbit were the biotinylated stored RBCs at 10-minute time point. Panel c) shows the best fit curve plotted as percentage of stored RBCs survival versus time. The MPL of stored RBCs can be calculated based on the equation. For interpretation of the references to color in this and all other figures, the reader is referred to the electronic version of this dissertation.

Table 5.1 – Percentage of Posttransfusion Survival of Stored RBCs at Various Time Points

Time/day	Rabbit No.1 CPD/AS-1	Rabbit No.3 CPD/AS-1	Rabbit No.2 CPD-N/AS-1N	Rabbit No.4 CPD-N/AS-1N
0	100	100	100	100
0.04	106	107	108	104
0.08	109	114	102	112
0.17	104	104	107	96
0.25	91	108	102	102
1	88	102	99	96
2	98	107	105	99
7	73	81	80	74
14	60	71	61	54

were only stored for 24-hour, the posttransfusion survival of stored RBCs were pretty high and there was not a significant difference between the hyperglycemic and normoglycemic storage.

6 rabbits were originally assigned to this study. However, a study of 4 rabbits was finished before writing. Thus, the first future work would be the completion of this study with all rabbits or with different study conditions (e.g., time in storage for cell samples). Also, considering the long term reversibility study in chapter 4, the permanent change has not occurred in the first day of storage. Thus, a significant difference could be expected between the hyperglycemic and normoglycemic conditions when the post-transfusion survival study was performed using the RBCs in longer storage (> 14 days).

5.3 Glucose Slow Release Device/Membrane Development

As mentioned in chapter 2, the normoglycemic conditions were maintained by a periodic glucose feeding treatment. However, this treatment is not perfect. First, the glucose feeding is provided every 5 days. During these 5 days, the glucose level of storage may decrease to ~ 1.4 mM, which may have an adverse effect on the RBCs, such as decreased glycolytic metabolism. Second, the glucose feeding is performed by using a very high concentration of glucose saline solution. The drop of concentrated glucose saline into storage would result in a local high glucose level and consequently sorbitol accumulation in the related RBCs. Thus, it is necessary to develop a glucose source that can release glucose slowly according to the glucose metabolism rate of stored RBCs at 4°C.

The first attempt at this was performed by our group using a polycarbonate membrane, which enables glucose to diffuse from one area to another. An experimental glucose diffusion chamber was constructed of a ~3 mL glass vial with a cap that held a circular piece of 0.4 μm pore membrane. The chamber was filled with 200 mM glucose in AS that was placed in 40 mL of AS without glucose. The entire setup was placed in a refrigerator at 4 C and samples were taken at various time points to determine the diffusion rate. By decreasing the diffusion area of the membrane to 0.2 mm^2 , the diffusion rate of glucose could be controlled at 1.4 ± 0.3 mM/day, which is close to the metabolism rate of stored RBCs. However, transforming this preliminary device to a commercial device that can be used in blood banking still needs tremendous efforts.

Another idea is to provide glucose-limited feeding by a secondary glucose source instead of the direct addition of glucose. Suitable secondary sources of glucose can be a glucose-containing oligosaccharide or polysaccharide and a glucosidase. The rate of glucose release therefore can be controlled by adjusting the glucosidase activity present. Neubauer *et al.* have shown that high cell density cultivations were achieved by enzyme controlled glucose auto-delivery.²⁸⁻²⁹ The secondary glucose source was the starch, formed as a metabolically inactive polymer, which could be hydrolyzed by the enzyme, glucoamylase, to glucose. A similar experiment was tried with the collaboration of Dr. Odom from the University of Kentucky. The secondary glucose source chosen was lactose together with the enzyme, lactase. The addition of 0.1 g of lactose and 0.01 g of lactase per mL of AS would allow to release glucose at a rate of approximately 1

mM/day for a week. However, the direct addition of lactose and lactase in the AS to store RBC resulted in an initial high glucose level of ~ 10 mM in the storage.

Overall, more efforts should be made to improve the glucose feeding system, to provide a reliable controlled glucose release into the storage. The glucose source or the material of the device should be chosen wisely to avoid the interruption of normal function and metabolism of the RBCs in storage. In addition, this device or source needs to be able to be applied to the current storage bags conveniently without large changes. The achievement of providing a physiologically normal glucose condition to the storage of RBCs may lead to improved function of stored RBCs after transfusion.

REFERENCES

REFERENCES

1. Hess, J. R., An Update on Solutions for Red Cell Storage. *Vox Sanguinis* 2006, *91* (1), 13-19.
2. Bergfeld, G. R.; Forrester, T., Release of ATP from Human Erythrocytes in Response to a Brief Period of Hypoxia and Hypercapnia. *Cardiovascular Research* 1992, *26* (1), 40-47.
3. Sprague, R. S.; Ellsworth, M. L.; Stephenson, A. H.; Lonigro, A. J., ATP: The Red Blood Cell Link to No and Local Control of the Pulmonary Circulation. *American Journal of Physiology* 1996, *271* (6 Pt 2), H2717-2722.
4. Zhu, H.; Zennadi, R.; Xu, B. X.; Eu, J. P.; Torok, J. A.; Telen, M. J.; McMahon, T. J., Impaired Adenosine-5'-Triphosphate Release from Red Blood Cells Promotes Their Adhesion to Endothelial Cells: A Mechanism of Hypoxemia after Transfusion. *Critical Care Medicine* 2011, *39* (11), 2478-2486.
5. Roback, J. D.; Neuman, R. B.; Quyyumi, A.; Sutliff, R., Insufficient Nitric Oxide Bioavailability: A Hypothesis to Explain Adverse Effects of Red Blood Cell Transfusion. *Transfusion* 2011, *51* (4), 859-866.
6. Sprague, R. S.; Ellsworth, M. L.; Stephenson, A. H.; Kleinhenz, M. E.; Lonigro, A. J., Deformation-Induced ATP Release from Red Blood Cells Requires Cftr Activity. *American Journal of Physiology* 1998, *275* (5 Pt 2), H1726-1732.
7. Olearczyk, J. J.; Stephenson, A. H.; Lonigro, A. J.; Sprague, R. S., Heterotrimeric G Protein Gi Is Involved in a Signal Transduction Pathway for ATP Release from Erythrocytes. *The American Journal of Physiology - Heart and Circulatory Physiology* 2004, *286* (3), H940-945.
8. Sprague, R. S.; Ellsworth, M. L.; Stephenson, A. H.; Lonigro, A. J., Participation of Camp in a Signal-Transduction Pathway Relating Erythrocyte Deformation to ATP Release. *The American journal of physiology - Cell Physiology* 2001, *281* (4), C1158-1164.
9. Tinmouth, A.; Fergusson, D.; Yee, I. C.; Hebert, P. C., Clinical Consequences of Red Cell Storage in the Critically Ill. *Transfusion* 2006, *46* (11), 2014-2027.
10. Ho, J.; Sibbald, W. J.; Chin-Yee, I. H., Effects of Storage on Efficacy of Red Cell Transfusion: When Is It Not Safe? *Critical Care Medicine* 2003, *31* (12 Suppl), S687-697.
11. Moroff, G.; Sohmer, P. R.; Button, L. N., Proposed Standardization of Methods for Determining the 24-Hour Survival of Stored Red Cells. *Transfusion* 1984, *24* (2), 109-114.

12. Mock, D. M.; Lankford, G. L.; Widness, J. A.; Burmeister, L. F.; Kahn, D.; Strauss, R. G., Measurement of Red Cell Survival Using Biotin-Labeled Red Cells: Validation against ⁵¹Cr-Labeled Red Cells. *Transfusion* 1999, 39 (2), 156-162.
13. Suzuki, T.; Dale, G. L., Biotinylated Erythrocytes: In Vivo Survival and in Vitro Recovery. *Blood* 1987, 70 (3), 791-795.
14. Mock, D. M.; Widness, J. A.; Strauss, R. G.; Franco, R. S., Posttransfusion Red Blood Cell (Rbc) Survival Determined Using Biotin-Labeled Rbcs Has Distinct Advantages over Labeling with (⁵¹) Cr. *Transfusion* 2012, 52 (7), 1596-1598.
15. Hillyer, C. D., *Blood Banking and Transfusion Medicine: Basic Principles & Practice*. 2 nd ed.; Philadelphia, PA : Churchill Livingstone/Elsevier: 2007.
16. Strauss, R. G.; Mock, D. M.; Widness, J. A.; Johnson, K.; Cress, G.; Schmidt, R. L., Posttransfusion 24-Hour Recovery and Subsequent Survival of Allogeneic Red Blood Cells in the Bloodstream of Newborn Infants. *Transfusion* 2004, 44 (6), 871-876.
17. Gilson, C. R.; Kraus, T. S.; Hod, E. A.; Hendrickson, J. E.; Spitalnik, S. L.; Hillyer, C. D.; Shaz, B. H.; Zimring, J. C., A Novel Mouse Model of Red Blood Cell Storage and Posttransfusion in Vivo Survival. *Transfusion* 2009, 49 (8), 1546-1553.
18. Russo, V.; Barker-Gear, R.; Gates, R.; Franco, R., Studies with Biotinylated Rbc: (1) Use of Flow Cytometry to Determine Posttransfusion Survival and (2) Isolation Using Streptavidin Conjugated Magnetic Beads. *Advances in Experimental Medicine and Biology* 1992, 326, 101-107.
19. Solomon, S. B.; Wang, D.; Sun, J.; Kanias, T.; Feng, J.; Helms, C. C.; Solomon, M. A.; Alimchandani, M.; Quezado, M.; Gladwin, M. T.; Kim-Shapiro, D. B.; Klein, H. G.; Natanson, C., Mortality Increases after Massive Exchange Transfusion with Older Stored Blood in Canines with Experimental Pneumonia. *Blood* 2013, 121 (9), 1663-1672.
20. Valeri, C. R.; Ragno, G., The 24-Hour Posttransfusion Survival of Baboon Red Blood Cells Preserved in Citrate Phosphate Dextrose/ Adsol (Cpd/as-1) for 49 Days. *Contemporary Topics in Laboratory Animal Science / American Association for Laboratory Animal Science* 2005, 44 (1), 38-40.
21. Mudge, M. C.; Walker, N. J.; Borjesson, D. L.; Librach, F.; Johns, J. L.; Owens, S. D., Post-Transfusion Survival of Biotin-Labeled Allogeneic Rbcs in Adult Horses. *Veterinary Clinical Pathology / American Society for Veterinary Clinical Pathology* 2012, 41 (1), 56-62.
22. d'Almeida, M. S.; Jagger, J.; Duggan, M.; White, M.; Ellis, C.; Chin-Yee, I. H., A Comparison of Biochemical and Functional Alterations of Rat and Human Erythrocytes Stored in Cpda-1 for 29 Days: Implications for Animal Models of Transfusion. *Transfusion Medicine* 2000, 10 (4), 291-303.

23. Sprung, R.; Sprague, R.; Spence, D., Determination of ATP Release from Erythrocytes Using Microbore Tubing as a Model of Resistance Vessels in Vivo. *Analytical Chemistry* 2002, 74 (10), 2274-2278.
24. Shafer, A. W.; Bartlett, G. R., Effect of Inosine on the Posttransfusion Survival of Stored Rabbit Erythrocytes. *The Journal of Clinical Investigation* 1960, 39, 69-71.
25. Donohue, D. M.; Finch, C. A., An Animal Assay Method for the Measurement of Post-Transfusion Survival of Stored Blood. *Vox Sanguinis* 1957, 2 (6), 369-375.
26. Owens, S. D.; Johns, J. L.; Walker, N. J.; Librach, F. A.; Carrade, D. D.; Tablin, F.; Borjesson, D. L., Use of an in Vitro Biotinylation Technique for Determination of Posttransfusion Survival of Fresh and Stored Autologous Red Blood Cells in Thoroughbreds. *American Journal of Veterinary Research* 2010, 71 (8), 960-966.
27. Laura Chiarantini; Magnani, M., Immobilization of Enzymes and Proteins on Red Blood Cells. In *Immobilization of Enzymes and Cells*, 1996; Vol. 1, pp 143-152.
28. Panula-Perala, J.; Siurkus, J.; Vasala, A.; Wilmanowski, R.; Casteleijn, M. G.; Neubauer, P., Enzyme Controlled Glucose Auto-Delivery for High Cell Density Cultivations in Microplates and Shake Flasks. *Microbial Cell Factories* 2008, 7, 31.
29. Glazyrina, J.; Krause, M.; Junne, S.; Glauche, F.; Storm, D.; Neubauer, P., Glucose-Limited High Cell Density Cultivations from Small to Pilot Plant Scale Using an Enzyme-Controlled Glucose Delivery System. *New Biotechnology* 2012, 29 (2), 235-242.